Investigation into discontinuous low temperature waste heat utilisation from a renewable power plant in rural India for absorption refrigeration

by Joel A W Hamilton, MEng

Thesis submitted to
The University of Nottingham
for the degree of Doctor of Philosophy
December 2016

The University of Nottingham

UNITED KINGDOM · CHINA · MALAYSIA

Abstract

This research focusses on utilising low temperature waste heat from a rural renewable power plant for absorption refrigeration. It forms part of a collaborative "Bridging the Urban Rural Divide" (BURD) research group across the United Kingdom and India investigating rural sustainable development through the provision of renewable electricity. The group is tasked with improving the educational environment and healthcare of a 45 household community (which is part of a larger village) in West Bengal, India.

Working in collaboration with the Indian Institute of Technology Bombay as part of this thesis, a projected daily electrical demand for the community of 55 kW·h per day was calculated, providing: lighting, fans and an electrical device charging station. To allow in excess of the daily electrical demand as well as for system ancillaries at 12 kW·h, solar trackers at 14 kW·h and 7 kW·h for hydrogen production, a power plant producing 90 kW·h was specified. This included daily electricity production of 70 kW·h during the daytime from solar via a 10 kW concentrated photovoltaic (CPV) system and 20 kW·h in the evening from a 5 kW biogas and hydrogen internal combustion engine electrical generator (genset). The biogas is produced from anaerobic digestion of food waste and aquatic weeds, and the hydrogen is produced from the electrolysis of water in an electrolyser powered by excess solar power.

An energy and exergy analysis identified the daily quantity and quality of recoverable waste heat sources at 25°C. These are the CPV with an energetic value of 109 kW·h and an exergetic value of 32 kW·h at 60°C and the genset

radiator with an energetic value of 32 kW·h and an exergetic value of 5 kW·h at 80°C. The exhaust heat from the genset has been allocated for other uses and, though calculated, is outside the scope of this research.

The thesis then focusses on using these low temperature waste heat sources for absorption refrigeration. The working fluids selected are acetone and zinc bromide as these had been proven in the literature to operate at temperatures below those of the expected waste heat sources without the need for rectification (the process of separating two fluid vapours from each other). Due to the local climate with high ambient temperatures, averaging 24°C to 35°C, and the relatively low waste heat source temperatures, a number of configurations of absorption refrigerator were investigated to achieve lower, and therefore more versatile, evaporator temperatures. Some of these involve utilising some of the cooling produced from either or both of the heat sources to cool the absorber and condenser.

The findings were that the most energy effective way of providing low evaporator temperatures was to use a small (2%) difference in weak and strong solution concentrations and not use a proportion of the cooling generated for the absorber or condenser. By operating two independent refrigerators powered by each heat source independently, the solution concentrations could be optimised to provide the lowest possible evaporator temperatures at a given ambient temperature.

At the 25°C reference ambient temperature used for the energy and exergy analysis, the CPV waste heat can provide 33.4 kW·h of continuous cooling per day at 6°C and the genset radiator 6.3 kW·h at 0°C. This cooling energy collectively is sufficient to replace 12.7 kW·h of electricity that would have been used to power a vapour compression refrigerator to provide the same amount of cooling, which is equal to 22% of the electrical power provided to the village.

The genset waste heat source used for absorption refrigeration can pro-

vide cooling for food and medicine storage equivalent to 6 to 8 domestic refrigerators. The CPV waste heat source can provide space cooling for a room in a health centre for 6 to 9 hours per day. The investigations within this thesis highlighted the need for intelligent control systems to optimise the availability and temperatures of the refrigerators during unfavourable ambient conditions.

Acknowledgements

Thank you for taking the time to read my thesis. It has been a long and satisfying journey.

I would like to thank my supervisors, the university, my examiners and all the technical and administrative staff for their support and perseverance with me. I would not have made it through this journey without them. At the same time I also thank the research group and fellow PhD students who were always there to keep me safe, on track and full of tea. It goes without saying that I would not have been able to do this without the support and distraction of family, friends, mentors and my menagerie of pets.

This work has been carried out as a part of the BioCPV project jointly funded by DST, India (Ref No: DST/SEED/INDO-UK/002/2011) and EPSRC, UK, (Ref No: EP/J000345/1). I acknowledge both funding agencies for their support. I also acknowledge the support of the partner universities which include: University of Exeter, Indian Institute of Technology Bombay, Indian Institute of Technology Madras, University of Nottingham, Herriot Watt University, Visva-Bharati (West Bengal) and University of Leeds.

Contents

List of Figures

List of Tables

Acronyms, Abbreviations, Definitions and Nomenclature

Acronyms, Abbreviations and Definitions

BioCPV - Collaborative research project name encompassing the use of biogas and CPV

CPV - Concentrated photovoltaic

Genset - Internal combustion engine electric generator

AD - Anaerobic digester

DNI - Direct normal irradiance

CoP - Coefficient of Performance

PV - Photovoltaic

Cell - PV cell assembly in CPV unit

$ZnBr_2$ - Zinc bromide

Weak solution - High–in–refrigerant

Strong Solution - Low–in–refrigerant

Nomenclature

T - Temperature (°C and K)

P - Pressure (bar)

h - Specific enthalpy ($kJ \cdot kg^{-1}$)

s - Specific entropy ($kJ \cdot kg^{-1} \cdot K^{-1}$)

X - Concentration $\frac{m_{ZnBr}}{m_{total}} \times 100$ (e.g $50\% = 50$)

C - Concentration $\frac{m_{ZnBr}}{m_{total}}(\%)$

m - Mass (kg) or mass flow (time period dependant modelling approach)

Q - Thermal energy (kJ), (kW) or (kW·h)

W - Work (kJ)

E - Electrical energy (kJ), (kW) or (kW·h)

ε - Exergy (kJ), (kW) or (kW·h)

A - Area (m^2)

η - Efficiency

n - Number of $[item]$

ϵ - Heat exchanger effectiveness

λ - Percentage of cooling energy used

c_p - Specific heat capacity ($kJ \cdot kg^{-1} \cdot K^{-1}$)

Δ - Difference

Energy Analysis

E_{CPV} - CPV electrical output

$Q_{CPV_{concentrator}}$ - Thermal energy entering the CPV concentrator

n_{CPV} - Number of CPV units

$\eta_{CPV_{optical}}$ - Optical efficiency of CPV concentrator

$A_{CPV_{concentrator}}$ - Area of CPV concentrator

$Q_{CPV_{cell}}$ - Thermal energy reaching PV cell assembly in CPV unit

$\eta_{CPV_{cell}}$ - PV cell efficiency

$Q_{CPV_{thermal}}$ - Thermal energy of the PV cell

Q_{genset} - Genset thermal energy requirement

$W_{genset_{ancillary}}$ - Genset ancillary losses

$Q_{genset_{exhaust}}$ - Thermal energy in genset exhaust

$m_{genset_{exhaust_i}}$ - Mass flow of individual components of genset exhaust

$h_{genset_{exhaust_i}}$ - Specific enthalpy of individual components of genset exhaust

$Q_{genset_{radiator}}$ - Thermal energy in genset radiator

Absorption Refrigerator

The following explains the general naming method for the symbols used in absorption refrigerator modelling in this thesis, where $Symbol_{1_{2_{3_4}}}$

Suffix 1: General

if blank it refers to both CPV and genset

AMB Ambient

c - Critical

s - Saturation

l - Liquid

v - Vapour

sh - Superheated

$genset$ - Internal combustion engine electrical generator

CPV - Concentrated photovoltaic

HTF - Heat transfer fluid

vc - Vapour compression refrigerator

Suffix 2: Component

BO - Boiler

CO - Condenser

RE - Reservoir

TH - Throttle

EV - Evaporator

AB - Absorber

Suffix 3: Fluid

WS - Weak (high-in-refrigerant) solution

SS - Strong (low-in-refrigerant) solution

R - Working refrigerant (used in condenser / evaporator)

Suffix 4: Flow Direction

in - Input

out - Output

Example

$T_{genset_{RE_{R_{out}}}}$

This refers to the temperature of the genset powered absorption refrigerator refrigerant reservoir's output:

- Temperature (T)
- Genset ($_{genset}$)
- Reservoir ($_{RE}$)
- Refrigerant $\left(_{R}\right)$
- Output $\left(_{out}\right)$

Chapter 1

Introduction

The following thesis investigates discontinuous (operating for a proportion of the day e.g. when the sun shines or the evening) low temperature waste heat utilisation for absorption refrigeration for a range of ambient conditions. The research forms part of a Bridging the Urban Rural Divide programme (BURD) called BioCPV aiming to provide a sustainable development solution to rural India through the provision of renewable power. The power plant proposed by the BioCPV research group and its location in rural India provide the criteria and input information for the investigations within this thesis.

The BioCPV project is a collaboration between three Indian and four British universities and the renewable power plant consists of 10 kW (electric) concentrated photovoltaic (CPV) and 5 kW (electric) biogas-hydrogen internal combustion engine electrical generator set (genset). The CPV is solar powered, the biogas is generated in an anaerobic digester powered by local food waste and aquatic weeds, and the hydrogen is produced from the electrolysis of water using excess solar power from the CPV. The waste heat sources being investigated are the CPV maintained at 60°C and the genset radiator at 80°C. Though the waste heat sources are modelled from a specific case study power plant the research within this thesis is applicable to a wide

range of waste heat sources from industrial to domestic applications in any environment where sustainable refrigeration is required.

There is a need to address the future global energy demands and the significance of the contribution of rural electrification in India. A presentation of a demand profiling method used to quantify the needs of the case study community in rural India is necessary to understand how an electricity generation plant will be used in the context of a rural village in India. An overview of the proposed power plant by the BioCPV group is provided to aid contextualisation of the analysis within this thesis. There is also a need to address the potential global low grade waste heat resource and how its use has the potential to reduce global energy consumption. This helps place a level of importance on the issue of waste heat utilisation.

The motivation for this research is that the case study community is located in West Bengal, India and due to its high ambient temperatures and traditional rural lifestyle a sustainable source of refrigeration has been considered a more beneficial use of waste heat than hot water. Refrigeration has the potential to provide food and medicine storage or cooling for a medical recovery area, whereas hot water from these low grade heat sources is not needed for heating and so would only provide more comfortable washing facilities. Providing sustainable refrigeration can have a significant impact on the development of this community without the need for a significant increase in electricity generation.

The research objective is to investigate discontinuous low temperature waste heat utilisation from a renewable power plant in rural India for absorption refrigeration.

The approach consists of:

- Assess and validate the needs of the community.

- Appraise refrigeration technologies to determine the most suitable to investigate.
- Quantify and qualify the waste heat sources.
- Investigate the operating limits of absorption refrigeration from the waste heat sources identified in a range of ambient temperatures.
- Investigate any alternative configurations that extend the operating limits.
- Quantify the benefits from the optimised configuration for the community.

The thesis structure:

- **Background and Motivation** outlines the main drivers, objectives and approach of this research. The rationale behind how low grade waste heat utilisation can help mitigate some of the negative effects of global energy consumption is presented. This is followed by a description of the case study community and their needs together with a projected electrical demand profile. The renewable power plant proposed by the BioCPV research group is then shown to identify the low grade heat sources which are used to power the absorption refrigeration systems modelled later in the thesis.
- **Refrigeration Technology Review** presents an appraisal of refrigeration technologies. Initially a history of refrigeration is introduced which is followed by a review of common refrigeration systems. An appraisal process of common refrigeration systems finds absorption refrigeration to be suitable for the conditions of the case study community and the heat sources available. This is followed by a detailed review of absorption refrigeration working fluids and system configurations. Acetone and zinc bromide solution is identified as suitable working

fluid pair and configurations that reduce evaporator temperatures are identified to be investigated.

- **Analytical Methodology** presents the approach used to calculate the results presented in the following three chapters. This includes the calculations for the energy analysis within which lies the modelling of the waste heat sources. This is followed by the modelling approach for the absorption refrigeration systems. Finishing with the approach for quantifying energy utilisation using exergy for the BioCPV power plant and a method for relating the cooling generated from the absorption refrigeration systems to avoided electricity consumption.
- **Power Plant Energy Utilisation** presents the results and discussions of an energy and exergy analysis of the rural renewable power plant proposed by the BioCPV research group. This process quantifies and qualifies the energy contained in the heat sources.
- **Absorption Refrigeration Experiment** presents the results and discussions from a lab scale absorption refrigerator used to provide insight into the absorption refrigeration system modelling assumptions in the analytical methodology and the operational challenges.
- **Absorption Refrigeration Modelling** presents the results and discussions of the absorption refrigeration system modelling, investigating the effects of operating limits and cycle configurations on cooling output and refrigeration temperature.
- **Conclusions and Further Work** describes the processes used for the investigations in this thesis and presents the main findings together with areas of further work that were identified during this research.

Chapter 2

Background and Motivation

Global energy demand and consumption is increasing and the associated environmental impacts of it are generally accepted amongst the scientific community. This thesis explores the optimisation of low grade waste heat sources for absorption refrigeration to address this increasing consumption. There have been several international conferences, frameworks and treaties from the United Nations Framework Convention on Climate Change (UNFCCC) in 1992 through to the Conference of the Parties (COP) 21 in 2015 where targets were set and plans made to mitigate and adapt to the effects of emmssions resulting from energy consumption. Non OECD (Organisation for Economic Co-operation and Development) countries are expected to account for the majority of this increase in energy consumption where projections show that by 2040 they could account for 2.5 times that of OECD countries (EIA 2015). This is largely the result of the economic growth of a country being directly related to the per capita energy consumption (Ghosh 2002).

In order to study this global issue, this research investigates a key contributing country, India. It has the second largest population, with approximately 1.25 billion people it accounts for approximately 17% of the global population (CIA 2015). India is one of the non OECD countries expected to develop rapidly in the coming years resulting in an increase in its en-

ergy consumption. According to the data of the Government of India 2011 census, approximately 69% of the total population (833 million people) live in 640,867 villages, of whom 56% (approximately 400 million people) are without grid connected electricity supply (Census of India, 2011). In rural areas energy is required for both domestic use and small-scale local industries, both of which contribute significantly to economic development. The geographical diversity and lack of infrastructure has become a barrier for the grid connection to the rural areas in India.

To illustrate this further, per capita annual grid connected electricity consumption in India during 2011 was 288 kW·h in urban areas and 96 kW·h in rural areas. This exceeds the World Energy Outlook (WEO) analysis of the International Energy Agency (IEA) in 2012 which considered 500 kW·h and 250 kW·h as the minimum household consumption levels for urban and rural areas respectively (with five people in each household). However if the 400 million people without grid connected electricity in rural India are to be provided with a source of electricity at the average consumption for rural areas of 96 kW·h per annum a crude approximation of the increase in annual energy consumption for rural India is 38 TW·h, which is roughly equivalent to the annual electricity consumption of Belarus or New Zealand (CIA 2015). This does not take into account the even greater increase in energy consumption resulting from rural communities becoming more affluent and the associated desire for more energy consuming appliances.

Decentralised hybrid power plants with a range of renewable technologies can provide efficient, cost effective and sustainable options for rural electrification (Bajpai and Dash 2012) (Ghosh 2002). The integration of a variety of renewable sources to complement each other, coupled with storage, can provide a sustainable development solution all year round. India had 20,556 MW of renewable power generation capacity by 30th June 2011 which was approximately 11% of the total power generation capacity of the country.

Through the Jawaharlal Nehru National Solar Mission (JNNSM) it is envisaged that India will have an installed solar capacity of 20,000 MW by 2020, 100,000 MW by 2030 and 200,000 MW by 2050. (Sharma et al. 2012).

Globally, waste heat is a huge energy resource, which if well utilised can reduce global energy consumption and the associated negative effects. Olulleye et al. (2016) state "process industries are responsible for 27% of global energy consumption" combined with 20% to 50% of industrial energy being wasted as heat (DOE 2008), indicates that approximately 10% of global energy consumption is industrial process waste heat. Considering that Haddad et al. (2014) state that low grade waste heat (defined as below 200°C) accounts for 66% of industrial waste heat, it is possible to approximate that 7% of global energy consumption is lost as low grade waste heat through the process industries. These figures should be used with caution, as Miró et al. (2015) describe that there are difficulties in obtaining waste heat data internationally. However the literature suggests that there is currently a significant amount of wasted low grade heat. If well utilised, these figures suggest that this energy source could either significantly reduce global energy consumption or allow greater levels of development growth without the associated increased energy demand.

The factors mentioned here led to the creation of a collaborative research group between institutions in the UK and India, called BioCPV, with the objective of providing a sustainable development solution to rural India through renewable power. This research group has chosen a small community in Santiniketan, West Bengal, India, which is adjacent to one of the partner organisations, Visva-Bharati, to provide renewable power to. In addition to providing sustainable sources of energy to supply the projected growth in energy consumption of the community, it is equally important to optimise the use of the energy produced as this, by its nature, can reduce the amount of energy needed and therefore consumed. Due to the nature of

renewable energy sources, renewable power plants tend to operate in a discontinuous fashion and have discontinuous sources of waste heat available. These elements provided the motive for the investigation of this thesis into discontinuous low temperature waste heat utilisation from a renewable power plant in rural India for absorption refrigeration.

2.1 Assessment of The Needs of The Case Study Community

Two rural tribal villages in the north-west of India (shown in Figure 2.1), Kaligung and Pearson-Palli, adjacent to Visva-Bharati University, Santiniketan have been selected because the majority of the tribal people in this area

Figure 2.1: Location of the case study community Kaligung and Pearson-Palli, Santiniketan, Bolpur District, West Bengal, India.

do not have access to electricity owing to their socio-economic conditions. Although there is a grid connection in the village, the supply is weak, only providing a few hours of electricity per day and not all the houses are connected to this grid. The villages comprise 179 households with a population of approximately 821. Most of the families in the village live below the poverty line as defined by the World Bank. Out of the total population, 52% are women and 10% are children. The average household income is approximately INR 2500 per month. The BioCPV research project selected 45 households out of these villages for the case study community to provide renewable power to.

Basic facilities such as drinking water and sanitation are not available which leads to an unhygienic lifestyle. The houses, shown in Figure 2.2 are

Figure 2.2: Typical house found in Kaligung and Pearson-Palli, made from bamboo or wood and mud.

typical for an Indian village made from bamboo or wood and mud. There is a basic health centre in the village which provides primary health care through an arrangement with Visva Bharati University, doctors and local health workers. Most of this care currently takes place outdoors. For more serious illness, villagers visit the Block Primary Health Centre (BPHC) or University Hospital (3 and 2 km away respectively).

Kaligung and Pearson-Palli are primarily tribal populations, mostly belonging to Santal tribes (indigenous group found in East India and Nepal). The villages come within the Visva-Bharati University (a member of the BioCPV project) core area. Historically, these native tribes found work in agriculture, gardening and forestation of the Santiniketan campus (Visva-Bharati, West Bengal). Despite being the oldest inhabitants of the area, from a socio-economic perspective they are lagging behind the rest of the local society.

2.1.1 Lifestyle and Culture

The people of Kaligung and Pearson-Palli are deprived of the basic privileges of a developed society lifestyle and education primarily due to the lack of infrastructure in rural areas. Research from Visva-Bharati looking at a sample of the villagers showed that 70% of households are not landowners and live on government land. The findings in Figure 2.3 show 53% of these two villages' populations are daily labourers, 24% are farmers and the remaining 23% are self-employed or private servants. Additionally 31% of people in the villages are literate, but not well educated. Typically the parents in the villages are illiterate but their children are in conventional school education. However acute poverty forces some children to leave school early in order to earn a living.

Women are involved in both household and income generating activities.

Household activities include: collecting leaf litters and fuel woods from the nearest forest area 2 to 3 km from the village for cooking and preparing meals for the rest of the family. Income generating activities include: spice grinding and making small handicrafts using bamboo and other locally available materials. Some of them are involved in Self Help Groups (SHG) to generate opportunities for small scale businesses to improve their economic conditions. The activities women are involved in are all time-intensive manual labour, which reduces their opportunity to undertake training and education to improve their quality of life.

Men are considered the primary income generator in families in the villages; this is typical for rural parts of this district. The Department of Statistics and Programme Implementation for the government of West Bengal (2011) state that 43% of the total population of the district are rural male primary income generators. When they are not working men spend a lot of time in public areas, therefore developing these public areas so that they are

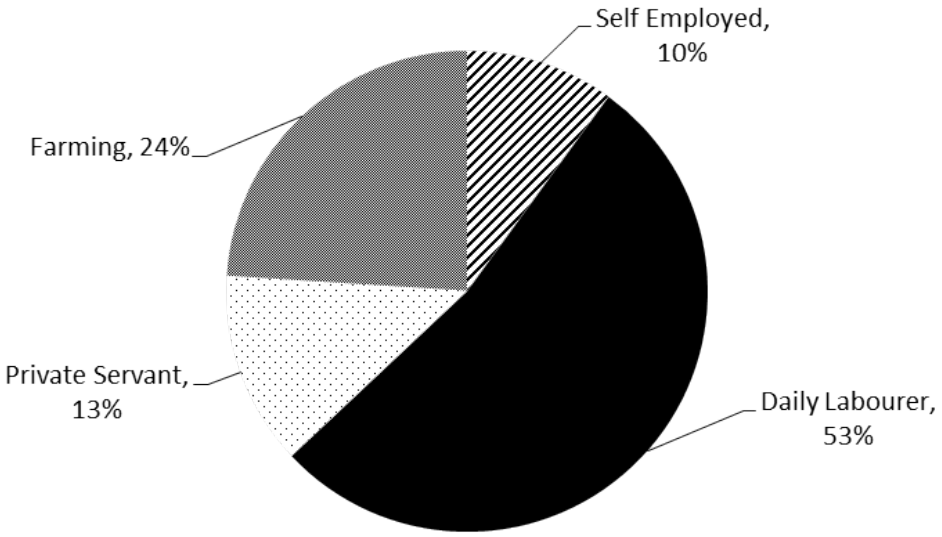

Figure 2.3: Occupations of working age residents of Kaligung and Pearson-Palli.

suitable for education and training could also provide a positive impact for the villagers.

There is inadequate indoor and outdoor lighting in the villages. This results in the majority of work and learning taking place during the day. A survey carried out by Visva-Bharati within the village found that it was difficult for children to study at home due to inadequate lighting. The current solution of kerosene lamps has health implications as their emissions reduce indoor air quality.

Due to a lack of reliable electricity it is not practical to provide refrigeration for food and medicine storage or space cooling (for example a recovery room in the medical centre).

The demographic and socio-economic needs described here can be addressed by providing reliable electricity to aid the development of this community. This will improve the educational environment through lighting and ventilation. It will reduce reliance on technologies damaging to health (such as kerosene lamps). It will also alleviate some of the time-intensive manual income generating activities potentially leading to an improved quality of life. Providing these infrastructural developments in a sustainable way, will help the long term needs of this community and act as a model for rural communities across the developing world.

2.1.2 Weather and Conditions

Like most of the remote areas of eastern India, the region of Kaligung and Pearson-Palli is warm and humid with generous rainfall. Based on data collected from a local weather station at Visva-Bharati, Santiniketan there is typically 1500 mm of rainfall from June to September and average temperatures of 24°C to 35°C with highs approaching 50°C.

2.1.3 Resources Available

India has an abundance of solar energy with annual daily average solar irradiance on a horizontal surface of 5 to 7 $kW \cdot h \cdot m^{-2}$. Nearly 58% of the geographical area represents regions of exceptional solar power potential (Ramachandra et al. 2011). The eastern part of India is rich in both solar irradiation and biomass resources (Reddy and Veershetty 2013) (Banerjee 2006). A survey by Visva-Bharati also estimated that there is access to a minimum of 200 kg food waste generated on a daily basis from the university hostels in the nearby area of the village and plenty of aquatic weeds provided by the nearby ponds, which can be used as a fuel source.

2.2 Community Power Demand Rationale

The following section describes the process for creating a demand estimation for the community and presents the renewable power plant proposed by the group. The following process was developed as part of this thesis and was a collaboration with the Indian Institute of Technology Bombay. A detailed overview of the technologies available allowing appropriate selection together with the design considerations and sizing calculations for each technology within the plant can be found in Appendix Paper titled "Design and initial assessments of a biomass/biogas and solar renewable power plant for rural electrification in India".

2.2.1 Demand Estimation

The World Energy Outlook analysis for the minimum electricity consumption of a five person household is calculated using the assumption that the following technologies could be used: a floor fan, a mobile telephone, and two compact fluorescent lamps (CFL) in rural areas, and might include: an

efficient refrigerator, a second mobile telephone, and another appliance, such as a small television or a computer, in urban areas. Electric lighting is seen to be an influential technology to provide development, from 2001 to 2011 the share of households in rural areas using electricity as their prime source of lighting changed from 43.5% to 55.3%, and in urban areas from 87.6% to 92.7% [Census of India, 2011].

In light of these findings and studies of the local needs, together with the desire to provide sustainable development through improving the educational environment and overall quality of life, this section describes the method used to calculate a demand profile for the community and others like it. Table 2.1 lists the items and quantities used in the demand profile and Figure 2.4 shows how the energy demand of the items in Table 2.1 would be distributed through a typical 24 hour period.

Previous work with these communities carried out by Visva-Bharati found that successful adoption of change requires a holistic approach where the villagers are involved throughout the project, training and education are provided and that everything is compatible with their customs and traditions. Alongside the engineering research there is work and research in promoting the system and its benefits to the local community. This is equally as important as the engineering design to avoid rejection of technology resulting from apprehension of significant change.

Ventilation - Fans

Fans are required for thermal comfort; it is common to see ceiling fans used in warm climates as they destratify the air providing a sensation of being cooler. Guidelines in the United Kingdom suggest 70 m^2 is required for a primary or middle school class of 30 students (NUT 2015). A typical ceiling fan such as Vent-Axia Reversible Hi-Line + requires 60 W at full load and suggests in tropical climates that they should be placed 3 m apart (and 6 m

in temperate climates) (Vent-Axia 2015). There are currently 104 students at the school which are accommodated in 2 large rooms (approximately 11 m x 5 m) and one small one (3 m x 4 m). The number of students can vary, and the building may have additional rooms built on to it, so, for the purposes of repeatable demand profiling, the remaining analysis is based on the guidelines mentioned here. Therefore the school would require 3 classrooms allowing for a comfortable learning environment for 90 children. Each 70 m^2 classroom can be allocated 2 fans depending on dimensions. An assembly hall which can house activities and exercise classes as well, is assumed to be the size of 3 classrooms and would require 6 fans. Another room the same size as a classroom used as an office for the teachers and staff would require a further 2 fans. This totals 14 fans, but it will be very unlikely that all the fans would be at maximum load at the same time. For the purposes of load estimating, an average fan load equivalent to 10 fans at 60 W each has been assumed.

Lighting

The efficacy of a CFL bulb is 55 $lm \cdot W^{-1}$ (NREL 2014). The lighting requirements for a bright office space requiring perception of detail is 200 lx and for dull workspaces not requiring perception of detail is 100 lx. (HSE 1997).

By definition

$$efficacy = \frac{lumen}{electrical\ power} \tag{2.1}$$

And

$$lux = \frac{lumen}{area} \tag{2.2}$$

Therefore using Equations 2.1 and 2.2 the lit area depending on the lighting requirements can be found using Equation 2.3

$$area = \frac{efficacy \times electrical\ power}{lux} \tag{2.3}$$

Table 2.1: Appliance itinerary to create demand profile, including typical energy consumption and quantity required.

	Power Per Item (W)	Quantity	Total Power (kW)
School / Public light bulb	15	40	0.75
Fan	60	10	0.6
Domestic light bulb	10	90	0.9
Lantern / Phone charging	10	100	1
Desktop PC	100	10	1
Small Machinery	200	8	1.6

Using this information a 15 W CFL should provide 4.125 m^2 of bright workspace and 8.25 m^2 of dull workspace. Therefore 40 $\times$ 15 W CFLs are considered for public lighting, providing a bright area of 165 m^2 and a dull area of 330 m^2. Taking natural light into consideration as well, the estimate of 40 bulbs provides an average load of public lighting to meet the daytime and evening needs. Public lighting refers to the lighting used for the school building, which is intended to be used as a communal area outside of school time.

Likewise the same analysis can be used to determine that 10 W CFLs in a domestic setting can provide the equivalent of 2.75 m^2 of bright workspace and 5.5 m^2 of dull workspace. Assuming that 2 rooms per household require lighting, then for 45 households, 90 $\times$ 10 W CFL bulbs are required.

Lantern and Phone Charging

Lantern and phone charging was based on modern high powered USB chargers outputting approximately 10 W for mobile phone charging, for example the Innergie ADP 21AW D. Since a large number of battery powered devices

can be charged by these it was assumed to be suitable for lanterns as well. It was assumed that there would be 2 lanterns per household and 10 phones in the community resulting in a quantity of 100 × 10 W devices requiring charge.

Desktop PC

The power demand for a typical PC found on the market is 100 W based on a basic specification of an HP 110-352na Desktop PC at 65 W and a typical monitor such as the HP ENVY 24 60.5 cm at 26 W to 54 W (HP 2015). It was assumed the school could have an average PC load of 10 PCs.

Small Machinery

Small machinery such as spice grinders and sewing machines were estimated at 200 W based on a range available in the market. A quantity of 8 was estimated allowing a gentle introduction of the technology, so that those who want to work together with the machinery can and those who prefer the traditional methods can maintain their current approach.

2.2.2 Demand Profile

Figure 2.4 shows the expected demand profile of the village over 24 hours. The demand is divided in to a day load which is from 09:00 to 17:00 and an evening load from 17:00 to 21:00. Public area lighting, fans, computers and the charging station are assumed to be used all day from 09:00 to 21:00. This is a result of the community buildings being used as a school during the day and then a community centre in the evening, where computers, lighting, fans and charging station will be used. The use of small machinery is assumed to only take place during the day; this is mainly because they are noisy.

2.2.3 System Requirements

The demand profiling analysis shown in Figure 2.4 and Table 2.1 has found that there is a minimum system requirement of 4.8 kW of electricity during the day (9:00 to 17:00) and 4.1 kW in the evening (17:00 to 21:00), totalling 55 kW·h per day of electrical supply to the village. An additional 33 kW·h has been allocated as: 12 kW·h for system ancillaries, 14 kW·h for solar trackers, and an electrolyser load for hydrogen production of 7 kW·h (1 kW for the 7 hours of CPV operation) based on discussions with the partner organisations. Therefore there is a minimum electrical generation requirement of 88 kW·h per day.

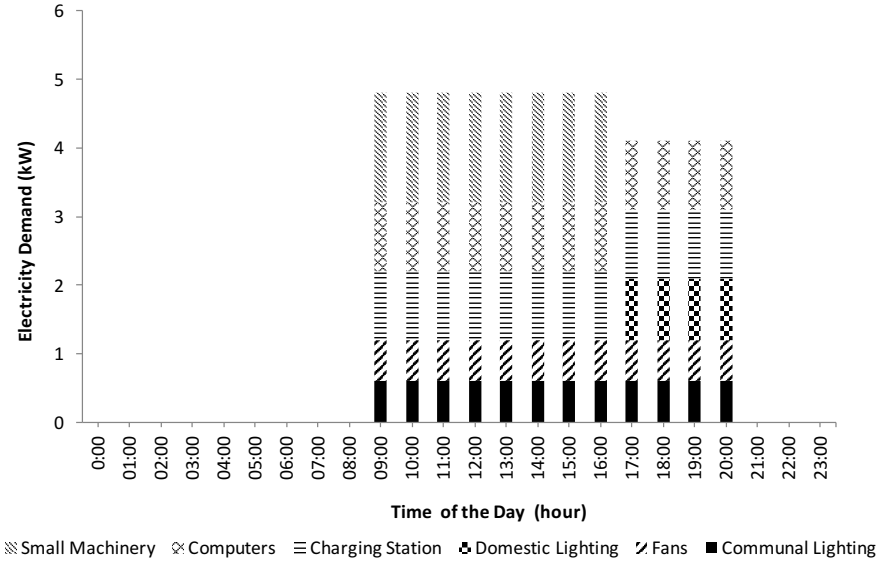

Figure 2.4: Maximum predicted demand profile elected for the community on a typical day irrespective of the season.

2.3 Proposed Renewable Power Plant Design

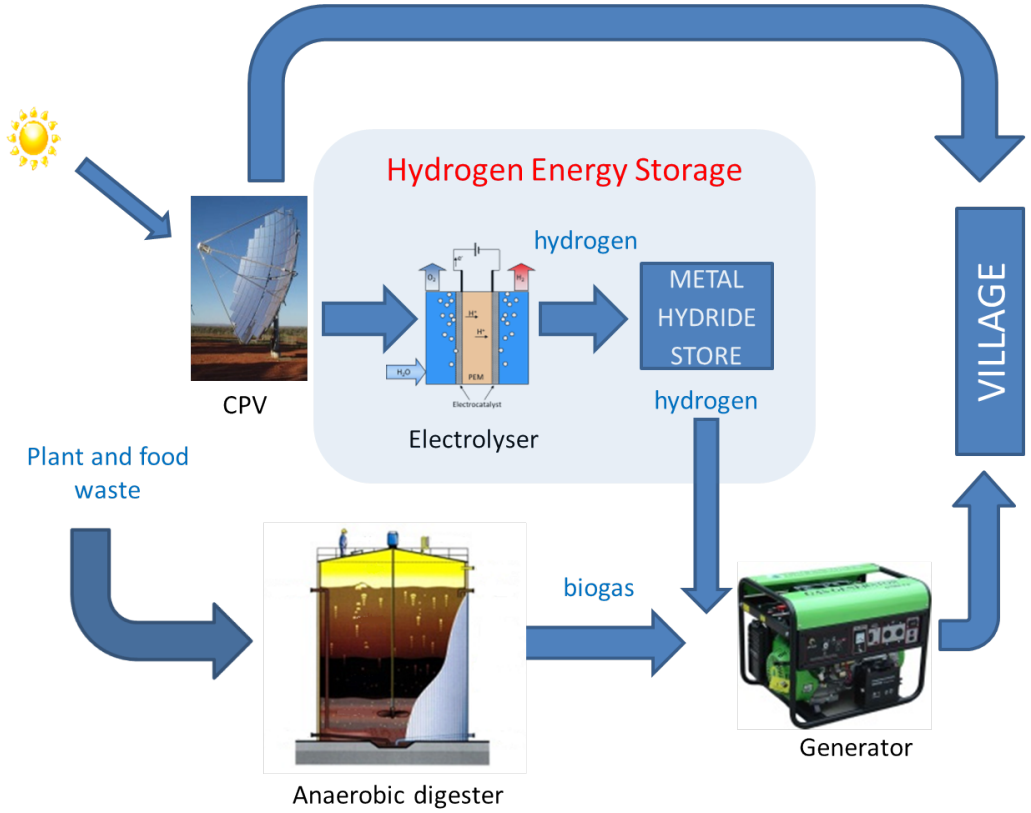

Figure 2.5: BioCPV renewable power plant schematic, consisting of: 10 kW concentrated photovoltaic (CPV), 5 kW biogas and hydrogen internal combustion engine electrical generator set (genset), electrolyser, metal hydride store and anaerobic digester.

Due to the abundance of solar irradiation and biomass in the vicinity, CPV and biogas; created by anaerobic digestion of food waste and aquatic weeds and used in an internal combustion engine electrical generator set (genset), were selected as the main electricity generation methods. These technologies complement each other as the biogas genset can be operated when the CPV is unavailable. Moreover the production and use of biogas are decoupled; therefore, depending on storage capacity, it can support both seasonal and diurnal variation. Hydrogen storage will be used to optimise

the use of solar electricity and increase the quality of the biogas. A schematic of the BioCPV power plant can be seen in Figure 2.5.

For system sizing purposes the BioCPV group agreed on a daily generation load of 90 kW·h per day as it exceeds the estimated daily demand of 88 kW·h. This can be allocated to a daytime solar generation load of 70 kW·h which can be simplified to 7 hours of generation at 10 kW (electric) and an evening biogas - hydrogen electrical generator load of 20 kW·h based on 5 kW (electric) for 4 hours per day.

The partners in the project have specified that the CPV PV cells module (hereinafter referred to as: PV, cell and CPV waste heat source) should operate at 60°C and will require a mechanism to remove the heat generated, from its operation, to maintain this temperature. Waste heat from the internal combustion engine electrical generator (genset) is also expected; typically the sources are the radiator at 80°C and the exhaust at 350°C. The CPV and genset waste heat sources will be discontinuous as the CPV will operate during the day for 7 hours and the genset at night for 4 hours.

2.4 Conclusion

There is a need to provide renewable power to drive the sustainable development of the selected community and communities similar to it internationally. The BioCPV group have proposed a rural renewable power plant based on the projected demand profile presented in this chapter and an assessment of locally available resources.

The community at present conducts most of its minor medical treatment outside and could benefit from some space cooling for a recovery room. They also have no means of refrigerating food and medicines. The potential benefits that refrigeration can bring without having a significant impact on the electricity demand has led to the focus of this research in investigating low

temperature discontinuous waste heat utilisation from a renewable power plant in rural India for absorption refrigeration.

Low temperature discontinuous waste heat sources are expected within the proposed power plant. These typically have a low energy quality and therefore are not suitable for the generation of work and electricity. Generally the most efficient uses of low temperature waste heat sources are space or water heating as this is a direct use, and if designed appropriately, could make use of almost all of the waste energy. The problem is that hot water and heating is not an important need in this location whereas refrigeration would be welcomed.

This situation is not unique to this community; there are many developing countries with warm climates where a sustainable source of refrigeration can improve the quality of life. Therefore, the findings and methods presented in this thesis can be applied to many situations internationally. Moreover, it was estimated in this chapter that low grade waste heat accounts for 7% of global energy use; making its efficient utilisation a significant factor in lowering global energy demand and the associated negative effects.

Chapter 3

Refrigeration Technology Review

Given the need for refrigeration in rural India identified in Chapters 1 and 2, this chapter aims to provide insight into the refrigeration choices made in this thesis. This is achieved by presenting a history of refrigeration, a description of common refrigeration systems and a detailed overview of the selected technology: absorption refrigeration.

Depending on the energy source available to drive a refrigerator there are a number of options, which can be broken down into thermally activated and mechanically activated. Thermally activated include: absorption, adsorption and desiccant cooling systems. Mechanically activated include: vapour compression (also known as reverse Rankine) cycle and gas (also known as reverse Brayton) cycle.

There are a number of other refrigeration technologies which are not discussed here as they are either only at lab scale or are not suitable for food storage and thermal comfort, which constitute the main refrigeration needs in rural India. Today the most common form of refrigeration is the vapour compression cycle, this is found in almost all domestic refrigerators,

air conditioning units and the majority of industrial refrigeration systems as well.

This chapter consists of the following sections:

- **History of Refrigeration** starts with references to the the earliest forms of refrigeration from ancient civilisations, followed by descriptions of the mechanical ancestors of various forms of refrigerating machines and provides some insight into the reasoning behind their development.
- **Review of Commonly Used Refrigeration Systems** describes the following refrigeration systems: vapour compression, adsorption, gas (or reverse Brayton), absorption and desiccant cooling. It concludes with a selection process for an appropriate refrigeration technology to utilise low temperature waste heat in rural India, found to be absorption refrigeration.
- **Detailed Overview of Absorption Refrigeration** describes absorption refrigeration in detail and includes the following:
  - **Challenges of Absorption Refrigeration** describes the fundamental challenge with absorption refrigeration which is created by the desire to maintain high condensing temperatures, low evaporator temperatures, high coefficient of performance (CoP) and low boiler temperatures.
  - **Fluids** describes the possible working fluids for absorption refrigeration systems.
  - **System Configurations to maximise heat utilisation** describes the following configurations: boiler absorber heat exchange (BAX, also known as GAX and DAHX), boiler heat recovery, half effect and dual cycle.

  - **System Configurations to Utilise Discontinuous Heat Sources** describes the systems to utilise discontinuous heat from solar power and focusses on the application of the refrigerant storage method with the single effect and double boiler cycles.
  - **System Configurations to Reduce the Evaporator Temperature** describes systems that allow cooling of the condenser and absorber to lower the pressure in the evaporator, these are evaporator tap-off and coupled cycle.
  - **Using Discontinuous Heat Sources and Controlling Evaporator Temperature** combines the ideas from the two previous subsections to create cycles that can utilise discontinuous waste heat to provide useful refrigeration in rural India.
  - **Appraisal of Absorption Refrigeration Systems** provides a comparison of the configurations described to allow selection of appropriate cycles for utilising low temperature discontinuous waste heat in rural India.

- **Conclusion of Refrigeration Technologies Review** summarises the technologies, their history and applications described in this chapter and justifies the choice of refrigerator technology.

3.1 History of Refrigeration

Jordan and Priesters book titled "Refrigeration and air conditioning" describes how there are poetry references from the Ancient Greeks, Chinese and Romans about using natural ice to cool food and drink. It also explains how during most of the 19th century natural ice was shipped all over the world to be used for cold storage and food processing. (Jordan and Priester 1950), (Freidberg 2009)

Artificial refrigeration, not by naturally forming ice, also dates back to ancient times:

> "As early as the fourth century AD the East Indians knew that certain salts, such as sodium nitrate when placed in water would result in lowering the temperature."(Jordan and Priester 1950)

An article in the New Scientist reviewing the book "A History of Refrigeration Throughout the World" by Roger Thevenot claims the first artificial refrigeration device was produced by William Cullen in 1755 (Howard 1980).

One of the earliest patents for a refrigeration machine is from 1834, shown in Figure 3.1. This device is the predecessor for the vapour compression cycle, which is currently the most common refrigeration cycle. The machine operates by compressing the refrigerant at position A increasing its pressure, then condensing it at position B by removing the heat that was generated from compression (A) and evaporation (C and D). At point C (throttle) the pressure is lowered, to correspond with the desired refrigeration temperature, through moving the piston to increase the volume. The flow of refrigerant is controlled with the throttle allowing the refrigerant to evaporate and fill the void created by the piston moving. Part of this void, position D, is called the refrigerator in this machine (also known as the evaporator in todays vapour compression machines). The evaporation taking place in the refrigerator (D)

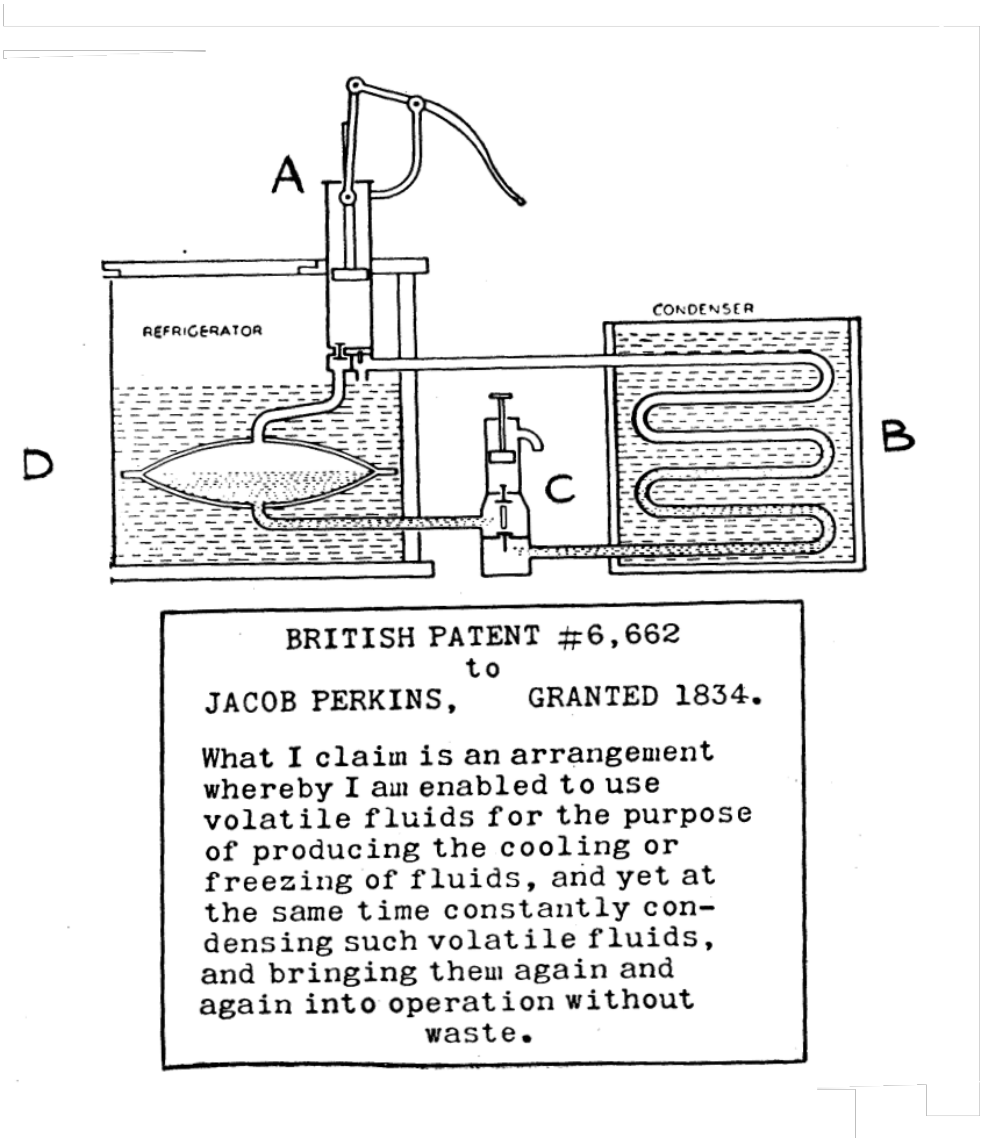

Figure 3.1: Earliest recorded patent for a refrigeration machine, issued in Great Britain in 1834. Where A is the compressor, B the condenser, C the throttle and D the evaporator (or refrigerator) (Jordan and Priester 1950).

draws in heat which provides the refrigeration effect. The refrigerant then enters the compressor at A and the cycle repeats.

Dr. John Gorrie designed a refrigeration machine that used compressed air as the refrigerant and received the first American patent for an ice machine in 1851. Sulphuric ether was the desired refrigerant for Prof A. C. Twining's ice making machine in New Haven, USA which followed the vapour compression cycle; he gained a patent for it in 1853. All these devices require some motive power to drive the compressor. (Jordan and Priester 1950)

During the mid nineteenth century there was little access to electricity which often resulted in vapour compression systems requiring a fossil fuelled

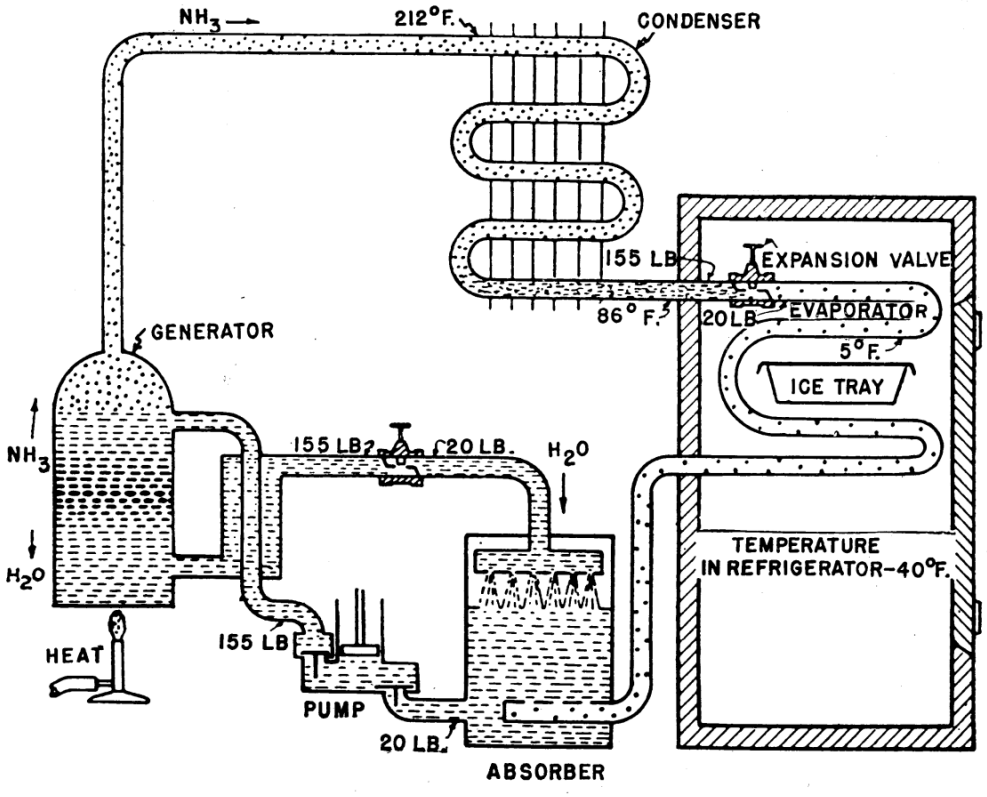

Figure 3.2: Diagrammatic sketch of Ferdinand Carré's absorption refrigeration machine for which he received a patent in the 1860s (Jordan and Priester 1950).

engine to provide the motive power. However mass production of internal combustion engines did not start until the late nineteenth century (Todd 1995), so the motive power for vapour compression refrigeration machines was limited to external combustion engines. This requirement for an external heat source to power a vapour compression refrigerator made absorption refrigeration more attractive as the systems could be directly powered by the heat source, potentially making them simpler and cheaper at the time. An early example of a commercial absorption refrigerator is Ferdinand Carré's machine, seen in Figure 3.2, which was used during the French civil war as the supply of ice from the north was cut off. This system used ammonia as the refrigerant and water as the absorbent (Jordan and Priester 1950). Carré received the first patent in the USA for a commercial absorption refrigerator in the 1860s (Deng et al. 2011). This machine changed the approach to refrigeration globally as ice could be generated locally and no longer had to be transported around the world. (Freidberg 2009) (Jordan and Priester 1950)

During the twentieth century electricity grids became more widespread which resulted in electric motor driven vapour compression refrigerators dominating the domestic market. These systems were often smaller, simpler and cheaper than any of the thermally activated refrigerators. However vapour compression systems often used highly toxic refrigerants. After an incident of a family being killed by a leaking refrigerator Albert Einstein and Leo Szilard developed a hermetically sealed absorption refrigerator with no moving parts to significantly reduce the likelihood of leaks and therefore poisoning from the refrigerant. Their design was based on the absorption refrigerator designed by Platen and Munters which was originally patented in 1923. Both refrigerators use heat to cause vapour bubbles to move the solution from one part of the fridge to another, Einstein and Szilard call it a bubble pump whereas Platen and Munters call it a thermo-siphon and both use a

pressure equalising fluid. (Moss 1989) (Dannen 1995) (Munters and Platen 1928) (Einstein and Szilard 1930)

As with *ab*sorption, *ad*sorption refrigeration was developed from the mid-nineteenth to the early twentieth century, when it was overtaken by vapour compression systems. The first recorded discovery of an adsorption refrigeration system was from Faraday with ammonia onto silver chloride in 1848. For food storage in trains during the 1920's Hulse investigated a silica gel and sulphur dioxide system which would reach evaporation temperatures of -12°C. (Wang and Oliveira 2006) (Deng et al. 2011)

Solid desiccant cooling systems were introduced in the 1930s using lithium chloride to dehumidify air (Deng et al. 2011). A desiccant air conditioning system will typically dehumidify the air with a desiccant and then cool the air with a separate refrigeration cycle. This technique reduces the need to over cool the air, often required with other forms of refrigeration for air conditioning, to allow for temperatures low enough so that the moisture can condense out. The first desiccant air conditioning cycle was patented in 1955 by Pennington. It used a rotary desiccant wheel and its objective was to dehumidify air in summer and humidify air in winter (Pennington 1955). Until the mid 1980s most desiccant air conditioning systems were restricted to contamination controlled environments such as pharmaceutical, electronics and food manufacture. In these sectors the cost of the desiccant system was outweighed by the prevented loss of manufacturing output. Some liquid desiccant systems can sterilise and clean air which has made them useful for air conditioning of medical buildings. Since 1985 supermarkets started using desiccant cooling as the cost benefit of switching from electrical to thermal energy became favourable. (Mei et al. 1992)

The development of vapour compression systems has been largely dictated by environmental laws restricting the refrigerants that can be used, such as banning chlorofluorocarbons (CFCs) in 1987 (ESRL 2015) and more recent

restrictions on the use of hydrofluorocarbons (HFCs) (EEB 2015). There are continuous efforts to reduce the energy consumption of vapour compression refrigerators which is achieved through improvements in compressor technology, electric motors, insulation materials and heat exchangers. (Tassou et al. 2010)

As thermally activated refrigerators can be driven by a variety of heat sources their interest and development has followed a similar path to most sustainable technologies, i.e. it is proportional to the cost of energy with additional spikes of interest occurring when the competing technology is found to be harmful. Interest in thermally activated refrigeration technologies re-emerged during the oil crises of the 1970s and has continued with rising fuel and electricity prices. Interest also increased in the late 1920s and again in the late 1980s when the harmfulness of the refrigerants in vapour compression cycles came into the public's view. Moreover as sustainable operation is becoming more profitable, both from a cost saving and marketing perspective, industries are making better use of waste heat sources, which can be used for thermally activated refrigeration. Interest in the domestic market is also growing with the development of tri-generation technologies, where electricity, heating and cooling are provided by either combustion engines or solar power. (Deng et al. 2011), (Wang and Oliveira 2006) (Dannen 1995) (Jordan and Priester 1950), (Freidberg 2009) (Mathkor et al. 2015) (Agnew et al. 2015)

3.2 Review of Commonly Available Refrigeration Systems

The following section provides an explanation of the working principles of some of the commonly available refrigeration systems. The section concludes with an appraisal process to determine the most suitable refrigeration technology for waste heat utilisation in the context of the BioCPV power plant.

3.2.1 Vapour Compression

The vapour compression cycle which is also known as the reverse Rankine cycle uses mechanical power, often provided by electricity, to drive a compressor so that a refrigerant can absorb heat at a low pressure and temperature and then reject it at a high pressure and temperature. Figure 3.3 illustrates

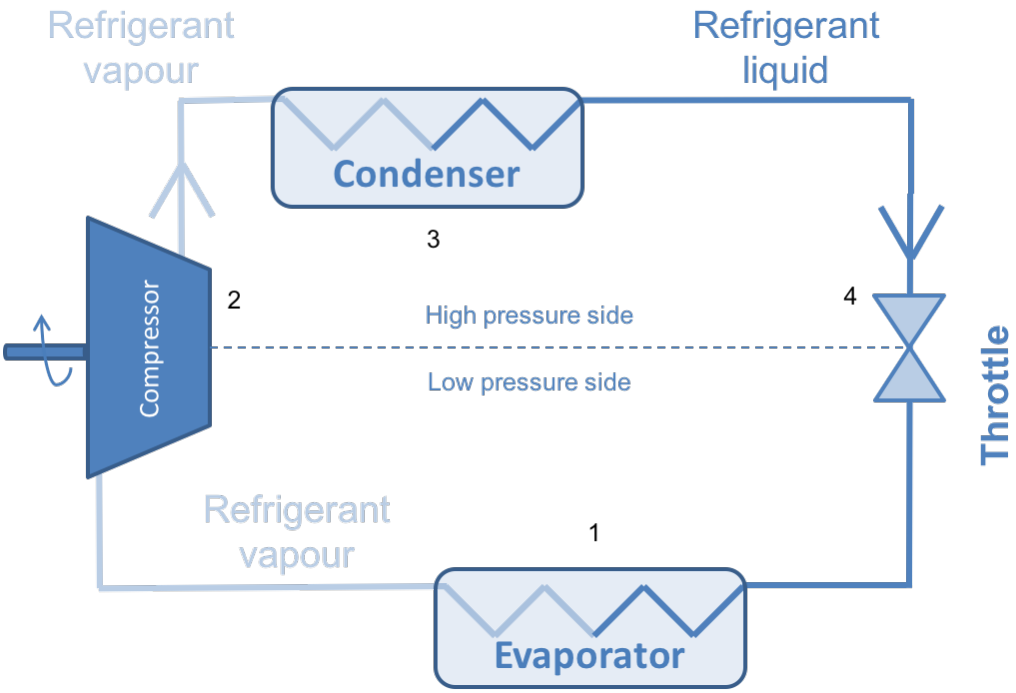

Figure 3.3: Schematic of a vapour compression refrigeration cycle.

the cycle. At position 1, the evaporator, the refrigerant enters as a liquid at low pressure and starts to evaporate absorbing heat from the space or object begin cooled. This absorption of heat and evaporation occurs because the low pressure side of the system has been designed to provide a saturation temperature for the desired refrigeration conditions. After leaving the evaporator the refrigerant vapour enters the compressor (2) where its pressure is raised so that the saturation temperature is above the ambient temperature. This results in the refrigerant vapour not being able to maintain its state and so it condenses back to a liquid in the condenser (3) rejecting the heat absorbed in the evaporator and compressor. The refrigerant liquid then passes through a throttle (4) which lowers the pressure so that the cycle can repeat when the refrigerant re-enters the evaporator (1). The throttle (4) and compressor (2) maintain the pressure difference between the high and low pressure sides. (Tassou et al. 2010) (Pita 1984)

3.2.2 Adsorption Refrigeration

Adsorption is the process whereby a substance is drawn on to the surface of another, usually in the form of a vapour 'sitting' on the surface of a solid. A common example is silica gel and water. This phenomenon coupled with thermal power can be used to drive a refrigeration circuit. The adsorber/desorber is usually a heat exchanger with the external surfaces covered in the adsorbent. In its simplest configuration the cycle is discontinuous.

Referring to Figure 3.4 the heat input causes desorption of the refrigerant in the adsorber/desorber (1). The refrigerant vapour passes through non-return valves (2, 4, 6 and 9) to prevent back-flow and resorption after each component. The refrigerant rejects its heat (gained from the adsorber/desorber) to the environment in the condenser (3), and is condensed back to a liquid. The refrigerant liquid is then stored in a reservoir (5) un-

til the heat source has expired. Once the adsorber/desorber (1) is cool, it provides a low pressure resulting from its ability to adsorb refrigerant. The refrigerant passes through a throttle to maintain the low pressure providing the necessary refrigeration temperature. The refrigerant then evaporates in the evaporator (8) drawing in heat and providing cooling. The refrigerant vapour is then adsorbed in the adsorber/desorber. The adsorber/desorber needs to have good heat transfer so that it can be cool during adsorption, which is exothermic, and be heated to provide desorption, which is endothermic. This can be challenging as adsorbents are typically powders, which as a result of the air gaps and small contact areas between particles generally have poor thermal conductivity. For example a silica gel adsorbent bed has a thermal conductivity of 0.17 $W \cdot m^{-1} \cdot K^{-1}$, though there are examples in the

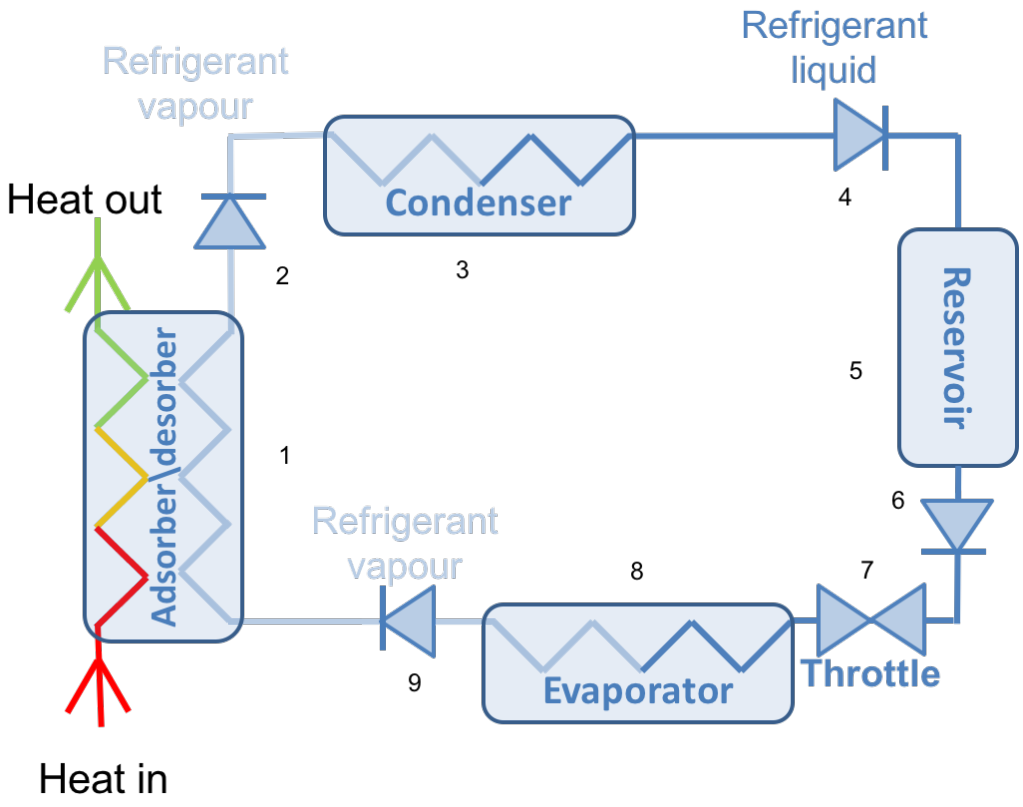

Figure 3.4: Schematic of an adsorption refrigeration system.

literature of 10 $W \cdot m^{-1} \cdot K^{-1}$ to 20 $W \cdot m^{-1} \cdot K^{-1}$ with composite blocks. (Wang and Oliveira 2006) (Deng et al. 2011) (Tassou et al. 2010)

3.2.3 Gas Cycle

The gas or reverse Brayton cycle, shown in Figure 3.5 operates with a refrigerant in the gas phase only, unlike vapour compression which operates in both the gas and liquid phase. It has the same components as a vapour compression system, however as the process occurs in the gas phase only the names used in multiphase refrigeration systems would be misleading. Therefore the evaporator becomes the expander and the condenser becomes a heat rejecter. These systems typically operate at very high pressures, in order to reject the heat absorbed in the expander. As the process is only in the gas phase the heat transfer is poor (in comparison to a phase change process) which tends to result in low coefficients of performance (CoPs). CoP, in terms of refrigeration, is the ratio of heat absorbed to provide cooling to

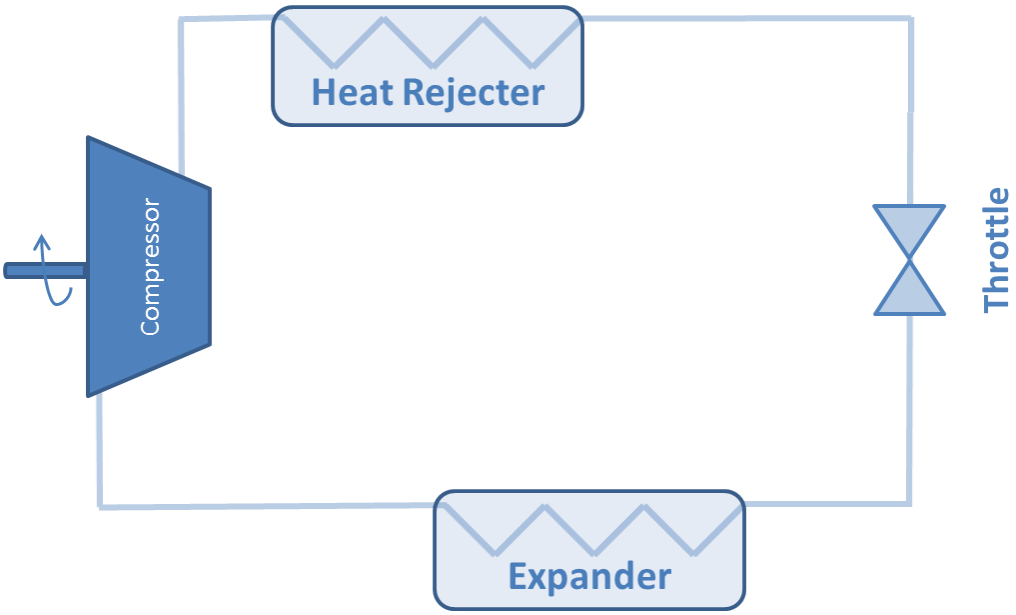

Figure 3.5: Schematic of a basic gas (or Reverse Brayton) cycle refrigerator.

the energy required to drive the refrigeration cycle. This can be improved with a cascading system where another refrigeration cycle is used to cool the heat rejection heat exchanger. They are often used to refrigerate to very low temperatures as the working pressures are not restricted to saturation conditions. (Deng et al. 2011) (Tassou et al. 2010) (Ge et al. 2009)

3.2.4 Absorption Refrigeration

Absorption is where one substance is drawn into another substance, for example the process of dissolving. Absorption refrigeration requires at least two substances (an absorbent and a refrigerant); the process of separating them, evaporating the refrigerant, and mixing them back together provides the refrigeration cycle.

Figure 3.6 illustrates this cycle; at position 1 heat is added to the boiler where it interacts with the high-in-refrigerant (weak) solution. The heat

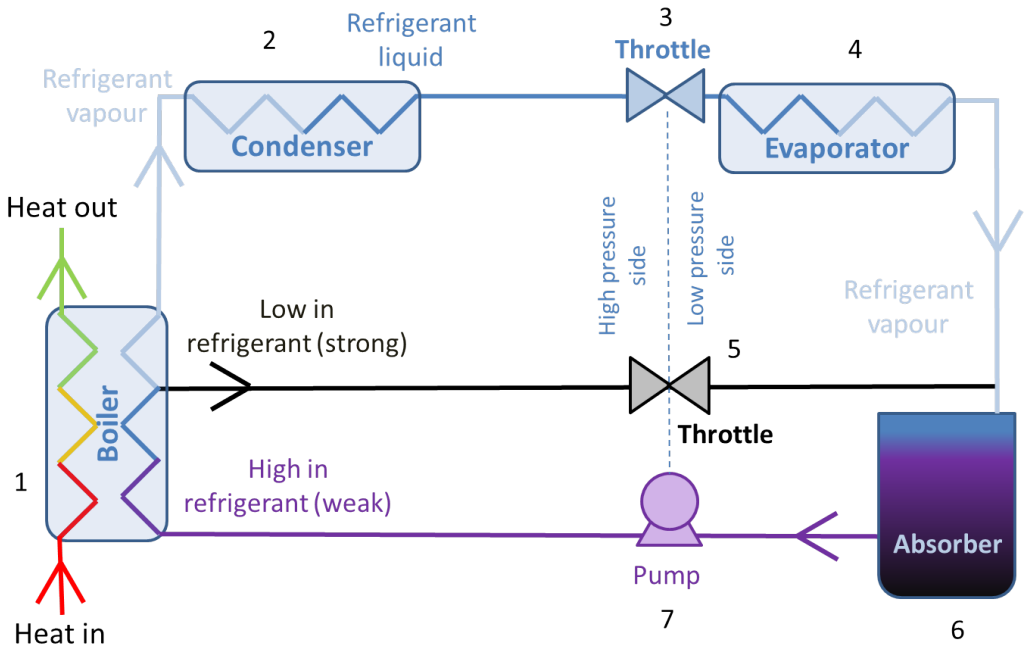

Figure 3.6: Schematic of a basic absorption refrigeration cycle

releases some of the refrigerant from the weak solution, leaving the low-in-refrigerant (strong) solution behind. The refrigerant vapour then enters the condenser (2) where the heat is removed (typically to the environment) and the refrigerant vapour condenses into a liquid. This liquid passes through a throttle (3) to maintain a pressure drop. The refrigerant then evaporates in the evaporator at a low pressure (and temperature) absorbing heat and providing the refrigeration effect. The refrigerant vapour leaving the evaporator (4) is absorbed into the strong solution from the boiler (1) in the absorber (6). Before reaching the absorber (6) the strong solution passes a throttle (5) to maintain the low pressure at the evaporator (4) and absorber (6). After the desired amount of refrigerant vapour has been absorbed into the strong solution the now weak solution is pumped (7) from the absorber (6) back to the boiler (1). (Herold 1996) (Deng et al. 2011) (Tassou et al. 2010)

3.2.5 Desiccant Cooling

Desiccant cooling is commonly used for air conditioning and can often be driven by low grade heat. The process separates latent and sensible cooling of air by using the desiccant to remove moisture before cooling the air (with another refrigeration method) to the desired temperature. The desiccant can either be a liquid or a solid. Liquid desiccants are used when it is simpler to move the desiccant to the heat source and solid desiccants can be used when the heat source can be moved to the desiccant. Solid desiccants tend to be in the form of powders in varying particle sizes and therefore often have poor heat transfer which can limit their application. Commonly used solid desiccant are: “silica, polymers, zeolites, alumina, hydratable salts and mixtures. Other available liquid desiccants are calcium chloride, lithium chloride, lithium bromide, tri-ethylene glycol, and a mixture of 50% calcium chloride and 50% lithium chloride” (Mohammad et al. 2013). Typical desic-

cant cooling systems are rotary wheels for solid desiccants and packed bed for both solid and liquid desiccants. All systems require a dehumidifier to absorb the moisture from the air and a regenerator (e.g. hot air) to remove the moisture from the desiccant. (Mei et al. 1992) (Pennington 1955)

3.2.6 Appraisal of Common Refrigeration Systems

This subsection provides a comparison of the refrigeration systems described earlier in this section to allow the selection of an appropriate technology for utilising low temperature discontinuous waste heat from distributed renewable power plants in rural India. The scale is 1 (undesirable) to 5 (desirable) and Applications refers to its applicability to rural India, HSE is Health Safety and Environmental considerations and Driving Energy refers to the versatility of the energy that powers the refrigeration system; in this study it is desirable to utilise low temperature (hence low quality) waste heat, therefore, 5 indicates low quality energy sources and 1 infers that the energy could be used for many applications e.g. electricity and work. Each factor investigated here was deemed to be of equal importance and therefore no weighting was applied.

The decision matrix in Table 3.1 finds that of the refrigeration technologies examined absorption, adsorption and desiccant cooling had a driving energy score of 5 as all of these can make use of low temperature waste heat. Desiccant cooling has an applications score of 1 as it is limited to air conditioning and requires a further cooling system. Absorption has greater potential for a variety of cooling applications than adsorption, shown by the application score of 3 in comparison to 1 respectively. Desiccant cooling, absorption and adsorption all score 4 for HSE though all of these technologies have a wide range of fluid choices with varying levels of HSE considerations. Both adsorption and solid desiccant systems are often powders which typi-

cally have poor thermal conductivity, which may be problematic in terms of removing waste heat from the source effectively.

This research is focussed on utilising waste heat sources from a discontinuous renewable electricity generation plant in rural India, where the waste heat is part of a cooling system for the components in the power plant. Therefore good heat transfer is important to ensure efficient operation of the components, ruling out solid desiccants and adsorption technologies. The variety of refrigeration applications is greater for absorption than liquid desiccant systems, scoring 4 and 1 respectively, resulting in the selected technology to investigate low temperature waste heat utilisation being absorption refrigeration.

Table 3.1: Appraisal and decision matrix of refrigeration technologies for their application in using low grade discontinuous waste heat in rural India, where 5 is desirable and 1 is undesirable.

Refrigeration Type	Description	Applications	HSE	Driving Energy	Total Score
Vapour Compression	One fluid system comprising of: evaporator, condenser, throttle and compressor. Uses saturation conditions and mechanical compression to move heat	Chilled and frozen food storage, cryogenic, air conditioning	Depends on refrigerants HFC, CFC, HCFC all have high global warming potential, others are: toxic and flammable or at very high pressures	Mechanical to drive the compressor, electricity in most cases	7
Score		5	1	1	
Adsorption	Two fluid system comprising of a refrigerant and adsorbent (can be either solid or liquid). Typically discontinuous, comprising of: Adsorber/desorber condenser, throttle, evaporator, reservoir and non-return valves between components. Uses saturation conditions and chemical compression to move heat	Air conditioning and chilled food storage	Depends on refrigerant-adsorbent pair some are harmless; most have no global warming potential; some are: irritants, flammable and toxic	Heat, temperature depends on refrigerant and adsorbent pair, min 60°C	12
Score		3	4	5	
Gas (Reverse Brayton)	One fluid system comprising of: compressor, expander, heat rejecter and a throttle. Uses mechanical compression in gas phase only to move heat	Industrial frozen food storage and cryogenics	High pressure	Mechanical to drive the compressor, electricity in most cases	6
Score		2	3	1	
Absorption	Two or more fluid system (refrigerant and absorbent) comprising of: evaporator, absorber, boiler, condenser, pump and (at least) two throttles. Uses saturation conditions and chemical compression to move heat	Domestic and industrial chilled (and in some cases frozen) food storage, air conditioning	Depends on refrigerant-absorbent pair, most have no global warming potential; some are harmless; some are: caustic, toxic, flammable, irritants and harmful to aquatic systems	Heat, depends on the choice of refrigerant and absorbent, min 50°C	13
Score		4	4	5	
Desiccant	Water vapour removed from air with desiccant before using another form of refrigeration, removing the need for latent cooling	Air conditioning and air purification	Some desiccants are corrosive, and/ or harmful to aquatic systems. Most will cause irritation	Low temperature heat for dehumidification, for cooling it depends on the refrigeration technology	10
Score		1	4	5	

3.3 Detailed Review of Absorption Refrigeration

Vapour absorption technology has been established for almost 200 years, however, as already mentioned, due to cheap and reliable electricity vapour compression refrigerators became more widespread. Therefore research has not been continuous and has been instigated by: oil crises, rising fuel prices and environmental concerns pushing more efficient use of energy sources. (Deng et al. 2011)

To the present day research is being conducted to find optimal working fluid combinations by either finding new combinations (Jelinek and Borde 1998) (Zohar et al. 2009) (Zacarías et al. 2011) or through using additives and surfactants to commonly used working fluids (Saravanan and Maiya 1998) (J. K. Kim et al. 2007). New configurations of refrigerator are being developed to utilise a wider variety of energy sources such as multiple effect systems (Deng et al. 2011), hybrids (J. Jeong et al. 2011), co-generation (Hua et al. 2014) and tri-generation (Mathkor et al. 2015). Others have been developing specific components of the refrigerator most commonly the absorber (Xie et al. 2012) (Tae Kang et al. 2000) (Zacarías et al. 2011). Many predictive models for specific components (Sieres and Fernández-Seara 2007) (Tae Kang et al. 2000) and entire systems (D. S. Kim and Infante Ferreira 2009) (J. Jeong et al. 2011) have been developed. There are also continuing efforts to model and verify the thermodynamic properties of the working fluids (Pátek and Klomfar 2006) (Ajib and Karno 2008).

Several manufacturers offer industrial scale absorption refrigerators which can be powered by a fuel source or waste heat such as York, Carrier, Mitsubishi and Thermax India. Absorption refrigerators are also available on a domestic scale and mostly used in motorhomes and environments where either silent operation is desirable or electricity is not available. There is

also interest in domestic absorption refrigeration systems for air conditioning as part of a tri-generation system, where heating, cooling and electricity is provided by one system (Deng et al. 2011) (Tassou et al. 2010).

This section contains:

- **Challenges of Absorption Refrigeration** a description of the overarching challenge of absorption refrigeration.
- **Fluids** the working fluids used in absorption refrigeration systems
- **System Configurations** a selection of system configurations investigated up to the present day and an appraisal process to determine suitability for the conditions expected from the BioCPV system.
- **Conclusions** concludes the main findings of this review and the appraisal processes.

3.3.1 Challenges of Absorption Refrigeration

Absorption refrigerators rely on a delicate balance of solution concentrations and solution temperatures. These decide how much refrigerant can be contained within the solution and, assuming perfect mass transfer, ultimately determine the saturation conditions of the pure refrigerant. The greater the capacity of the solution to hold refrigerant the lower the vapour pressure as the solution is providing a sucking force for the refrigerant vapour to be absorbed. This is achieved with low-in-refrigerant (strong) solution concentrations and cold temperatures. A strong solution concentration causes little refrigerant to be available and the low temperature results in the refrigerant not having enough energy to leave the surface of the solution. Conversely weak solution concentrations and high temperatures provide a large quantity of refrigerant with enough energy to leave the surface of the solution resulting in high pressures. The pressure caused by the solution concentration and its

temperature determine the saturation conditions of the pure refrigerant in the condenser and evaporator, especially when a salt is used as the absorbent as the vapour will only contain refrigerant.

However the condenser temperature is usually limited by the temperature of the cold reservoir (plus a few degrees for heat transfer), e.g. ambient air, rivers, lakes, etc. The evaporator temperature is often limited by the application e.g. air conditioning, short or long term food storage and their related temperature requirement. Moreover it is the exit conditions of the solution leaving the boiler and absorber that determine the operating pressures and therefore limiting temperatures of the condenser and evaporator respectively. Which means; the strong solution concentration and the boiler temperature determine the maximum condenser temperature. The weak solution concentration and the absorber temperature determines the minimum evaporator temperature. However high condenser temperatures are desirable as it allows smaller heat exchangers, choice over the cooling fluid and whether passive or active cooling is used. Low evaporator temperatures are desirable as they are more versatile.

This creates a conflict; dilute strong solution concentrations are desirable for high condenser temperatures whereas concentrated weak solution concentrations are desirable for low evaporator temperatures. Yet the strong solution concentration has to be more concentrated than the weak solution, by definition. Moreover the difference in solution concentrations is proportional to the mass ratio of working refrigerant to total solution. The working refrigerant is the refrigerant that goes through the condenser and evaporator and is responsible for providing the refrigeration effect in the evaporator. Therefore it will be more efficient if the heat source is used to separate more refrigerant from solution rather than heating a large amount of solution to provide little working refrigerant.

The challenge in summary:

By definition,

$$X_{SS} > X_{WS} \tag{3.1}$$

Where X_{WS} is weak solution concentration, X_{SS} is strong solution concentration and solution concentration is defined as $\frac{m_{absorbent}}{m_{solution}}$.

And

$$m_{WS} = m_{SS} + m_R \tag{3.2}$$

Where m_{WS} is mass of weak solution, m_{SS} is mass of strong solution and m_R the mass of the working refrigerant or the refrigerant that is used in the evaporator and condenser.

However a high condenser temperature (T_{CO}) is desirable but is proportional to the strong solution concentration (X_{SS}), and the boiler temperature (T_{BO}).

$$T_{CO} \propto f(X_{SS}, T_{BO}) \tag{3.3}$$

Yet a low evaporator temperature is desirable but is proportional to the weak solution concentration (X_{WS}), and absorber temperature (T_{AB}).

$$T_{EV} \propto f(X_{WS}, T_{AB}) \tag{3.4}$$

To add further complication, the difference in solution concentrations is proportional to the ratio of working refrigerant; which is the refrigerant that goes through the evaporator, (m_R) to weak solution (m_{WS}).

$$X_{XS} - X_{WS} \propto \frac{m_R}{m_{WS}} \tag{3.5}$$

This ratio affects the coefficient of performance (CoP) of the refrigerator as it relates the amount of heat that is used in generating the working refrigerant to the amount of heat used to warm the solution, and the quantity of working refrigerant determines how much cooling can be provided.

$$\frac{m_R}{m_{WS}} \propto CoP \tag{3.6}$$

3.3.2 Fluids

The fluids for absorption refrigerators can be split into two main categories: two fluid systems such as a lithium bromide and water refrigerator and three fluid systems such as the Platen-Munters and Einstein-Szilard refrigerators. However, rather confusingly, the two fluid system category includes additives which can bring the number of fluids in the system above two. To eliminate this confusion, three fluid systems are referred to as systems with a pressure equalising fluid and two fluid systems are those without. A pressure equalising fluid is an auxiliary gas providing pressure equalisation for the working refrigerant between the condenser and evaporator in the Platen-Munters and Einstein-Szilard style refrigerators. (Herold 1996)

Eames and Wu (2003) and Saravanan and Maiya (1998) suggest that the presence of the pressure equalising fluid reduces mass transfer as it provides additional resistance and is responsible for the low CoPs of systems with a pressure equalising fluid. This may explain why there is considerably more research available on systems without. An example of the low CoP achieved from systems with a pressure equalising fluid is found in research by Delano (1998) using isobutene-ammonia-water, butane-ammonia-water, neopentane-ammonia-water, pentane-ammonia-water and butane-hydrogen chloride-water. The highest CoP achieved was 0.225 with isobutene-ammonia-water, which he discusses is largely due to the high ratio of refrigerant to solution and the small temperature difference with the absorber/condenser and evaporator temperatures.

Zohar et al. (2009) investigated the following refrigerants with an organic absorbent (DMAC - dimethylacetamide) and helium as the pressure equalising inert gas. The following refrigerants were investigated: R22 (chlorodifluoromethane), R32 (difluoromethane), R124 (1-chloro-1,2,2,2-tetrafluoroethane), R125 (pentafluoroethane) and R134a (1,1,1,2-tetrafluoroethane). As with

Delano (1998) the CoPs were low, under 0.24. Boiler temperatures ranged from 135°C to 160°C, condenser temperatures 33°C to 43°C and evaporator temperatures −9°C to 6°C. (Zohar et al. 2009)

The opinions of Eames and Wu (2003) and Saravanan and Maiya (1998) together with the results from Delano (1998) and Zohar et al. (2009) indicate that systems with a pressure equalising fluid are not as effective at converting a heat source into refrigeration when compared with systems that do not require a pressure equalising fluid. Deng et al. (2011), González-Gil et al. (2011), Balghouthi et al. (2012), Jelinek, Levy, et al. (2002), Jelinek and Borde (1998), state CoPs in the range of 0.2 to 1.7, depending on the fluid choice and system configuration, are achievable from systems that do not require a pressure equalising fluid.

The category of fluid systems that do not require a pressure equalising fluid can be split into two distinct groups: those requiring rectification (the process of separating one fluid from another, in the vapour phase, when they both follow Dalton's Law) and those that do not. Systems where the absorbent and refrigerant have close (less than 200°C) boiling temperatures, typically when the absorbent is a liquid, tend to need rectification as there will be a proportion of the absorbent in the refrigerant vapour leaving the boiler. If the absorbent vapour is not removed (or at least reduced in proportion) from the refrigerant vapour it reduces the volatility of the working refrigerant (as it is a mixture) which results in less heat being absorbed in the evaporator (the refrigeration effect) and therefore reduces the performance of the refrigerator. The most common fluid pair which requires rectification is ammonia and water; according to Deng et al. (2011) these systems can provide cooling temperatures of -60°C to 10°C and have CoPs from 0.25 to 1.2 depending on system configuration.

Systems that do not require rectification typically use a salt for the absorbent, as salts generally have high boiling temperatures in comparison to

the refrigerants used and are therefore not volatile. The most common fluid pair in this category is water and lithium bromide. All systems where pure water (i.e. without additives) is used as the refrigerant are limited to cooling temperatures above 0°C due to the water freezing in the evaporator and blocking it at sub zero temperatures. Deng et al. (2011) suggests that CoPs of lithium bromide-water systems are 0.5 to 1.7 depending on system configuration. This slight increase in CoP compared with water and ammonia systems is likely to be a result of not requiring rectification as well as typically higher evaporator temperatures causing a smaller temperature difference between condenser/absorber and evaporator due to using water as a refrigerant.

Sun et al. (2012) provides an extensive review of the various working fluids for absorption refrigeration, where acetone and zinc bromide seem to operate at the lowest boiler temperatures. The acetone and zinc bromide system described by Sun et al. (2012) has been proven to work with low temperature heat sources by Karno and Ajib (2008), with reports of an experimental CoP of 0.4 and theoretical of 0.6 from a heat source below 60°C. Acetone has a melting point of -94.6°C (Lide 2004) and therefore has the potential to provide sub 0°C cooling temperatures when used as a refrigerant. Zinc bromide has a boiling point of 650°C (Lide 2004) and is not volatile; it will therefore not be a constituent of the vapour released from the boiler temperatures investigated in this thesis and will not need rectification. Acetone and zinc bromide are therefore the fluid pair chosen for investigation in this thesis.

3.3.3 System Configurations to Maximise Heat Utilisation

Several different configurations of absorption refrigeration have been investigated in the literature for a variety of applications. The following review of cycle configurations has a greater focus on systems that can use discontinu-

ous low temperature heat sources, such as those found in the rural renewable electricity plant defined in Chapter 2. If the focus is on system simplicity and using low grade heat sources (<100°C) then single effect cycles are useful. Multiple effect cycles can be used for higher grade heat sources, though the system complexity increases. When high utilisation of the heat source is important then configurations that allow preheating of the weak solution into the boiler such as boiler heat recovery can be used. When high utilisation of the waste heat generated in the refrigerator is important then boiler-absorber heat exchanger (BAX) also known as generator-absorber heat exchanger (GAX) and desorber/absorber heat exchanger (DAHX) is used. Conversely when evaporator temperatures are important, for example refrigeration of food, then configurations that provide cooling of the absorber are used such as: Coupled cycle and evaporator tap-off. And, if utilising waste heat at temperatures too low to drive a single effect cycle then the half effect cycle can be used. The following subsections provide an overview of these configurations, their applications and merits.

Boiler Absorber Heat Exchanger (BAX)

The boiler absorber heat exchanger (BAX) or generator absorber heat exchanger (GAX) or desorber/absorber heat exchanger (DAHX), depicted in Figure 3.7, utilises the rejected heat from the absorber to drive off refrigerant from the weak solution before the main heat source in the boiler completes the desorbing process. As the absorber waste heat is reused for latent heating of the high-in-refrigerant solution, the heating process has to take place in the boiler as the refrigerant vapour needs to be removed from the solution. (Srikhirin et al. 2001)

Boiler Heat Recovery

The boiler heat recovery configuration (known as absorber heat recovery configuration by Srikhirin et al. (2001)), shown in Figure 3.8, uses the warm low-in-refrigerant solution from the boiler to preheat the high-in-refrigerant solution entering the boiler after leaving the absorber. This is a sensible heating process and therefore does not need to occur inside the boiler as no separation of refrigerant from solution occurs.

Half Effect

The half effect cycle allows an absorption refrigerator to operate from boiler temperatures that would otherwise be too low for a single effect cycle. The effect of a low boiler temperature is that either the condenser temperature would need to be very low or the evaporator temperature very high, both of which are undesirable; the theory of this is explained in Section 3.3.1. This

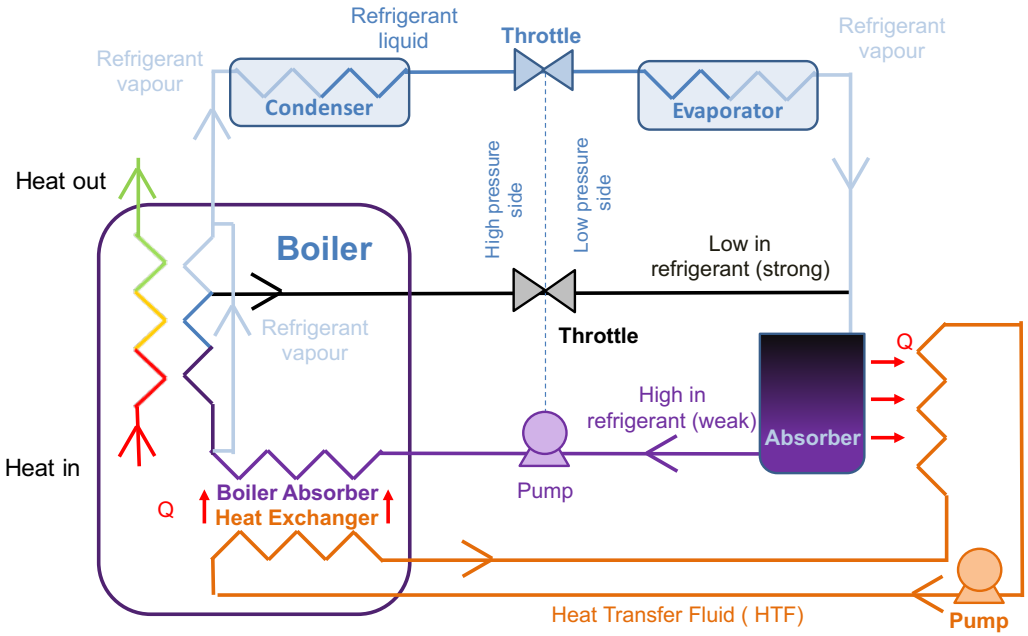

Figure 3.7: Schematic of the boiler absorber heat exchanger (BAX) cycle on a single effect cycle.

cycle is achieved by splitting the heat source over two boilers. One with a high-in-refrigerant solution strong enough to create the low pressure for a low evaporator temperature. The other to provide a low-in-refrigerant solution weak enough to create the high pressure for a usable condenser temperature. (Herold 1996)

Referring to Figure 3.9 the heat enters the system at 1. It is split across the intermediate pressure boiler (2) and the high pressure boiler (6). The refrigerant vapour released from the intermediate pressure boiler (2) is then absorbed by the low-in-refrigerant solution leaving the high pressure boiler (6) in the intermediate pressure absorber (3). This ensures that the low-in-refrigerant solution leaving the high pressure boiler (6) is weak enough to provide a usable condenser temperature. The pressure in the intermediate pressure absorber is maintained by the throttle (4). The refrigerant vapour leaving the high pressure boiler (6) is then condensed in the condenser (7).

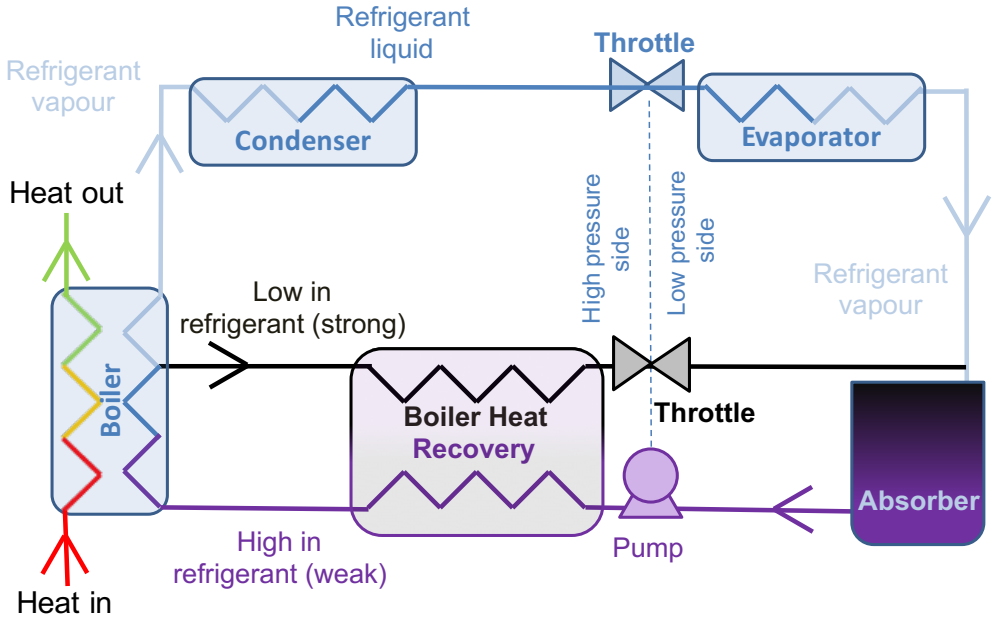

Figure 3.8: Schematic of the boiler heat recovery cycle on a single effect cycle.

It then passes through a throttle (8) which maintains the pressure difference between the high and low pressure sides. As the refrigerant enters the low pressure side and the evaporator (9) it draws in heat and evaporates providing the refrigeration effect. The refrigerant vapour is then absorbed in the low pressure absorber (10) into the low-in-refrigerant solution from the intermediate pressure boiler (2). The throttle (11) for the low-in-refrigerant solution from the intermediate pressure boiler (2) helps maintain the pressure

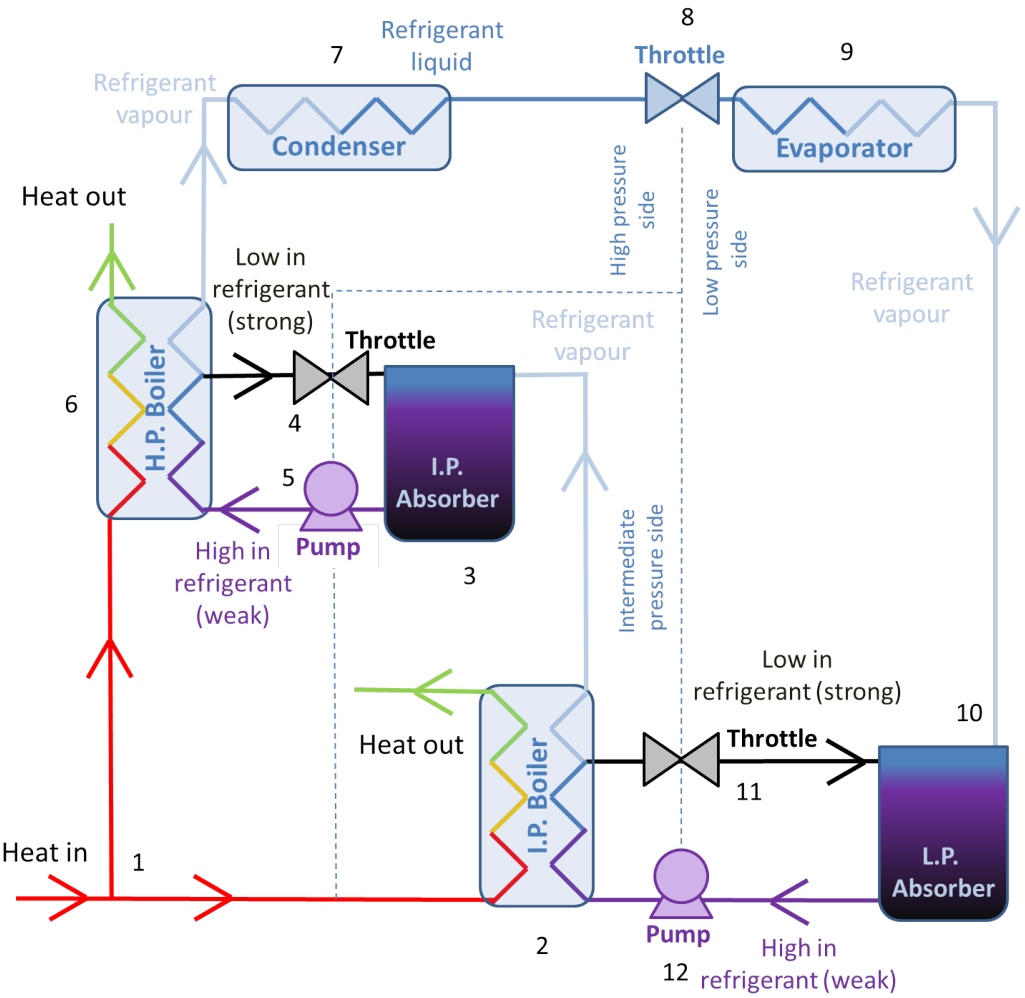

Figure 3.9: Schematic of half effect cycle, which can operate with low boiler temperatures at the expense of some of the energy input, where L.P, I.P. and H.P. are low pressure, intermediate pressure and high pressure respectively.

difference between the intermediate and low pressure sides of the refrigerator.

By operating at three different pressure levels and four different solution concentrations the half effect cycle allows an absorption refrigerator to be driven by a boiler temperature that would otherwise be too low. There is a thermodynamic penalty for this; the heat that is used in the intermediate pressure boiler has little energetic effect on the useful output of the refrigerator (heat that can be absorbed by the evaporator). This is because the vapour that is released at the intermediate pressure (I.P.) boiler is reabsorbed before being used as a working refrigerant. It therefore results in a low CoP in terms of energy. However the ability to use low temperature heat may be advantageous in terms of exergy.

Dual Cycle

The dual cycle as described by Srikhirin et al. (2001) cascades the input heat through two absorption refrigerators. The heat is used to drive a standard single effect cycle, while the rejected heat from the condenser and absorber is used to drive another cycle. This system tends to be used with different working fluids and concentrations in each refrigerator.

3.3.4 System Configurations to Utilise Discontinuous Heat Sources

Said et al. (2012) describe the possible configurations for providing continuous cooling through absorption refrigeration from solar power (a discontinuous heat source). The three main options are:

Hot storage

The heat from the heat source is stored and is released at the required rate to power the refrigerator, for example insulated hot water tanks, phase changing materials and thermal mass.

Cold storage

The cooling output of the refrigerator is stored, this could be in the form of ice blocks or any working fluid stored in an insulated vessel.

Refrigerant storage

This is where the refrigerant is stored after condensing back to a liquid. It also requires the low-in-refrigerant solution to be stored between the boiler and absorber, as well as the weak solution between the absorber and boiler. If condensing occurs at or above ambient temperature the refrigerant will not require any insulation. Similarly, as the low-in-refrigerant solution temperature is high as it leaves the boiler, it too will benefit from cooling to ambient as less energy will have to be removed from the absorber to maintain the desired evaporator temperature. This is described as chemical storage by Herold (1996).

Only a few details about the simulation method are presented and the heat source used by Said et al. (2012) was at 120°C. The CoP for refrigerant storage was reported to be 0.427 compared to cold storage at 0.372 and hot storage at 0.434. Due to the desire to use low temperature heat sources (<100°C) in this thesis and the high ambient temperatures in rural India, the refrigerant storage method is more suitable, as it should not degrade the temperature of the heat source or cold generated as much as the other methods.

Ammar, Joyce, et al. (2012) have investigated a similar system to the refrigerant storage method proposed by Said et al. (2012) across large areas to connect waste heat from the process industry to users requiring heating or cooling. This type of absorption system uses the waste heat source for the boiler process; after which, providing that condensing occurs at (or above) ambient temperature, the condensed refrigerant can be moved across large distances without any concern for insulation. Likewise the strong and weak

solutions, providing they transfer their respective thermal energy near to the source or user, can also be transported with little consideration for insulation. Ammar, Joyce, et al. (2012) found an economic distance of 30 km for heating and 27 km for cooling from an 80°C heat source using an ammonia and water absorption refrigeration system. "The economic distance here refers to the length of system corresponding to an investment for a payback period of three years". (Ammar, Chen, et al. 2011)

Single Effect Cycle with Reservoirs

The single effect cycle with reservoirs configuration shown in Figure 3.10 uses the refrigerant storage method described by Said et al. (2012) and Herold (1996) so that discontinuous heat sources can provide continuous refrigeration. Multiple single effect cycles can be considered when there is more than one heat source and the distance between the heat sources is uneconomical

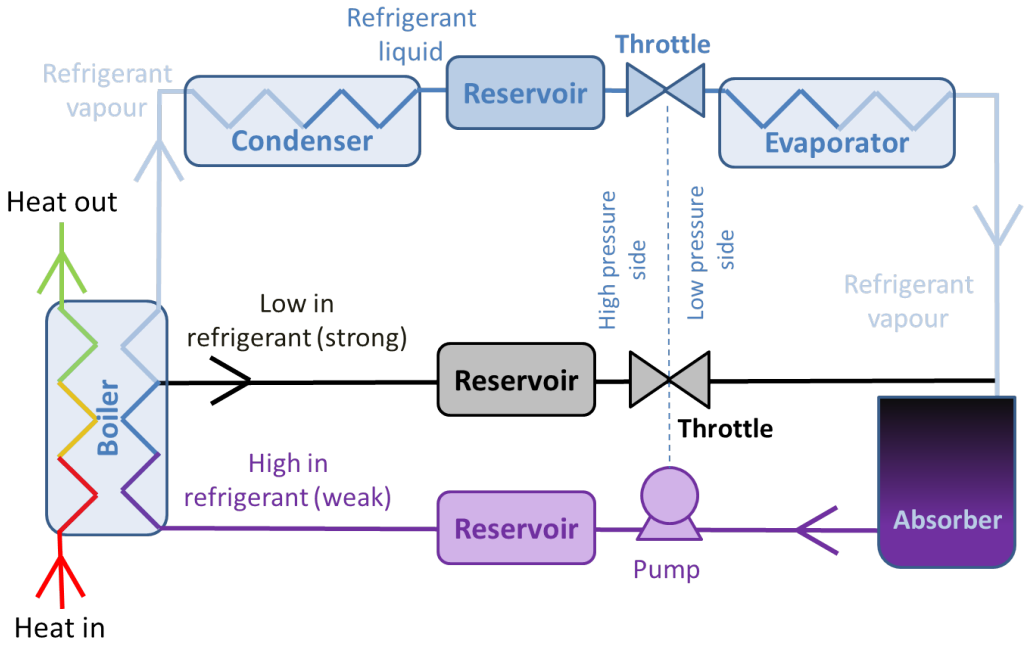

Figure 3.10: Single effect with reservoirs to allow for continuous cooling from discontinuous heat sources.

to warrant one of the other cycles described in this section. If desired this cycle can be improved with either or both the heat utilisation configurations in Section 3.3.3 and the lowering evaporator temperature configurations described in Section 3.3.5.

Double Boiler with Reservoirs

The double boiler cycle in Figure 3.11 is similar to the single effect cycle except it uses two heat sources. This cycle differs from the half effect cycle as it does not have an intentional intermediate pressure, though different pressures may occur if the heat sources are at different temperatures which may add a control requirement. The reservoirs act in the same way as in the

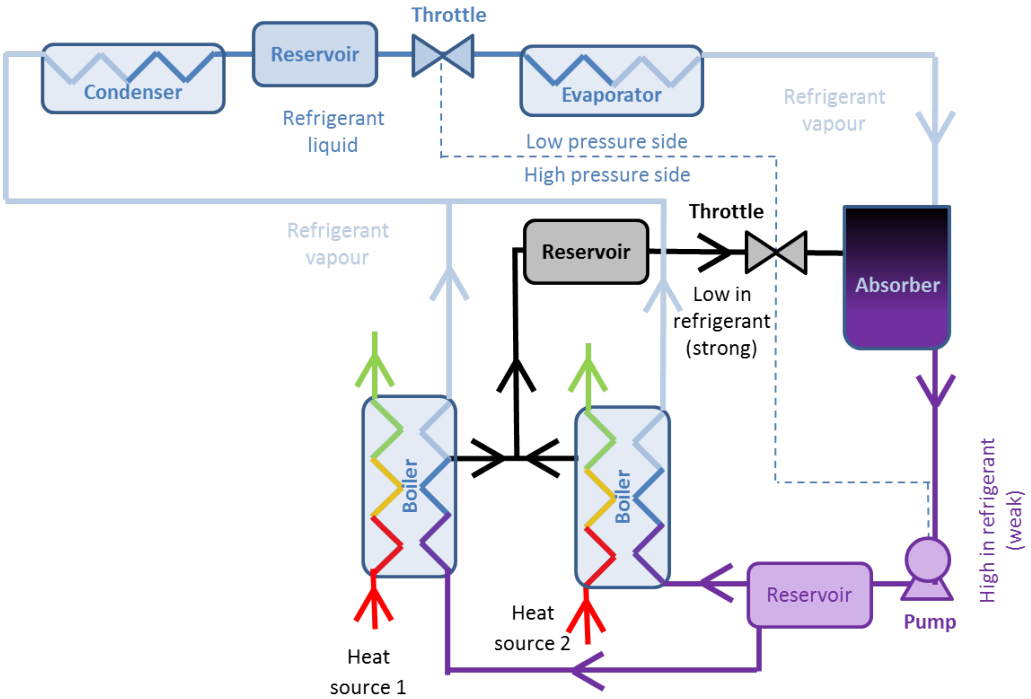

Figure 3.11: Double boiler cycle schematic; showing one absorption refrigerator powered by two discontinuous heat sources through two separate boilers with reservoirs to allow for continuous cooling from discontinuous heat sources.

single effect cycle with reservoirs cycle allowing continuous refrigeration from discontinuous heat sources, with the advantage that in this system multiple heat sources can be used.

3.3.5 System Configurations to Reduce the Evaporator Temperature

For all refrigeration systems the evaporator temperature determines the appropriate applications. With absorption refrigerators there are two main strategies to manipulate evaporator temperature: control absorber temperature and / or control solution concentration.

Control of the solution concentration is limited by the condenser temperature and the crystallisation limit (conditions where salt crystals form in the solution, typically before the absorber). The crystallisation limit can be reduced by increasing operating temperatures, though the crystallisation limit should generally be avoided to prevent unexpected blockages and therefore operation close to it will not be considered in this thesis. However, configurations using the idea of the half effect cycle can provide condenser temperatures and evaporator temperatures that would not be possible with a single effect cycle. The alternative is actively cooling the condenser, through using some of the heat absorbing potential of the evaporator (evaporator tap-off or coupled cycle) or by an external cold sink, such as: a river, lake or sea to improve heat transfer over basic ambient air cooling.

The absorber temperature can be controlled by active cooling such as: the external cold sinks mentioned in this section, coupled cycle and evaporator tap-off. It can also be controlled through the physical design to increase heat and mass transfer such as: adiabatic absorbers (Zacarías et al. 2011), falling film absorbers (Tae Kang et al. 2000), (Castro et al. 2009), (D. S. Kim and

Infante Ferreira 2009) and bubble absorbers (Tae Kang et al. 2000), (Castro et al. 2009).

The following subsection only describes the potential system configurations for reducing evaporator temperatures and not the specifics of absorber design as it is outside of the scope of this research. Moreover the configurations are focused on adaptations of the refrigerant storage method described by Said et al. (2012) and not the hot and cold storage method. Though the other methods are possible with a heat transfer fluid this research is focussed on using low temperature heat in a high temperature environment and the process of storing the heat or cold would degrade their temperatures as a result of heat transfer losses and the limits of insulation, whereas the refrigerant storage method does not.

The approach discussed later uses a proportion of the heat absorbing potential of the evaporator to cool either or both the condenser and absorber of the refrigerator. Both of which can lower the evaporator temperature. As cooling the condenser allows a stronger low-in-refrigerant solution concentration, which enables a stronger high-in-refrigerant solution concentration, which results in lower absorber and therefore evaporator pressures. Likewise cooling the absorber also lowers the evaporator pressure. This can be achieved through the evaporator tap-off technique or using an independent refrigerator to cool the absorber and / or condenser of another such as the coupled cycle. The following cycles have been influenced by the literature presented here however they are the ideas developed in this thesis.

Evaporator Tap-Off

The evaporator tap-off method thermally couples the evaporator to the condenser and / or absorber. This can be achieved through direct coupling where some or all of the evaporator heat exchanger is in direct contact with

or built into the absorber and / or condenser heat exchangers. Or an indirect method such as a heat transfer fluid can be used as shown in Figure 3.12.

Figure 3.12 shows how heat can be transferred from the condenser and absorber to the heat transfer fluid. The heat transfer fluid then rejects as much heat as possible to the environment in the ambient heat dump and is then further cooled by rejecting heat to the evaporator. The cold heat transfer fluid then flows back to the absorber and condenser. The flow rates can be controlled through the use of valves.

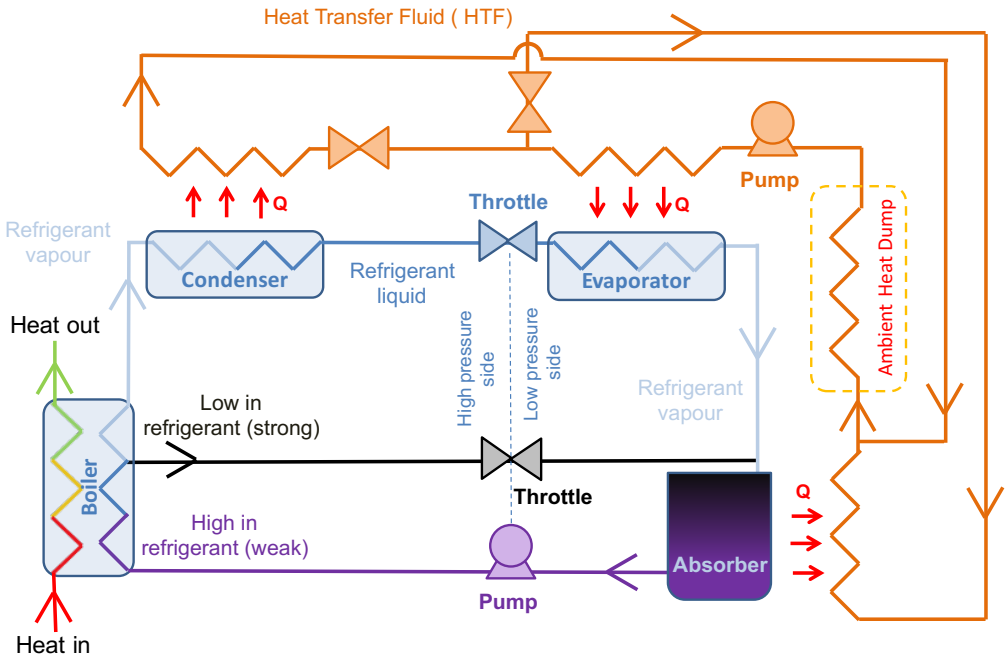

Figure 3.12: Single effect cycle with evaporator tap-off schematic; where the thermal coupling is shown as a heat transfer fluid (orange section).

Coupled Cycle

The coupled cycle refrigerator in Figure 3.13 consists of two refrigerators powered by two separate heat sources. It uses one refrigerator to cool either or both the condenser and absorber of the other refrigerator. As with the evaporator tap-off method it can be achieved either through a heat transfer fluid as shown by the orange section of Figure 3.13 or through direct thermal coupling. This cycle allows each refrigerator to have different solution concentrations to each other, which could lead to greater optimisation opportunities.

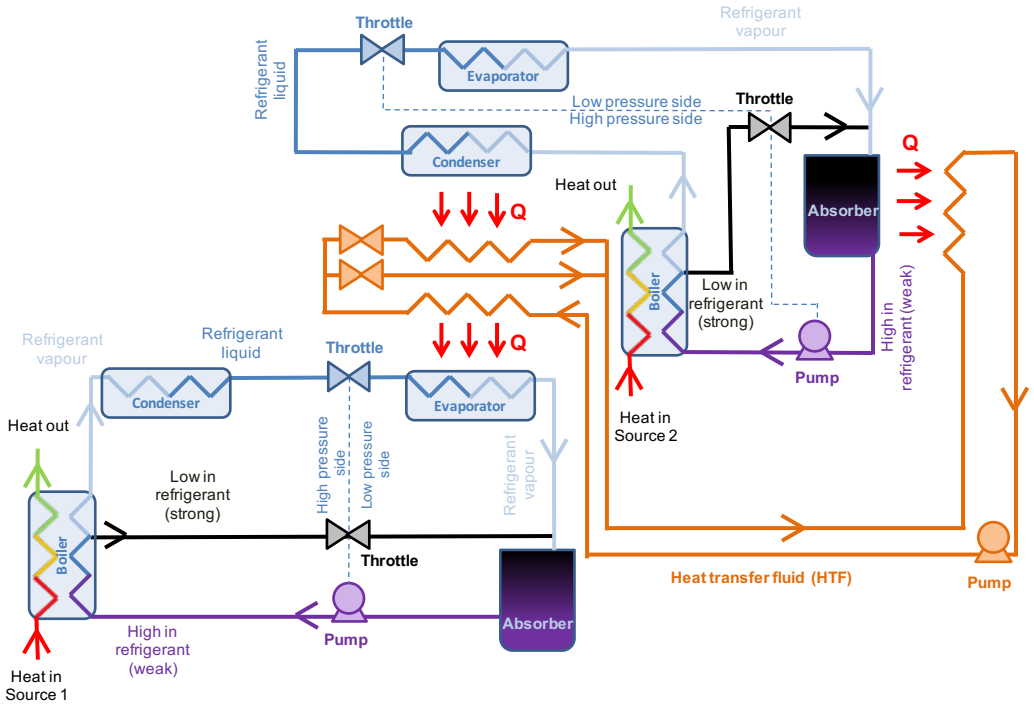

Figure 3.13: Coupled cycle schematic; where two absorption refrigerators are powered by two separate heat sources and are thermally coupled between the evaporator of one and the absorber and condenser of the other. The thermal coupling is illustrated as a heat transfer fluid (orange section).

3.3.6 Using Discontinuous Heat Sources and Controlling Evaporator Temperature

The concepts already mentioned to utilise discontinuous heat sources and control evaporator temperature can be combined creating the following cycles:

Single Effect with Reservoirs and Evaporator Tap-Off

The single effect with reservoirs and evaporator tap-off combines the concepts in Sections 3.3.4 and 3.3.5 to allow both continuous cooling from discontinuous heat sources and control over the evaporator temperature. This is achieved through reservoirs to store the solutions and refrigerant between

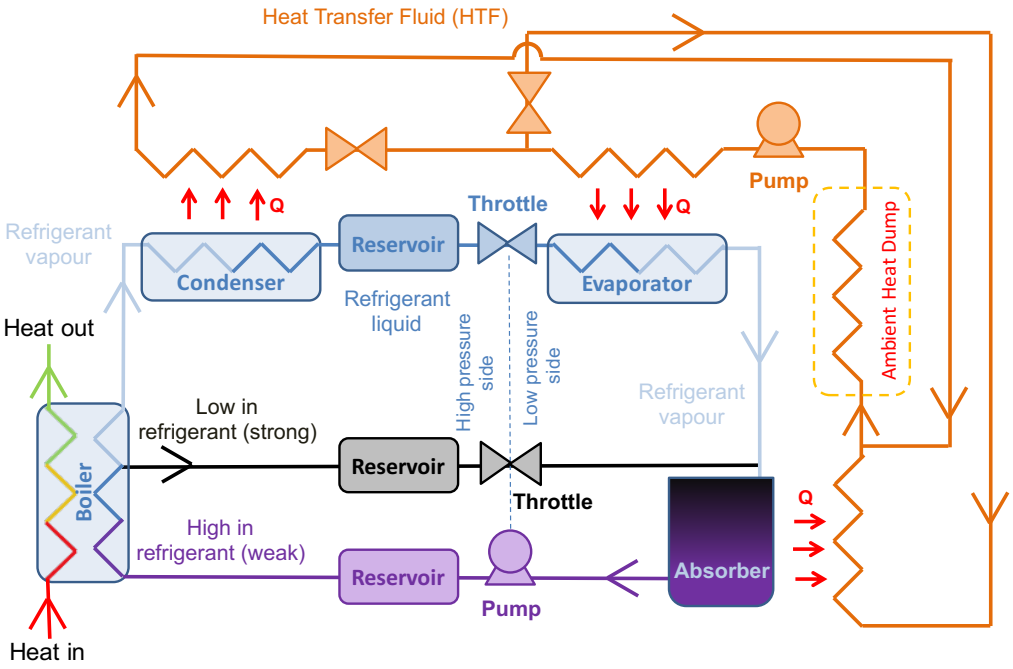

Figure 3.14: Single effect cycle with reservoirs and evaporator tap-off. This cycle allows both continuous refrigeration from discontinuous heat sources and control over the evaporator temperature. The thermal coupling is illustrated as a heat transfer fluid (orange section).

components and a heat transfer fluid (as shown in Figure 3.14) or through direct coupling of the evaporator to the absorber and / or condenser (not shown in the diagram).

Coupled Cycle with Reservoirs

The coupled cycle also described in Section 3.3.5 can be combined with the refrigerant storage method to provide continuous cooling from discontinuous heat sources. This cycle allows both heat sources to occur at any time independent of each other. As both refrigerators can provide continuous cooling,

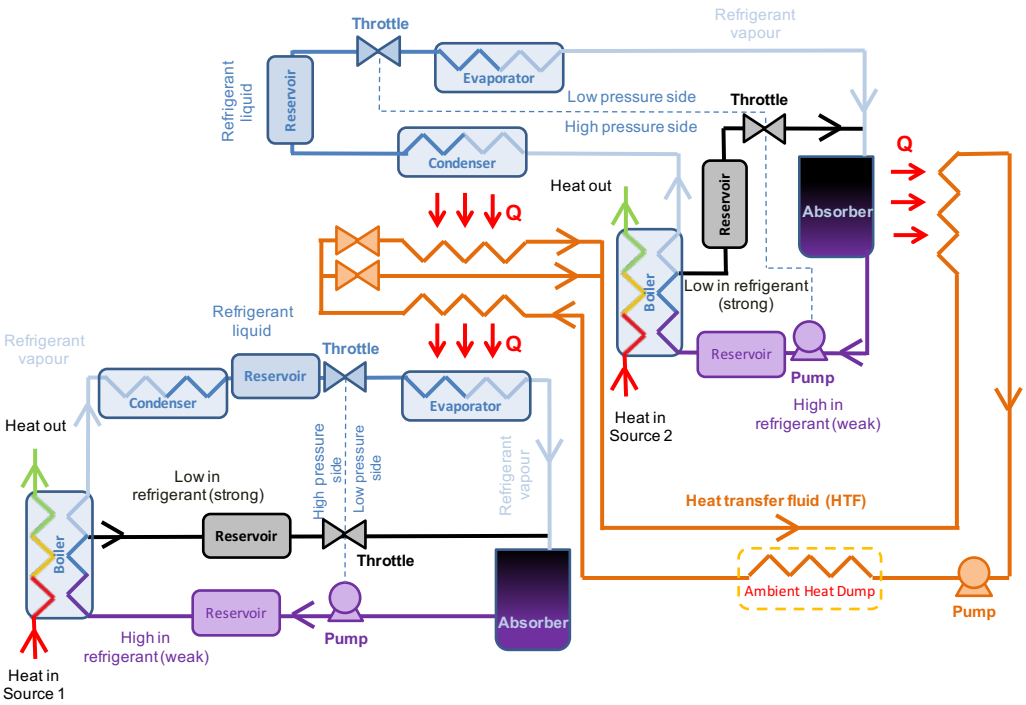

Figure 3.15: Coupled cycle schematic combined with reservoirs, allowing continuous cooling from discontinuous heat sources; where two absorption refrigerators are powered by two separate heat sources and are thermally coupled between the evaporator of one and the absorber and condenser of the other. The thermal coupling is illustrated as a heat transfer fluid (orange section).

this cycle provides a high level of control over the output evaporator temperature (from the refrigerator powered by heat source 2) as the refrigerator powered by heat source 1 can be optimised for the desired operating temperatures of the absorber and / or condenser of the refrigerator powered by heat source 2.

Double Boiler Cycle with Reservoirs and Evaporator Tap-Off

The double boiler cycle in Figure 3.16 has been described in Section 3.3.4, however here it incorporates the evaporator tap-off technique described in

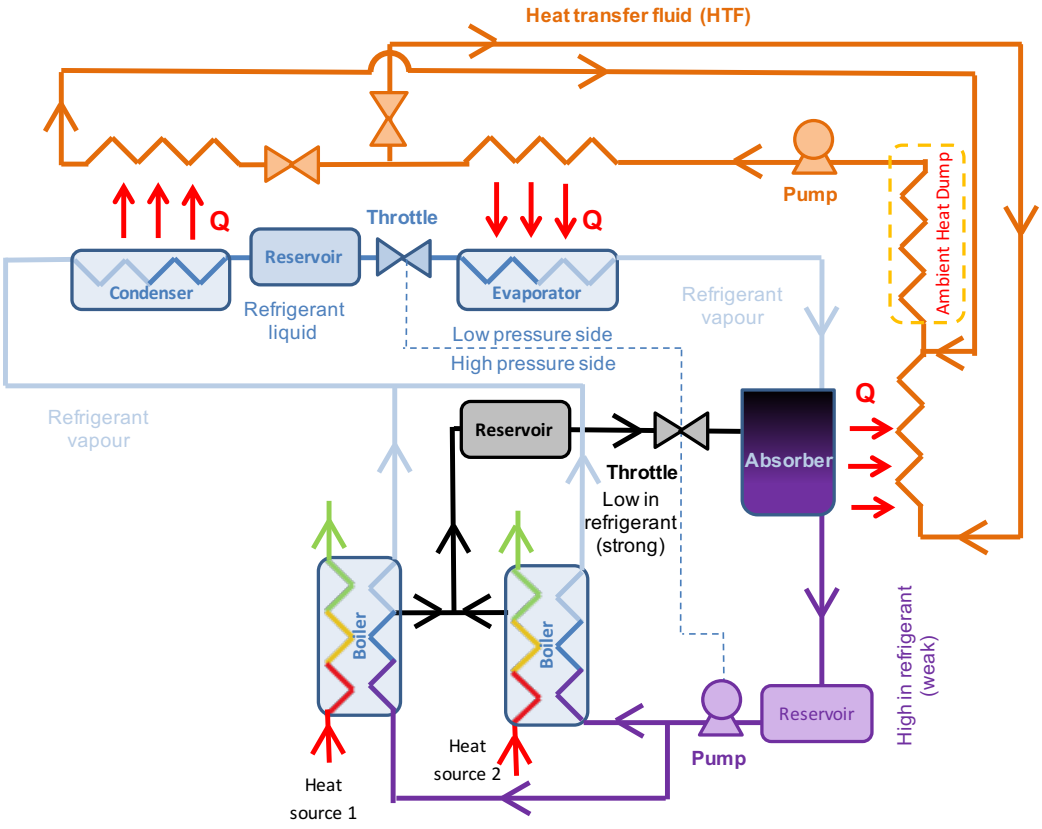

Figure 3.16: Double boiler with reservoirs and evaporator tap-off cycle schematic; showing one absorption refrigerator powered by two heat sources through two separate boilers. The thermal coupling is illustrated by the heat transfer fluid (orange section).

Section 3.3.5 to allow both continuous cooling from more than one discontinuous heat source and control over the evaporator temperature. This configuration only requires one condenser, absorber and evaporator with multiple boilers.

3.3.7 Appraisal of Absorption Refrigeration Systems

Table 3.2 shows the appraisal mechanism which aims to summarise the previously described system configurations and technologies available for absorption refrigeration. The table includes descriptions which highlight the applications, advantages and disadvantages of the systems in question, as well as a decision matrix to aid the comparison process when applied to the needs of the community described in Section 2.1, where:

- Heat Source Suitability refers to its ability to use low temperature discontinuous heat.
- Cooling Application refers to the possible refrigeration uses 5 being versatile (a range of temperatures) 1 not versatile (limited temperatures e.g. air conditioning only).
- Impact on CoP refers to the effect on refrigerator performance in terms of energy 5 is significantly improves CoP and 1 is significantly worsens CoP.
- Evaporator Temperature refers to the direct impact on evaporator temperature where 5 is lowering the temperature and 1 is increasing it.

The ranked factors in the decision matrix have equal importance and therefore no weighting was applied.

Table 3.2: Appraisal and decision matrix of absorption refrigeration cycles to use low grade discontinuous waste heat in rural India, where 5 is desirable and 1 is undesirable.

Refrigeration Type	Description	Applications	Advantages	Disadvantages	Total Score	References
Configurations for improving heat utilisaition						
Boiler Absorber Heat Exchanger (BAX / GAX / DAHX)	Uses heat generated from absorber to provide latent heating of the weak solution as a desorbing stage in the boiler	High evaporator temperatures (resulting from the required high absorber temperatures) such as air conditioning	- Reuses the low temperature heat absorbed in the evaporator and upgrades it for desorption - Improves the efficiency of the heat exchange process in the boiler by raising the weak solution's initial temperature - Allows a greater difference between the weak and strong solution concentrations	- Increases evaporator temperature through requiring high absorber temperatures - Limited to high boiler temperatures - Heat exchange needs to allow for refrigerant get to the condenser - Increased system complexity	**9**	Srikhirin et al. (2001)
Considerations	**Heat Source Suitability**	**Cooling Applications**	**Impact on CoP**	**Evaporator Temperature**		
Score	2	1	5	1		
Boiler Heat Recovery	Preheating the weak solution before it enters the boiler with warm strong solution leaving the boiler	All absorption refrigeration systems	Improves overall heat utilisation and therefore CoP of the refrigerator	Increased system complexity	**18**	Srikhirin et al. (2001)
Considerations	**Heat Source Suitability**	**Cooling Applications**	**Impact on CoP**	**Evaporator Temperature**		
Score	5	5	5	3		
Half Effect	Allows boiler temperatures that would otherwise be too low to operate the refrigerator by creating three pressure levels and four solution concentrations by splitting the input heat over two boiler stages	When low temperature heat is available such as flat plate solar collectors and condensers from process or power industry	Can utilise low temperature heat sources	- Thermodynamic penalty approximately half the CoP of a single effect cycle - Increased system complexity	**13**	Herold (1996)
Considerations	**Heat Source Suitability**	**Cooling Applications**	**Impact on CoP**	**Evaporator Temperature**		
Score	4	5	1	3		
Dual Cycle	Two single effect absorption refrigerators where the waste heat from the condenser and absorber of one is used to drive the other absorption refrigerator	- High temperature heat is available - Environments where two different temperatures are required e.g. frozen food and fresh food storage	- High utilisation of initial heat sources - Allows multiple refrigeration applications	- Requires high temperature heat source - Increased system complexity	**15**	Srikhirin et al. (2001)
Considerations	**Heat Source Suitability**	**Cooling Applications**	**Impact on CoP**	**Evaporator Temperature**		
Score	1	5	5	4		

Refrigeration Type	Description	Applications	Advantages	Disadvantages	Total Score	References
Configurations for discontinuous heat sources						
Single Effect with Reservoirs	Uses reservoirs to store the refrigerant, strong and weak solution so that discontinuous heat sources can provide continuous refrigeration	Any intermittent heat sources from power, process industry or domestic where decoupled cooling is required e.g. air conditioning and food storage	- Can provide continuous (or decoupled) refrigeration from discontinuous heat sources - Not reliant on insulation	Increased system complexity	14	Ammar, Joyce, et al. (2012)
Considerations	**Heat Source Suitability**	**Cooling Applications**	**Impact on CoP**	**Evaporator Temperature**		
Score	5	3	3	3		
Double Boiler with Reservoirs	Two (or more) boilers are connected to a single effect cycle with reservoirs to store the refrigerant, strong and weak solution between components allowing continuous refrigeration from multiple discontinuous heat sources	Multiple discontinuous waste heat sources from power generation or process industry	Relatively simple system as it only requires one condenser, evaporator and absorber for more than one boiler	- Little flexibility over solution concentrations - No flexibility over working fluids	14	Ideas developed in this thesis influenced by Ammar, Joyce, et al. (2012)
Considerations	**Heat Source Suitability**	**Cooling Applications**	**Impact on CoP**	**Evaporator Temperature**		
Score	5	3	3	3		
Configurations to control evaporator temperature						
Evaporator Tap-Off	Some of the cooling potential of the evaporator is used to cool either or both the absorber and condenser through either direct coupling or a heat transfer fluid	Any refrigeration application where control over the evaporator temperature is required which could not be achieved by external heat sinks such as rivers, lakes or the sea	- Does not rely entirely on external heat sinks to control evaporator temperature - Provides a level of independence from ambient conditions	Some of the refrigeration output is lost to cooling components resulting in lowering the CoP	16	Idea developed in this thesis, influenced by using low pressure steam to preheat boiler feed water in steam generation boilers
Considerations	**Heat Source Suitability**	**Cooling Applications**	**Impact on CoP**	**Evaporator Temperature**		
Score	4	5	2	5		
Coupled Cycle	Two single effect cycles where the evaporator of one is used to cool the condenser and / or absorber of the other either through direct coupling or through a heat transfer fluid	Any refrigeration application where control over the evaporator temperature is required which could not be achieved by external heat sinks such as rivers, lakes or the sea	- Reduces reliance on external heat sinks to control evaporator temperature - Provides a level of independence from ambient conditions - Allows different solution concentrations in each refrigerator - Allows different working fluids in each refrigerator	High system cost due to the complexity of having two complete refrigerators	15	Ideas developed in this thesis
Considerations	**Heat Source Suitability**	**Cooling Applications**	**Impact on CoP**	**Evaporator Temperature**		
Score	4	5	1	5		

Refrigeration Type	Description	Applications	Advantages	Disadvantages	Total Score	References
Configurations for discontinuous heat sources and evaporator temperature control						
Single Effect with Reservoirs and Evaporator Tap-Off	Single effect cycle with refrigerant, strong and weak solution reservoirs to allow continuous cooling from discontinuous heat sources combined with the evaporator tap-off method to extract some of the cooling potential from the evaporator to cool the absorber and / or condenser.	Any refrigeration application where control over evaporator temperature is required which could not be achieved by external heat sinks such as rivers, lakes or the sea and the heat source is discontinuous e.g. flat plate solar collectors in hot climates.	- Reduces reliance on ambient conditions - Reduces reliance on external heat sinks to control evaporator temperature - Allows continuous cooling from discontinuous heat sources	- Some of the refrigeration output is lost to cooling components resulting in lowering the CoP	**17**	Ideas developed in this thesis
Considerations	**Heat Source Suitability**	**Cooling Applications**	**Impact on CoP**	**Evaporator Temperature**		
Score	5	5	2	5		
Coupled Cycle with Reservoirs	Two refrigerators where the evaporator of one is used to cool the condenser and / or absorber of the other. Both refrigerators have refrigerant, strong and weak solution reservoirs to allow continuous cooling from discontinuous sources	- Any refrigeration application where control over the evaporator temperature is required which could not be achieved by external heat sinks such as rivers, lakes or the sea - More than one discontinuous heat source e.g. hybrid renewable power plants	- Reduces reliance on ambient conditions - Reduces reliance on external heat sinks to control evaporator temperature - Allows continuous cooling from discontinuous heat sources	All of the refrigeration output from one of the refrigerators is lost to cooling the other, lowering the system CoP	**16**	Ideas developed in this thesis
Considerations	**Heat Source Suitability**	**Cooling Applications**	**Impact on CoP**	**Evaporator Temperature**		
Score	5	5	1	5		
Double Boiler with Reservoirs and Evaporator Tap-Off	Single effect cycle with two (or more) boilers with refrigerant, strong and weak solution reservoirs to allow continuous cooling from discontinuous sources, combined with the evaporator tap-off method to use some of the cooling potential from the evaporator to cool the absorber and / or condenser	- Any refrigeration application where control over the evaporator temperature is required which could not be achieved by external heat sinks such as rivers, lakes or the sea - More than one discontinuous heat source e.g. hybrid renewable power plants	- Reduces reliance on ambient conditions - Reduces reliance on external heat sinks to control evaporator temperature - Allows continuous cooling from discontinuous heat sources	Some of the refrigeration output is lost to cooling components lowering the system CoP	**17**	Ideas developed in this thesis
Considerations	**Heat Source Suitability**	**Cooling Applications**	**Impact on CoP**	**Evaporator Temperature**		
Score	5	5	2	5		

Table 3.2 allows immediate identification of systems that are not suitable for the types of heat sources and community which this research is based around, which tends to be scores under 16. For example, boiler absorber heat exchanger has a total score of 9 which is a result of it being a technology suited for higher temperature heat sources and higher temperature cooling. Likewise the half effect cycle was deemed unsuitable as it has a total score of 13 which is largely a result of the impact on CoP (scoring 1) from half of the input energy being used internally.

Interestingly the boiler heat recovery is the highest scoring system (18) but it will not be carried forward in this research. This is largely due to the additional modelling complexity. Though it should be noted that, as a technology, it can be applied to almost any absorption system to recover the waste heat in the strong solution at the boiler exit.

The systems that are either for discontinuous heat sources or to control evaporator temperature but not both scored 14 and 15, apart from the evaporator tap-off which scored 16. This was slight increase is a result of it having a less serious impact on CoP than the coupled cycle, scoring 2 and 1 respectively.

The cycles that can utilise discontinuous heat sources and evaporator temperature control scored 16 and 17 indicating that they are the most suitable for the heat sources in this particular setting. The single effect with reservoirs and evaporator tap-off, coupled cycle with reservoirs and double boiler with reservoirs and evaporator tap-off all provide the ability to use discontinuous heat for continuous cooling while also providing some control over the evaporator temperature. These features are particularly useful in rural India where the cold sinks may be limited and / or not be effective and hot, humid weather will not provide the conditions to maintain suitable absorber and condenser temperatures.

3.4 Conclusion of Refrigeration Technology Review

This refrigeration technology review described the history of refrigeration and an overview of common refrigeration systems. From which it appeared that absorption refrigeration would be an appropriate technology to utilise low temperature discontinuous waste heat from a renewable power plant in rural India. It therefore included a detailed review of absorption refrigeration including the working fluids available and potential system configurations. The application for which this research is based has two discontinuous low temperature (<100°C) heat sources in a hot environment with only poor quality cold sinks (e.g. hot humid air) available. Currently acetone and zinc bromide solution has proven to work from heat source temperatures lower than 60°C and has no need for rectification.

The use of reservoirs and cooling of the condenser and / or the absorber by either the evaporator tap-off or from an independent refrigerator is an extension of the work by Said et al. (2012), Ammar, Joyce, et al. (2012), Jelinek and Borde (1998) and Gutiérrez-Urueta et al. (2011). The system configurations that can utilise discontinuous low temperature waste heat and are less reliant on environmental cold sinks are: single effect with reservoirs and evaporator tap-off, coupled cycle with reservoirs and double boiler with reservoirs and evaporator tap-off. These configurations with acetone and zinc bromide will be investigated in this thesis.

There appears to be a knowledge gap in the literature about using acetone and zinc bromide absorption systems to utilise low temperature discontinuous waste heat from renewable power plants in the high ambient temperatures expected in rural India. Moreover, though there is substantial knowledge about absorption refrigerator configurations and their effect, there is a knowledge gap in determining the operating limits when utilising these configurations

for low temperature waste heat sources to provide low refrigerating temperatures in high ambient conditions. Investigating these knowledge gaps will identify the limits of suitability for absorption refrigeration for requirements of the case study community identified in Chapter 2.

Chapter 4

Analytical Methodology

The following chapter describes the modelling used in the investigation of absorption refrigeration from utilising low temperature discontinuous waste heat from a renewable power plant in rural India. The heat sources are based on those in the proposed power plant which are a 10 kW (electric) concentrated photovoltaic (CPV) system and the radiator of a 5 kW (electric) hydrogen-biogas internal combustion engine electric generator (genset radiator). The working fluids for the absorption refrigeration system are acetone and zinc bromide.

This chapter consists of the following sections:

- **Energy Profiling and Heat Source Modelling** describes how the energy flows in the BioCPV power plant are quantified. This process provides the data for a Sankey diagram which includes the waste heat sources used to drive the absorption refrigerators.
- **Fluid Properties** describes the calculations required to model the working fluids in the absorption refrigerator system. This includes acetone in its pure form as well as acetone and zinc bromide as a solution.

- **Absorption Refrigerator Modelling** describes the process used to model a basic single effect absorption refrigerator and the alternative configurations used in this thesis.

- **Energy Utilisation** describes the method of qualifying energy utilisation within the BioCPV power plant and the absorption refrigerators. This uses exergy for the power plant energy flows and presents an alternative to exergy for the absorption refrigerators relating the cooling to avoided electrical consumption from a vapour compression cycle.

4.1 Energy Profiling and Heat Source Modelling

The following section describes the method used to model the electrical and heat output of the 10 kW (electric) CPV system and the radiator of the 5 kW (electric) genset.

4.1.1 Concentrated Photovoltaic

The proposed CPV system has been designed by the project partners at the University of Exeter and the Indian Institute of Technology Madras. The following information has been provided by them for the analysis in this thesis.

The CPV system aims to achieve optical efficiencies of 80% by addressing issues of concentrated light such as fuzziness at the receiver and reducing losses in the optical components. The CPV system consists of four CPV units with two axis tracking. Each CPV unit consists of two primary concentrators and receivers. The primary concentrator is a parabolic dish with a square opening, made up of four sections to achieve an overall entry aperture area of $9m^2$, though the actual collecting area is calculated to be 7.565 m^2 to provide

a total system output of 10 kW. Each receiver is designed to be 580 cm^2 and consists of a solar cell assembly of 144 solar cells, secondary concentrator (Crossed Compound Parabolic Concentrator (CCPC)) and cooling system. The specifications of the CPV units required for energy modelling are given in Table 4.1 and to aid contextualisation a CAD model of the system is provided in Figure 4.1 from the partners at the Indian Institute of Technology Madras.

The CPV system modelled in this investigation has been designed to the specifications in Table 4.1. The following equation calculates the solar radiation entering the CPV system ($Q_{CPV_{concentrator}}$).

$$Q_{CPV_{concentrator}} = A_{CPV_{concentrator}} \times DNI \tag{4.1}$$

Then using the solar energy entering the CPV concentrator ($Q_{CPV_{concentrator}}$) and optical efficiency ($\eta_{CPV_{optical}}$), the solar energy falling on the CPV's PV cell can be calculated.

$$Q_{CPV_{cell}} = Q_{CPV_{concentrator}} \times \eta_{CPV_{concentrator}} \tag{4.2}$$

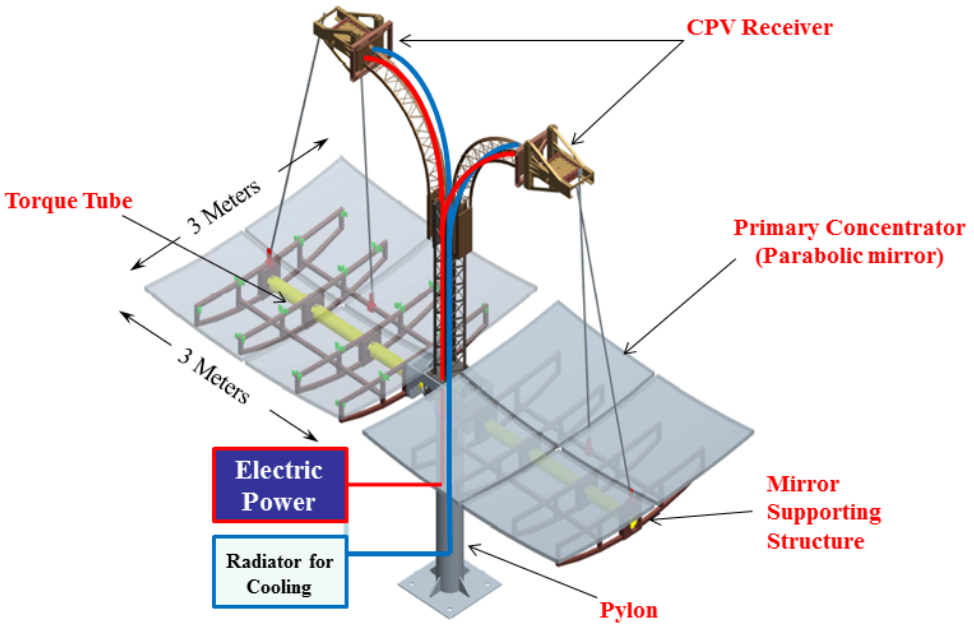

Figure 4.1: CAD model of one of the four CPV modules provided by partners at Indian Institute of Technology Madras and University of Exeter.

Table 4.1: CPV specifications provided by partners at Indian Institute of Technology Madras and University of Exeter.

Total Installation power rating	E_{CPV}	10 kW
Number of CPV modules	n_{CPV}	8
Solar irradiance considered	DNI	550 W·m^{-2}
Concentration ratio	CR_{CPV}	500X
Concentrator optical efficiency	$\eta_{CPV_{optical}}$	80%
Concentrator entry aperture area	$A_{CPV_{concentrator}}$	7.565 m^2

Likewise the electricity generated from the PV cell (E_{CPV}) can be calculated using the cell efficiency ($\eta_{CPV_{cell}}$) and the solar energy falling on the PV cell ($Q_{CPV_{cell}}$).

$$E_{CPV} = Q_{CPV_{cell}} \times \eta_{CPV_{cell}} \tag{4.3}$$

However the cell efficiency is affected by its temperature and the concentration ratio. This system is designed to operate at a high concentration ratio (500 suns). The cell manufacturer (Azur Space) state a cell temperature operating range of 25°C to 80°C. However, in the interest of reliability and avoidance of localised over heating the partners responsible for the CPV system want to maintain the cell temperature at 60°C. The cell manufacturer has supplied the following equation at 500 suns to relate PV cell temperature ($T_{CPV_{cell}}$) in degrees Celsius to PV cell efficiency ($\eta_{CPV_{cell}}$), in confidential communication (at the time) to Prof. Tapas Malik, University of Exeter.

$$\eta_{CPV_{cell}} = 0.39 - 0.0004134 \times (T_{CPV_{cell}} - 25) \tag{4.4}$$

The optical losses ($Q_{CPV_{optical}}$) can be calculated from the difference in the energy entering the CPV concentrator ($Q_{CP_{concentrator}}$) and the energy directed on the PV cell assembly ($Q_{CPV_{cell}}$).

$$Q_{CPV_{optical}} = Q_{CPV_{concentrator}} - Q_{CPV_{cell}} \tag{4.5}$$

Reflective losses from the PV cell assembly are included in the concentrator efficiency. Therefore the remaining losses at the PV cell assembly are assumed to be heat. This thermal energy in the CPV system ($Q_{CPV_{thermal}}$) is calculated from the difference between the solar energy falling on the PV cell ($Q_{CPV_{cell}}$) and the electrical output (E_{CPV}).

$$Q_{CPV_{thermal}} = Q_{CPV_{cell}} - E_{CPV} \tag{4.6}$$

4.1.2 Electrical Generator Radiator Heat Source

The biogas-hydrogen electrical generator set (genset) will be a commercially available 5 kW biogas internal combustion engine modified to take a biogas-hydrogen mix; a mixture of the locally produced anaerobic digester product gas and hydrogen from a local water electrolyser powered by excess electrical supply from the CPV system. The electrical efficiency, was estimated at 25% based on common electrical efficiencies of 5 kW natural gas generators found in the market, for example Yanmar CP5WN (Yanmar 2016).

For this analysis the ratio of hydrogen is 2% of the fuel mix by mass. This is based on the expected daily production of hydrogen from 7 kW·h per day of solar electricity via a 60% efficient electrolyser providing 4 kW·h per day of hydrogen. These figures are based on communication with electrolyser manufacturer ITM power and the responsible academic parters at the time. The hydrogen forms part of the daily fuel energy required for the genset, calculated in Equation 4.7 and presented in Table 4.2, though in reality the hydrogen content may vary depending on availability and need. Conveniently results from C. Jeong et al. (2009) show that there are diminishing returns from ratios greater than 2.3% hydrogen to fuel mix by mass because the hydrogen displaces air and reduces volumetric efficiency. They also state the most significant increase in efficiency of 3.34% was achieved from 0% to 0.7% hydrogen to fuel mix by mass, when compared to an increase of 1.24% with hydrogen ratios from 1.5% to 2.3%.

Table 4.2: Genset expected efficiency and electrical output.

Electrical output	E_{genset}	5 kW
Genset efficiency	η_{genset}	25%
Energy input (fuel)	Q_{genset}	20 kW

Using the genset electrical efficiency (η_{genset}) stated in Table 4.2 together with the required electrical output (E_{genset}), the energy input of the genset (Q_{genset} i.e. the energy of the fuel) can be calculated. The electrical generation losses between the work out of the internal combustion engine and the electrical generator are assumed to be negligible, based on personal industrial experience.

$$Q_{genset} = \frac{E_{genset}}{\eta_{genset}} \tag{4.7}$$

The US Department of Energy suggest that there are 10% ancillary losses ($W_{genset_{ancillary}}$) on average with automotive internal combustion engines (DOE 2014). This was assumed to be a reasonable assumption for a generator set as there would be a similar ancillary load to maintain the plant. Discussions independent of this project with generator suppliers in the industrial sector confirmed this value to be reasonable for modelling purposes.

$$W_{genset_{ancillary}} = Q_{genset} \times 0.1 \tag{4.8}$$

The energy content (or losses contained) within the exhaust ($Q_{genset_{exhaust}}$) was calculated by assuming a biogas - hydrogen fuel mix (2% hydrogen by mass) and the products of combustion leave the exhaust at 350°C. This figure is the average of the exhaust temperatures determined by Tamura (2008) on natural gas engines. The partners responsible for the anaerobic digester have suggested the biogas to be 60% methane and 40% carbon dioxide. Tamura (2008) also found that an excess air ratio (to stoichiometric combustion) of 1.2 was a minimum to allow complete combustion. Therefore combustion here is

assumed to take place with an excess air ratio of 1.2 times the stoichiometric air fuel ratio and for simplicity the excess air in the exhaust remains as oxygen and nitrogen (i.e. no NOx formed). The enthalpy data was extracted from Cengel and Boles (2006) using linear extrapolation for 350°C (623K) and taking the environmental temperature to be 25°C (298K). Subscript i denotes a particular component of the products of combustion in the exhaust, h is enthalpy, m is the mass flow rate.

$$Q_{genset_{exhaust}} = \sum m_{genset_{exhaust_i}} \times h_{genset_{exhaust_i}} \tag{4.9}$$

For simplicity the radiator is assumed to contain the remaining losses ($Q_{genset_{radiator}}$), though in reality there will be losses through the engine casing to atmosphere.

$$Q_{genset_{radiator}} = Q_{genset} - Q_{genset_{ancillary}} - Q_{genset_{exhaust}} - E_{genset} \tag{4.10}$$

4.2 Fluid Properties

This section is required for the absorption refrigerator modelling described in Section 4.3. The following equations and coefficients have been taken from Ajib and Karno (2008) to estimate the thermodynamic and thermophysical properties of acetone and zinc bromide solution and the enthalpy of pure acetone. Saturation pressures and temperatures use the Antoine equation provided by NIST Webbook (2011). Ajib and Karno (2008) suggest that acetone and zinc bromide absorption refrigeration systems can operate with solution concentrations between a range of 30% to 70% $\left(\frac{m_{ZnBr_2}}{m_{solution}}\right)$ to avoid crystallisation.

4.2.1 Pure Acetone

The following section describes the calculations for pure acetone. Figure 4.2, a pressure enthalpy (ph) graph, has been included to aid visualisation of the fluid properties.

Pure acetone Enthalpy

For the following set of equations h denotes specific enthalpy in kJ·kg^{-1}, T temperature in °C and P pressure in bar. The subscripts $_l$ is for liquid, $_v$ vapour, $_{sh}$ superheated and $_s$ saturation.

The enthalpy of acetone as a saturated liquid (Ajib and Karno 2008):

$$h_l = 177.185 + 2.154T_s + 1.06 \times 10^{-5}T_s^3 \ \text{(kJ·kg}^{-1}\text{)} \tag{4.11}$$

The enthalpy of acetone as a saturated vapour (Ajib and Karno 2008):

$$h_v = \frac{1}{0.001336 - 2.172 \times 10^{-6}T_s + 2 \times 10^{-11}T_s^3} \ \text{(kJ·kg}^{-1}\text{)} \tag{4.12}$$

The enthalpy of superheated acetone where pressure P is in bar (Ajib and Karno 2008):

$$h_{sh} = exp(6.62 + 0.0017T - 0.003P) \ \text{(kJ·kg}^{-1}\text{)} \tag{4.13}$$

Pure Acetone Saturation pressure

The saturation vapour pressure (P_s) of pure acetone provided by the Antoine equation from NIST Webbook (2011) uses a conversion from Kelvin to Celcius from Rogers and Mayhew (1995). This form of the equation is simpler to that from Ajib and Karno (2008) making the extraction of saturation temperature algebraically easier when the pressure is known. (NIST Webbook 2011)

$$P_s = 10^{4.42448 - \left(\frac{1312.253}{T_s + 240.705}\right)} \ (bar) \tag{4.14}$$

Pure Acetone Saturation Temperature

The saturation temperature can be found by rearranging Equation 4.14 in terms of saturation temperature (T_s), where saturation pressure (P_s) is in bar (NIST Webbook 2011).

$$T_s = \frac{1312.253}{4.42448 - log_{10}(P_s)} - 240.705 \ (°\text{C}) \tag{4.15}$$

Table 4.3: Vapour pressure calculation coefficients (a_{ij}) for solutions of acetone and zinc bromide to use in Equation 4.16 where subscript $_i$ corresponds to T^i and subscript $_j$ corresponds to X^j (Ajib and Karno 2008).

a_{00}	-2.41	a_{10}	5.35×10^{-2}	a_{20}	-2.13×10^{-4}
a_{01}	1.72×10^{-2}	a_{11}	-1.16×10^{-4}	a_{21}	3.66×10^{-6}
a_{02}	-5.58×10^{-4}	a_{12}	2.38×10^{-6}	a_{22}	-4.61×10^{-8}

4.2.2 Acetone and Zinc Bromide Solution

The following describes the calculations for an acetone and zinc bromide solution. Figure 4.3 has been included to aid visualisation of the solution properties and indicate the crystallisation limit. It also includes the saturation temperatures of pure acetone in red next to the corresponding vapour pressure.

Acetone and Zinc Bromide Solution Vapour pressure

As with the previous set of equations the following nomenclature corresponds to an acetone and zinc bromide solution: m is mass in kg (or mass flow over a desired time period), T is temperature in °C, P pressure in bar and h enthalpy in kJ·kg^{-1}. The solution concentration X is in the form $\frac{m_{ZnBr_2}}{m_{solution}} \times 100$ e.g. when $X = 50\%$ use 50, this is the form used by Ajib and Karno (2008).

The vapour pressure of acetone and zinc bromide solution ($P_{Acetone-ZnBr_2}$) can be calculated using Table 4.3 (Ajib and Karno 2008):

$$P_{Acetone-ZnBr_2} = exp \sum_{i=0}^{2} \sum_{j=0}^{2} a_{ij} T^i X^j \text{ (bar)} \tag{4.16}$$

Ajib and Karno (2008) report a good correlation from solution concentrations of 30% to 70% and solution temperatures of 0°C to 70°C. Maximum deviations of 15.85% in solution vapour pressure occurred for solutions at 30% and 58.1°C and the data is only validated up to 70°C.

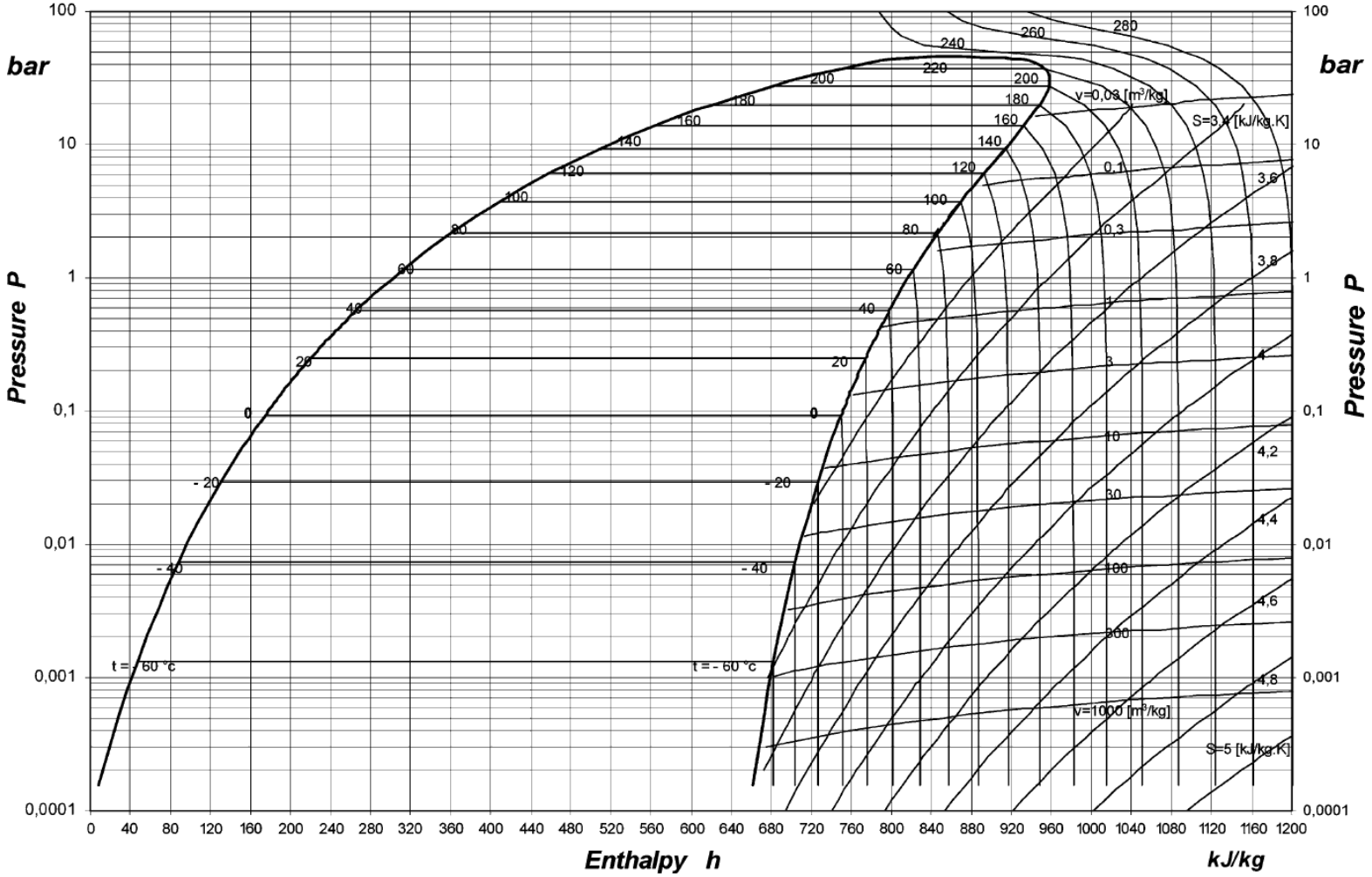

Figure 4.2: Pressure and enthalpy (ph) graph for pure acetone (Ajib and Karno 2008).

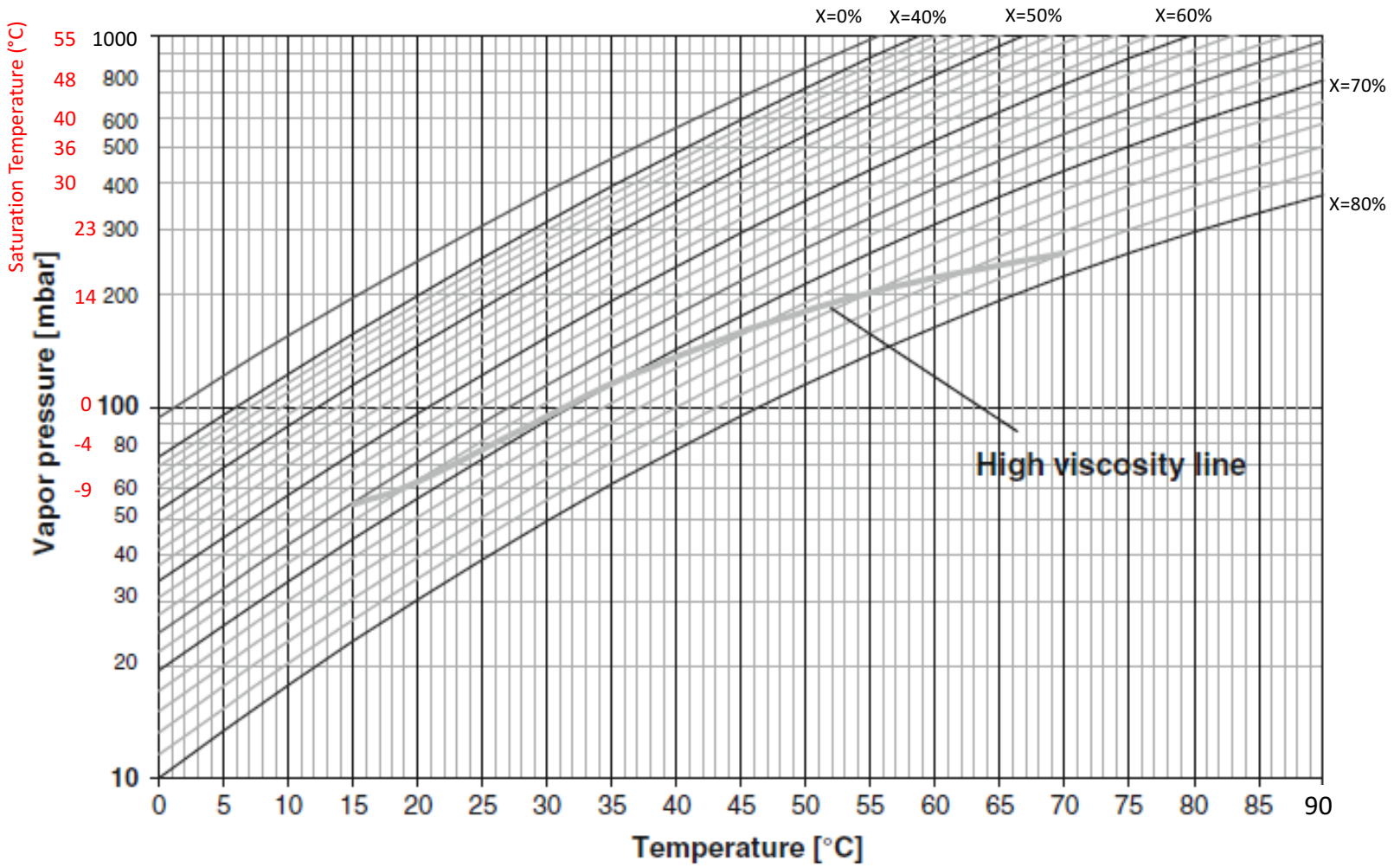

Figure 4.3: Pressure and temperature graph for acetone and zinc bromide solution, where the saturation temperature of pure acetone (red) is next to the corresponding vapour pressure and X is solution concentration in $\frac{m_{ZnBr_2}}{m_{solution}}$ (Ajib and Karno 2008).

Table 4.4: Solution enthalpy calculation coefficients (b_{ij}) to use in Equation 4.17 where subscript $_i$ corresponds to X^i and subscript $_j$ corresponds to T^j (Ajib and Karno 2008).

b_{00}	176.64	b_{10}	-2.95
b_{01}	1.892	b_{11}	-1.31×10^{-2}
b_{02}	-1.616×10^{-4}	b_{12}	2.8735×10^{-5}
b_{03}	1.486×10^{-5}	b_{13}	-5.02×10^{-7}
b_{04}	-2.439×10^{-8}	b_{14}	1.755×10^{-9}

Acetone and Zinc Bromide Solution Enthalpy

The coefficients for the following solution enthalpy ($h_{Acetone-ZnBr_2}$) calculations can be found in Table 4.4 (Ajib and Karno 2008):

$$h_{Acetone-ZnBr_2} = \sum_{i=0}^{1} \sum_{j=0}^{4} b_{ij} X^i T^j \ (\text{kJ}\cdot\text{kg}^{-1}) \tag{4.17}$$

4.3 Absorption Refrigerator Model

The following section describes the approach used to model the investigated absorption refrigerators, using the thermodynamic and thermophysical properties described in the previous section.

4.3.1 Solution Concentrations

In this study the condenser is assumed to be air cooled and therefore dependant on ambient conditions and the effectiveness of the heat exchanger used. To calculate the minimum condenser temperature, the following heat exchanger effectiveness equation can be used as $\dot{m}_{air} c_{p_{air}} > \dot{m}_{CO} c_{p_{CO}}$ due to the nearly infinite mass of air. (Shah et al. 1988)

$$\epsilon = \frac{T_{hi} - T_{ho}}{T_{hi} - T_{ci}} \tag{4.18}$$

In the case of the condenser the hot flow input temperature (T_{hi}) is the refrigerant leaving the boiler at the boiler temperature (T_{BO}), the hot output flow (T_{ho}) is the temperature of the condenser (T_{CO}) and the cold input flow (T_{ci}) is the air ambient temperature (T_{AMB}). Therefore condenser temperature can be found using Equation 4.18 in the following form:

$$T_{CO} = T_{BO} - \epsilon_{CO}\left(T_{BO} - T_{AMB}\right) \tag{4.19}$$

The boiler temperature (T_{BO}), the ambient temperature (T_{AMB}) and the condenser heat exchanger effectiveness (ϵ_{CO}) set a limit for the minimum condenser temperature. This has a corresponding saturation pressure, which is the minimum possible condenser pressure (P_{CO}) for those conditions. This pressure can be calculated using Equation 4.14 in the following form:

$$P_{CO} = 10^{4.42448 - \left(\frac{1312.253}{T_{CO}+240.705}\right)}\ (bar) \tag{4.20}$$

Assuming no losses between components, this pressure is also the minimum boiler pressure (P_{BO}).

$$P_{BO} = P_{CO} \tag{4.21}$$

Equation 4.16 in the context of the boiler is

$$P_{BO} = exp \sum_{i=0}^{2} \sum_{j=0}^{2} a_{ij} T_{BO}^{i} (X_{SS})^{j}\ \text{(bar)} \tag{4.22}$$

Equation 4.22 rearranged to find the low-in-refrigerant or strong solution concentration (X_{SS}) is a quadratic equation. Therefore, the general solution to a quadratic equation, together with Table 4.3 can provide the minimum strong solution concentration at which evaporation of the refrigerant, from solution, in the boiler is possible for a given boiler pressure and temperature.

$$aX_{SS}^{2} + bX_{SS} + c = 0 \tag{4.23}$$

Becomes

$$X_{SS} = \frac{-b \pm \sqrt{b^2 - 4ac}}{2a} \tag{4.24}$$

Where

$$a = a_{02} + a_{12}T_{BO} + a_{22}T_{BO}^2 \tag{4.25}$$

$$b = a_{01} + a_{11}T_{BO} + a_{21}T_{BO}^2 \tag{4.26}$$

$$c = a_{00} + a_{10}T_{BO} + a_{20}T_{BO}^2 - ln(P) \tag{4.27}$$

Ajib and Karno (2008) report working solution concentration limits of 30% to 70% ($\frac{m_{ZnBr_2}}{m_{solution}}$) and the equations provided by them are only valid in this range. Beyond this the solution is approaching the crystallisation limit which can cause blockages in the system, particularly at the absorber inlet. When the conditions provide a strong solution concentration which is stronger than 70%, 70% will be used in this model. For conditions which will provide solution concentrations weaker than 30% it is unlikely that any useful cooling will be generated due to the resulting high operating pressures.

The weak solution concentration can be set at any concentration weaker than the strong solution but stronger than 30%. Due to the challenges of absorption refrigeration described in Section 3.3.1 investigations into the optimal difference between strong and weak solution concentrations are required. This is because more concentrated weak solution concentrations provide lower evaporator temperatures, while less concentrated strong solution concentrations provide higher condenser temperatures. Yet, the weak solution concentration has to be less concentrated than the strong solution concentration and the difference between them is proportional to the ratio of working refrigerant (the refrigerant used in the condenser and evaporator) to total solution, which ultimately determines how much cooling can take place.

4.3.2 Boiler

For the purposes of this study it is assumed that perfect heat exchangers are used between the waste heat source (PV cell and genset radiator) and the

boiler resulting in their temperatures being equal. The quantities of heat available for the boiler (Q_{BO}) in Equation 4.28 can be found from the energy analysis in Section 4.1.

$$Q_{CPV_{BO}} = Q_{CPV_{thermal}} \tag{4.28}$$

or

$$Q_{genset_{BO}} = Q_{genset_{radiator}} \tag{4.29}$$

The boiler energy balance is calculated below where Q_{BO} is the boiler energy, m_{WS} is the mass of the weak solution, $h_{BO_{WS}}$ is the enthalpy of the weak solution as it enters the boiler, m_R is the mass of the working refrigerant leaving the boiler, h_{BO_R} is the enthalpy of the refrigerant as it leaves the boiler, m_{SS} is the mass of the strong solution and $h_{BO_{SS}}$ is the strong solution enthalpy as it leaves the boiler. (Karno and Ajib 2008)

$$Q_{BO} = m_{WS}h_{BO_{WS}} - m_R h_{BO_R} - m_{SS}h_{BO_{SS}} \tag{4.30}$$

The high-in-refrigerant (weak) solution temperature ($T_{BO_{WS}}$) entering the boiler is assumed to be at ambient temperature. This is because it is assumed that there is no heat transfer between the low-in-refrigerant (strong) solution leaving the boiler and, due to the discontinuous nature of the boiler, the weak solution would have remained in its uninsulated reservoir for some time.

$$T_{BO_{WS}} = T_{AMB} \tag{4.31}$$

Weak solution concentration is set by the model operator relative to the strong solution concentration (calculated as a function of ambient temperature and condenser heat exchanger effectiveness). The weak solution enthalpy is calculated using Equation 4.17 and Table 4.4.

$$h_{BO_{WS}} = \sum_{i=0}^{1}\sum_{j=0}^{4} b_{ij}(X_{WS})^i T_{BO_{WS}}^j \ \ (\mathrm{kJ{\cdot}kg^{-1}}) \tag{4.32}$$

The strong solution leaving the boiler is assumed to be at the boiler temperature due to thermal equilibrium. Its enthalpy is calculated using Equation 4.17 and Table 4.4.

$$h_{BO_{SS}} = \sum_{i=0}^{1}\sum_{j=0}^{4} b_{ij}(X_{SS})^i T_{BO}^j \ \ (\text{kJ}\cdot\text{kg}^{-1}) \tag{4.33}$$

The refrigerant is assumed to be in a superheated state when leaving the boiler; as it will be at the boiler temperature due to thermal equilibrium, but will be at a pressure lower than the saturation pressure for that temperature due to the pressure gradient from the solution. Its enthalpy is calculated using Equation 4.13.

$$h_{BO_R} = exp\,(6.62 + 0.0017 \times T_{BO} - 0.003 \times P_{BO}) \ \ (\text{kJ}\cdot\text{kg}^{-1}) \tag{4.34}$$

The boiler pressure required P_{BO} for Equation 4.34 is calculated in Equations 4.20 and 4.21.

Daily mass requirement

The energy inputs to the boiler are known from Equation 4.28; the heat flux from the CPV and the genset radiator. The solution concentrations are calculated in Section 4.3.1 using ambient temperature and condenser heat exchanger effectiveness to determine the saturation temperature with Equation 4.19 and converted saturation pressure in the condenser using Equation 4.20 and boiler pressure using Equation 4.21. This is combined with the boiler temperature to determine the strong solution concentration using Equations 4.22 and 4.24. Therefore an energy balance across the boiler with the definition of solution concentration can be used to find the daily mass requirements in the system. Moreover the mass of zinc bromide is a constant because it is not heated beyond its boiling temperature.

To avoid confusion with the symbol X for solution concentration which is in terms of percentage number e.g. 50% is 50 a new symbol for solution concentration (C) where 50% would be 0.5 is required, it is defined as:

$$C = \frac{m_{ZnBr_2}}{m_{solution}} \tag{4.35}$$

Therefore the mass of strong solution (m_{SS}) in terms of its solution concentration is

$$m_{SS} = \frac{m_{ZnBr_2}}{C_{SS}} \tag{4.36}$$

The mass of the weak solution (m_{WS}) in terms of its solution concentration is

$$m_{WS} = \frac{m_{ZnBr_2}}{C_{WS}} \tag{4.37}$$

Also the mass of working refrigerant m_R is the mass difference between the strong and weak solutions. This is the refrigerant that is used in the condenser and evaporator.

$$m_R = m_{WS} - m_{SS} \tag{4.38}$$

When combined with Equations 4.36 and 4.37 Equation 4.38 becomes

$$m_R = \frac{m_{ZnBr_2}}{C_{WS}} - \frac{m_{ZnBr_2}}{C_{SS}} \tag{4.39}$$

Combining Equations 4.30, 4.36, 4.37, 4.39 and 4.38, and rearranging for mass of zinc bromide (m_{ZnBr_2})

$$m_{ZnBr_2} = \frac{Q_{BO} C_{SS} C_{WS}}{C_{WS}\left(h_{BO_{SS}} - h_{BO_R}\right) + C_{SS}\left(h_{BO_R} - h_{BO_{WS}}\right)} \tag{4.40}$$

Then using Equations 4.36, 4.37 and 4.38 with the outputs of Equations 4.19 to 4.24 the mass of the strong and weak solutions as well as the working refrigerant can be found.

4.3.3 Condenser

The condenser temperature is known from Equation 4.19. The mass of refrigerant going through the condenser will be the difference between the mass of the weak and strong solutions (Equation 4.38).

An energy balance can determine the thermal energy that needs to be removed from the condenser (Q_{CO}). (Karno and Ajib 2008)

$$Q_{CO} = m_{CO_R} \left(h_{CO_{in}} - h_{CO_{out}} \right) \tag{4.41}$$

Assuming no losses between the boiler and condenser, the enthalpy of the refrigerant entering the condenser ($h_{CO_{in}}$) is

$$h_{CO_{in}} = h_{BO_R} \tag{4.42}$$

The refrigerant leaves the condenser as a saturated liquid so the condenser output enthalpy ($h_{CO_{out}}$) can be calculated using Equation 4.11

$$h_{CO_{out}} = 177.185 + 2.154 \times T_{CO} + 1.06 \times 10^{-5} \times T_{CO}^3 \tag{4.43}$$

Where condenser output temperature T_{CO} is calculated in Equation 4.19.

4.3.4 Refrigerant Reservoir

The refrigerant reservoir, initially shown in Figure 3.10, acts as storage so that continuous cooling can be provided from discontinuous heat sources. It also provides space for the refrigerant to cool to ambient temperature. It is assumed that the refrigerant is in a saturated liquid state within the reservoir at all times, and that there is no left over refrigerant in the reservoir when the boiler starts to operate.

The refrigerant reservoir inlet enthalpy $\left(h_{RE_{R_{in}}} \right)$ is equal to the outlet enthalpy of the condenser assuming there are no losses between them.

$$h_{RE_{R_{in}}} = h_{CO_{out}} \tag{4.44}$$

The refrigerant reservoir outlet enthalpy $\left(h_{RE_{R_{out}}} \right)$ is calculated using Equation 4.11, where the refrigerant reservoir outlet temperature (T_{RE_R}) is

$$T_{RE_R} = T_{AMB} \tag{4.45}$$

and the enthalpy

$$h_{RE_{R_{out}}} = 177.185 + 2.154 \times T_{RE_R} + 1.06 \times 10^{-5} \times T_{RE_R}^3 \text{ (kJ·kg)} \tag{4.46}$$

4.3.5 Refrigerant Throttle

The refrigerant is assumed to be a saturated mixture of liquid and vapour when leaving the throttle. The throttle is assumed to be an isenthalpic process. Therefore the refrigerant enthalpy leaving the throttle ($h_{TH_{R_{out}}}$) will be equal to its enthalpy entering the throttle ($h_{TH_{R_{in}}}$) which, assuming no losses, is equal to its enthalpy leaving the refrigerant reservoir between the condenser and evaporator ($h_{RE_{R_{out}}}$).

$$\begin{aligned} h_{TH_{R_{out}}} &= h_{TH_{R_{in}}} \\ &= h_{RE_{R_{out}}} \end{aligned} \tag{4.47}$$

4.3.6 Evaporator

The heat energy absorbed by the evaporator (Q_{EV}) is the refrigeration effect and it is found using an energy balance. (Karno and Ajib 2008)

$$Q_{EV} = m_{EV_R} \left(h_{EV_{out}} - h_{EV_{in}} \right) \tag{4.48}$$

The evaporator input enthalpy ($h_{EV_{in}}$) is equal to the throttle output enthalpy ($h_{TH_{out}}$), calculated in Section 4.3.5.

$$h_{EV_{in}} = h_{TH_{out}} \tag{4.49}$$

The refrigerant is assumed to be a dry saturated vapour when leaving the evaporator to maximise its heat absorbing potential, its enthalpy ($h_{EV_{out}}$) is calculated using Equation 4.12.

$$h_{EV_{out}} = \frac{1}{0.001336 - 2.172 \times 10^{-6} T_{EV} + 2 \times 10^{-11} T_{EV}^3} \ (\text{kJ}\cdot\text{kg}^{-1}) \tag{4.50}$$

The maximum temperature of the evaporator (T_{EV}) is calculated using Equation 4.51, which is derived from Equation 4.15.

$$T_{EV} = \frac{1312.253}{4.42448 - log_{10}(P_{EV})} - 240.705 \ (^{\circ}\text{C}) \tag{4.51}$$

The maximum evaporator temperature is determined by the maximum vapour pressure in the evaporator which, assuming no losses between the

absorber and evaporator, is equal to the maximum vapour pressure in the absorber. The maximum absorber pressure is governed by the weak solution leaving the absorber.

$$P_{EV} = P_{AB} \tag{4.52}$$

4.3.7 Strong Solution Reservoir

The strong solution reservoir serves two purposes: It allows the strong solution generated in the boiler to be stored and released at a constant rate, it is also a space for the strong solution to cool between the boiler and absorber.

An energy balance can be used to calculate the heat released from the strong solution reservoir ($Q_{RE_{SS}}$), where: $m_{RE_{SS_{in}}}$ and $h_{RE_{SS_{in}}}$ are the mass and enthalpy of the strong solution input to the reservoir, and $m_{RE_{SS_{out}}}$ and $h_{RE_{SS_{out}}}$ are the mass and enthalpy of the strong solution output from the reservoir.

This is presented here for completeness as there is a heat dissipation requirement in the strong solution reservoir, however it is not evaluated in the thesis.

$$Q_{RE_{SS}} = m_{RE_{SS_{in}}} h_{RE_{SS_{in}}} - m_{RE_{SS_{out}}} h_{RE_{SS_{out}}} \tag{4.53}$$

Assuming no losses between components, the input enthalpy ($h_{RE_{SS_{in}}}$) will be equal to output enthalpy of the strong solution from the boiler ($h_{BO_{SS}}$), calculated in Equation 4.33.

$$h_{RE_{SS_{in}}} = h_{BO_{SS}} \tag{4.54}$$

The strong solution temperature at the outlet ($T_{RE_{SS_{out}}}$) will be at ambient temperature (T_{AMB}) assuming the solution is held in the reservoir for long enough.

$$T_{RE_{SS_{out}}} = T_{AMB} \tag{4.55}$$

This is required to calculate the outlet enthalpy ($h_{RE_{SS_{out}}}$) using Equation 4.17

$$h_{RE_{SS_{out}}} = \sum_{i=0}^{1} \sum_{j=0}^{4} b_{ij} (X_{SS})^i T_{RE_{SS}}^j \text{ (kJ·kg)} \tag{4.56}$$

4.3.8 Strong Solution Throttle

The strong solution throttle is assumed to be isenthalpic, therefore its output enthalpy ($h_{TH_{SS_{out}}}$) is equal to its input enthalpy ($h_{TH_{SS_{in}}}$) which, assuming no losses, is equal to the strong solution reservoir output enthalpy

$$\begin{aligned} h_{TH_{SS_{out}}} &= h_{TH_{SS_{in}}} \\ &= h_{RE_{SS_{out}}} \end{aligned} \tag{4.57}$$

4.3.9 Absorber

The absorber calculation requires an iterative approach due to its relationship with the evaporator. The inputs are the strong solution from the throttle after the strong solution reservoir and the refrigerant leaving the evaporator. The output is the weak solution.

The pressure of the absorber determines the evaporator conditions. However the evaporator output is an input into the absorber which contains the majority of the thermal energy that has to be removed in the absorber. The absorber heat exchanger effectiveness determines the absorber operating temperature which determines the absorber pressure and ultimately the evaporator temperature. The evaporator temperature and the assumption that the refrigerant leaves the evaporator as a saturated vapour determines the input conditions to the absorber.

The amount of cooling required for the absorber (Q_{AB}) can be calculated using an energy balance, where m_R and h_{AB_R} are the mass and enthalpy of the refrigerant entering the absorber, m_{SS} and $h_{AB_{SS}}$ are the mass and enthalpy of the strong solution entering the absorber and m_{WS} and $h_{AB_{WS}}$ are the mass and enthalpy of the weak solution leaving the absorber. (Karno and Ajib 2008)

$$Q_{AB} = m_R h_{AB_R} + m_{SS} h_{AB_{SS}} - m_{WS} h_{AB_{WS}} \tag{4.58}$$

Assuming no losses the enthalpy of the strong solution entering the absorber ($h_{AB_{SS}}$) is equal to its enthalpy leaving the strong solution throttle ($h_{TH_{SS_{out}}}$) calculated from Equation 4.57.

$$h_{AB_{SS}} = h_{TH_{SS_{out}}} \tag{4.59}$$

Assuming no losses the enthalpy of the refrigerant entering the absorber is equal to the enthalpy leaving the evaporator, calculated from Equation 4.50. However the evaporator enthalpy is determined by its temperature which is determined by the pressure resulting from the weak solution concentration and temperature as it leaves the absorber. The weak solution temperature is determined by the effectiveness of the heat exchanger used in the absorber. An iterative approach is required to calculate this.

Initially an estimate is required to find the refrigerant enthalpy entering the absorber, denoted with subscript $_1$. Since the weak solution leaving the absorber determines the pressure in the evaporator. The pressure in the evaporator determines the temperature of the refrigerant and hence its enthalpy leaving the evaporator and entering the absorber. For this analysis the initial estimate is based on the assumption that the weak solution leaves the absorber at ambient temperature.

$$T_{AB_{WS_1}} = T_{AMB} \tag{4.60}$$

Assuming no losses between evaporator and absorber their pressures (P_{EV} and P_{AB}) are equal.

$$P_{EV} = P_{AB} \tag{4.61}$$

The estimated absorber pressure (P_{AB_n}) is found using the weak solution concentration and its estimated temperature, where subscript $_n$ is an iteration indicator.

$$P_{AB_n} = exp \sum_{i=0}^{2} \sum_{j=0}^{2} a_{ij} T^i_{AB_{WS_n}} (X_{WS})^j \text{ (bar)} \tag{4.62}$$

Using Equations 4.61, 4.62 and 4.15 to estimate the evaporator temperature (T_{EV_n}) we get:

$$T_{EV_n} = \frac{1312.253}{4.42448 - log_{10}(P_{EV})} - 240.705 \text{ (°C)} \tag{4.63}$$

With this temperature and the assumption that the refrigerant leaves the evaporator and enters the absorber as a saturated vapour its enthalpy can be found using Equation 4.12.

$$h_{EV_{out_n}} = \frac{1}{0.001336 - 2.172 \times 10^{-6} T_{EV_n} + 2 \times 10^{-11}} \text{ (kJ·kg}^{-1}\text{)} \tag{4.64}$$

Assuming no losses between components the output enthalpy of the evaporator ($h_{EV_{out_n}}$) is the input enthalpy of the refrigerant into the absorber ($h_{AB_{R_n}}$).

$$h_{AB_{R_n}} = h_{EV_{out_n}} \tag{4.65}$$

As this is an ambient air cooled system Equation 4.18 can be used, however the hot inlet temperature (T_{hi}) needs to be calculated. The hot inlet temperature is the adiabatic temperature of the weak solution leaving the absorber. This can be found by calculating the enthalpy of the adiabatic weak solution leaving the absorber ($h_{AB_{WS_{adiabatic_n}}}$) using the masses and enthalpies in the absorber of the refrigerant ($m_R h_{AB_{R_n}}$) and strong solution ($m_{SS} h_{AB_{SS}}$) and the mass of the weak solution in the absorber (m_{WS}).

$$h_{AB_{WS_{adiabatic_n}}} = \frac{m_R h_{AB_{R_n}} + m_{SS} h_{AB_{SS}}}{m_{WS}} \tag{4.66}$$

Then the solution enthalpy equation (Equation 4.17) can be used to determine the adiabatic temperature of the weak solution leaving the absorber ($T_{AB_{WS_{adiabatic}}}$).

$$h_{AB_{WS_{adiabatic_n}}} = \sum_{i=0}^{1} \sum_{j=0}^{4} b_{ij} (X_{WS})^i T^j_{AB_{WS_{adiabatic_n}}} \text{ (kJ·kg}^{-1}\text{)} \tag{4.67}$$

This creates the following quartic equation, the coefficients can be found in Table 4.4

$$a_1 T^4_{AB_{WS_{adiabatic_n}}} + b_1 T^3_{AB_{WS_{adiabatic_n}}} + c_1 T^2_{AB_{WS_{adiabatic_n}}} + d_1 T_{AB_{WS_{adiabatic_n}}} + e_1 = 0 \tag{4.68}$$

Where

$$a_1 = b_{04} + b_{14}(X_{WS}) \tag{4.69}$$

$$b_1 = b_{03} + b_{13}(X_{WS}) \tag{4.70}$$

$$c_1 = b_{02} + b_{12}(X_{WS}) \tag{4.71}$$

$$d_1 = b_{01} + b_{11}(X_{WS}) \tag{4.72}$$

$$e_1 = b_{00} + b_{10}(X_{WS}) - h_{AB_{WS_{adiabatic}}} \tag{4.73}$$

This can be solved algebraically or computationally, care must be taken to select the root that is sensible. In this thesis it was solved computationally.

Once the estimated adiabatic weak solution temperature ($T_{AB_{WS_{adiabatic}}}$) has been determined, Equation 4.18 can be used to determine the estimated output temperature of the weak solution ($T_{AB_{WS_{n+1}}}$) based on the heat exchanger effectiveness (ϵ_{AB}).

$$T_{AB_{WS_{n+1}}} = T_{AB_{WS_{adiabatic_n}}} - \epsilon_{AB}\left(T_{AB_{WS_{adiabatic_n}}} - T_{AMB}\right) \tag{4.74}$$

The new weak solution temperature leaving the absorber ($T_{AB_{WS_{n+1}}}$) can then be used to replace the old weak solution temperature ($T_{AB_{WS_n}}$) in Equation 4.62.

$$T_{AB_{WS_n}} = T_{AB_{WS_{n+1}}} \tag{4.75}$$

The process using Equations 4.62 to 4.75 can be repeated until the difference between the new and old weak solution absorber outlet temperature is deemed negligible, for this investigation that difference was 0.001°C.

If

$$|T_{AB_{WS_{n+1}}} - T_{AB_{WS_n}}| \geq 0.001°\text{C} \tag{4.76}$$

Then

$$T_{AB_{WS_n}} = T_{AB_{WS_{n+1}}} \tag{4.77}$$

Else

$$T_{AB_{WS_{n+1}}} = T_{AB_{WS}} \tag{4.78}$$

The process presented in Equations 4.58 to 4.78 provides the operating conditions and energy flow in the absorber which also provides the information to calculate the conditions and energy flow in the evaporator.

4.3.10 Coefficient of Performance (CoP)

The Coefficient of Performance (CoP) of a refrigerator is its practical efficiency (rather than thermodynamic). For absorption refrigeration (where pumping load is considered negligible) it is calculated from the ratio of heat absorbed in the evaporator (cooling energy) to heat absorbed in the boiler (waste heat source for this investigation). (Karno and Ajib 2008)

$$CoP = \frac{Q_{EV}}{Q_{BO}} \tag{4.79}$$

4.3.11 Alternative Configurations

The method described above will calculate the single effect with reservoirs system. All other systems in this analysis require a heat transfer fluid which will be water. The purpose of the alternative configurations is to investigate whether some of the cooling can be used to improve the performance of the refrigerators in the conditions expected in rural India.

The heat transfer fluid absorbs the heat from the condenser and absorber and rejects as much as possible to the environment at ambient conditions. It is then further cooled by an evaporator from the respective system. The heat

transfer fluid then enters the condenser and absorber at a lower temperature than ambient ultimately lowering the evaporator temperature.

Heat Transfer Fluid

To allow a comparative analysis in all cases there will be a heat transfer fluid will have an approach temperature of 2°C from the hot inlet. This figure is based on personal experience with water as a heat transfer fluid in industrial vapour compression systems. The heat transfer fluid is assumed to have cooled to ambient before entering at the cold inlet of the heat exchanger. This information can be used with an energy balance to find the mass flow rate of the heat transfer fluid.

For the case of the condenser the heat transfer fluid inlet temperature ($T_{HTF_{CO_{in}}}$) is

$$T_{HTF_{CO_{in}}} = T_{AMB} \tag{4.80}$$

and the heat transfer outlet temperature ($T_{HTF_{CO_{out}}}$) is

$$T_{HTF_{CO_{out}}} = T_{CO_{in}} - 2°\text{C} \tag{4.81}$$

Therefore the mass flow rate of the heat transfer fluid in the condenser ($m_{HTF_{CO}}$) can be calculated by rearranging a heat balance between the heat transfer fluid and the condenser. This uses the heat rejected from the condenser (Q_{CO}), the specific heat capacity of the heat transfer fluid ($C_{P_{HTF}}$) together with the outlet and inlet temperatures of the heat transfer fluid ($T_{HTF_{CO_{out}}}$ and $T_{HTF_{CO_{in}}}$).

$$\dot{m}_{HTF_{CO}} = \frac{Q_{CO}}{C_{P_{HTF}}\left(T_{HTF_{CO_{out}}} - T_{HTF_{CO_{in}}}\right)} \tag{4.82}$$

Likewise for the heat transfer fluid in the absorber the inlet temperature ($T_{HTF_{AB_{in}}}$) is

$$T_{HTF_{AB_{in}}} = T_{AMB} \tag{4.83}$$

and the heat transfer fluid outlet temperature ($T_{HTF_{AB_{out}}}$) is

$$T_{HTF_{AB_{out}}} = T_{AB_{adiabatic_{out}}} - 2°\text{C} \tag{4.84}$$

Therefore the mass flow rate of the heat transfer fluid in the absorber ($m_{HTF_{AB}}$) is

$$\dot{m}_{HTF_{AB}} = \frac{Q_{AB}}{C_{P_{HTF}}\left(T_{HTF_{AB_{out}}} - T_{HTF_{AB_{in}}}\right)} \tag{4.85}$$

Evaporator Tap-Off

To model the evaporator tap off method for cooling either the absorber or the condenser the quantity of cooling required to lower the heat transfer fluid from ambient by a set number of degrees Celsius ($\Delta T_{HTF_{Tap\,Off}}$) can be calculated with an energy balance.

$$Q_{HTF_{Tap\,Off}} = C_{P_{HTF}} \Delta T_{HTF_{Tap\,Off}} m_{HTF} \tag{4.86}$$

This can then be quantified as a percentage of the evaporator cooling energy (λ)

$$\lambda = \frac{Q_{HTF_{Tap\,Off}}}{Q_{EV}} \tag{4.87}$$

For the condenser and absorber, the temperature that the heat transfer fluid has been reduced to becomes the new cold inlet temperature, replacing what was previously ambient temperature. The respective calculations are rerun and the change in evaporator temperature can be compared to the amount of cooling required to achieve it.

4.4 Energy Utilisation

To quantify how well the energy is utilised in the proposed system, a method of scaling the different energy types based on their quality is required. The most common method of doing this is exergy. Exergy rationalises energy

in terms of its quality. It does this by relating the energy to its maximum possible theoretical work output relative to its environment. As work is (generally) independent of environmental temperature it has the highest energy quality therefore its exergy and energy values are equal. As electricity can almost entirely be converted to work, its energy and exergy are also equal. Other forms of energy have to be exergetically rationalised. An alternative way to view exergy is the quantity of reversible work from a given energy source. Conversely exergy losses are irreversibilities. (Cengel and Boles 2006)

However exergy analysis falls short when trying to quantify the quality of the cooling produced from a refrigerator powered by a waste heat source. This is because an exergy analysis will tell you the reversibility of the energy exchange between the evaporator and environment. A more appropriate measure of the energy utilisation of a waste heat driven absorption refrigerator is to quantify how much electricity would be required to power a generic vapour compression refrigerator to provide the same amount of cooling. This approach allows a direct comparison to electrical output and therefore performance of the renewable power plant. Moreover, as electricity has equal energetic and exergetic quantities this approach allows a direct comparison to the thermal exergy of the CPV and genset radiator waste heat.

4.4.1 Concentrated Photovoltaic System Exergy

The following describes how to calculate the exergy of the CPV system.

Solar Exergy (Radiative)

This section extrapolates the exergetic analysis of a PV cell technique described by Petela (2010) to a CPV system.

Petela (2010) calculates the total thermal exergy ($\varepsilon_{PV_{cell}}$) from the sun falling on a PV cell, where $F_{SunEarth}$ is the Sun-Earth Factor, σ is the

Table 4.5: Data for radiative exergy calculations (Petela 2010).

σ	Stephan-Boltzmann coefficient	$5.67 \times 10^{-}8$ $\mathrm{J{\cdot}s^{-1}{\cdot}m^{-2}{\cdot}K^{-4}}$
$F_{Sun-Earth}$	Sun-Earth factor (dimensionless)	2.16^{-5}
T_{Sun}	Temperature Sun's surface	5800 K
T_{AMB}	Ambient temperature	298 K

Stephan-Boltzmann constant, T_{Sun} is temperature of the surface of the sun and T_{AMB} is the ambient temperature. Values can be found in Table 4.5.

$$\varepsilon_{PV_{cell}} = F_{SunEarth}\frac{\sigma}{3}A_{PV} \times (3T_{Sun}^4 + T_{AMB}^4 - 4T_{AMB}T_{Sun}^3) \tag{4.88}$$

To extrapolate for the 8 CPV modules being used in this analysis and treating the concentrator as Petela (2010)'s PV cell, an effective area ($A_{effective}$) has to be used based on Petela (2010) energy calculation of a PV cell, where:

$$A_{effective} = \frac{Q_{CPV_{concentrator}}}{F_{SunEarth} \times \sigma \times T_{Sun}} \tag{4.89}$$

The solar exergy entering the CPV concentrator ($\varepsilon_{CPV_{concentrator}}$) is

$$\varepsilon_{CPV_{concentrator}} = F_{SunEarth}\frac{\sigma}{3}A_{effective} \times n_{CPV} \times (3T_{Sun}^4 + T_{AMB}^4 - 4T_{AMB}T_{Sun}^3) \tag{4.90}$$

The exergy analysis on the CPV uses the following information:

- **Input** Radiative solar exergy
- **Optical losses** 20% (from 80% optical efficiency)
- **Electrical output** 10 kW
- **Heat output** Thermal exergy

Exergy of PV Cell Waste Heat (Thermal)

Thermal exergy uses the Carnot efficiency to calculate the maximum work output of a given heat source. The Carnot efficiency uses the temperature difference between a hot source (T_{hot}), in this case the PV cell, and a cold source (T_{cold}), in this case the surroundings, to predict the efficiency of an ideal heat engine. (Cengel and Boles 2006) (Bejan 1997)

$$\eta_{Carnot} = \frac{T_{hot} - T_{cold}}{T_{hot}} \tag{4.91}$$

$$\varepsilon_{thermal} = Q \times \eta_{Carnot} \tag{4.92}$$

Therefore the following equation calculates the exergy of the PV cell using the cell temperature ($T_{CPV_{cell}}$), ambient temperature (T_{AMB}) and the thermal energy in the PV cell ($Q_{CPV_{cell}}$) calculated in Equation 4.6.

$$\varepsilon_{CPV_{cell}} = Q_{CPV_{cell}} \times \frac{T_{CPV_{cell}} - T_{AMB}}{T_{CPV_{cell}}} \tag{4.93}$$

4.4.2 Internal Combustion Engine Electrical Generator Exergy

Fuel Exergy (Chemical)

Chemical exergy quantifies the maximum work output of a chemical reaction in a given environment. The chemical exergy of fuels has been tabulated by Bejan (1997) at 25°C and 1 atmosphere. This conveniently lies within the conditions expected for the BioCPV power plant environment, and is compatible with the data for the CPV system which is rated to the same conditions.

- Hydrogen = 235.2 kJ· mol^{-1} (Bejan 1997)
- Methane = 830.2 kJ· mol^{-1} (Bejan 1997)

Exhaust Exergy (Flow)

Exhaust gases are a flow, (whereas the radiator is a stationary heat source) so flow exergy (ε_{flow}) will be used. Flow exergy uses the entropy generated in the surroundings to determine the maximum reversible work output of a flow. It has been simplified here by neglecting the kinetic and potential terms. (Cengel and Boles 2006) (Bejan 1997)

$$\begin{aligned}\varepsilon_{flow} = \dot{m}[(h_{flow} - h_{surroundings}) - \\ T_{surroundings}(s_{flow} - s_{surroundings})]\end{aligned} \tag{4.94}$$

When there are several components of a flow composition the previous equation can be altered to sum the individual components, where subscript i denotes a single component of the flow composition. In the case of the exhaust exergy ($\varepsilon_{genset_{exhaust}}$) this will be the products of combustion.

$$\begin{aligned}\varepsilon_{genset_{exhaust}} &= \sum \varepsilon_{flow_i} \\ &= \sum \dot{m}_i[(h_i - h_{surroundings}) - \\ &T_{surroundings}(s_i - s_{surroundings})]\end{aligned} \tag{4.95}$$

Radiator Exergy (Thermal)

The exergy contained in the radiator ($\varepsilon_{genset_{radiator}}$) is a stationary heat source and therefore uses the same approach as the PV cell. The exergy contained in the radiator is calculated using the genset radiator temperature ($T_{genset_{radiator}}$), ambient temperature (T_{AMB}) and the heat energy contained in the radiator ($Q_{genset_{radiator}}$) calculated with Equation 4.10.

$$\varepsilon_{genset_{radiator}} = Q_{genset_{radiator}} \times \frac{T_{genset_{radiator}} - T_{AMB}}{T_{genset_{radiator}}} \tag{4.96}$$

4.4.3 Refrigeration Exergy Replacement

Equivalent Electricity Consumption of a Vapour Compression Refrigerator

Calculating the avoided electrical consumption that would have been used to provide the same amount of cooling as the absorption refrigerators modelled in this analysis provides an alternative metric to exergy. The exergy output (cooling) of an absorption refrigerator, quantifies the irreversibility of the cooling provided which is challenging to relate back to the main output of the BioCPV power plant, electricity. Whereas using the avoided electrical consumption provides a metric that can easily be related to the electrical output of the power plant. The following section provides the modelling approach for this.

Using R134a (1,1,1,2 - tetrafluoroethane) as a refrigerant and the following assumptions:

1. No losses between components.
2. Throttle is isenthalpic.
3. Compressor has an electrical efficiency of 50% (based on personal industrial experience).
4. The refrigerant leaves the evaporator as a saturated vapour.
5. Condenser temperature is 8°C above ambient based on average difference found in absorption refrigerator modelling.
6. Refrigerant leaves the compressor as a superheated vapour calculated as 10 kJ·kg^{-1} above the enthalpy of dry saturated vapour at the condenser temperature.

The thermal energy absorbed by the evaporator of the vapour compression refrigerator ($Q_{EV_{VC}}$) is equal to the thermal energy absorbed by the evaporator of the absorption refrigerator (Q_{EV}).

$$Q_{EV_{VC}} = Q_{EV} \tag{4.97}$$

Enthalpy data has been extracted from the Technical Information Sheet for HFC-134a provided by DuPont Suva Refrigerants (DuPont Suva 2016) and copied into a spreadsheet. A series of lookup functions find the necessary values within the model.

The evaporator output enthalpy ($h_{EV_{out_{VC}}}$) can be found using the evaporator temperature from the absorption refrigerator and the assumption that the refrigerant leaves the evaporator as a saturated vapour. The evaporator input enthalpy can be found with the assumptions for the condenser temperature.

$$T_{CO_{VC}} = T_{AMB} + 8\ (^{\circ}\mathrm{C}) \tag{4.98}$$

The condenser output enthalpy ($h_{CO_{out_{VC}}}$) can be found using the assumption that that it leaves the condenser as a saturated liquid. This enthalpy can then be used with the assumptions that there are no losses between components and that the throttle is isenthalpic. The input and output enthalpies of the throttle ($h_{TH_{inVC}}$ and $h_{TH_{out_{VC}}}$) as well as the evaporator input enthalpy ($h_{EV_{in_{VC}}}$) all equal the condenser output enthalpy.

$$\begin{aligned} h_{CO_{out_{VC}}} &= h_{TH_{in_{VC}}} \\ &= h_{TH_{out_{VC}}} \\ &= h_{EV_{in_{VC}}} \end{aligned} \tag{4.99}$$

Using a rearranged energy balance the mass of the refrigerant in the vapour compression cycle ($m_{R_{VC}}$) can be calculated, where $Q_{EV_{VC}}$ is the cooling energy of the vapour compression refrigerator, $h_{EV_{out_{VC}}}$ and $h_{EV_{in_{VC}}}$ are the output and input enthalpies of the evaporator of the vapour compression refrigerator respectively.

$$m_{R_{VC}} = \frac{Q_{EV_{VC}}}{h_{EV_{out_{VC}}} - h_{EV_{in_{VC}}}} \tag{4.100}$$

Assuming no losses, the compressor input enthalpy ($h_{comp_{in_{VC}}}$) equals the evaporator output enthalpy ($h_{EV_{out_{VC}}}$).

$$h_{comp_{in_{VC}}} = h_{EV_{out_{VC}}} \tag{4.101}$$

Likewise the compressor output enthalpy ($h_{comp_{out_{VC}}}$) equals the condenser input enthalpy ($h_{CO_{in_{VC}}}$).

$$h_{comp_{out_{VC}}} = h_{CO_{in_{VC}}} \tag{4.102}$$

Therefore the ideal compressor work ($E_{comp_{VC_{ideal}}}$) can be calculated using an energy balance across the compressor.

$$E_{comp_{VC_{ideal}}} = m_{R_{VC}} \left(h_{comp_{out_{VC}}} - h_{comp_{in_{VC}}} \right) \tag{4.103}$$

Taking the compressor efficiency into account ($\eta_{comp_{VC}}$) the actual electrical consumption of the compressor and therefore the vapour compression refrigerator ($E_{comp_{VC}}$) can be calculated.

$$E_{comp_{VC}} = \frac{Q_{comp_{VC_{ideal}}}}{\eta_{comp_{VC}}} \tag{4.104}$$

This provides the metric to compare the performance of the absorption refrigerators investigated in this thesis to the electrical output of the BioCPV power plant.

4.5 Presentation of Results and Discussions

The following three chapters present the results and discussions for the investigation of low temperature discontinuous waste heat utilisation from a renewable power plant in rural India for absorption refrigeration, using acetone and zinc bromide as the working fluid. They are separated as follows:

- **Power Plant Energy Utilisation** presents an assessment of the energy and exergy of the power plant described in Section 2.3 using the methods described in Section 4.1 and 4.4. This allows quantification of the amount of waste heat available and its quality.

- **Absorption Refrigeration Experiment** presents the findings of a physical experiment used to provide insight into the validity of the modelling assumptions and the practicalities of operating an absorption refrigeration system.
- **Absorption Refrigeration Modelling** presents the findings from investigations using the modelling approach described in Section 4.3, to utilise the waste heat from an internal combustion engine electrical generator set (genset) radiator and a concentrated photovoltaic (CPV) system for absorption refrigeration in the conditions expected in rural India. It also investigates the viability of the absorption refrigerator system configurations selected in the Chapter 3.

  The approach initially identifies the important variables, some of their operating limitations and their effects on the operation of absorption refrigeration systems in the conditions expected in rural India using the specified heat sources. The impact of factors such as ambient temperature and heat exchanger effectiveness on key components (such as the condenser and absorber) and solution concentration limits form part of this analysis.

  The theoretical cooling output from single effect absorption refrigeration systems powered by each heat source is presented at a variety of ambient temperatures. The effect of the difference in strong and weak solution concentration is examined with refrigeration systems powered by both heat sources at varying ambient temperatures. This is followed by an investigation of the evaporator tap-off method, which uses water as a heat transfer fluid to cool the absorber and condenser. The results are extrapolated to assess the viability of the configurations identified in Chapter 3.

Chapter 5

Power Plant Energy Utilisation

The following chapter presents the energy and exergy profile of the BioCPV rural renewable power plant. The energy and exergy flows through power plant originate with solar power entering the concentrated photovoltaic (CPV) and a biogas fuel, which is later mixed with hydrogen before being consumed by the internal combustion engine electrical generator set (genset). These flows are broken down into losses (such as optical, ancillary and heat) and electricity. The electrical flow can then be followed to the users which in this case is the 45 household community within the villages of Kaligung and Pearson-Palli to determine the systems energetic and exergetic (or rational) efficiency.

5.1 Energy Profile

The following section presents the energy profile of the BioCPV renewable power plant. The CPV and genset are assessed to quantify the input energy into the power plant and the losses from electricity generation. Assumptions from the partners in the BioCPV research group are used to quantify the electrical losses within the system. This process provides the information

Table 5.1: CPV energy balance.

	Power kW	Daily Energy kW·h	Percentage of Solar Input
Solar Input Energy	33.3	233	100%
Optical Losses	6.7	47	20%
Thermal Losses	16.6	116	50%
Electrical Output	10	70	30%

for a Sankey diagram to be generated allowing a visual representation of the energy flows through the power plant.

The energy profile of the CPV and generator are calculated differently as the generator is an "off the shelf" component where generic operating assumptions have been used. Conversely the CPV is being designed by some of the partners and details of the specific operating conditions are from their design specification.

5.1.1 Concentrated Photovoltaic

To simplify the modelling process the CPV is assumed to operate at a constant load for 7 hours per day, this was a collective decision of the research partners at the time of the initial designs. The electrical output of the CPV system has been calculated from Section 4.1.1. The heat output is based on the assumption that all the unused energy falling on the PV cell will be converted to heat due the optical efficiency taking into account any reflective losses. Using the rated conditions which are 25°C and 1 atmosphere Table 5.1 shows the energy balance of the CPV system. This data is later used to form a Sankey diagram.

CPV Efficiency Analysis

The electrical and heat output of the CPV are a function of PV cell efficiency which is a function of cell temperature and concentration ratio, as the concentration ratio is fixed at 500 suns by the design specification from University of Exeter and Indian Institute of Technology Madras, the following analysis only considers PV cell temperature. Figure 5.1 is a graph of the relationship between PV cell efficiency and PV cell temperature. The graph uses Equation 4.4 provided by the PV cell manufacturer Azur Space for typical performance of their triple junction PV cells. It shows that raising the cell temperature from 25°C to 100°C decreases the efficiency by 3%. This, combined with the already mentioned risks of localised overheating is not considered to be significant to warrant an analysis of operating the CPV at different temperatures.

The manufacturer provides an operating range of 25°C to 80°C, and 60°C

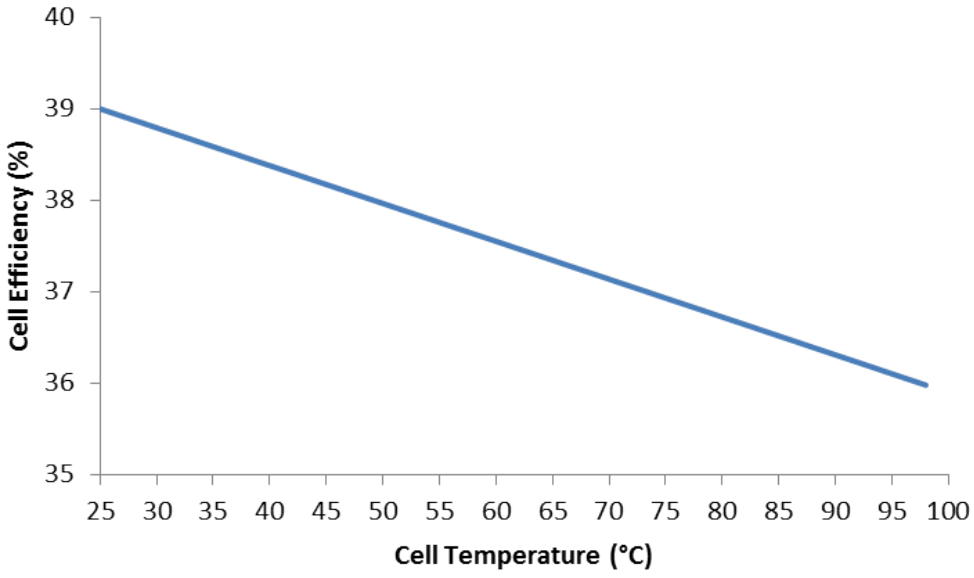

Figure 5.1: PV cell efficiency as a function of cell temperature using Equation 4.4 provided in confidence by PV manufacturer Azur Space.

Table 5.2: Combustion calculation to find the energy contained within the exhaust from the hydrogen part of the fuel.

		$2H_2$	+	$1.2O_2$	+	$4.512N_2$	→	$2H_2O$	+	$4.512N_2$	+	$0.2O_2$
Moles	kmol	2		1.2		4.512		2		4.512		0.2
Molar mass	$kg \cdot kmol^{-1}$	2.016		31.999		28.013		18.015		28.013		31.999
Molar mass x mass	kg	4.03		38.4		126.4		36		126.4		6.4
Mass ratio		0.024		0.227		0.749		0.213		0.749		0.038
Mass flow rate	$kg \cdot s^{-1}$	7.05E-06		6.72E-05		2.21E-04		6.30E-05		2.21E-04		1.12E-05
h at 350°C	$kJ \cdot kg^{-1}$							3176		657		583
h at 25°C	$kJ \cdot kg^{-1}$							105		309		271
Energy in exhaust	kW							0.19		0.077		0.003
Total energy from hydrogen in exhaust				**0.27kW**								

has been selected as the desired operating temperature by the partners responsible for the CPV. During testing without cooling the partners responsible for the CPV found that the PV cells failed from over heating. This finding provides a motive for utilising the waste heat from the CPV system as the system requires some form of heat removal for stable operation.

5.1.2 Internal Combustion Engine Electrical Generator

The generator input energy is calculated as a function of the assumed efficiency of 25% and electrical output requirement of 5 kW over 4 hours providing a daily electrical energy of 20 kW·h and fuel input of 80 kW·h. The biogas composition by volume is assumed to be 60% methane and 40% carbon dioxide (based on the specifications from University of Leeds and Visva-Bharati) and the hydrogen available is equivalent to 4 kW·h per day which equates to 5% the fuel input energy (2% of the fuel mixture by mass). The hydrogen availability is based on 7 kW·h per day of excess electricity from the CPV. The design specifications of the electrolyser and metal hy-

Table 5.3: Combustion calculation to find the energy contained within the exhaust from the biogas part of the fuel.

		$0.67CO_2$ +	CH_4 +	$2.4O_2$ +	$9.024N_2$ →	CO_2 +	$2H_2O$ +	$9.024N_2$ +	$0.4O_2$
Moles	kmol	0.67	1	2.4	9.024	1.67	2	9.024	0.4
Molar mass	$kg \cdot kmol^{-1}$	44.01	16.043	31.999	28.013	44.01	18.015	28.013	31.999
Molar mass x moles	kg	29.3	16.0	76.8	252.8	73.4	36	252.8	12.8
Mass ratio		0.078	0.043	0.205	0.674	0.196	0.096	0.674	0.034
Mass flow rate	$kg \cdot s^{-1}$	6.26E-04	3.42E-04	1.64E-03	5.39E-03	1.56E-03	7.68E-04	5.39E-03	2.73E-04
h at 350°C	$kJ \cdot kg^{-1}$					531	3176	657	583
h at 25°C	$kJ \cdot kg^{-1}$					213	105	309	271
Energy in exhaust	kW					0.5	2.36	1.87	0.085
Total energy from biogas in exhaust			**4.82 kW**						

dride energy storage system expect a combined efficiency of 60%, which has been provided in parallel with this research by the University of Nottingham as part of the BioCPV project.

Higher heating values have been used as it is assumed that the heat in the vapour of the exhaust gases will be used through condensing heat exchangers. The calculated fuel mass flow rates:

- Hydrogen: 7.05×10^{-6} $kg \cdot s^{-1}$
- Biogas: 6.26×10^{-4} $kg \cdot s^{-1}$

Tables 5.2 and 5.3 show the calculation for the energy within the exhaust gases using a combination of combustion chemistry and textbook enthalpy values for the assumed temperature of the exhaust gases at 350°C and an ambient temperature of 25°C from Rogers and Mayhew (1995).

Table 5.4, the generator energy balance, can be drawn by summing the results of Tables 5.2 and 5.3 and using the assumptions stated in the Analytical Methodology Chapter Section 4.1.2.

Table 5.4: Internal combustion engine electrical generator energy balance.

	Power kW	Daily Energy kW·h	Percentage of Fuel Input
Fuel Input Energy	20	80	100%
Electrical	5	20	25%
Exhaust Losses	5	20	25%
Ancilleries Losses	2	8	10%
Radiator Losses	8	32	40%

5.1.3 Renewable Power Plant Energy Flow

The data presented earlier in this section has been used to draw Figure 5.2 a Sankey diagram which shows the flow of energy through the BioCPV renewable power plant. It uses the following additional assumptions provided by the partners in the project:

- The solar trackers use 2 kW and are active during CPV operation (7 hours), providing a daily energy load of 14 kW·h.
- The system ancillaries equal 0.5 kW but run for 24 hours, providing a daily load of 12 kW·h.
- Electricity generation (rated) values are 10 kW for CPV and 5 kW for genset
- Waste heat sources are:
  - 60°C for CPV
  - 80°C for genset radiator
  - 350°C for genset exhaust

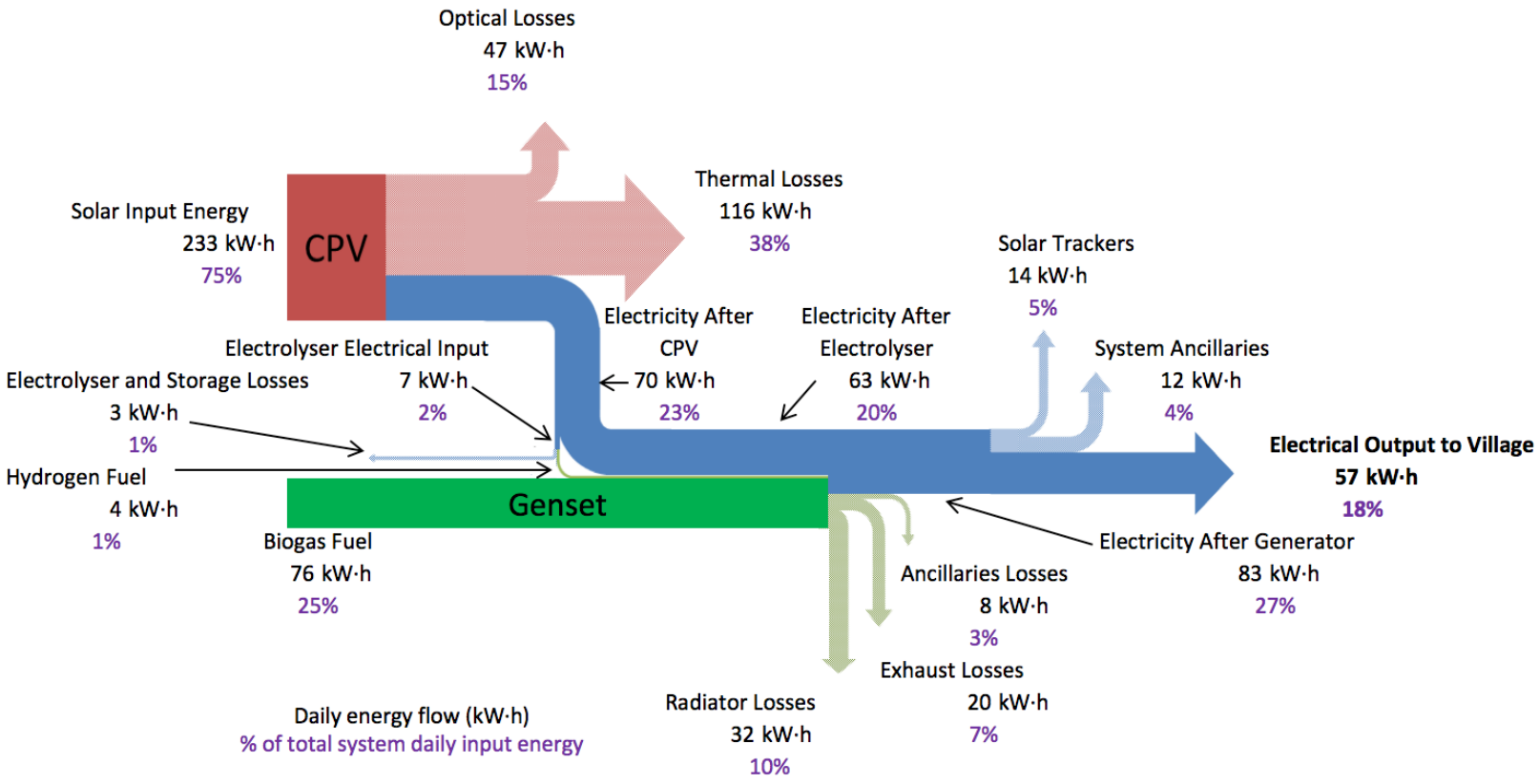

Figure 5.2: Sankey diagram of daily energy flow in BioCPV power plant.

Figure 5.2 is a Sankey or energy flow diagram of the BioCPV rural renewable power plant for a 24 hour period. Figure 5.2 shows that 18% (57 kW·h) of the total energy input goes to the village as electricity, therefore the system has an electrical efficiency of 18%. The unrecoverable losses are: the optical losses at 15%, solar trackers at 5%, system ancillaries at 4%, electrolyser and hydrogen storage losses at 1% and genset ancillaries at 3%. Unrecoverable losses equal 28% (85 kW·h) of total energy input. The single largest loss, which is also recoverable is the thermal losses from the CPV at 38% of the total energy input. The other recoverable losses are the genset radiator losses at 10% and the exhaust losses at 7%.

The exhaust heat due to its high temperature is being considered for a water purification process and is outside the scope of this research. There is 116 kW·h per day of low temperature thermal energy lost from CPV, which equates to 38% of the total system input energy. The utilisation of this significantly large proportion of the total system input energy is investigated later in Chapter 7 for absorption refrigeration.

The exergy analysis in Figure 5.3 of the BioCPV plant over a 24 hour period in the following section, relates these energy values to their energy quality in a 25°C environment. Broadly speaking, in this analysis, it can be considered as the maximum theoretical work that can be achieved from the energy source in a 25°C environment.

5.2 Exergy Profile

In a similar process to the previous section, this section displays the results of the exergy analysis. In which the exergy flows of the BioCPV power plant are calculated, using the process outlined in Section 4.4, to allow the construction of a Grassman diagram. The following subsections calculate

Table 5.5: CPV exergy balance.

	Exergy Power kW	Daily Exergy kW·h	Percentage of Solar Input
Solar Input Exergy	31	217	100%
Electricity	10	70	32%
Exergetic optical losses	6.2	43	15%
Thermal exergy	1.7	12	6%
Exergy destroyed	13.1	91	47%

the exergy flows in the CPV and genset separately and are followed by the graphic presentation the results in a Grassman diagram.

5.2.1 Concentrated Photovoltaic

The exergy flows through the CPV are calculated using the approach described in Section 4.4.1 and are presented in Table 5.5. The input solar exergy is calculated using an effective collector area adapted from Petela (2010) energy and exergy calculation of a PV cell. The exergetic optical losses are based on the design criteria of an 80% optical efficiency. The exergy content in the thermal losses uses the thermal energetic loss calculated in Section 5.1.1 and the Carnot efficiency of the CPV heat source. The remaining exergy is known as the exergy destroyed and is an indicator of the irreversibility of the CPV system.

The exergy contained in the radiation from the sun has a lower value than its energy, 217 kW·h compared with 233 kW·h. This is to be expected as the efficiencies of solar powered technologies indicate that it is not possible to entirely convert radiative energy into work. Likewise the optical losses have reduced from 47 kW·h per day to 43 kW·h. The most significant reduction is from the thermal losses from 116 kW·h per day to 12 kW·h, this is to be expected as the Carnot efficiency of a 60°C heat source in a 25°C environment is 10.5% resulting in little work potential.

Table 5.6: Calculation of flow exergy within the genset exhaust by separating each product of combustion of the biogas-hydrogen fuel mix.

		CO_2	+	H_2O	+	N_2	+	O_2
Molar Mass	$kg \cdot mol^{-1}$	44.01		18.015		28.013		31.999
Enthalpy at 25°C	$kJ \cdot kg^{-1}$	213		550		309		271
Enthalpy at 350°C	$kJ \cdot kg^{-1}$	531		1179		652		580
$h_{623K} - h_{298K}$	$kJ \cdot kg^{-1}$	318		629		342		309
Entropy at 25°C	$kJ \cdot kg^{-1} \cdot K^{-1}$	4.86		10.48		6.84		6.41
Entropy at 350°C	$kJ \cdot kg^{-1} \cdot K^{-1}$	5.57		11.90		7.61		7.11
$s_{623K} - s_{298K}$	$kJ \cdot kg^{-1} \cdot K^{-1}$	0.71		1.42		0.77		0.70
Mass	$kg.s^{-1}$	1.56E-03		8.31E-04		5.61E-03		2.84E-04
Exergy	kW	0.17		0.17		0.63		0.03
Total Exergy in Exhaust					**1**	kW		

5.2.2 Internal Combustion Engine Electrical Generator

The exergy flows through the genset are calculated using the approach described in Section 4.4.2 and presented in Table 5.7. This required calculating the exergy content of the fuel mixture and the exhaust. The thermal energy in the radiator of the genset calculated in Section 5.1.2 can be converted to exergy using the Carnot efficiency. The remaining exergy is known as the exergy destroyed and is an indicator of the irreversibly of genset system.

The exergy in the exhaust presented in Table 5.6 was calculated using Equation 4.95 for flow exergy and the products of combustion calculated in Tables 5.2 and 5.3. Table 5.6 shows the flow exergy within the exhaust is 1 kW which over 4 hours operation will provide 4 kW·h per day of exergy compared to the energetic value of 20 kW·h per day. This indicates that maximum theoretical efficiency for a system generating work from the exhaust would only be 20% and further justifies the use of the exhaust heat for water purification.

Table 5.7 presents the exergy flow through the genset. The exergy con-

Table 5.7: Genset exergy balance.

	Exergy Power kW	Daily Exergy kW·h	Percentage of Fuel Input
Fuel Input Energy	18.5	74	100%
Electrical	5	20	27%
Exhaust Losses	1	4	5%
Ancilleries Losses	2	8	11%
Radiator Losses	1.2	5	7%
Exergy Destroyed	9.3	37	50%

tent of the fuels was calculated using the molar exergetic heating values from Bejan (1997) and converted with their respective molar masses to be used with the mass flow rates calculated in Tables 5.2 and 5.3. The information in Table 5.6 provides the exhaust exergy. The exergy in the radiator was calculated using the Carnot efficiency of the radiator and the thermal energy contained in the radiator calculated in Table 5.4. The electrical energy generated has an equal exergetic value and the remaining exergy is the exergy destroyed.

The exergy content of the biogas-hydrogen fuel mixture is 74 kW·h compared to an energetic value of 80 kW·h indicating a relatively small (7.5%) irreversibility of chemical energy of the fuel source. The radiator exergy output is low at 5 kW·h per day compared with an energetic value of 32 kW·h indicating that this energy source is highly irreversible and the generation of work would not utilise it well. 37 kW·h of exergy would be destroyed daily with this system which is equivalent to 50% of the total fuel exergy input. Table 5.7 also shows the exergetic or rational efficiency of the genset is 27%. This is higher than the energetic efficiency of 25% because exergy takes into account the exergetic value of the inputs which in this case is fuel.

5.2.3 Renewable Power Plant Exergy Flow

Figure 5.3 is a Grassman or exergy flow diagram of the BioCPV rural renewable power plant over a 24 hour period. It shows that the electrical output is 20% of the total exergy input, therefore the system has a rational efficiency of 20%. This increase from energetic to exergetic efficiency is a result of the energy inputs (solar and biogas) being rationalised in terms of exergy. It also shows that the recoverable waste energy sources have low exergetic values compared to their energetic values: thermal losses from the CPV are 12 kW·h per day in comparison to 116 kW·h per day and radiator losses are 5 kW·h per day in comparison to 32 kW·h per day. The low temperature waste heat sources collectively have a combined theoretical maximum work output of 17 kW·h per day which could change the rational efficiency of the whole system from 20% to 26%. Comparing this to their energy values in Figure 5.2 of 148 kW·h, which would raise the system energy efficiency from 18% to 66%, indicates the importance of effective energy utilisation when energy quality is vastly different.

The exergy of these heat sources is quantified by the maximum work output of a Carnot heat engine. Carnot engines present the maximum theoretical efficiency between a hot and cold source. A common form heat engine for low temperature waste heat applications is an organic Rankine cycle. The results of Glover et al. (2015), Peris et al. (2015) Desideri et al. (2016) on organic Rankine cycle generators, suggest efficiencies of 1% to 5% from heat sources under 100°C. Exergy analysis provides a useful theoretical tool to compare energy sources in terms of quality. However, practical outputs need to be taken into consideration when comparing the utilisation of an energy source to its exergetic quantity.

The main outcome of this analysis is that these low temperature waste heat sources have a low energy quality and therefore should not be consid-

ered for the generation of work and electricity. However, these waste heat sources can be better used elsewhere. Generally the optimum uses of low temperature waste heat sources are space or water heating as this is a direct use and if designed appropriately could make use of almost all of the waste energy. The problem is that hot water is not an important need in this location whereas refrigeration, which could be used to store food and medicines or cool a recovery room in a health centre, would be welcomed. This energy and exergy analysis together with the practical needs of the community and the objectives of the collaborative research group provides the motive for this body of research in investigating the utilisation of low temperature waste heat sources from a renewable power plant in rural India for absorption refrigeration.

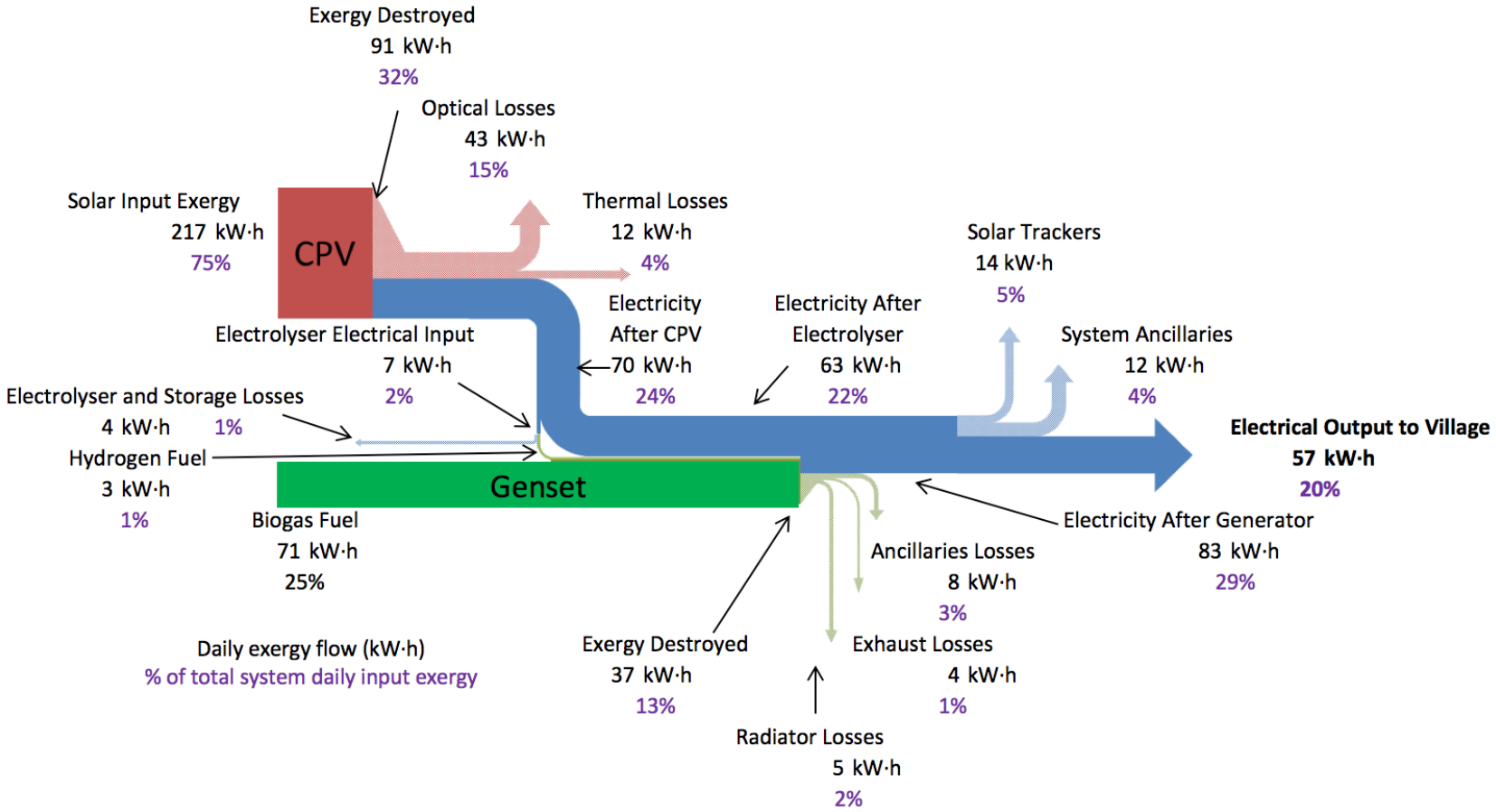

Figure 5.3: Grassman diagram of daily exergy flow in BioCPV power plant.

Chapter 6

Absorption Refrigeration Experiment

This chapter presents the results of a lab scale experimental test rig. A once through single effect cycle with reservoirs absorption refrigerator was built to gain insight in to the operational performance and challenges of an acetone and zinc bromide absorption refrigerator. Using reservoirs also provided the opportunity to assess the possibility of using discontinuous heat sources to provide continuous refrigeration. Continuous refrigeration in this context refers to refrigeration that occurs over 24 hour period, 7 days a week, without disruption.

This chapter consists of:

- **Test Description** presents the test rig together with the aid of a schematic describing the process of the experiment.
- **Results** presents the results of this experimental test.
- **Conclusions** presents the main findings of this experiment.
- Photos of the experimental test rig are presented at the end of the chapter to help visualise the system. Some of the photos also provide evidence for the fluid state.

6.1 Test Description

The test rig, shown schematically in Figure 6.1 and physically in Figures 6.9 to 6.12, consists of a 1 litre loading reservoir which holds the weak solution. The boiler simulates the heat from CPV or genset radiator by using a 250 W strip heater mounted to a flat plate heat exchanger with 5 k-type thermocouples positioned along it, shown schematically in Figure 6.3. The strong solution leaving the boiler enters the strong solution reservoir which uses a Dreschel bottle attachment to separate the refrigerant from the strong solution. The refrigerant vapour flows up to the condenser (a Leibig condenser) which is connected to the refrigerant reservoir. The strong solution leaves the strong solution reservoir via a valve at the base and flows into the absorber which also uses a Dreschel bottle attachment connected to a Leibig condenser. The refrigerant flows from the refrigerant reservoir through the evaporator (another Leibig condenser) where it evaporates and absorbs heat. It then meets the strong solution in the absorber from the other Dreschel port. The weak solution leaving the absorber is collected in a second weak solution reservoir, where the test ends.

Cooling of the condenser and absorber, as well as the heat source for the evaporator was provided by mains supply water, through the cooling jacket of the Leibig condenser vessels used for each of these. The condenser had a dedicated tap supplying cooling water whereas the evaporator and absorber shared a tap. This was due to limited availability of mains water taps and that the condenser is likely to have the highest demand for cooling water. The flow rate and temperature of the cooling water were not controllable as they would fluctuate depending on other users in the building. Flow rate tests conducted at the end of the experiment showed 11 to 12 $g \cdot s^{-1}$ in the absorber and evaporator and 24 $g \cdot s^{-1}$ in the condenser.

Between each component there is a k-type thermocouple and there are five

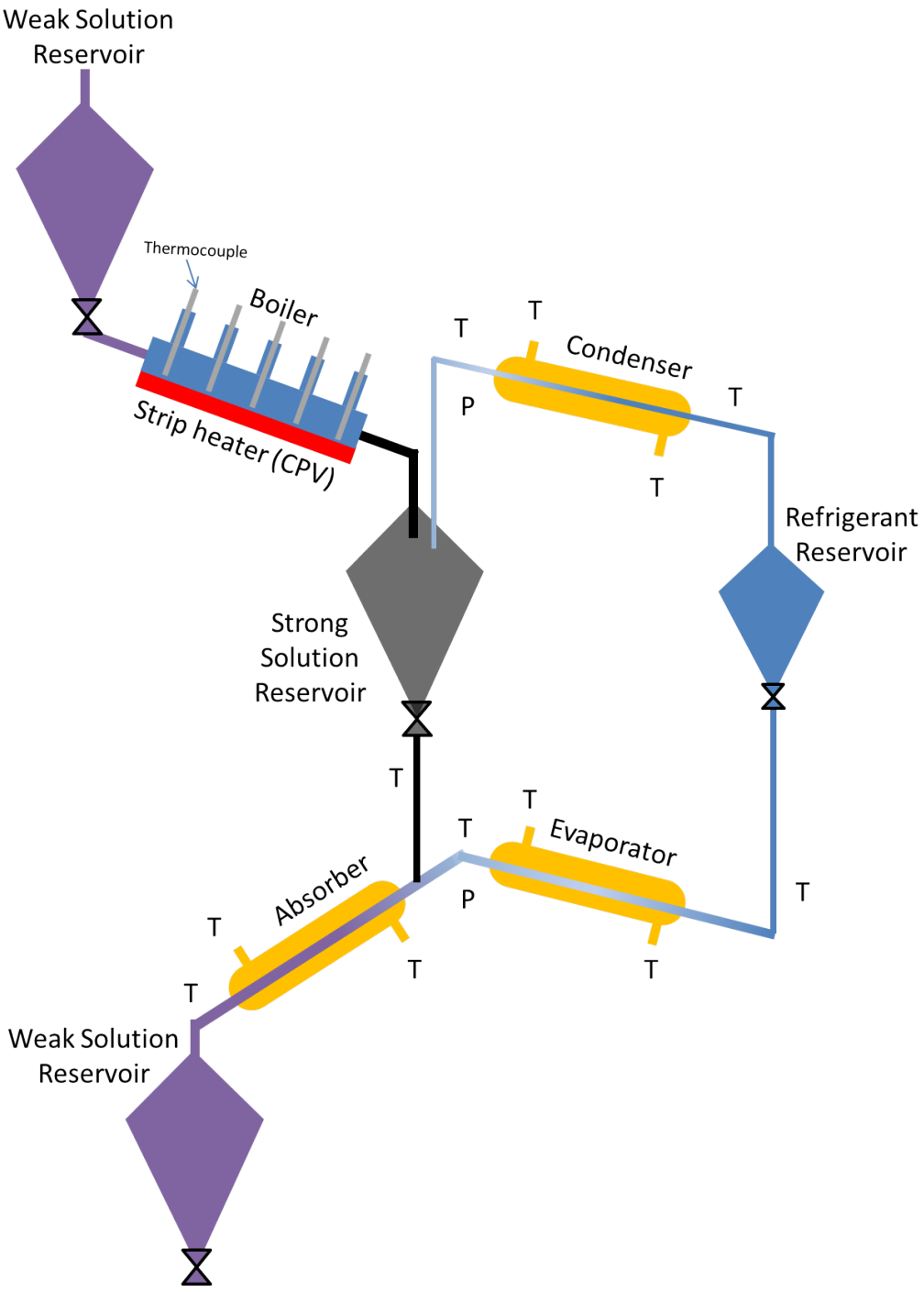

Figure 6.1: Absorption refrigerator experiment testing equipment schematic (P denotes pressure transducer and T thermocouple).

thermocouples placed along the boiler. The thermocouples are sealed with graphite ferrules into Swagelok unions. There are two GE Unik 5000 pressure transducers; one 0 to 3 bar absolute for the high pressure side between the strong solution reservoir and the condenser, and another 0 to 2 bar absolute for the low pressure side between the evaporator and absorber. The pressure transducers are also connected to Swagelok unions. The Swagelok unions are sealed to the glass fittings using EPDM hose and o-clips. All the glass to glass contacts were sealed using Dow Corning High Vacuum Grease. The system requires the air to be evacuated before commencing a test to minimise the gas mixing effect of the air and acetone vapour.

The fluids are moved by gravity and vapour pressure alone. The test is a once through; starting at the highest point and ending at the lowest. At the end of the test, as part of the reloading procedure, air is let in from the top to help flush the remaining solution through. When this is complete the components are cleaned, seals re-greased and the air evacuated. The collected solution is then transferred to the weak solution reservoir used for loading at the top of the rig. Tests were repeated to ensure the reproducibility of results, the results presented here are not all from the same test run.

6.2 Results

The following subsections present the results and are broken down as follows:

- **Overview** presents the results for the temperature of the boiler and the evaporator and provides information about the operating times of the boiler and evaporator.
- **Boiler** presents a number of tests related to the boiler operation including the solutions ability to maintain a boiler operating temperature and the conditions that determine the pressure of the high pressure side.

- **Condenser** presents the findings to suggest the input and output state of the refrigerant in the condenser.
- **Evaporator** presents the findings to indicate the input and output state of the refrigerant in the evaporator.
- **Absorber** presents the findings to indicate the operation of the absorber and provides insights into fluid state within the component.

6.2.1 Overview

Figure 6.2 shows an overview of the experimental results. The blue line corresponds to the average boiler temperature. The sudden rise in the blue line after 574 seconds shows the heater was turned on. The sudden drop at 701 seconds is when the weak solution was released into the boiler. The period between 701 and 904 seconds is when the boiler is heating the weak solution and the period after is when the weak solution had stopped flowing through the boiler and the temperature rose rapidly. The heater was turned off shortly after as indicated by the period of cooling after 1001 seconds.

The boiler heating period indicates that an acetone and zinc bromide solution can be used to cool the heat source in these conditions to below 60°C, suggesting that an acetone and zinc bromide solution can be used to cool the heat source by utilising that heat for absorption refrigeration. This also indicates that in the wider context of this project an acetone and zinc bromide absorption refrigerator can be used to cool the CPV system to below 60°C. This finding can be further justified with Figure 6.4.

The red line corresponds to the evaporator temperature. At 942 seconds the drop in temperature indicates the evaporator working and providing cooling. The evaporator continues to provide cooling until 2668 seconds. The decay at this point could be a result of several factors including: the weak solution in the absorber and end weak solution reservoir warming up, the

strong solution and refrigerant had been used up, or a slow rate of heat transfer into the components once the test had finished.

The difference in the operating times between the boiler and evaporator, 203 seconds and 1,726 seconds respectively, indicates that an absorption refrigerator with reservoirs can use a discontinuous heat source to provide a considerably longer period of cooling. If a solution pump was used, this system could provide continuous cooling from a discontinuous heat source.

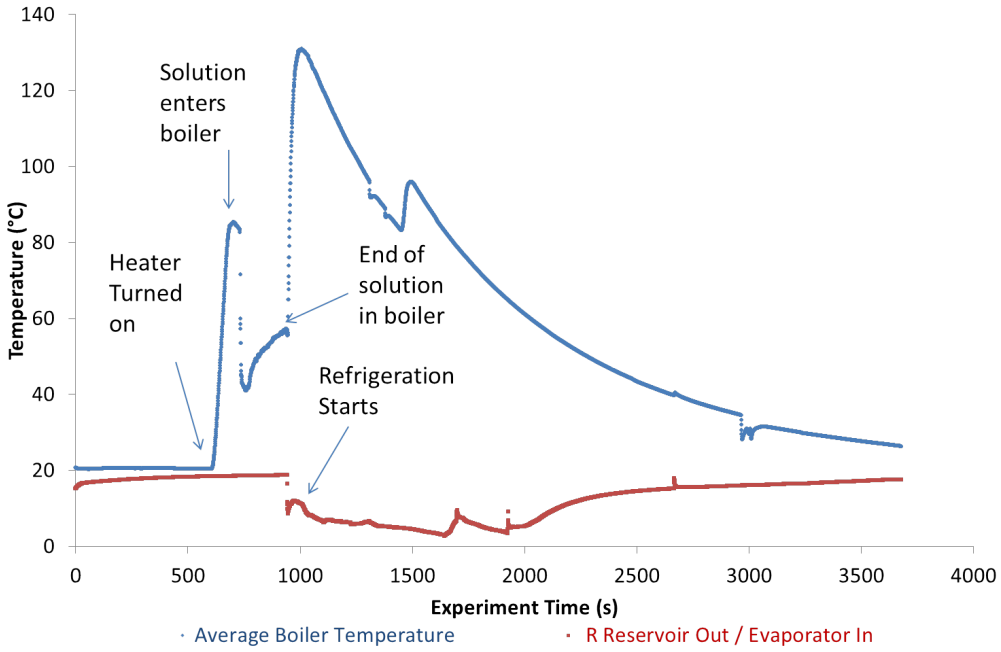

Figure 6.2: Boiler temperature and evaporator temperature with respect to experiment time, where the blue line corresponds to the average boiler temperature and the red line is the evaporator inlet temperature. Test details: weak solution concentration $\left(\frac{m_{ZnBr_2}}{m_{solution}}\right)$ at inlet 62% and 703 g of solution collected.

6.2.2 Boiler

Figure 6.3 is a schematic of the boiler showing the position of the five thermocouples used to measure the temperature profile across the boiler. Figure 6.4 shows the temperature recorded by the 5 thermocouples during a boiler operation test. The solution reaches the boiler at 498 seconds, indicated by the sudden drop in temperature at all thermocouple positions, and the solution stops flowing through the boiler at 992 seconds, indicated by the sudden rise in temperature at all thermocouple positions. There is a small rise of 11°C at 829 seconds at thermocouple position 5 (T_{BO_5}) which is near the exit of the boiler. This is likely to be a result of the solution flow rate slowing down at the end of the test.

A consistent temperature is achievable at each thermocouple position. This indicates that a solution of acetone and zinc bromide can be used to cool and maintain the temperature of a heat source like the CPV or genset radiator. However the difference in temperature between the thermocouple positions indicates that there is a need to investigate the heat exchanger

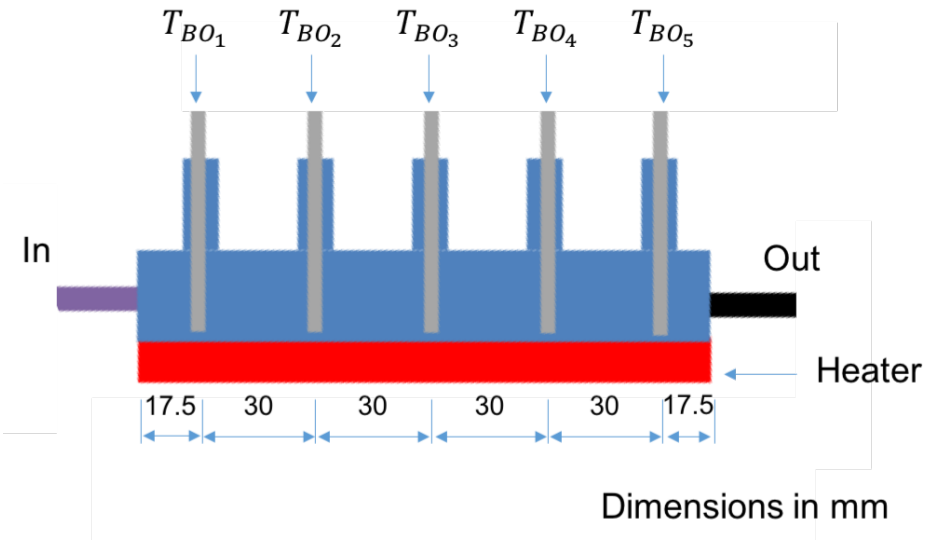

Figure 6.3: Boiler schematic showing the positions of all five thermocouples.

design, particularly for the CPV, to ensure the thermal management is satisfactory.

In Figure 6.5 the blue line shows the average boiler temperature. The red line is the pressure from the high pressure side which is measured between the strong solution reservoir and the condenser. During the period of boiler operation between 701 to 904 seconds the pressure and average boiler temperature follow the same profile. After 904 seconds the solution is no longer entering the boiler and the temperatures correspond to the boiler heating without fluid flowing through. This graph shows that the pressure in the high pressure side is maintained after the boiler stops. However it should be noted that the pressure was measured between the strong solution reservoir

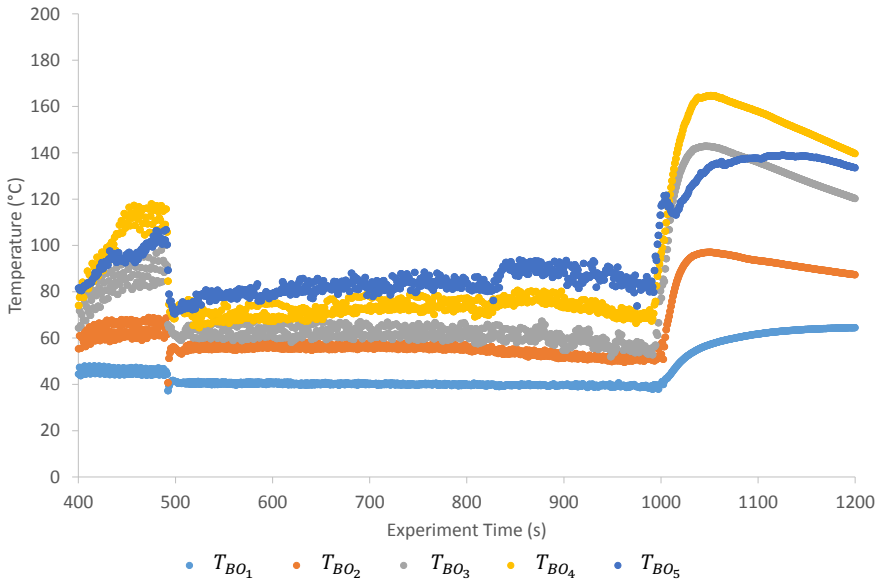

Figure 6.4: Boiler temperature showing the temperature readings from all five thermocouples in the boiler T_{BO_1} to T_{BO_5} (using the thermocouple locations shown in Figure 6.3). Test details: weak solution concentration $\left(\frac{m_{ZnBr_2}}{m_{solution}}\right)$ at inlet 51.7% and 1171 g of solution collected.

and the condenser. Temperature stratification throughout the strong solution reservoir (hot at the top and cooler at the bottom) was identified by touching the wall of the reservoir. Considering the pressure was maintained after boiler operation. This indicates that the conditions at the top of the reservoir determine the pressure of the high pressure side, which gradually cools as shown by the steady drop in pressure in Figure 6.5. This finding shows the importance of boiler exit and strong solution reservoir inlet design to maintain the solution temperature until the refrigerant has condensed.

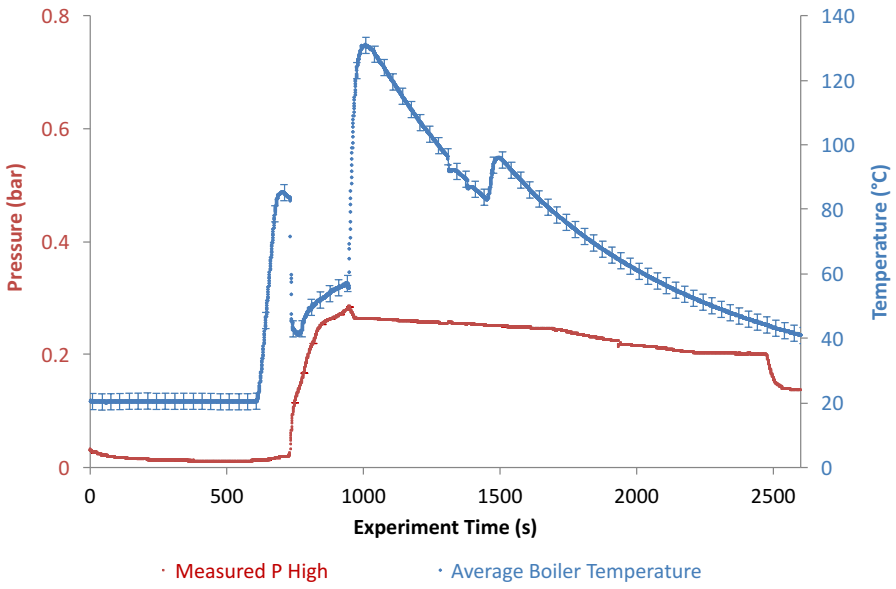

Figure 6.5: Average boiler temperature (blue line, right axis) and pressure of the high pressure side measured by the transducer between the strong solution reservoir and the condenser (red line, left axis). Test details: weak solution concentration $\left(\frac{m_{ZnBr_2}}{m_{solution}}\right)$ at inlet 62% and 703 g of solution collected.

6.2.3 Condenser

Figure 6.6 shows that once steady state is achieved in the condenser (at 1716 seconds) the red line which is the input to the condenser (from the boiler) is at a higher temperature than the condenser output temperature (green line). The condenser output and the saturation temperature based on the pressure at this point of the experiment appear to follow each other closely, this indicates that the acetone entering the condenser is in a superheated state. From visual inspection and shown in Figure 6.11 the refrigerant was a liquid at the exit of the condenser and its temperature (the green line) is at the saturation temperature (blue line). In Figure 6.6 it is likely that

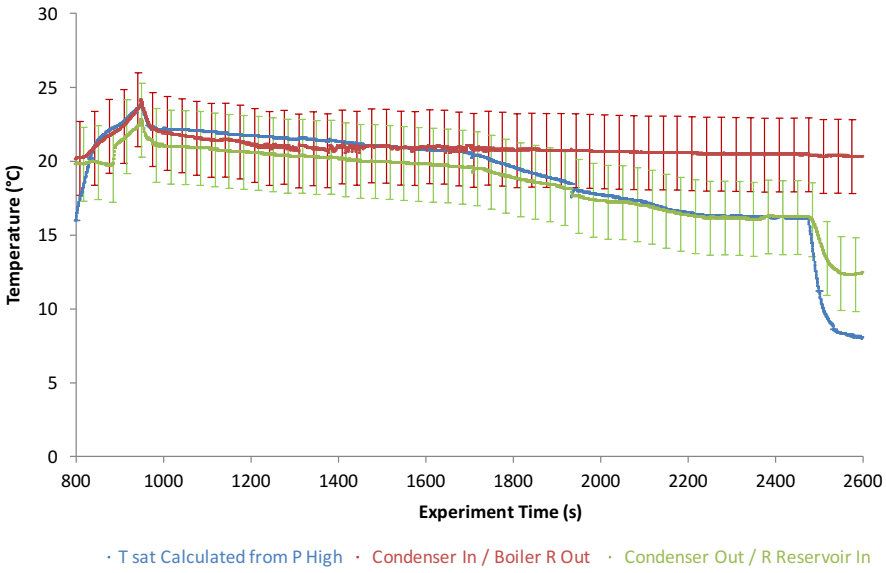

Figure 6.6: Operating temperatures of the condenser (green line for inlet and red line for outlet) with the high pressure converted to acetone saturation temperature using Equation 4.15 (blue line). Test details: weak solution concentration $\left(\frac{m_{ZnBr_2}}{m_{solution}}\right)$ at inlet 62% and 703 g of solution collected.

the period before steady state in the condenser was heavily influenced by the boiler operation and the decay in the period of steady state by the slow cooling of the strong solution in the strong solution reservoir shown in Figure 6.5.

6.2.4 Evaporator

In Figure 6.7 the green line is the output temperature of the evaporator, the red line is the input temperature of the evaporator and the blue line is the saturation temperature of acetone calculated (using Equation 4.15) from the low pressure reading, measured between the evaporator and absorber. The

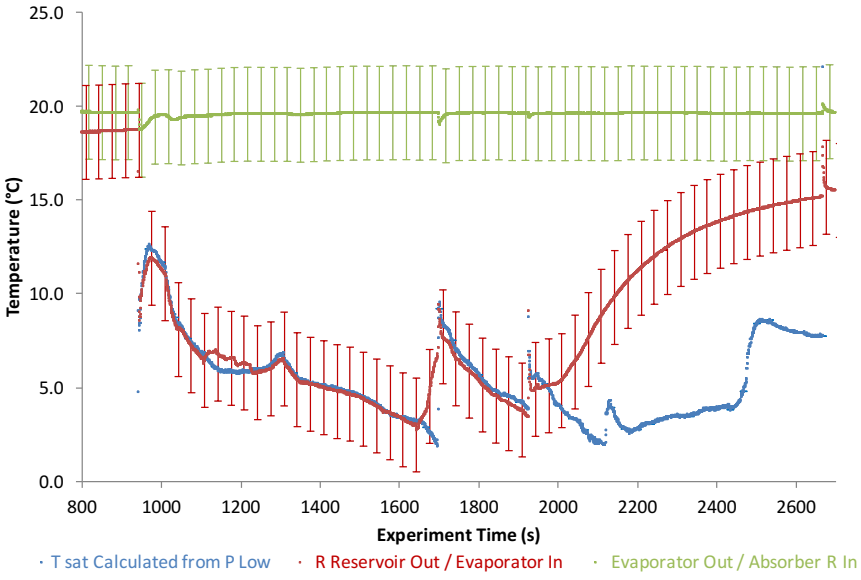

Figure 6.7: Operating temperatures of the evaporator (red line for inlet and green line for outlet) with the low pressure converted to acetone saturation temperature using Equation 4.15 (blue line). Test details: weak solution concentration $\left(\frac{m_{ZnBr_2}}{m_{solution}}\right)$ at inlet 62% and 703 g of solution collected.

blue and red lines follow each other for the majority of the test indicating that the refrigerant enters the evaporator at saturation conditions. Moreover due to the transparency of the equipment it was visible that the acetone was a liquid at this state, see Figure 6.12. The presence of vapour bubbles in the photo further validates the acetone being at saturation conditions. However the green line (evaporator out) is maintained at 20°C indicating that the refrigerant leaves the evaporator as superheated vapour rather than a saturated one. This may be a result of a large heat load provided by the flow of water at a relatively high temperature compared to the evaporator inlet. There is also the potential for measuring equipment error resulting from the thermocouple location.

6.2.5 Absorber

In Figure 6.8 the blue line is the temperature of the weak solution leaving the absorber, the red line is the strong solution entering the absorber and the green line is the pressure of the low pressure side, measured between the absorber and evaporator. The average strong solution input temperature during steady state 1311 seconds to 1914 seconds is 32°C and the average weak solution output temperature is 25.5°C. As the mixing of acetone and zinc bromide is exothermic these results indicate good heat transfer in the absorber to the cooling jacket.

The pressure is presented in this graph to aid the investigation of patterns arising in the temperature data. There are some peaks at 1697 seconds and 1918 which correspond to peaks in the weak solution temperature and slightly smaller troughs in the strong solution temperature. These are likely to be a result of the flow rate of the strong solution being slightly reduced. Reducing the strong solution flow rate would reduce the amount of heat transferred to the strong solution thermocouple housing (stainless steel Swagelok T union)

allowing the solution to cool slightly to ambient conditions. However the slow flow rate of solution would allow more time for the refrigerant vapour to be absorbed and the exothermic reaction would cause the now more dilute weak solution to warm up. As there is little control over the refrigerant vapour absorption into the strong solution in the absorber the increased dilution and temperature of the weak solution can cause a slight pressure rise thus explaining the peaks in pressure and weak solution temperature.

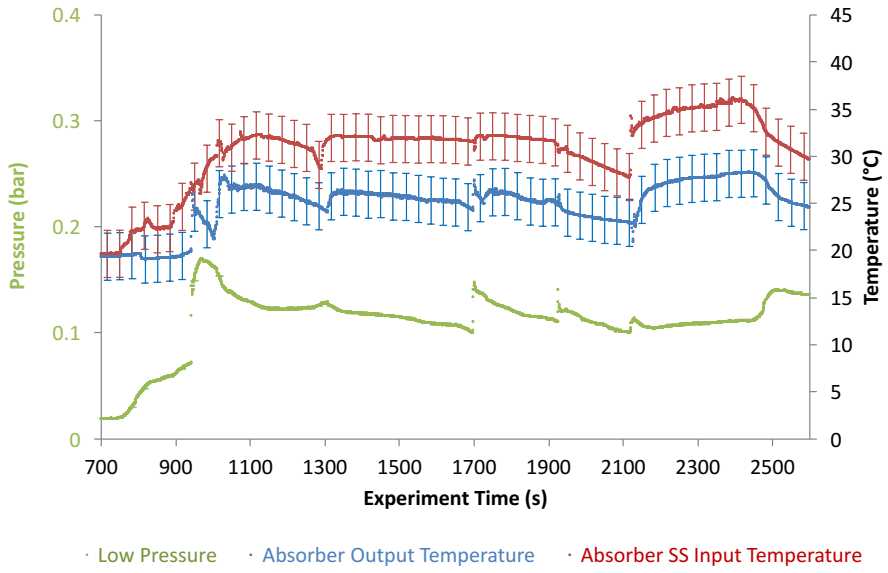

Figure 6.8: Operating input (red line, right axis) and output (blue line, right axis) temperatures of the absorber along with the pressure between the absorber and evaporator (green line, left axis). Test details: weak solution concentration $\left(\frac{m_{ZnBr_2}}{m_{solution}}\right)$ at inlet 62% and 703 g of solution collected.

6.2.6 Error Analysis

Measuring equipment used in this experiment had the following tolerances: Thermocouples ±2.5°C and the pressure transducers ±0.04% of full scale deflection (2 bar and 3 bar for low and high pressure sides respectively) resulting in ±0.0008 bar and ±0.0012 bar on the low and high pressure sides respectively. These errors were converted using the respective state equations depending whether pressure or temperature was required when analysing pure acetone. Pressure and temperature measurement frequency was 3 Hz, this provided an accurate picture of the trends taking place with the experiment. Unfortunately there were issues with leaks and control of the flow rates. For example the heat transfer fluid (mains water) did not have adequate flow control to calculate an accurate cooling output, making calculating an accurate physical CoP impractical.

6.3 Absorption Refrigeration Experiment Conclusion

This experiment consisted of a once through single effect absorption refrigerator with reservoirs and provided insight into the physical workings and challenges of an acetone and zinc bromide absorption refrigerator with reservoirs. It also provided some confidence in the modelling approach used in the next chapter. The use of glass allowed visual inspection of the fluid and its state throughout the cycle. This also aided the understanding of the system and the operating complexities. The instrumentation allowed reasonable analysis of the workings of each component with the system.

The experiment showed considerably longer period of cooling heat transfer in the evaporator to that of the heat transfer in the boiler, indicating that the use of reservoirs could allow continuous cooling from discontinuous heat

sources. The stable temperatures achieved at each thermocouple position in the boiler indicated that acetone and zinc bromide could be used to cool and maintain the CPV PV cells at a suitably low temperature while utilising that extracted heat to provide refrigeration. The pressure in the high pressure side is maintained after boiler operation indicating the importance of boiler exit and strong solution reservoir inlet design to optimise condensing, together with effective heat exchange in the condenser, all of which determine the concentration of the strong solution. The results from the condenser indicated that the inlet was a superheated vapour and outlet was a saturated liquid. Interestingly the evaporator showed a superheated outlet which was unexpected, this is likely to be a result of a large heat load applied to the evaporator.

Issues such as leaks and control would have caused some of the sources of error which were extremely challenging to measure, such as the continuously varying flow rates of the solution and the effects these had on solution concentrations. The errors resulting from the accuracy of the measuring equipment and human errors were not sufficient to interfere with the key observations of the test which showed generally well the predicted behaviour of the system. This test procedure provided insight into the operation an acetone and zinc bromide absorption refrigerator and provided confidence for the modelling approach described in Chapter 4.

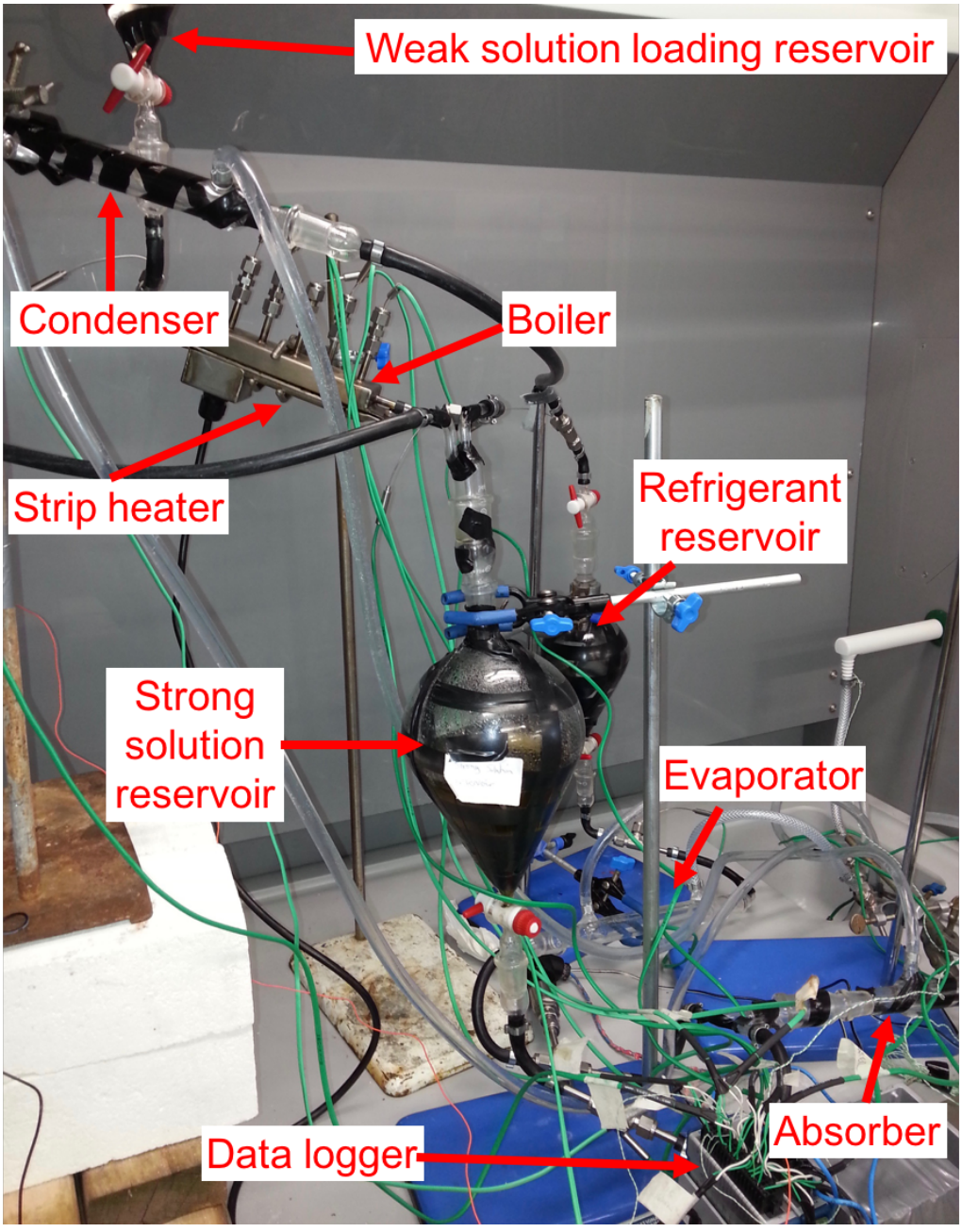

Figure 6.9: Photo of the left hand side of the absorption refrigerator test rig, showing all of the high pressure side and some of the low pressure side.

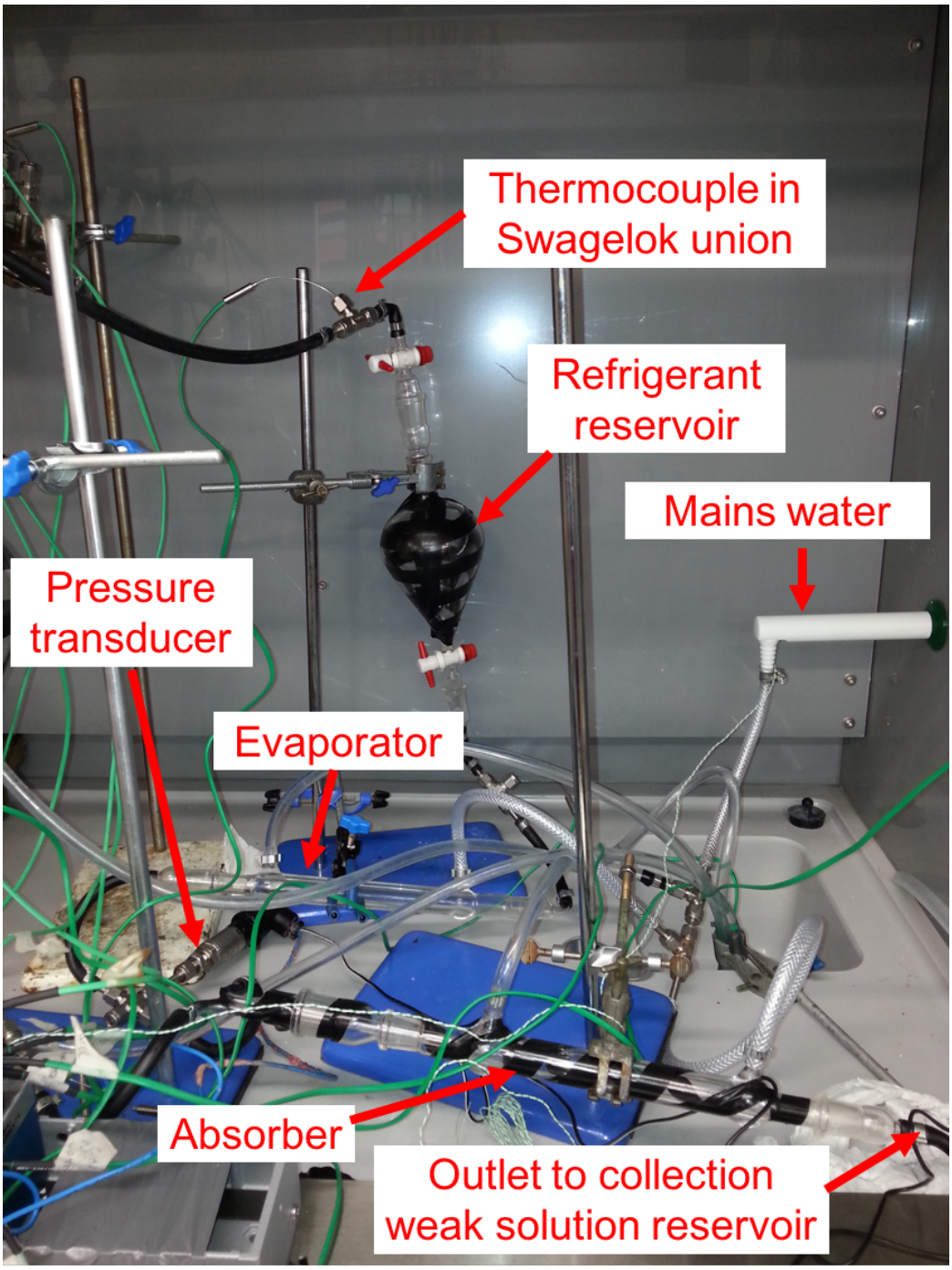

Figure 6.10: Photo of the right hand side of the absorption refrigerator experimental test rig, mainly the low pressure side.

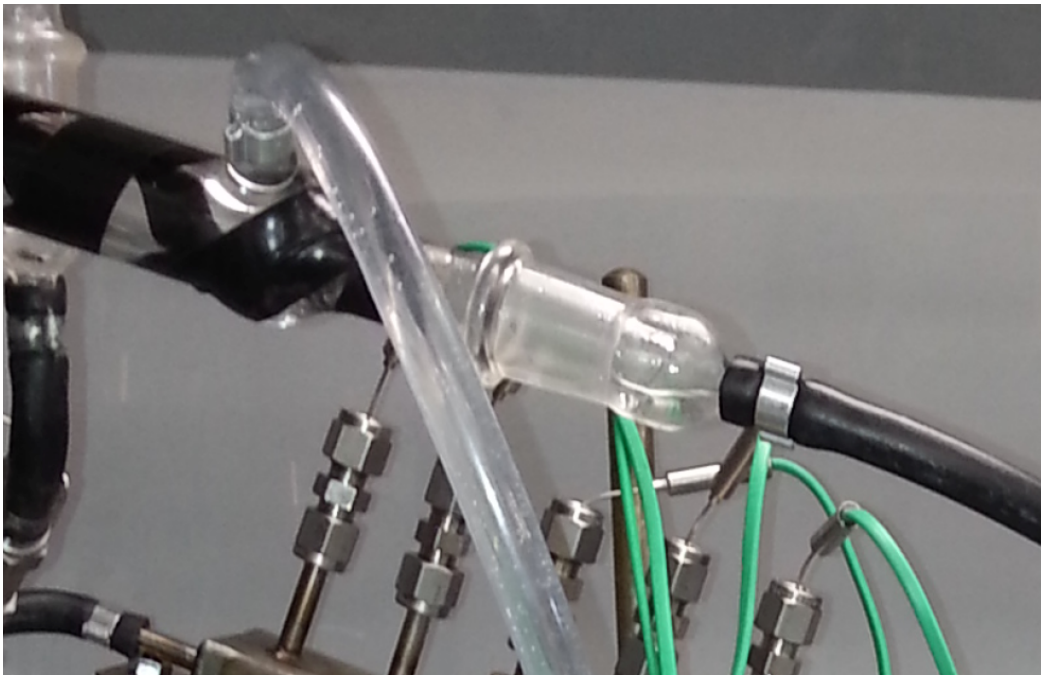

Figure 6.11: Photo of the condenser in the absorption refrigerator experimental test rig showing the refrigerant leaving the condenser as a liquid.

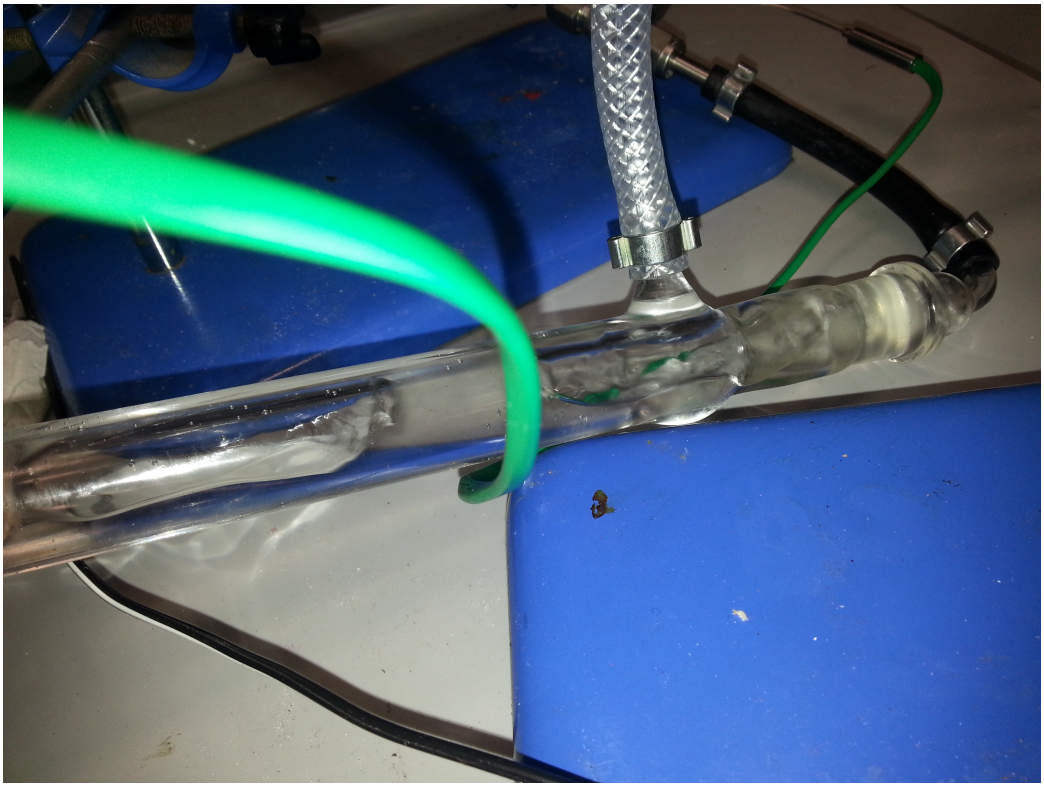

Figure 6.12: Photo of the evaporator in the absorption refrigerator experimental test rig showing the refrigerant as a liquid entering the evaporator and vapour bubbles forming inside the evaporator.

Chapter 7

Absorption Refrigeration Modelling

The following chapter investigates using the waste heat from the CPV and genset radiator for absorption refrigeration. Initially the operating limits have been investigated to provide the boundaries of investigation for the different configurations of absorption refrigerator, which were identified as suitable in Chapter 3. Each heat source is then investigated separately to be used in independent absorption refrigerators. This is followed by an evaluation of the evaporator tap off method investigating how each heat source could independently optimise the evaporator temperature. Based on these results the combined cycle and double boiler with evaporator tap off cycle will be evaluated, as will the need for further modelling.

For refrigeration benchmarking purposes the Food Standards Agency in the UK recommend refrigerator temperatures of 5°C and freezer temperatures of -18°C. (FSA 2015). They also stipulate "Food that is likely to support the growth of pathogenic micro-organisms or the formation of toxins must be kept at a temperature of 8°C or below." (FSA 2007). Harrison (1996) states that some root vegetables such as potatoes, sweet potatoes,

pumpkins and winter squash can be stored at 10°C to 15°C for over 2 months. A domestic refrigerator such as the Blomberg SSM9450 has an annual energy consumption of 132 kW·h per year (0.37 kW·h per day) which could be considered as an average electrical power load of 15 W (Cameo 2016). Assuming a typical CoP range of 2 to 3 food refrigeration can be approximated to 1 kW·h cooling load per day. Thermal comfort requirements are typically based on an indoor temperature of 24°C which in rural India could require between 3 kW to 5 kW air conditioning systems for a 20 m^2 to 30 m^2 room in a health centre, based on consultation with building design engineers and guidelines from Hawkins (2011).

The World Health Organisation (WHO) provide guidelines on medicine storage (WHO 2016):

- Store frozen: below -20°C, e.g. longer storage of certain vaccines.
- Store refrigerated: 2°C to 8°C e.g. medicines that cannot be frozen and can only be stored for a short period of time.
- Keep cool: 8°C to 15°C.
- Store at room temperature: 15°C to 25°C.

This chapter contains the following sections:

- **Operating Limits** presents the relationships between and effects of components within the absorption refrigerator to determine operating limits for the later analysis.
- **Single Effect Cycle Analysis Powered by the CPV and Genset Radiator Heat Sources** investigates the refrigeration outputs using the two heat sources and the effect of the difference between the strong and weak solution concentrations.
- **Absorption Refrigerator Configuration Analysis** investigates methods of lowering evaporator temperatures. Using the evaporator tap off

a proportion of the cooling from the evaporator along with ambient cooling is used to lower the operating temperatures of the condenser and absorber. This analysis is then used to evaluate the practicality of the other systems identified in Section 3.3.7.

- **Configuration Conclusion** presents the outcome of the configuration analysis and models the daily outputs of the selected configuration of absorption refrigerators over a range of ambient temperatures.
- **Within Day Analysis** investigates the performance within a day of the CPV powered absorption refrigerator for typical conditions expected in the region using historical weather data.
- **Absorption Refrigerator Modelling Conclusion** presents the main findings of this analysis and its application elsewhere.

7.1 Operating Limits

The primary challenge with absorption refrigeration is a balancing act described in the Challenges of Absorption Refrigeration (Section 3.3.1). This subsection addresses the challenge with the following investigations:

- The parameter effects on strong solution concentration on the high pressure side of the refrigerator, the parameters are: condenser temperature, boiler temperature, ambient temperature and condenser heat exchanger effectiveness.
- The parameter effects on evaporator temperature on the low pressure side of the refrigerator, the parameters are: weak solution concentration, ambient temperature, absorber temperature and absorber heat exchanger effectiveness.
- The effect of the difference between strong and weak solution concentrations on evaporator temperature.

- The minimum absorber heat exchanger effectiveness limit to provide evaporator temperatures lower than ambient.

7.1.1 Effect of the Boiler and Condenser Conditions on Strong Solution Concentration

In the waste heat recovery scenario investigated here the waste heat temperature is low (below 100°C) and the ambient temperature is high (above 20°C). High ambient temperatures result in a requirement for high condenser temperatures which lead to less concentrated strong solutions being suitable, as described in the Challenges of Absorption Refrigeration (Section 3.3.1). The model determines the strongest permissible strong solution concentration

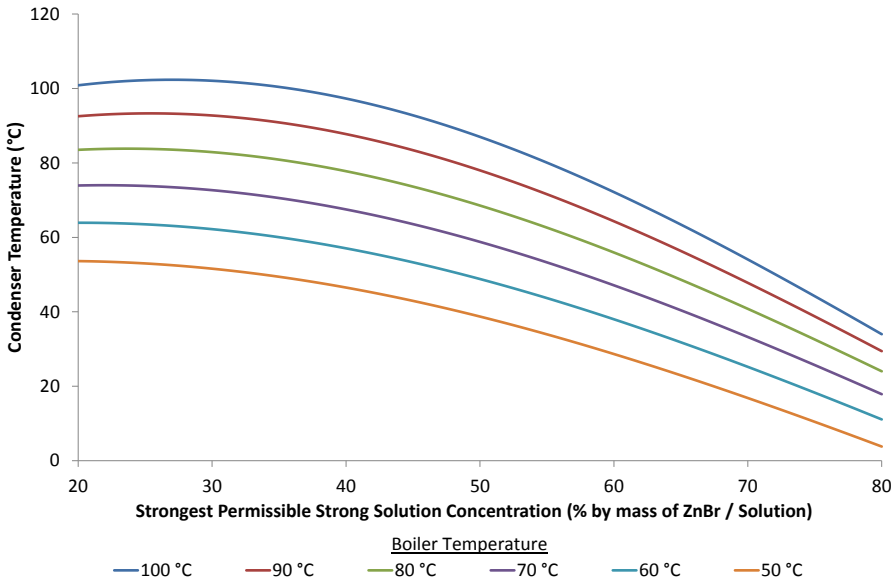

Figure 7.1: Graph of the operating limits of the boiler and condenser showing the effect of strong solution concentration on condenser temperature for boiler temperatures of 100°C to 50°C.

based on the condenser temperature. Figure 7.1 investigates this relationship with varying boiler temperatures. It uses the solution pressure equation (Equation 4.16) and the pure acetone saturation temperature equation (Equation 4.15) to determine the condenser temperature from varying solution (boiler) temperatures and concentrations. For all boiler temperatures the condenser temperature decreases with strengthening the strong solution concentration. As the boiler temperature increases higher condenser temperatures can be achieved. Figure 7.1 therefore illustrates the need for both a higher boiler temperature and a more dilute strong solution in order to have high condensing temperatures, which allow operation in higher ambient temperatures.

$$\boxed{\uparrow T_{CO} = \uparrow T_{AMB}} \tag{7.1}$$

$$\boxed{\uparrow T_{BO} = \uparrow T_{CO} = \uparrow T_{AMB}} \tag{7.2}$$

$$\boxed{\uparrow X_{SS} = \downarrow T_{CO} = \downarrow T_{AMB}} \tag{7.3}$$

7.1.2 Effect of Heat Exchanger Effectiveness on Condenser Temperature

The condenser heat exchanger effectiveness and ambient temperature play an important role in determining the maximum permissible condenser temperature, as the condenser loses heat to the surroundings at ambient temperature. The analysis in Figure 7.2 investigates the effects of heat exchanger effectiveness on condenser temperature. The conditions investigated were a boiler temperature of 60°C at ambient temperatures of 10°C to 40°C. Figure 7.2 is calculated using Equation 4.19.

Figure 7.2 shows that as the heat exchanger effectiveness increases (gets closer to 1) the condenser temperature falls until reaching the ambient temperature. The ambient temperature affects the gradient; as it decreases the

gradient increases. This is to be expected since Equation 4.19 is a straight line equation where $(T_{AMB} - T_{BO})$ is the gradient and boiler temperature (T_{BO}) is the y intercept.

$$\boxed{\uparrow \epsilon_{CO} = T_{CO} \rightarrow T_{AMB}} \tag{7.4}$$

If the heat exchanger effectiveness and the ambient temperature are known the condenser temperature can be calculated. The condenser temperatures can then be converted into saturation pressures using Equation 4.20. These pressures along with Equation 4.16 can computationally (in this case using lookup tables) find the strongest permissible solution concentration at the chosen boiler temperature. To illustrate this for a boiler temperature of 60°C Figure 7.3 shows the effect of heat exchanger effectiveness on the

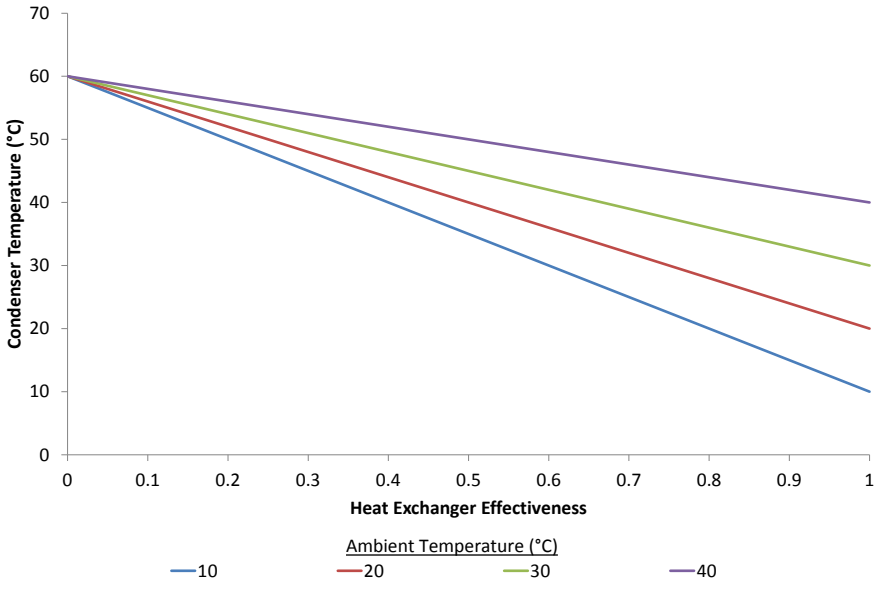

Figure 7.2: Graph of the effect of condenser heat exchanger effectiveness on condenser temperature, for a boiler temperature of 60°C at ambient temperatures of 40°C to 10°C.

strongest permissible strong solution concentration. Figure 7.3 shows that as heat exchanger effectiveness increases so does the strongest permissible strong solution concentration. As ambient temperature decreases both the gradient and the strongest permissible strong solution concentration increase.

The analysis presented in Figures 7.1 and 7.3 show how both the boiler temperature, ambient temperature and condenser heat exchanger effectiveness affect the strength of the strong solution. The maximum strength of the strong solution ultimately determines the maximum strength of the weak solution which (together with absorber temperature) determines the evaporator temperature.

$$\boxed{\uparrow X_{SS} = \uparrow X_{WS} = \downarrow T_{EV}} \tag{7.5}$$

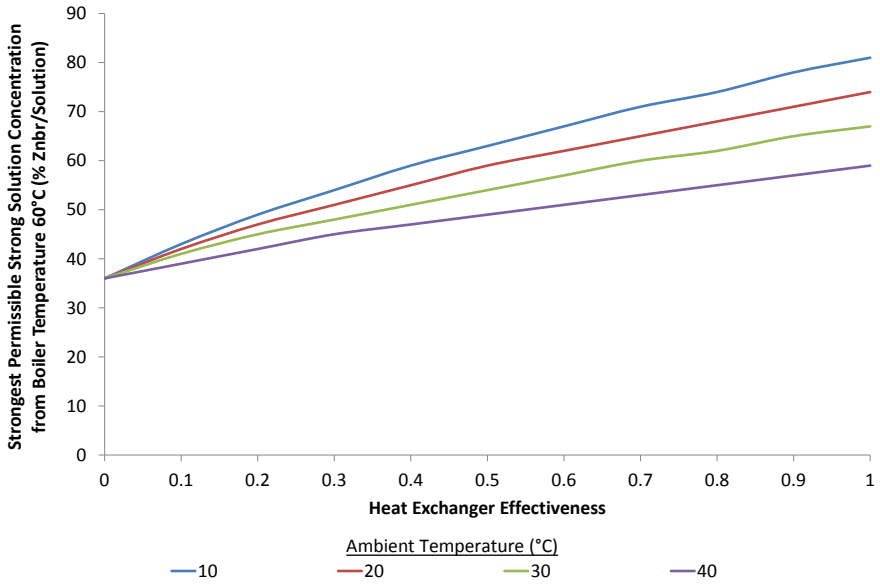

Figure 7.3: Graph of the effect of condenser heat exchanger effectiveness on the strongest permissible strong solution concentration based on a boiler temperature of 60°C at ambient temperatures of 40°C to 10°C.

$$\boxed{\uparrow \epsilon_{CO} = \uparrow X_{SS} = \downarrow T_{EV}} \tag{7.6}$$

$$\boxed{\uparrow T_{AMB} = \downarrow X_{SS} = \uparrow T_{EV}} \tag{7.7}$$

7.1.3 Effect of Weak Solution on Absorber and Evaporator

Figure 7.4 extends the same analysis used in Figure 7.1 for the weak solution concentration and absorber temperature. Figure 7.4 demonstrates the evaporator temperature with weak solution concentration variation and absorber temperature variation. The findings show lower evaporator temperatures, which can provide more versatile cooling, can be achieved by reducing absorber temperature and strengthening the weak solution concentration leav-

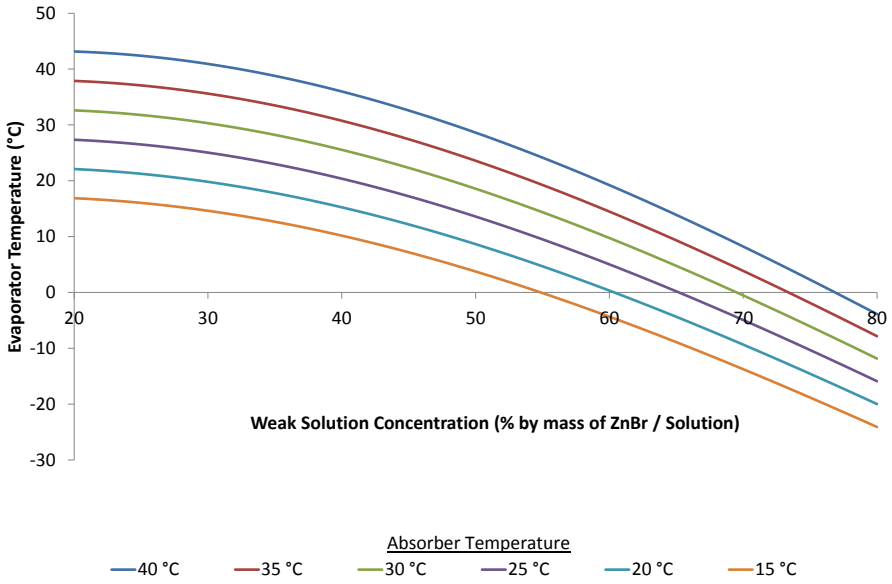

Figure 7.4: Graph of the operating limits of the absorber and evaporator showing the effect of weak solution concentration on evaporator temperature for absorber temperatures of 40°C to 15°C.

ing the absorber. In warmer climates this presents a problem as more concentrated weak solutions require more concentrated strong solutions which require low condenser temperatures and hence low ambient temperatures. Moreover the absorber needs to reject heat to the surroundings and its temperature is therefore also governed by ambient temperature, unless there is additional cooling available.

$$\boxed{\uparrow X_{WS} = \downarrow T_{EV}} \tag{7.8}$$

$$\boxed{\uparrow T_{AB} = \uparrow T_{EV}} \tag{7.9}$$

7.1.4 Effect of Absorber to Ambient Heat Exchanger Effectiveness

The output conditions of the absorber are the weak solution concentration and temperature. In the model used for this subsection the solution concentrations are fixed variables. The mixing of refrigerant into solution is exothermic and the solution vapour pressure is a function of solution temperature and concentration. In the absorber the refrigerant is being absorbed into the strong solution and heat is generated. The ability to remove this heat in the absorber will determine the output conditions of the absorber. In this model, as the solution concentrations are fixed, the heat exchanger effectiveness of the absorber determines the weak solution temperature (absorber output); which determines the vapour pressure of the solution. The weak solution at the outlet of the absorber has reached maximum capacity to absorb refrigerant at those conditions, therefore determining the vapour pressure in the absorber. The absorber and evaporator require the free flow of refrigerant vapour between the components in order to allow the absorption process of refrigerant vapour into solution. This results in the pressure of the absorber equalling the pressure in the evaporator. The pressure in the

evaporator determines the saturation conditions in the evaporator. The evaporator is assumed to operate at saturation conditions. Therefore the vapour pressure produced from the output conditions of the absorber determines the evaporator temperature.

The analysis shown in Figures 7.5 and 7.6 determines the conditions in the absorber for a range of ambient temperatures where example solution concentrations of 60% strong and 54% weak $\frac{m_{ZnBr}}{m_{solution}}$ are used. These solution concentrations are based on the analysis in Figure 7.1 which shows a strong solution concentration of 60% should operate in the ambient conditions expected at the CPV desired operating temperature. The weak solution concentration (54%) was arbitrarily selected as starting point of this investigation based on typical strong and weak solution concentration differences found in the literature. The calculation method is described in Section 4.3.9. The hot inlet is calculated from the adiabatic mixing of the refrigerant leaving the evaporator and the strong solution from its reservoir at ambient temperature. The cold stream (which could be air or the heat transfer fluid cooling to ambient and not below ambient) is at ambient conditions and the hot outlet is the weak solution leaving the absorber.

$$\boxed{\uparrow \epsilon_{AB} = \downarrow T_{AB_{WS}}} \tag{7.10}$$

$$\boxed{\uparrow T_{AMB} = \uparrow T_{AB_{WS}}} \tag{7.11}$$

Figure 7.5 presents the relationship between absorber outlet (weak solution) temperature and absorber heat exchanger effectiveness at a range of ambient temperatures for strong and weak solution concentrations of 60% and 54% respectively. It shows that as the heat exchanger effectiveness increases the absorber outlet temperature decreases for all ambient temperatures investigated. Increasing ambient temperature increases the weak solution temperature for the range of heat exchanger effectiveness analysed here.

This analysis can be converted into evaporator temperature through calculating the saturation pressure, with Equation 4.16, at the outlet conditions of the absorber and converting that pressure to a saturation temperature, with Equation 4.15, for pure acetone, the results of which are shown in Figure 7.6.

Figure 7.6 shows that, for the conditions selected (strong and weak solution concentrations of 60% and 54% respectively), as absorber heat exchanger effectiveness increases evaporator temperature decreases and when ambient temperature decreases the gradient of the trend decreases slightly. The most important finding is that for fixed solution concentrations there is an absorber heat exchanger effectiveness limit to achieve evaporator temperatures lower than ambient, shown with the orange dashed line. For example at an ambient temperature of 30°C and heat exchanger effectiveness of 0.6 the

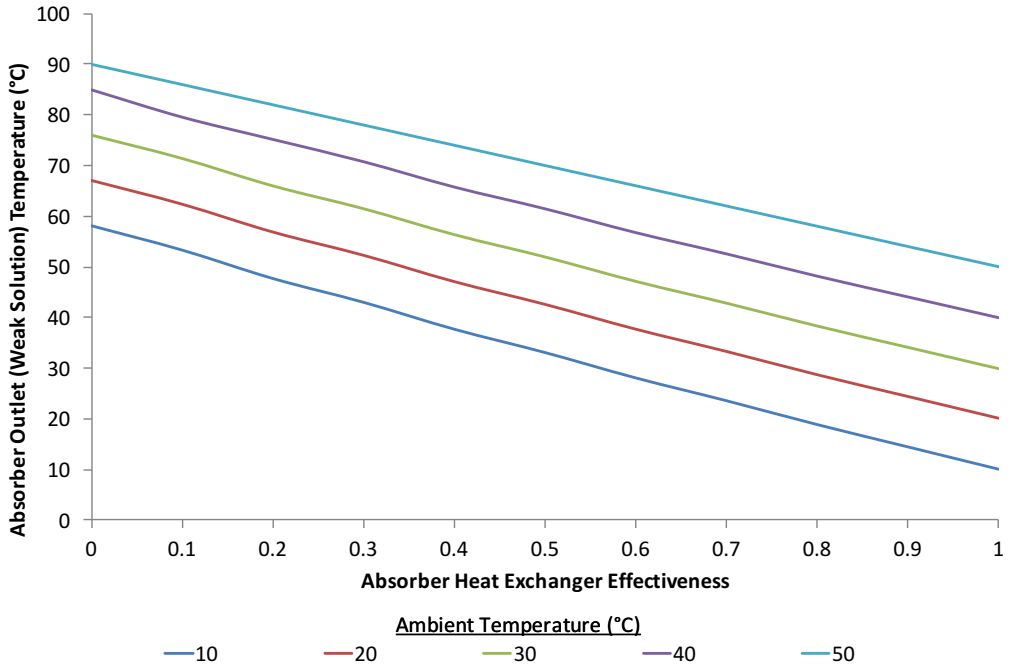

Figure 7.5: Effect of absorber heat exchanger effectiveness on absorber outlet (weak solution) temperature for a strong solution concentration of 60% and weak solution concentration of 54% $\left(\frac{m_{ZnBr_2}}{m_{solution}}\right)$ for ambient temperatures of 10°C to 50°C.

evaporator temperature would be 32°C; in this example a refrigerator would not be necessary as cooler temperatures can be achieved from ambient conditions. This minimum heat exchanger effectiveness to achieve evaporator temperatures at or below ambient temperature can be found by taking the straight line equations from the data in Figure 7.6 and finding the minimum absorber heat exchanger effectiveness when the evaporator temperature is equal to the respective ambient temperature.

$$\boxed{\uparrow \epsilon_{AB} = \downarrow T_{EV}} \tag{7.12}$$

$$\boxed{\uparrow T_{AMB} = \uparrow T_{EV}} \tag{7.13}$$

The dashed orange line in Figure 7.6 shows that for a strong solution concentration of 60% and a weak solution concentration of 54% at ambient

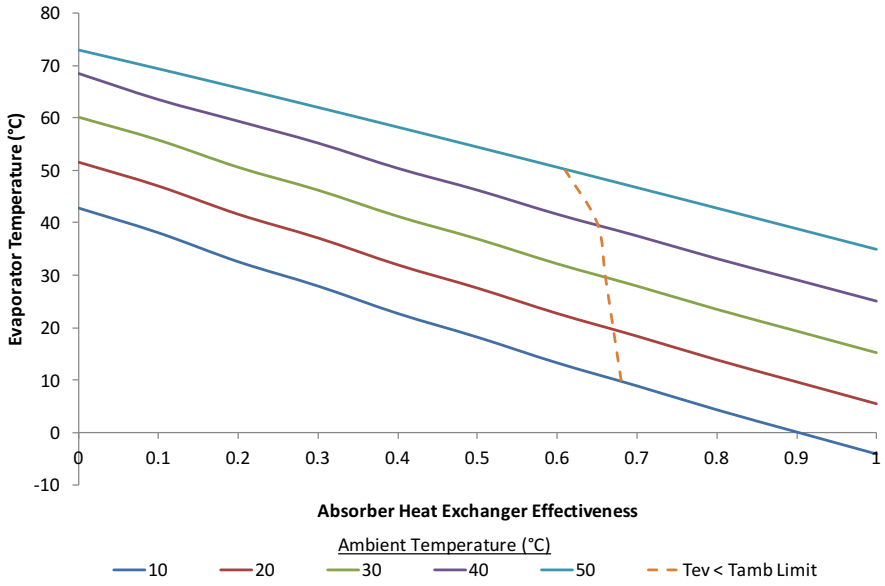

Figure 7.6: Effect of absorber heat exchanger effectiveness on evaporator temperature for a strong solution concentration of 60% and weak solution concentration of 54% $\left(\frac{m_{ZnBr_2}}{m_{solution}}\right)$ for ambient temperatures of 10°C to 50°C.

temperature of 10°C there is a heat exchanger effectiveness limit of 0.68 this falls to 0.61 for an ambient temperature of 50°C. To illustrate the effect of the difference in concentration between the strong and weak solution the analysis shown in Figures 7.5 and 7.6 is presented for a strong solution concentration of 60% and a weak of 56% in Figures 7.7 and 7.8.

$$\boxed{\uparrow_{AMB} = \downarrow \epsilon_{AB} \; such \; that \; T_{EV} < T_{AMB}} \tag{7.14}$$

Changing the weak solution concentration from 54% in Figure 7.5 to 56% in Figure 7.7 lowers the weak solution temperature at 0 heat exchanger effectiveness by 11°C for an ambient temperature of 50°C and by 16°C for an ambient temperature of 10°C. The reason for this is that the ratio of refrigerant to solution will be smaller with a more concentrated strong solution

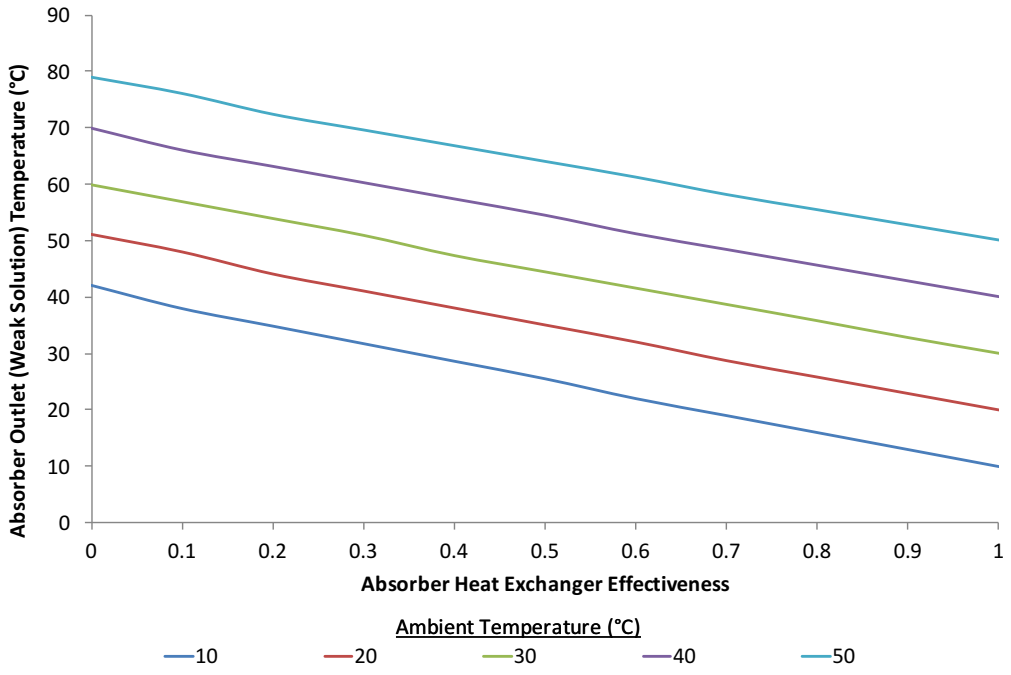

Figure 7.7: Effect of absorber heat exchanger effectiveness on absorber outlet (weak solution) temperature for a strong solution concentration of 60% and weak solution concentration of 56% ($\frac{m_{ZnBr}}{m_{solution}}$) for ambient temperatures of 10°C to 50°C.

and the saturation pressure (absorber and evaporator pressure) caused by this will be lower. The low saturation pressure will cause lower evaporator temperatures, the refrigerant leaving the evaporator as a saturated vapour will be at this lower temperature and therefore has a lower specific enthalpy, seen in Figure 4.2. This lower specific enthalpy results in a reduction in the energy removal requirement from the absorber with a smaller difference in solution concentrations. It has no effect on the weak solution temperature for a perfect heat exchanger (1) as at these values the weak solution equals ambient temperature.

$$\boxed{\downarrow (X_{SS} - X_{WS}) = \downarrow Q_{AB} = \downarrow T_{AB_{WS}}} \tag{7.15}$$

The effect of absorber heat exchanger effectiveness and difference in strong

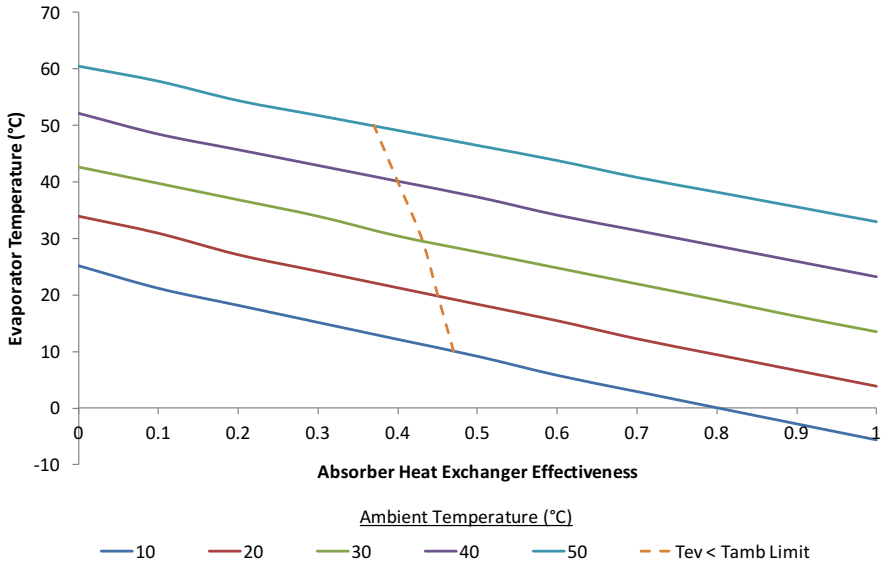

Figure 7.8: Effect of absorber heat exchanger effectiveness on evaporator temperature for a strong solution concentration of 60% and weak solution concentration of 56% ($\frac{m_{ZnBr}}{m_{solution}}$) for ambient temperatures of 10°C to 50°C.

and weak solution concentrations on evaporator temperature can be seen in the difference between Figures 7.6 and 7.8. When ambient temperature is 50°C the evaporator temperature is 12.5°C lower for a weak solution of 56% at a heat exchanger effectiveness of 0 but only 2°C lower for a perfect heat exchanger. However at an ambient temperature of 10°C the difference in evaporator temperatures for a 0 heat exchanger effectiveness is 17.7°C and 1.6°C for a perfect heat exchanger. This indicates that if the heat exchangers are highly effective a greater concentration difference between the strong and weak solutions can be used without having a significant effect on evaporator temperature.

$$\boxed{\uparrow X_{WS} =\downarrow T_{EV}} \tag{7.16}$$

When comparing the dashed orange line, which indicates the limit where evaporator temperature is equal to ambient temperature in Figures 7.6 and 7.8, changing the weak solution concentration from 54% to 56%, while maintaining a strong solution concentration of 60%, decreases the heat exchanger effectiveness limit to achieve evaporator temperatures lower than ambient. For example for an ambient temperature of 10°C the limit reduces from 0.68 to 0.47 reducing by 0.21 and for an ambient temperature of 50°C the limit reduced from 0.61 to 0.37 reducing by 0.24. These results show that a small difference in strong and weak solution concentrations reduces the impact of absorber heat exchanger effectiveness.

$$\boxed{\downarrow (X_{SS} - X_{WS}) =\downarrow \epsilon_{AB} \; such \; that \; T_{EV} < T_{AMB}} \tag{7.17}$$

This illustration of the effect of keeping the strong solution at 60% and changing the weak from 54% to 56% also shows that more concentrated weak solution concentrations provide lower evaporator temperatures. The ratio of working refrigerant to solution is proportional to the solution concentration difference, as it increases more energy needs to be removed from the absorber. This results in the absorber heat exchanger effectiveness having a

greater effect on the evaporator temperature for large solution concentration differences. In conclusion if the absorber heat exchangers are ineffective due to a lack of cold sinks a small difference in solution concentration should be used to provide low evaporator temperatures.

This analysis provides insight into the need for highly effective heat exchangers and the strongest possible weak solution while also having the weakest possible strong solution, to operate an absorption refrigerator from low temperature heat sources in a hot climate. Based on these findings and consultation with individuals who have industrial experience in heat exchangers a conservative heat exchanger effectiveness of 0.75 has been used for all heat exchangers in subsequent models

$$\boxed{\downarrow (X_{SS} - X_{WS}) = \downarrow T_{EV}} \tag{7.18}$$

$$\boxed{\uparrow \epsilon_{AB} = \downarrow T_{EV}} \tag{7.19}$$

The following section presents the theoretical outputs of the various cycle configurations discussed in Chapter 3. There is further analysis on the effect of adjusting the difference between the strong and weak solution as part of the analysis on the Single Effect Cycle.

7.2 Single Effect Cycle Analysis Powered by the CPV and Genset Radiator Heat Sources

The previous section explored the effects of varying the solution concentration difference with a fixed strong solution concentration focussing on the absorber and evaporator. This section investigates a single effect cycle powered by the heat sources in the BioCPV power plant. These heat sources have fixed operating temperatures of 60°C for the CPV and 80°C for the genset radiator. The following section investigates a single effect cycle powered by

the CPV heat source first with the difference in strong and weak solution concentrations of 2%, 4% and 6% at ambient temperatures varying from 0°C to 50°C in Figures 7.9 and 7.10. The same analysis is then conducted for the genset radiator at 80°C in Figures 7.11 and 7.12.

7.2.1 CPV Waste Heat Powered Absorption Refrigerator

Figure 7.9 investigates the temperature drop from ambient (ambient temperature - evaporator temperature) that a single effect absorption refrigerator can achieve. Solution concentration difference of 2% consistently achieved greater temperature drops from ambient than 4% and 6%. This is to be ex-

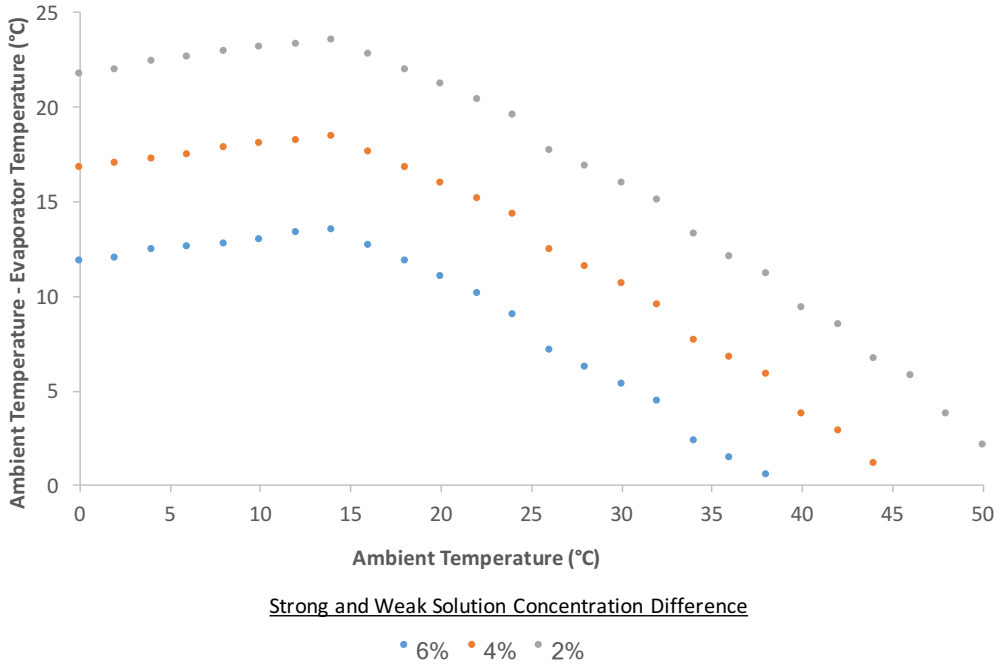

Figure 7.9: Analysis of difference between ambient and evaporator temperatures with strong and weak solution concentration differences of 2%, 4% and 6% and a boiler temperature of 60°C at ambient temperatures varying from 0°C to 50°C in a single effect cycle.

pected as the model would find the same strong solution concentration for all cases but the 2% increase will have a less concentrated weak solution than 4% and 6%, causing lower pressures in the low pressure side of the refrigerator and therefore lower evaporator temperatures. The knee in all the curves at 14°C indicates that up to this point the strong solution concentration was at the maximum limit to avoid crystallisation (70% $\frac{m_{ZnBr_2}}{m_{solution}}$). The x-axis intercept indicates that the evaporator and ambient temperatures are equal. This is the limit where it is not theoretically (and practically) possible to generate any cooling at ambient conditions. A 6% and 4% difference cannot operate theoretically at ambient temperatures above 38°C and 46°C respectively. At and close to these ambient temperatures, the cooling would not practically be useful as the evaporator temperature will be close to or at ambient and it is unlikely that the evaporator will be able to absorb any heat from an ambient source, as it will not have perfect heat exchangers. That being said it could be used to cool something warmer than ambient when passive ambient cooling is insufficient.

Figure 7.10 shows for the same set of conditions their effect on CoP. For all cases CoP rises with ambient temperature, this is partly a result of the assumption that the weak solution input to the boiler is at ambient temperature. The 2% difference in strong and weak solution concentrations has CoPs approximately half of the 6% concentration difference. However from Figure 7.9 the 2% difference in solution concentrations has colder evaporator temperatures. This indicates that lowering the solution concentration difference reduces the cooling energy available but the temperatures achieved are more versatile.

7.2.2 Genset Radiator Waste Heat Powered Absorption Refrigerator

Figures 7.11 and 7.12 show the same analysis for the genset radiator waste heat at 80°C. Figure 7.11 shows the temperature drop from ambient for a single effect cycle powered by an 80°C heat source at varying ambient temperatures and solution concentration differences. It follows a similar pattern to Figure 7.9. However there is a positive temperature difference from ambient at all ambient temperatures analysed here, indicating that this heat source can provide usable cooling with a solution concentration difference of 2% to 6% at ambient temperatures from 0°C to 50°C. The temperature drop at 0°C ambient is the same for both Figures 7.9 and 7.11 but the knee moves from

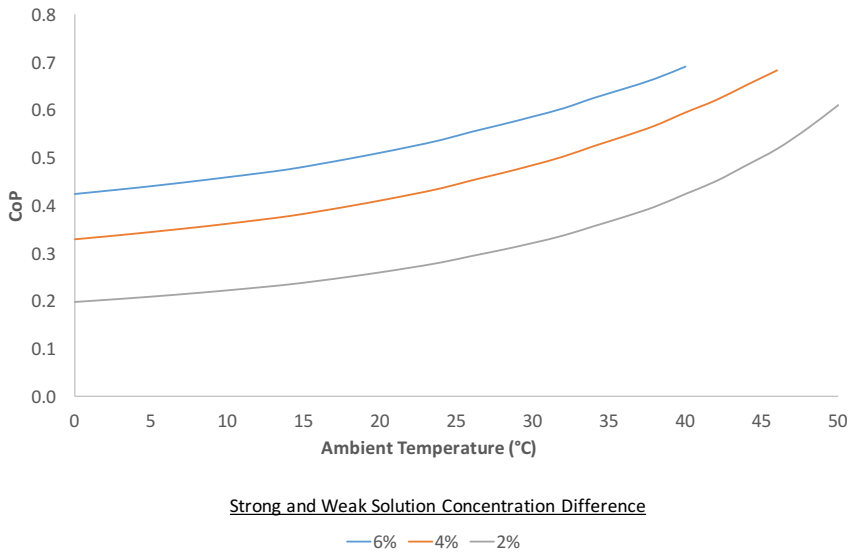

Figure 7.10: Analysis of single effect cycle CoP with varying the strong and weak solution concentration difference of 2%, 4% and 6%, with a boiler temperature of 60°C at ambient temperatures varying from 0°C to 50°C.

14°C to 28°C. This indicates that stronger solution concentrations can be used at higher ambient temperatures as a result of the higher boiler temperature. This also indicates that at higher boiler temperatures the refrigerator can operate close to the crystallisation limit at higher ambient temperatures. The result of this is that lower temperature cooling is available from the genset radiator heat source at higher ambient temperatures.

Figure 7.12 shows the CoP from the genset radiator heat source at varying ambient temperatures and solution concentration differences. The CoPs vary from 0.15 at an ambient temperature of 0°C with a 2% concentration difference to 0.57 at an ambient temperature of 50°C with 6% solution concentration difference. These are lower than the analysis for CPV waste heat powered absorption refrigerator in Figure 7.10 by 0.05 to 0.08 at 0°C ambient.

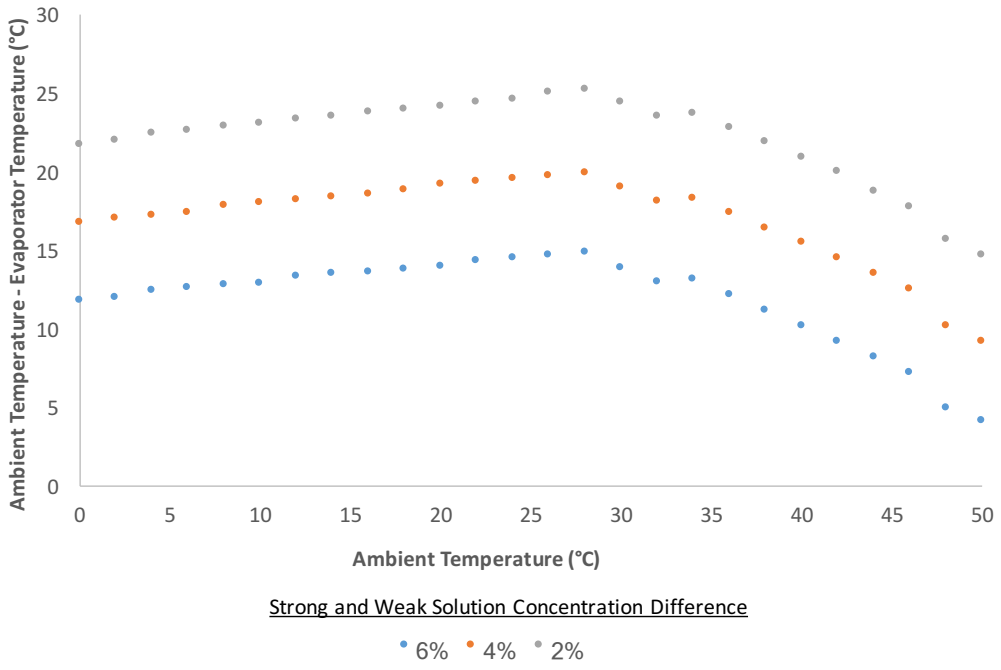

Figure 7.11: Analysis of difference between ambient and evaporator temperatures with strong and weak solution concentration differences of 2%, 4% and 6%, and a boiler temperature of 80°C at ambient temperatures varying from 0°C to 50°C in a single effect cycle.

This difference in CoP between the CPV powered refrigerator and genset radiator powered refrigerator increases as ambient temperature increases (e.g. 0.17 to 0.19 at 40°C).

In general terms the CPV waste heat can provide up to 96% higher CoPs but with up to 39% higher (therefore less versatile) evaporator temperatures than the genset radiator waste heat. As the CPV has considerably more waste heat available the following section investigates the effects of alternative configurations to utilise this energy effectively.

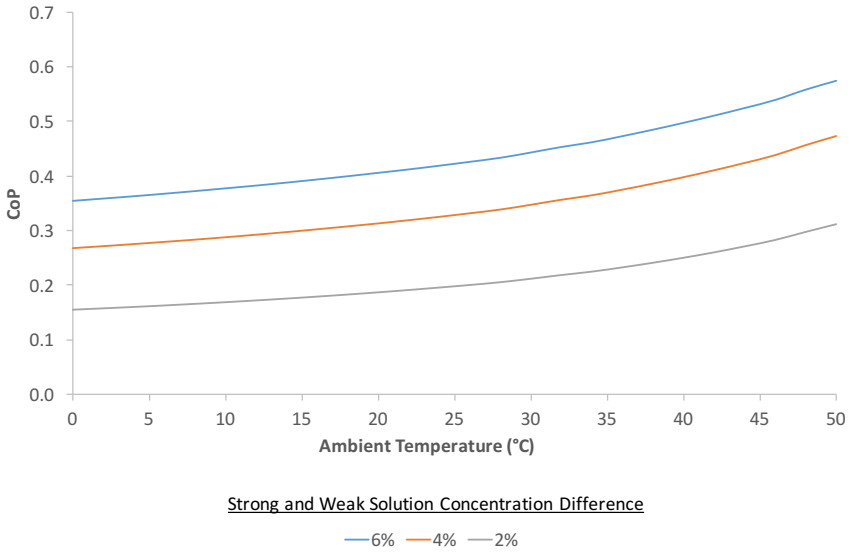

Figure 7.12: Analysis of single effect cycle CoP with varying the strong and weak solution concentration difference of 2%, 4% and 6% with a boiler temperature of 80°C at ambient temperatures varying from 0°C to 50°C.

7.3 Absorption Refrigerator Configuration Analysis

The previous section identified that the CPV heat source at high ambient temperatures cannot provide low evaporator temperatures. For example an ambient temperature of 35°C, at best (2% solution concentration difference), provides an evaporator temperature of 22°C. These high evaporator temperatures may be useful for space cooling but are not versatile enough to provide cooling for food or medicine. However, the thermal losses in the CPV accounts for 38% of the total power plant input energy. Therefore, ways to lower the evaporator temperature of the CPV powered absorption refrigerator need to be investigated to maximise the usefulness of this large energy source.

The following analysis assesses the potential to generate lower evaporator temperatures using the evaporator tap off method described in Chapter 3. It continues from the previous section by comparing the effect of reducing the solution concentration difference in a single effect cycle to the evaporator tap off method in a single effect cycle. The evaporator tap off method uses water as a heat transfer fluid to transfer some of the cooling from the evaporator to the absorber and condenser of the absorption refrigerator. The heat transfer fluid achieves this by initially rejecting the collected heat from the absorber and condenser to ambient, reducing its temperature to ambient, after which it is then further cooled by the evaporator. This allows the condenser and absorber to potentially operate at temperatures lower than ambient. The modelling approach is described in the Analytical Methodology Chapter Section 4.3.11. The findings from this analysis are then extrapolated to assess the viability of the combined cycle with reservoirs and double boiler with reservoirs and evaporator tap off absorption refrigerator system configurations.

7.3.1 Effect of using Evaporator Energy to Cool the Absorber

In Section 7.1 of this chapter the effect of absorber outlet temperature on evaporator temperature is described. The following analysis investigates the amount of cooling required to use the evaporator tap off method to lower the absorber temperature, which lowers the evaporator temperature. To calculate the energy used by the evaporator tap off method, the mass flow rate of the water (heat transfer fluid between absorber, ambient and evaporator)

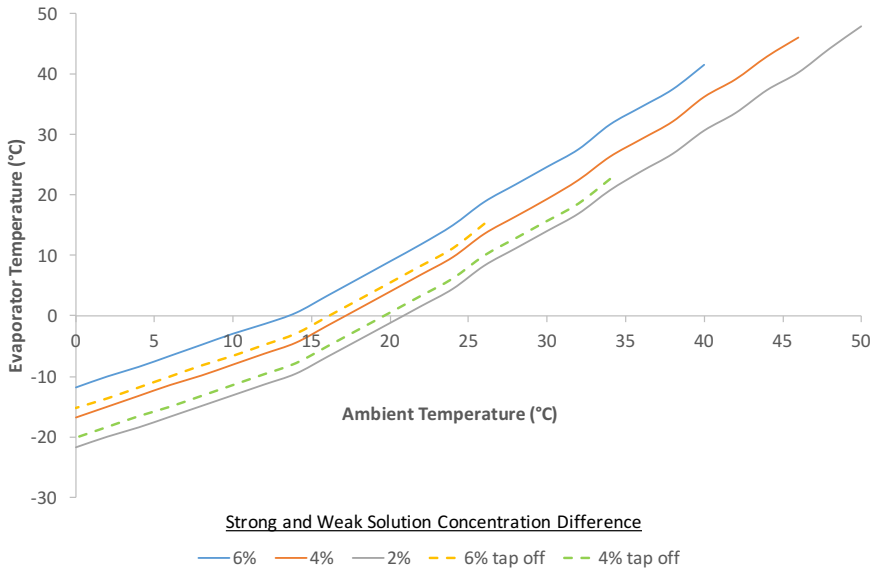

Figure 7.13: Analysis of evaporator temperatures achieved with a boiler temperature of 60°C at ambient temperatures varying from 0°C to 50°C, with evaporator tap off on a single effect cycle with solution concentration differences of 6% (yellow dashed line) and 4% (green dashed line) and single effect cycles with solution concentration differences of 6% (blue line) to 4% (orange line) and 2% (grey line).

was calculated using an energy balance when cooling the absorber to ambient. This quantity of water was then further cooled by 1°C to 5°C (from ambient). The energy required to do this was then subtracted from the evaporator cooling energy. The results presented here show the evaporator tap off method when the water used to remove heat from the absorber is cooled 5°C below ambient.

To determine whether the evaporator tap off method is effective for the CPV waste heat driven absorption refrigerator, it has been compared to changing the solution concentration difference from 6% to 4% and from 4% to 2%, in Figures 7.13 and 7.14.

Figure 7.13 shows the evaporator temperatures achieved at varying ambient temperatures for these system configurations. The blue, orange and grey lines show a single effect cycle with solution concentration differences of 6%, 4% and 2% respectively. The yellow and green dashed lines show systems using the evaporator tap off method, cooling the heat transfer fluid in the absorber by 5°C for solution concentration difference of 6% and 4% respectively. At 2% solution concentration difference the evaporator tap off required more cooling than was physically available and is therefore not presented in this analysis.

The general trends in Figure 7.13 show that in all cases lower evaporator temperatures are achieved by reducing the solution concentration difference rather than using the evaporator tap off configuration. Using a 6% solution concentration difference with the evaporator tap off in these conditions is only usable up to an ambient temperature of 26°C after which point the evaporator temperatures are not low enough to provide a 5°C reduction from ambient in the heat transfer fluid. Likewise this situation occurs at 34°C with the 4% solution concentration difference with the evaporator tap off configuration.

Figure 7.13 indicates that, in terms of providing low evaporator temperatures, the evaporator tap off method is less effective than lowering the

solution concentration difference. Dropping the solution concentration difference from 6% to 4% provided evaporator temperatures on average 1.5°C lower than using the tap off configuration for a solution concentration difference of 6%. Likewise dropping the solution concentration difference from 4% to 2% provided on average 1.7°C lower evaporator temperatures than using the tap off configuration on a solution concentration difference of 4%. In order to determine how this affects the energy performance of the absorption refrigerator the percentage of evaporator cooling (or heat absorbing) energy used by the evaporator tap off configuration has been compared to the loss

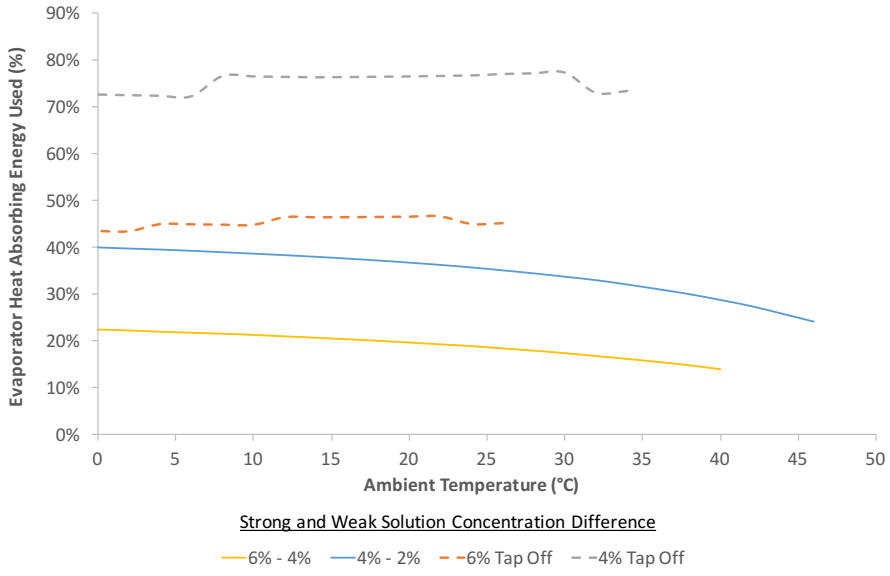

Figure 7.14: Analysis of evaporator heat absorbing energy used with a boiler temperature of 60°C at ambient temperatures varying from 0°C to 50°C, when comparing evaporator tap off on a single effect cycle with solution concentration differences of 4% (grey dashed line) and 6% (orange dashed line) against reducing the solution concentration difference from 6% to 4% (yellow line) and 4% to 2% (blue line).

in evaporator cooling energy from using a solution concentration difference of 6% to 4% and 4% to 2%. Figure 7.14 shows this.

The general trends observed from Figure 7.14 show that the tap off configuration uses more of the evaporator cooling energy than the reduction in evaporator cooling energy from lowering the solution concentration difference. The average cooling energy penalty from using a 4% solution concentration difference over 6% is 25 percentage points lower than using the tap off configuration with a 6% solution concentration difference. Likewise for solution concentration differences of 4% to 2% compared to 4% with tap off is 38 percentage points lower. The cooling energy penalty of going from 6% solution concentration difference to 4% is half that of 4% to 2%. Combining the results of Figures 7.13 and 7.14 in terms of providing lower evaporator temperatures and maximising cooling energy it is more effective to use lower solution concentration differences than the evaporator tap off method.

The result of this analysis is that an absorption refrigerator powered by a 60°C heat source in high ambient temperatures should use a 2% or lower solution concentration difference to provide cooling up to ambient conditions of 50°C. The evaporator tap off method is not effective at high ambient temperatures as the evaporator temperature is not low enough to cool the heat transfer fluid effectively. Moreover the evaporator tap off method has too high an energy penalty in comparison to lowering the solution concentration difference.

Conducting the same analysis for the genset radiator heat source which is assumed to be at 80°C in Figures 7.15 and 7.16. These figures show the evaporator temperatures and the cooling energy penalty respectively for the same conditions other than the boiler temperature. The general patterns are the same as those for a 60°C heat source, with the main difference being that the evaporator tap off method can operate at higher ambient temperatures, up to 46°C for a 6% solution concentration difference compared to 26°C

with the CPV heat source at 60°C. A 4% solution concentration difference with genset radiator waste heat tap off is viable for all ambient temperatures tested here.

The main finding is that the most energy effective way of achieving a lower evaporator temperature, with acetone and zinc bromide as the working fluids, is using a small solution concentration difference. The evaporator tap off configuration does not appear to utilise the waste heat sources well in terms of reducing evaporator temperature through cooling the absorber.

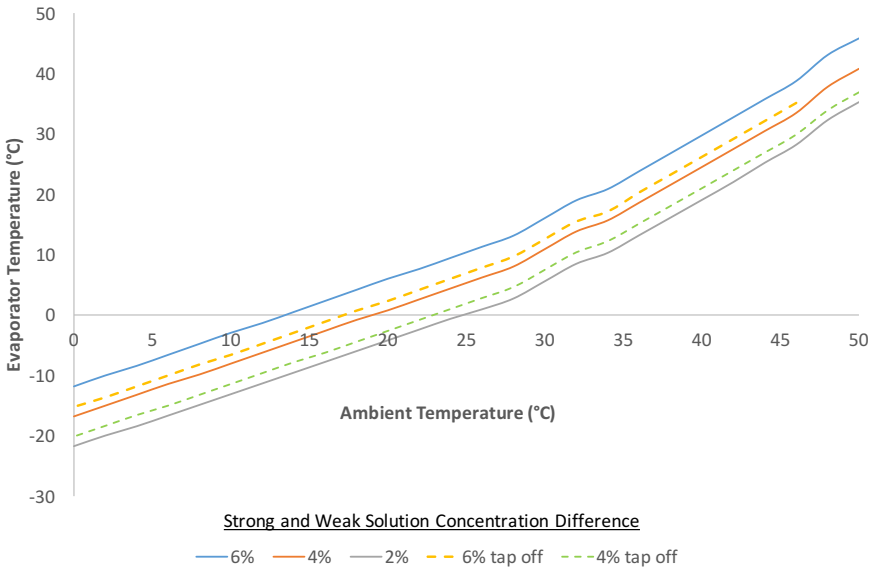

Figure 7.15: Analysis of evaporator temperatures achieved with a boiler temperature of 80°C at ambient temperatures varying from 0°C to 50°C, with the evaporator tap off on a single effect cycle with solution concentration differences of 6% (yellow dashed line) and 4% (green dashed line) and single effect cycles with 6%,(blue line) 4% (orange line) and 2% (grey line).

7.3.2 Effect of using Evaporator Energy to Cool the Condenser

The alternative to cooling the absorber to provide lower evaporator temperatures is cooling the condenser. The condenser temperature and the corresponding saturation pressure determine the strength limit of the strong solution leaving the boiler. If more concentrated strong solutions can be used then more concentrated weak solutions are possible. More concentrated weak solutions provide lower saturation pressures which can lead to lower

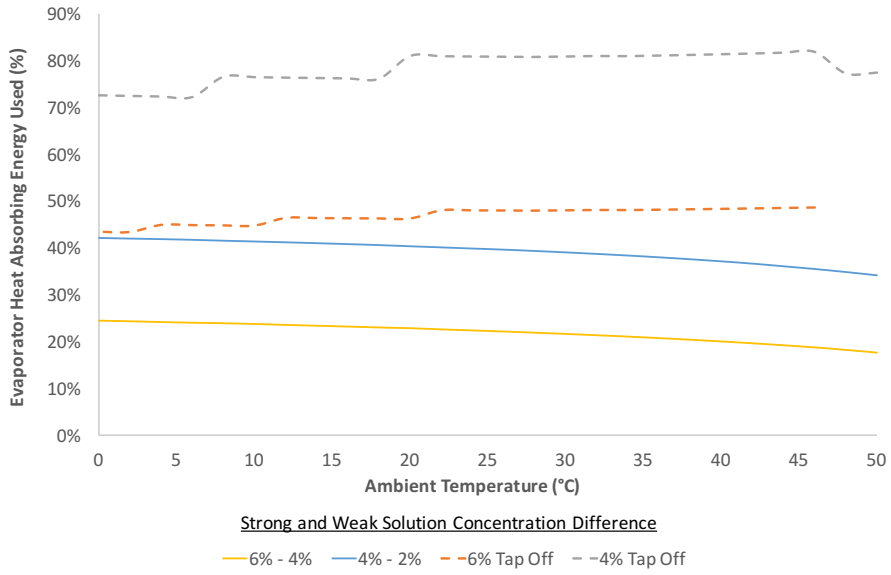

Figure 7.16: Analysis of evaporator heat absorbing energy used with a boiler temperature of 80°C at ambient temperatures varying from 0°C to 50°C, when comparing evaporator tap off on a single effect cycle with solution concentration differences of 4% (grey dashed line) and 6% (orange dashed line) against reducing the solution concentration difference from 6% to 4% (yellow line) and 4% to 2% (blue line).

evaporator temperatures.

Modelling tests investigated using up to 50% of the cooling generated in the evaporator to cool the condenser, using a similar calculation approach to cooling the absorber in the previous subsection. Using 50% of the evaporator cooling energy at ambient temperatures from 10°C to 50°C and boiler temperatures of 60°C and 80°C only allowed a maximum reduction of 1% and 2% respectively in the strong solution concentration. The resulting slight lowering of evaporator temperatures (less than 3°C) did not warrant the use of this much cooling potential, when compared with using a lower solution concentration difference described in the previous subsection.

These results align with the operational theory; when considering the specific enthalpy of the flows through the boiler the refrigerant (due to its phase change) contains most of the boiler input energy. The subsequent heat removal requirement in the condenser will be considerable resulting in the need for a large mass flow of heat transfer fluid. The energy requirement to lower the temperature of this large flow of heat transfer fluid will also be considerable. Taking into consideration that the highest CoP in this analysis is less than 0.7 and the typical range depending on solution concentration difference is 0.2 to 0.5 it is unlikely that there will be sufficient energy to provide useful cooling of the condenser heat transfer fluid. Cooling the condenser with the evaporator tap off method in the conditions addressed in this thesis can be considered ineffective.

7.4 Error Analysis

Effective error analysis in this kind of modelling is extremely difficult, there are errors that arise from the equations of state for both the solution and refrigerant. Some, but not all, of which are presented in Ajib and Karno

(2008) and NIST (2011). Further errors are created from the lookup table resolution; a resolution of 1°C and 1% of solution concentration was used.

One approach to simplify this process is to determine the most significant cause of error in the model and use the model to quantify it. The resolution of the lookup tables is likely to be the most significant error as these determine the key variables within the system when conditions change.

A resolution of 1% in solution concentration will only affect the strong solution concentration (as the weak solution concentration is calculated from adding the desired difference to the strong solution). A 1% change in strong solution concentration caused a maximum change in evaporator temperature of 2°C. The evaporator temperature is determined from a lookup table of the absorber outlet conditions which has a resolution of 1°C. Changing the weak solution temperature at the outlet of the absorber by 1°C affects the evaporator by a maximum of 1°C. Taking the larger of these, 2°C, provides a conservative error for the evaporator temperature. Changing the evaporator temperature by 2°C has a 0.5% change to cooling energy of the evaporator. The CoPs calculated were all less than 1 which would reduce this error when carried through to CoP, to provide a conservative estimate for the CoP error 0.5% will be used.

Karno and Ajib (2008) present simulation results providing a CoP 0.6 when the experimental result was approximately 0.4. This is likely to be a result of a number of modelling assumptions for example: there are no losses between components, the effectiveness of the heat exchangers, the effectiveness of the mass transfer in the boiler, homogeneity of the working fluids and errors in the thermophysical and thermodynamic property equations. Though this figure should be used with caution, its presents the reality that a simulation result can be over 30% greater than a physical result.

7.5 Configuration Conclusion

The findings from this analysis indicate that using evaporator tap off would not be effective with the double boiler configuration due to the high quantity of energy consumed in lowering the absorber temperature rather than using lower solution concentration differences. Moreover lower evaporator temperatures can be achieved by keeping the refrigerators separate as different solution concentrations can be used.

These findings also show the coupled cycle approach where the cooling provided by the genset radiator absorption refrigerator would be used to cool the absorber and / or condenser of the CPV absorption refrigerator would not provide any benefit to the evaporator temperature. This is a result of the genset radiator heat load being equivalent to 28% of the CPV heat load and the results showed that over 40% of the cooling provided by the CPV would need to be used for the evaporator tap off with a 6% solution concentration difference, and over 70% for a 4% solution concentration difference. Therefore there would not physically be enough cooling available to achieve results which are not as desirable as those found from lowering the solution concentration difference.

The half effect cycle suffers an energy penalty from splitting the heat source. It is generally used when the boiler temperatures are too low to operate in a given environment. As the single effect cycle modelled can work in the conditions expected it was therefore considered unnecessary to investigate it.

The most effective method of achieving low evaporator temperatures from heat sources at 60°C and 80°C is to use a small solution concentration difference, in this analysis 2%. The following set of results shows the expected outputs of single effect absorption refrigerators powered by the low temperature heat sources found in the BioCPV Rural Renewable Power Plant. These

are the CPV with 116 kW·h per day at 60°C and the genset radiator with 32 kW·h per day at 80°C, both with a 2% concentration difference. Ambient temperatures of 0°C to 50°C are investigated in all of the following analyses.

7.5.1 CPV Waste Heat Powered Absorption Refrigerator

Figure 7.17 shows the evaporator temperatures achieved with the CPV waste heat source powering an absorption refrigerator with varying ambient temperatures. It shows that sub 0°C evaporator temperatures can be achieved at ambient temperatures below 21°C and evaporator temperatures lower than 10°C at ambient temperatures below 27°C. Combining this analysis with Figure 7.9 the CPV heat source can provide a 10°C drop from ambient up

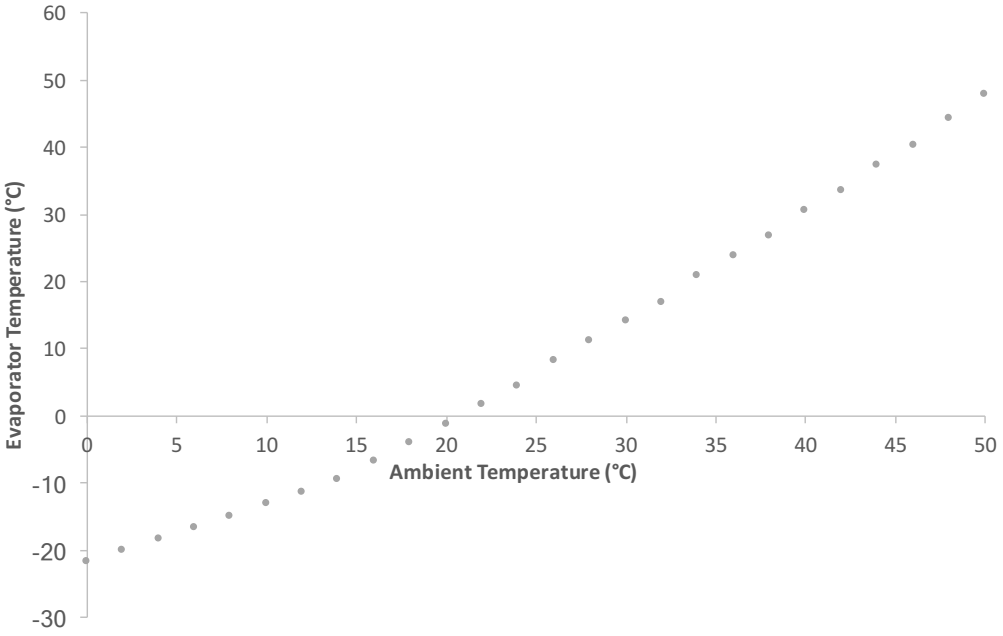

Figure 7.17: Evaporator temperature of a single effect cycle using the CPV waste heat as a heat source at 60°C with a 2% solution concentration difference at ambient temperatures from 0°C to 50°C.

to an ambient temperature of 38°C, which would provide a noticeable relief from the heat though it would be hotter than the recommended indoor temperature of 24°C.

Up to ambient temperatures of 24°C a CPV waste heat powered absorption refrigerator in this configuration could provide cooling for food in line with Food Standards Agency safe food storage requirement of below 8°C. Ambient temperatures between 24°C and 30°C from this analysis appear to be suitable for the refrigeration of root vegetables (10°C to 15°C). Refrigeration temperatures generated at ambient temperatures above 30°C may prolong the life of some foods in the short term but would be more suited for space cooling.

Figure 7.18 shows the daily cooling energy (or evaporator heat absorb-

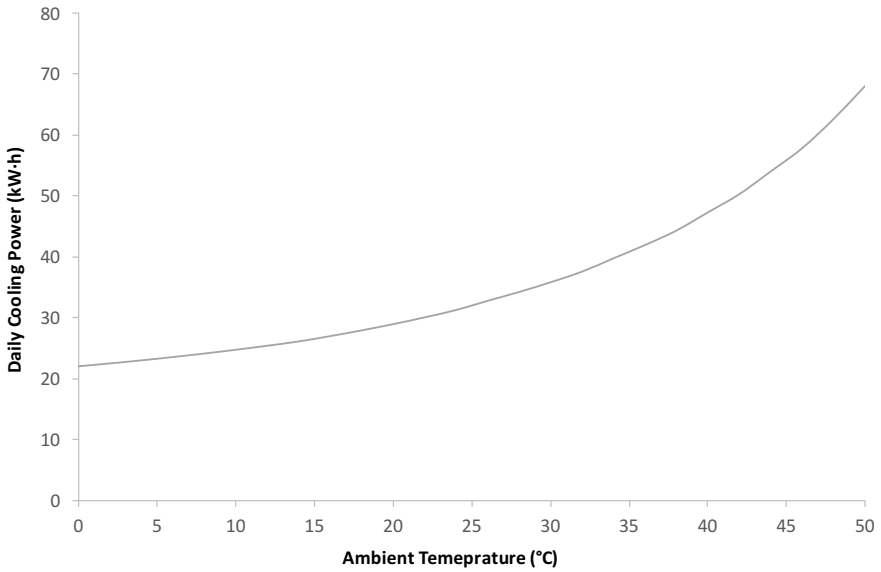

Figure 7.18: Cooling energy (evaporator heat absorbing energy) of a single effect cycle using the CPV waste heat as a heat source at 60°C with a 2% solution concentration difference at ambient temperatures from 0°C to 50°C.

ing energy) that an absorption refrigerator could produce when powered by the CPV waste heat with a 2% solution concentration difference in ambient temperatures from 0°C to 50°C. The graph shows that there is the potential to provide 23 kW·h at an ambient temperature of 0°C to 71 kW·h at an ambient temperature of 50 °C. The increasing quantity of cooling with ambient temperature is a result of the weak solution being warmer at higher ambient temperatures when it enters the boiler and that higher evaporator temperatures (seen in Figure 7.17) are generated.

Combining this analysis with the information in Figure 7.17 refrigeration of food in line with the Food Standard Agency requirements can be provided up to ambient temperatures of 24°C which corresponds to a cooling power of

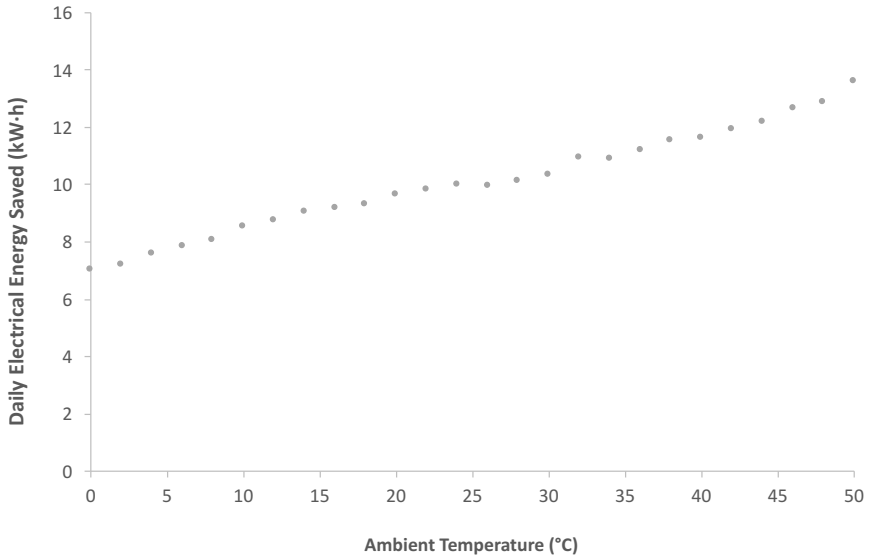

Figure 7.19: Daily electrical energy saved (avoided) from not using a vapour compression refrigerator to provide the same cooling as a single effect cycle using the CPV waste heat as a heat source at 60°C with a 2% solution concentration difference at ambient temperatures from 0°C to 50°C.

32.6 kW·h per day. This can be considered equivalent to 23 to 32 domestic refrigerator units. However the temperatures in the location of the power plant are expected to exceed this.

If the cooling generated at ambient temperatures above 24°C is used for space cooling, then there would be 32 kW·h at 24°C to 46.2 kW·h at 40°C. In terms of a 5 kW air conditioning system for a room in a medical centre this cooling can be considered equivalent to 6 to 9 hours per day of cooling.

To quantify the benefit of this cooling in terms of the electricity, Figure 7.19 presents the daily electrical energy that would have been used by an electrically driven vapour compression refrigerator to provide the same output as the absorption refrigerator powered by the CPV waste heat at varying ambient temperatures. The graph shows that between 7 kW·h and 14 kW·h can be saved per day in ambient conditions of 0°C to 50°C respectively. To put this in perspective of the energy analysis shown in Figure 5.2 the 116 kW·h of waste heat at 60°C in a 25°C environment can provide the same amount of cooling as 10 kW·h of electricity would provide which is approximately 17.5% of the electrical output of the renewable power plant.

7.5.2 Genset Radiator Waste Heat Powered Absorption Refrigerator

Figure 7.20 shows the evaporator temperatures achieved with the genset radiator waste heat source at 80°C powering a single effect absorption refrigerator with varying ambient temperatures. It shows that sub 0°C temperatures can be achieved at ambient temperatures below 25°C and lower than 10°C at ambient temperatures below 33°C. This refrigerator can provide a temperature drop from ambient greater than 20°C up to ambient temperatures of 41°C, even at 50°C it can provide an evaporator temperature of 35°C.

In terms of food storage this configuration of absorption refrigerator would

achieve the Food Standards Agency requirements of sub 8°C cooling up to ambient temperatures of 31°C and temperatures suitable for root vegetable storage (10°C to 15°C) up to ambient temperatures of 37°C. Above this the refrigeration temperatures are more suitable for space cooling.

Figure 7.21 shows the daily cooling energy (evaporator heat absorbing energy) available from a single effect absorption refrigerator powered by the genset radiator at 80°C at varying ambient temperatures. This ranges from 5 kW·h at an ambient temperature of 0°C to 10 kW·h at 50°C. At the conditions used for the energy analysis (25°C) there is 6.3 kW·h of cooling available. The cooling provided by this refrigerator is suitable for food storage for the average ambient temperatures expected in the case study location Kalingung - Pearson Pally, Santiniketan, West Bengal, India (24°C to 35°C). This refrigerator provides the equivalent cooling to 6 to 8 domestic scale re-

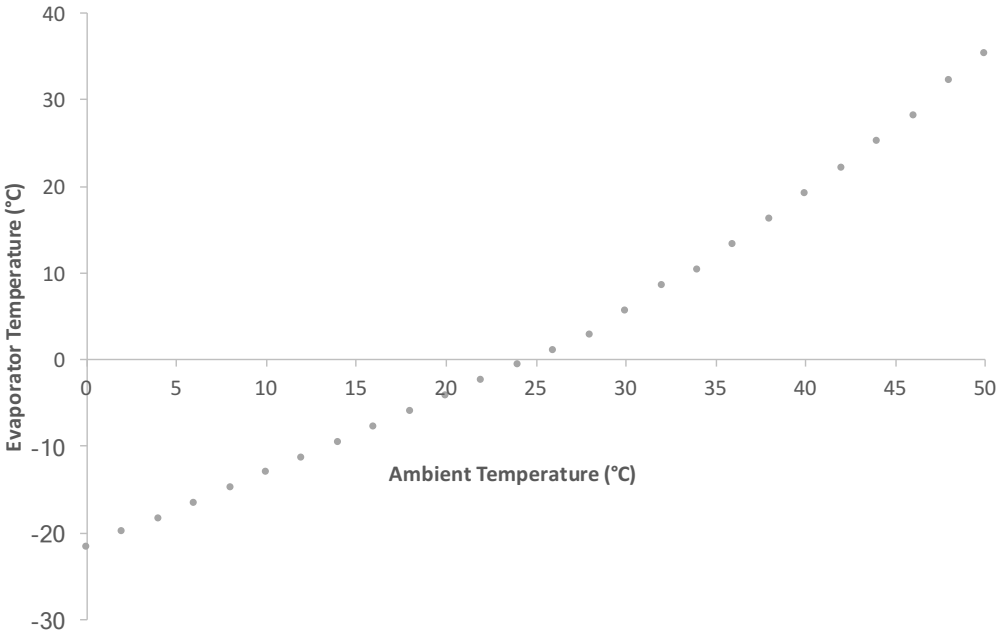

Figure 7.20: Evaporator temperature of a single effect cycle using the genset radiator waste heat as a heat source at 80°C with a 2% solution concentration difference at ambient temperatures from 0°C to 50°C.

frigerators. To ensure the preservation of food when ambient temperatures are above 30°C chilled food storage areas could be separated based on access requirements to keep the units sealed as long as possible, reducing the unnecessary loss of cooling to the environment.

Figure 7.22 shows the amount of electricity that would have been used (i.e. saved) if a vapour compression refrigerator was generating the same amount of cooling as the genset radiator waste heat powered absorption refrigerator. The results find that from ambient temperatures of 0°C to 50°C between 1.6 kW·h and 2.9 kW·h per day of electricity can be saved respectively. To compare with the energy analysis in Figure 5.2 at an ambient temperature of 25°C, 2.3 kW·h per day of electrical energy would have been used if a vapour compression refrigerator was used to provide this cooling. This equates to

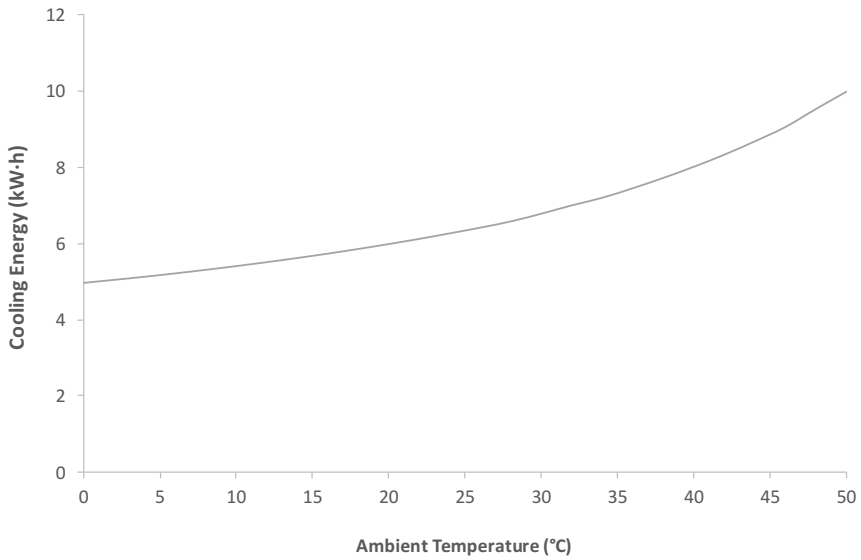

Figure 7.21: Daily cooling energy of a single effect cycle using the genset radiator waste heat as a heat source at 80°C with a 2% solution concentration difference at ambient temperatures from 0°C to 50°C.

4% of the electricity being provided to the village.

The analysis in this section also alludes to the possible benefits of operating the CPV at higher temperatures, particularly during high ambient temperatures; when space cooling and refrigeration of food and medicines is required most. Analysing Figures 7.9 and 7.11 the evaporator temperatures are over 15°C lower than ambient temperatures up to ambient temperatures of 50°C with an 80°C boiler temperature whereas at a boiler temperature of 60°C this is only achievable with ambient temperatures lower than 32°C. The CoP penalty, from Figures 7.10 and 7.12, for operating at 80°C rather than 60°C is between 25% to 50% at ambient temperatures of 0°C and 50°C respectively. As the CPV has approximately 3.6 times more waste heat available to power an absorption refrigerator than the genset radiator, a re-

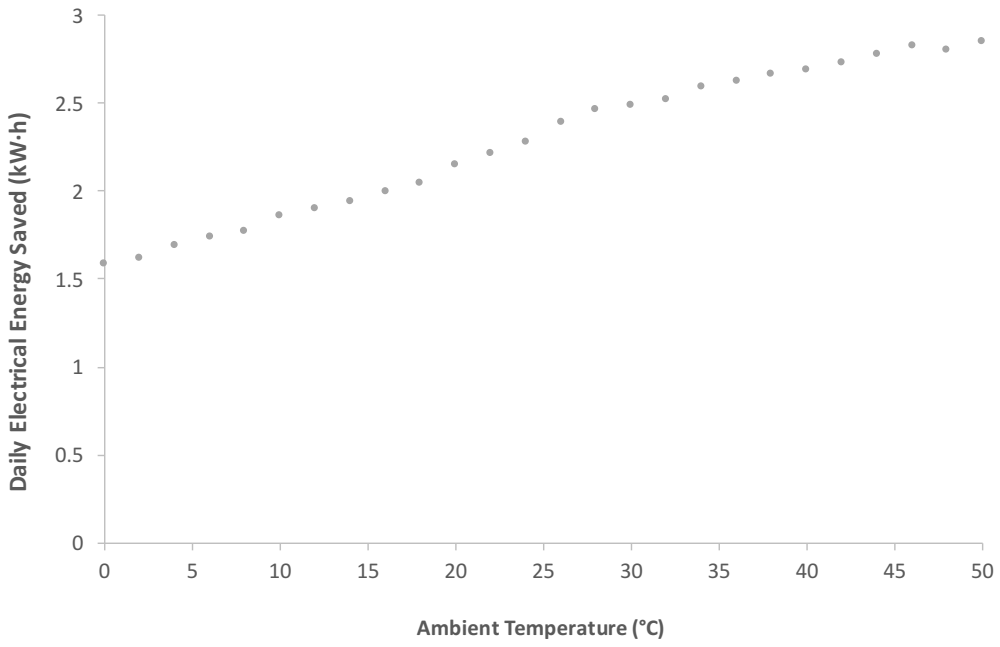

Figure 7.22: Daily electrical energy saved (avoided) from not using a vapour compression refrigerator to provide the same cooling as a single effect cycle using the genset radiator waste heat as a heat source at 80°C with a 2% solution concentration difference at ambient temperatures from 0°C to 50°C.

duction in cooling output in favour of lower evaporator temperatures during the hottest periods is beneficial. In practice, during high (32°C to 50°C) ambient temperatures, a control mechanism allowing the CPV waste heat powered absorption refrigerator to operate at 80°C could provide evaporator temperatures ranging from 8°C to 35°C with CoPs ranging from 0.2 to 0.3. It should be noted that operating the CPV at higher temperatures creates a risk of localised overheating if the heating and cooling profiles of the PV cells are not uniform. Therefore, careful monitoring of the PV cell temperature at multiple locations will be required together with adequate flow control through the heat exchangers of the PV cells.

Assuming that it is possible to operate an absorption refrigerator from the CPV operating at 80°C, this creates an opportunity for further investigation into the use of the coupled cycle system where the CPV powered absorption refrigerator could cool the genset powered absorption refrigerator. At ambient temperatures of 50°C an absorption refrigerator operating with a boiler temperature of 80°C generates an evaporator temperature of 35°C. Assuming this could cool both the absorber and condenser to simulate ambient conditions between 35°C and 40°C, evaporator temperatures of 10°C to 19°C are achievable respectively. These suggested evaporator temperatures could allow medicines with storage requirements of keep cool and store at room temperature as well some root vegetables to not perish during the hottest periods of the year.

7.6 Within Day Analysis

In order to gain some insight in how the system will operate on a day-to-day basis, this section provides an analysis of some typical days that would be experienced in the region. The typical day criteria are, high DNI, low DNI, high temperature and low temperature. DNI and ambient temperature data

are provided from NREL India Solar Resource Data using from using the nearest cell to Santiniketan 87.65° E, 23.65° N (NREL 2016).

The CPV operates during the daytime where ambient temperature and DNI vary significantly. Ambient temperature affects the maximum permissible strength of the strong solution, as described in Section 7.1 and DNI indicates the input energy in to the CPV, which is used to generate electricity and heat. The model assumes that the PV cell temperature is kept constant at 60°C, this could be achieved with thermostatic valves or variable speed drives on the cooling circuit of the PV cells.

Due to the ambient temperatures and operation of the genset being reasonably consistent throughout the evening, it was deemed unnecessary to conduct the following analysis for the genset radiator powered absorption refrigerator.

The systems are analysed such that the heating period and cooling period are separated. The heating period occurs the day before the cooling period where the heat input powers the boiler which fills the strong solution reservoir and refrigerant reservoir (via the condenser) for the following day. The cooling occurs over 24 hours on the following day (from midnight to midnight). If this operational strategy were implemented in a physical system, the inlets and outlets to the reservoirs would need to be monitored so that the stored quantity in the reservoirs are known. Then a control strategy could be implemented to ensure the stored quantity at the end of the heating period is sufficient to provide cooling for the following day.

It should be noted that the model is set up in a way where it determines the most concentred strong solution concentration permissible for a given boiler temperature and ambient temperature, the weak solution concentration is then set at a desired number of percentage points above this. Due to the previous analysis in this chapter finding 2% difference in strong and weak solutions to be optimal for low evaporator temperatures, 2% was used.

In reality the weak solution being fed into the boiler may be at varying concentrations, which will require control over the flow rates in the boiler and management of the heat transfer at the boiler exit to assist in optimising the strong solution concentration. For if the strong solution leaving the boiler cools too quickly the strong solution may reabsorb refrigerant faster than it can be condensed in the condenser.

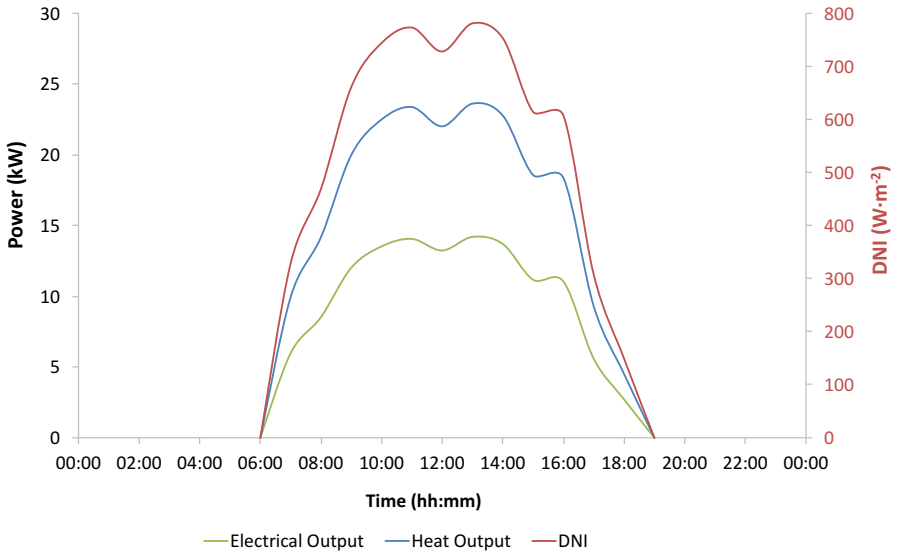

Figure 7.23: High DNI day analysis of the CPV electrical (green line, left axis) and heat (blue line, left axis) outputs together with the corresponding DNI (red line, right axis), to be used for the heating side of the CPV waste heat powered absorption refrigerator using ambient temperature and DNI data from the 20th August 2011 from NREL (2016).

7.6.1 High DNI Day

The 20th August 2011 had particularly high DNI using the data from the India solar resource data set provided by NREL (NREL 2016) and sorting the data to find an occasion with a high DNI. Figure 7.23 shows this high DNI day where the DNI is shown by the red line (right axis), the electrical output by the green line (left axis) and the heat output by the blue line (left axis). Sunlight was available between 06:00 and 19:00, peaking with 781 $W \cdot m^{-2}$ at 13:00. There appears to be some cloud cover or minor shading at midday as

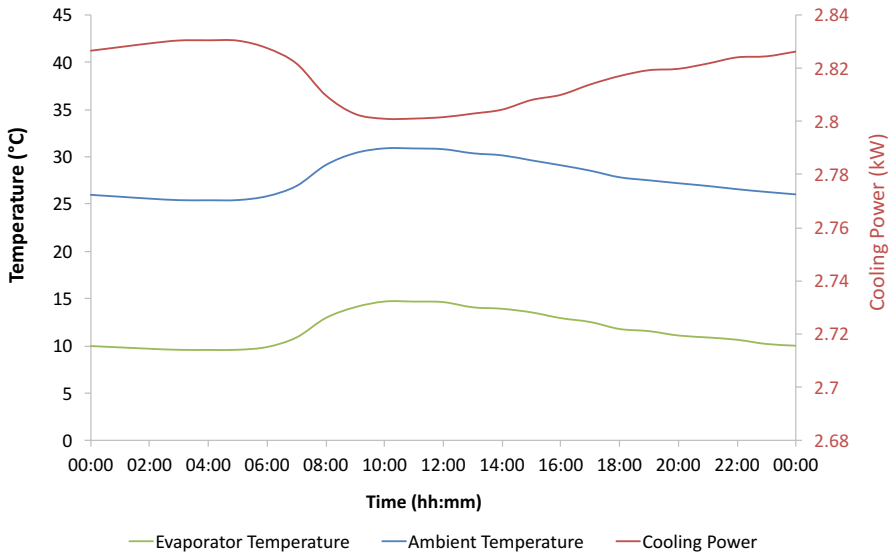

Figure 7.24: High DNI day analysis of the CPV waste heat powered absorption refrigerator showing the evaporator temperature (green line, left axis), ambient temperature (blue line, left axis) and cooling power (red line, right axis). Using the ambient temperature from the 21st August 2011 where the previous day was used to fill the strong solution and refrigerant reservoirs. Data from NREL (2016).

the DNI dropped to 728 $W \cdot m^{-2}$. The DNI profile determines the electrical and heat output profiles peaking at 14.2 kW and 23.6 kW respectively also at 13:00. The majority of the solar irradiance falls in the period of 09:00 and 16:00 with a steep rise and fall over the 3 hours either side of this respectively. This profile provides confidence in the modelling approach used in the earlier parts of this chapter where the irradiance lasted 7 hours at a constant value.

The analysis shown in Figure 7.23 provides the heat input to power the absorption refrigerator. Due to the changing ambient temperatures, the strong solution concentration varied from 63% at the coldest period (07:00, 26.1°C) and 60% at the hottest (11:00 to 14:00, 30.7°C to 31.2°C).

Once the heating period is complete the fluids that will be used for the cooling part of the circuit the following day can be calculated. The strong solution concentration mixture was calculated as 60.7%. The strong solution mass for the cooling period was calculated as 13,595 kg and the working refrigerant 463 kg.

Taking the mass flow rates over the 24 hour cooling period of the strong solution and refrigerant together with the ambient temperature of the following day, 21st October 2011, the cooling output of the refrigerator can be calculated. Figure 7.24 shows the cooling power (red line, right axis), the ambient temperature (blue line, left axis) and evaporator temperature (green line, left axis). The ambient temperature rises from 26°C at night to a peak of 30.9°C at 10:00 and the hot period (above 29°C) was from 08:00 to 16:00. As the cooling part of the model uses constant flow rates and solution concentrations the evaporator temperature rises proportionally from 10°C at night and peaking at 14.7°C at 10:00. This is to be expected as the evaporator temperature is calculated from the ability to exchange heat from the absorber to ambient conditions.

The cooling power ranges from 2.80 kW to 2.83 kW interestingly it follows an inverse shape to the evaporator and ambient temperatures. This is likely

to be a result of the modelling assumption of the evaporator entry and exit conditions; the refrigerant enters through an isenthalpic throttle and leaves as a saturated vapour. This causes a small difference in enthalpy (4.8 $kJ \cdot kg^{-1}$) between the highest and lowest temperature in the day, while flow rates remain constant. This can be seen in Figure 4.2 from the shape of the dry vapour side of the curve.

The evaporator temperatures correspond reasonably with the results presented in Figure 7.17 for example at an ambient temperature of 26°C Figure 7.24 shows an evaporator temperature of 10°C compared to Figure 7.17 showing an evaporator temperature of 8.3°C. Likewise at an ambient temperature of 30°C Figure 7.17 has an evaporator temperature of 14°C and Figure 7.24 shows an evaporator temperature 14.9°C. The slight difference is a result of the modelling methods where in Figure 7.17 the model optimises the solution concentrations for one ambient temperature during which heating and cooling occurs. Whereas, in this section, the analysis has varying ambient temperatures during the strong solution generation (during the heating day) and so the strong solution is not optimised for the ambient temperature at the point of cooling.

When comparing the cooling output in this analysis (Figure 7.23) with the analysis in Section 7.2 and Figure 7.18 the daily cooling energy is quite different, 67.6 kW·h and 37.3 kW·h respectively. The reason for this difference is that the analysis in Section 7.2 and Figure 7.18 uses a flat DNI profile of 550 $W \cdot m^{-2}$ for 7 hours totalling 3.85 $kW \cdot h \cdot m^{-2}$ compared the total DNI over the 24 hour heating period in this analysis of 6.915 $kW \cdot h \cdot m^{-2}$. The outcome of this finding is that, for longer days with high DNI the analysis in Section 7.2 is conservative and higher cooling energy outputs can be expected.

7.6.2 Low DNI Day

The 22nd June 2004, had significantly low DNI throughout the day to be used for a low DNI day analysis (NREL 2016). Figure 7.25 shows the solar irradiance (red line, right axis) along with the heat (blue line, left axis) and electrical output (green line, left axis) of the CPV if it were to operate in these conditions. Solar irradiance was only available between 9:00 and 17:00 where it peaks at 152 $W \cdot m^{-2}$ at 13:00 and drops to 136 $W \cdot m^{-2}$ at 14:00. For the remaining hours where sunlight is available the DNI is very low 16 $W \cdot m^{-2}$ to 37 $W \cdot m^{-2}$ in the morning and 12 $W \cdot m^{-2}$ to 26 $W \cdot m^{-2}$ in the afternoon.

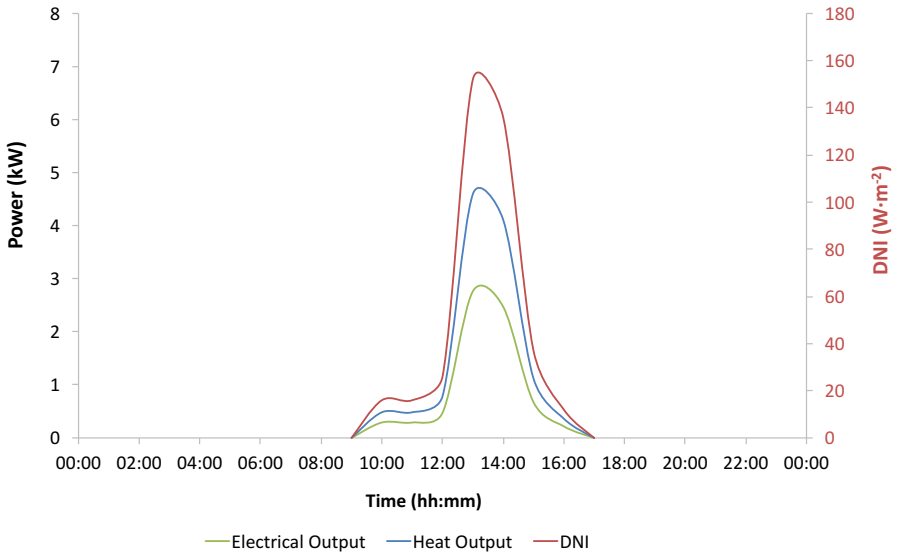

Figure 7.25: Low DNI day analysis of the CPV electrical (green line, left axis) and heat (blue line, left axis) outputs together with the corresponding DNI (red line, right axis), to be used for the heating side of the CPV waste heat powered absorption refrigerator using ambient temperature and DNI data from the 22nd June 2004 from NREL (2016).

This low DNI provided low heat and electrical generation from the CPV peaking 4.6 kW and 2.8 kW respectively at 13:00 and less than 0.5 kW for the remaining sunlight hours. It is worth noting that, with such low outputs, further investigation is required to determine how much recoverable waste heat would actually be produced from the CPV in these conditions. However this analysis provides insight into the absorption refrigerator operation if the heat were to be recoverable.

The conditions shown in Figure 7.25 provided strong solution concentrations in the range of 60% to 61%. The heating cycle generated 793 kg at

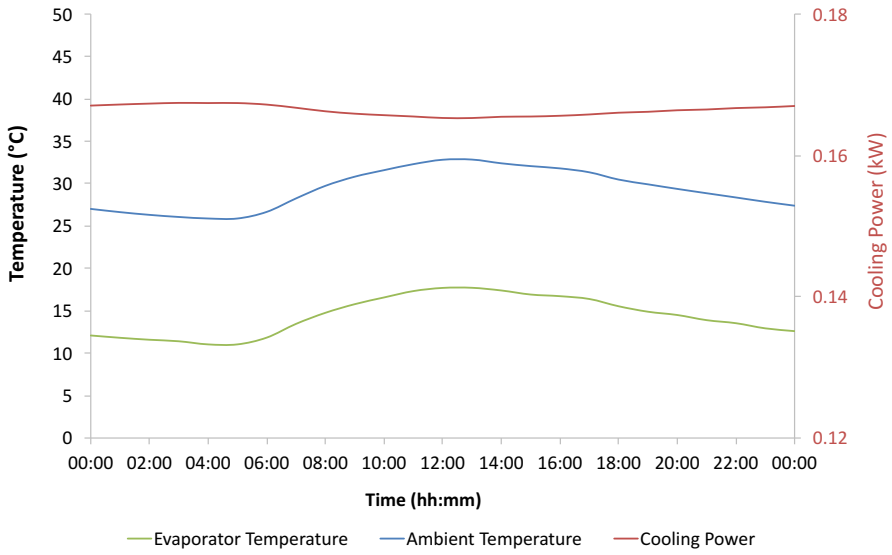

Figure 7.26: Low DNI day analysis of the CPV waste heat powered absorption refrigerator showing the evaporator temperature (green line, left axis), ambient temperature (blue line, left axis) and cooling power (red line, right axis). Using the ambient temperature from the 23rd June 2004 where the previous day was used to fill the strong solution and refrigerant reservoirs. Data from NREL (2016).

60% of strong solution and 27 kg of refrigerant to be used over a 24 hour period the following day. The model used uses these fluids and simulates the refrigeration for the following day (23rd June 2004), Figure 7.26 shows the cooling output (red line, right axis), the ambient temperature (blue line, left axis) and evaporator temperature (green line, left axis). The cooling output is expectedly low 0.165 to 0.167 kW though evaporator temperatures were between 14.7°C and 15.1°C below ambient throughout the 24 period. Indicating that in these conditions, useful cooling temperatures for space cooling or root vegetable storage is possible but there is little cooling energy (approximately 5 domestic refrigerators or 5% of a typical air conditioning unit for a small room). These outputs indicate the need to consider an alternative operational approach, where the strong solution and refrigerant storage time is longer than 24 hours so that cooling can be provided when DNI is low. If weather forecasting data was integrated with a control strategy together with suitably sized reservoirs a system could be designed to continue to operate effectively over these conditions.

The evaporator temperatures do not correspond as well with the analysis in Section 7.2 and Figure 7.17 as the high DNI day. For example at an ambient temperature of 26°C the evaporator temperatures of Figures 7.26 and 7.17 were 11.4°C and 8.3°C respectively. Though at an ambient temperature of 30°C the evaporator temperatures of Figures 7.26 and 7.18 were 15°C and 14°C respectively. The difference is likely to be a result of the majority of the solar irradiance being available when the ambient temperature was closer to 30°C.

Due to the nature of this analysis, showing how the system would behave on a very low DNI day, the cooling output across the whole day is significantly lower than anything shown in the analysis in Section 7.2. The low DNI day had a total DNI over the day of 0.4 $kW \cdot h \cdot m^{-2}$ and cooling output energy of 4.16 kW·h in comparison to the lowest cooling output in Figure

7.18 of 23 kW·h for a 24 hour period which had a total daily DNI of 3.85 kW·h·m^{-2}. Though poor performance is expected in these conditions, these results emphasise the need to investigate control strategies that can mitigate the effects of poor weather conditions.

7.6.3 High Temperature Day

The high temperature days chosen for this analysis occurred on the 11th and 12th May 2011, these days had peak temperatures of 43.9°C and 43.4°C respectively. Figure 7.27 shows the DNI (red line, right axis), electrical (green

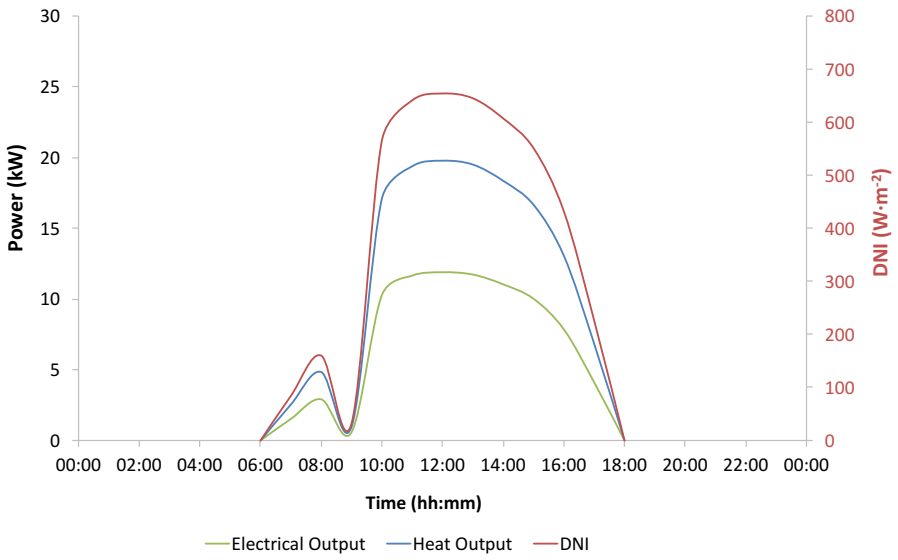

Figure 7.27: High temperature day analysis of the CPV electrical (green line, left axis) and heat (blue line, left axis) outputs together with the corresponding DNI (red line, right axis), to be used for the heating side of the CPV waste heat powered absorption refrigerator using ambient temperature and DNI data from the 11th May 2011 from NREL (2016).

line, left axis) and heat (blue line, left axis) output of the CPV for the 11th May 2011. The DNI peaked 654 W·m^{-2} at 12:00 and maintained a DNI greater than 550 W·m^{-2} from 10:00 to 15:00. Interestingly this day appears to have some shading at 09:00 where the DNI dropped to 32 W·m^{-2}, this could be a result of heavy cloud cover or something physically blocking the sensor. The electrical and heat output of the CPV peak at 12:00 with 19.8 kW and 11.9 kW respectively, and maintained outputs greater than 10 kW and 16 kW respectively from 10:00 to 15:00. These conditions generated strong solution concentrations ranging from 62% when ambient temperature

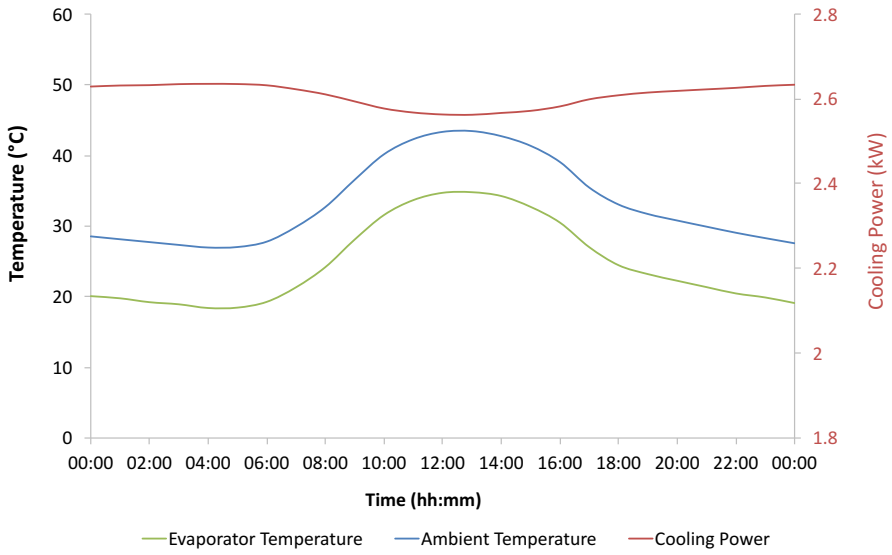

Figure 7.28: High temperature day analysis of the CPV waste heat powered absorption refrigerator showing the evaporator temperature (green line, left axis), ambient temperature (blue line, left axis) and cooling power (red line, right axis). Using the ambient temperature from the 12th May 2011 where the previous day was used to fill the strong solution and refrigerant reservoirs. Data from NREL (2016).

was 29°C at 07:00 to 51% when ambient temperature was 43.9°C at 13:00. At the end of the heating period there was 10,852 kg of strong solution at 53.1% and 425 kg of refrigerant to be used the following day for 24 hours of cooling.

Figure 7.28 shows the ambient temperature (blue line, left axis), evaporator temperature (green line, left axis) and cooling power (red line, right axis). The results show a good quantity of cooling available, between 2.56 kW and 2.63 kW, the dip occurring around midday as seen in the high DNI day analysis. However it appears the quality and therefore versatility of the cooling is poor as the evaporator temperature is between 8.4°C and 8.7°C lower than ambient temperature for the full 24 hour period. This indicates that for the conditions over these two days the refrigerator could provide space cooling as the temperature drop would be noticeable, though small. It may be worth considering some form of separate dehumidification to improve the thermal comfort if this cooling were used in this manner.

These evaporator temperatures correspond to the findings in Section 7.2 where Figure 7.9, the difference between ambient temperature and evaporator temperatures is shown to be between 9.4°C and 6.7°C at ambient temperatures of 40°C to 44°C, which is within the range of ambient temperatures in Figure 7.28. When comparing the total amount of cooling available over the 24 period this analysis shows 62.6 kW·h in comparison to 50.9 kW·h from Figure 7.18 using an ambient temperature of 41°C, as this was the average temperature during the bulk of the DNI. This is largely a result of the difference in DNI used for both models in this analysis the DNI over the heating day totalled 4.6 $kW \cdot h \cdot m^{-2}$. There is also the already mentioned factor of the analysis in Section 7.2 being optimised for a single ambient temperature.

7.6.4 Low Temperature Day

The low temperature day analysis uses data from the 4th and 5th January 2004 where the peak temperatures were 23.4°C and 22.3°C respectively. Figure 7.29 shows the DNI (red line, right axis), electrical (green, left axis) and heat (blue, left axis) outputs from the CPV for the conditions on the 4 January 2004. DNI is available from 07:00 to 16:00 and peaks at 455 W·m^{-2} at both 11:00 and 12:00. The electrical and heat output from the CPV peak at 13.8 kW and 8.3 kW respectively also at 11:00 and 12:00. The majority of the DNI and therefore electrical and heat output occurs between 10:00 and

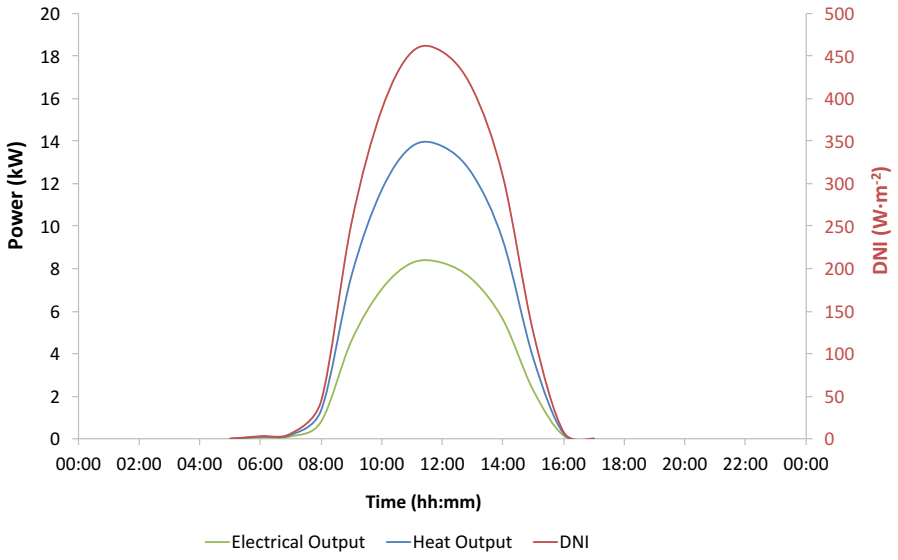

Figure 7.29: Low temperature day analysis of the CPV electrical (green line, left axis) and heat (blue line, left axis) outputs together with the corresponding DNI (red line, right axis), to be used for the heating side of the CPV waste heat powered absorption refrigerator using ambient temperature and DNI data from the 4 January 2004 from NREL (2016).

14:00. This heating period generated strong solution concentrations ranging from 70% before 08:00 when ambient temperature was less than 17°C to 65% from 12:00 to 14:00 when ambient temperature was 22.9°C and 23.4°C respectively. At the end of the heating period there was 4,355 kg of strong solution at 66% and 136 kg of refrigerant.

Figure 7.30 shows the cooling output (red line, right axis), ambient temperature (blue line, left axis) and evaporator temperature (green line, left axis) for the conditions on the 5 January 2004, if the heating period took place the day before. The cooling power is reasonably low in comparison to

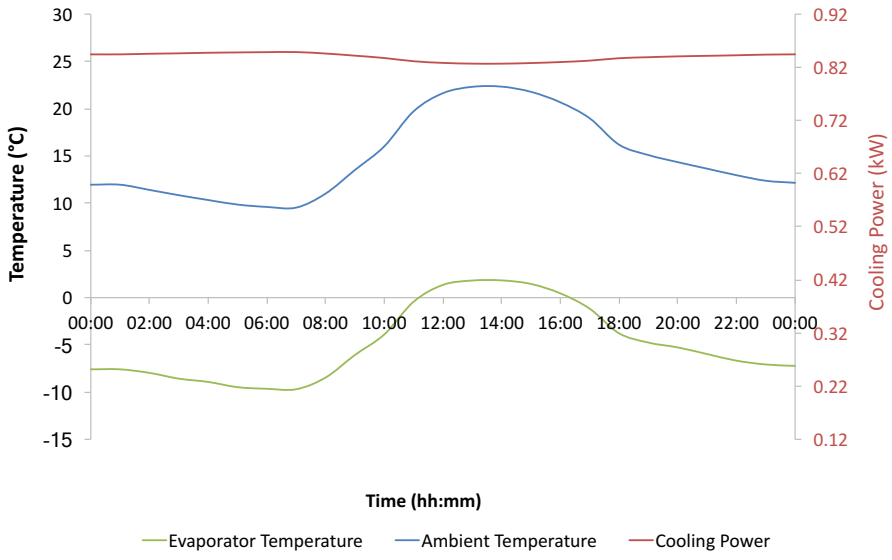

Figure 7.30: Low temperature day analysis of the CPV waste heat powered absorption refrigerator showing the evaporator temperature (green line, left axis), ambient temperature (blue line, left axis) and cooling power (red line, right axis). Using the ambient temperature from the 5 January 2004 where the previous day was used to fill the strong solution and refrigerant reservoirs. Data from NREL (2016).

the high DNI and high temperature days, ranging from 0.83 kW to 0.85kW, the dip occurring around midday. The difference between ambient temperature and evaporator temperature is between 16.5°C and 17.6°C, where sub zero evaporator temperatures achieved during the evening and morning up to 10:00. The highest evaporator temperature was at 14:00 at 4.8°C which is still cold enough for most food and 'store refrigerated' medicines.

Comparing the low temperature day findings with the results in Section 7.2 using Figures 7.17 and 7.30, at an ambient temperature of 22°C the evaporator temperatures are both 1.6°C, whereas at an ambient temperature of 10°C the evaporator temperatures are -9.2°C and -13.1°C respectively. This is a result of the already mentioned difference in modelling approaches.

There is a substantial difference in cooling energy over the 24 hours between the low temperature day and the analysis in Section 7.2, using the equivalent average temperature for the bulk of the solar irradiance on the heating day (22°C). The results in Figure 7.18 suggest 30.8 kW·h of cooling energy per day whereas the analysis in Figure 7.29 indicates 20.2 kW·h of cooling over 24 hours. This is likely to be a result of the difference in total DNI on the heating day to that used in Figure 7.18, 2.46 $kW \cdot h \cdot m^{-2}$ and 3.85 $kW \cdot h \cdot m^{-2}$ respectively.

The within day analysis has provided insight into the operational performance of the absorption refrigerator with storage of one day. The results have highlighted the difference in performance resulting from different levels of DNI and ambient temperature that can be expected from typical days in this region. In particular, to mitigate the effect of low DNI and high temperature days there is a need to investigate longer refrigerant and strong solution storage times together with integrating weather forecasting so that in practice the refrigerator can have some resilience to these conditions.

7.7 Absorption Refrigeration Modelling Conclusion

The results presented here investigated the waste heat sources which were quantified in terms of energy and exergy at an ambient temperature of 25°C in Chapter 5. In terms of energy these are CPV at 60°C with 116 kW·h per day equivalent to 38% of the total system input energy and the genset radiator at 80°C with 32 kW·h equivalent to 10% of the system input energy. However in terms of exergy they dwindle to 12 kW·h and 5 kW·h respectively, indicating that there is a high quantity of energy but it is of low quality. This provided a benchmark for the analysis of absorption refrigeration in terms of waste heat utilisation. Experimental results in Chapter 6 provided confidence in the modelling assumptions used for the results presented in this chapter.

The challenge of absorption refrigeration, described in Section 3.3.1, is managing the trade-offs between conflicting variables, the following were investigated in this analysis:

- The desire to operate in high ambient temperatures requires dilute strong solutions whereas the desire to have low evaporator temperatures require concentrated weak solutions.
- Condenser heat exchanger effectiveness limits the strength of the strong solution, which either limits the minimum boiler temperature or pushes the strong solution to be more dilute which causes the weak solution to be more dilute and therefore increases the evaporator temperature.
- Absorber heat exchanger effectiveness limits the minimum temperature of the weak solution outlet of the absorber which limits the minimum evaporator temperature.
- Reducing the difference in strong and weak solution concentration reduces the effect of the absorber heat exchanger effectiveness and can

provide lower evaporator temperatures.

The configuration analysis of the absorption refrigerators found that lower evaporator temperatures can be achieved by using a small (2%) difference in the strong and weak solution concentrations than the methods described to cool the condenser and absorber. Using a small solution concentration difference was also more energy efficient than the other methods presented.

Using a 2% solution concentration difference in two separate refrigerators powered by each waste heat source independently, at the same conditions as the energy and exergy analysis, can provide 33.4 kW·h of cooling per day at 6°C and 6.3 kW·h at 0°C. These can be considered to be equivalent to 12.7 kW·h of electricity that would have been used powering a vapour compression refrigerator which equates to 22% of the total electricity provided to the village.

For the average ambient temperatures expected in the case study area (Kaligung Pearson-Palli, Santiniketan, West Bengal, India) of 24°C to 35°C an absorption refrigerator powered by the CPV would provide 6 to 9 hours of space cooling of a room in a medical centre. An absorption refrigerator powered by the genset radiator could provide the equivalent of 6 to 8 domestic refrigerator units. Collectively these refrigeration options could also be used for medicines with the following storage requirements: keep refrigerated, keep cool and store at room temperature.

The following typical within day conditions were investigated with a resolution of one hour: high temperature, low temperature, high DNI and low DNI. The results provided insight into the application of the bulk of this research which uses a resolution of one day with a constant ambient temperature and DNI. An important outcome was that further research is required to extend the refrigerant and strong solution storage time beyond 24 hours together with weather forecasting data to provide resilience to weather conditions that cause poor performance, such as low DNI and high ambient

temperatures.

Low grade waste heat was estimated at 7% of global energy consumption in Chapter 2. Extrapolating the results of this chapter, where at the 25°C reference ambient temperature the waste heat utilisation to avoided electrical consumption for cooling efficiency was 8.6%, the 7% global wasted energy (as low grade heat) if used through absorption refrigeration could mitigate electrical consumption equal to 0.6% of global energy consumption. 0.6% of global energy consumption is approximately equal to the energy consumption of Poland (CIA 2015). These figures provide a crude but useful analysis of the global benefits of utilising low grade waste heat for absorption refrigeration. It should be noted that this analysis compares electricity avoided to global energy consumption and does not take into consideration the conversion efficiency of producing electricity due to the variances of electricity generation methods globally.

Chapter 8

Conclusion of Thesis and Further Work

This thesis focusses on utilising the low grade waste heat sources within a renewable power plant in rural India for absorption refrigeration. Refrigeration is more useful than low grade heat for communities in rural India as it can provide food and medicine storage, or space cooling which could be used for medical centres, recovery rooms or education environments.

This body of research forms part of a larger project called BioCPV which is a collaboration between British and Indian universities to design and provide a renewable power plant to a 45 household community within a small rural village in West Bengal, India with the intention of promoting sustainable development. The renewable power plant specified by the BioCPV research group provided the modelling boundaries to conduct the analysis within this thesis. Though the analysis is focussed on this particular plant the findings are applicable to a wide range of circumstances where low grade waste heat is available and sustainable refrigeration could be used.

An analysis of the sustainable development needs of the community identified that lighting, fans, a charging station, computers and small scale ma-

chinery would improve the education environment, reduce exposure to indoor air pollution and alleviate some of the labour intensive work currently undertaken. A daily energy profile of these items for the community concluded the projected electrical demand to be 55 kW·h. The total power demand including system ancillaries, solar trackers and electrolyser load was estimated at 88 kW·h per day. The power plant proposed by the BioCPV research group was specified to provide a daily generation of 90 kW·h, through 10 kW of concentrated photovoltaic (CPV) for 7 hours and a 5 kW biogas-hydrogen internal combustion engine generator set (genset) for 4 hours. The low grade waste heat sources from this power plant, which were investigated in this thesis, are the CPV at 60°C and the genset radiator at 80°C.

An assessment of common forms of refrigeration concluded that absorption refrigeration combines the ability to provide adequate heat removal at the heat source as well as the potential to provide cooling from low grade heat. A review of working fluids showed acetone and zinc bromide solution to be able to work at the waste heat temperatures expected without the need for rectification.

An energy and exergy analysis of the renewable plant at the rated conditions found that the plant has a daily electrical output of 57 kW·h with an electrical efficiency of 18%. The greatest energy losses were the low grade waste heat from the CPV at 116 kW·h per day which is 38% of the total energy input and the genset radiator at 32 kW·h per day which is 10% of the total energy input. Due to the low temperature of these heat sources their exergetic values at a 25°C environment were much lower, 12 kW·h and 5 kW·h respectively. This indicated that converting these energy sources to work is not effective and provided a case for their use in heat powered refrigeration.

A lab scale, once through, experimental absorption refrigerator was built and tested as part of this thesis in order to investigate the operational perfor-

mance and challenges of an absorption refrigerator with reservoirs using acetone and zinc bromide. The results indicated that the modelling approach in terms of fluid state was appropriate. Interestingly, observations of the boiler and evaporator temperatures and operating time, found that the evaporator provided cooling for a significantly longer period than the boiler provided heat. Indicating that, if a solution pump was present and suitable control over valve opening were available, this system could have been controlled to allow continuous cooling from a discontinuous heat source. The findings also showed that the pressure was maintained after the boiler operation ceased and drew attention to the importance of boiler exit and strong solution reservoir inlet design to maximise the condensing potential and therefore the concentration of the strong solution. Temperature measurements across the boiler, which simulated the heat sources in the power plant, suggested that with adequate flow control constant temperatures can be maintained. These observations coupled with the system successfully providing refrigeration through an absorption cycle indicated that absorption refrigeration can be used to extract waste heat from the power plant components and provide refrigeration while maintaining the desired operating temperatures of the power plant components.

The assessment of absorption refrigerator configurations to lower evaporator temperatures in high ambient temperatures concluded that the evaporator tap off method is ineffective for low temperature driven absorption refrigerators. The method uses a proportion of the evaporator cooling output in addition to ambient cooling to cool the absorber and / or condenser below ambient temperature. Cooling the absorber required double the cooling loss of lowering the solution concentration difference by 2% and provided on average 1.5°C higher evaporator temperatures. Cooling the condenser, which leads to stronger weak and strong solutions being usable, had negligible effect on evaporator temperatures whilst using up to 50% of the evaporator

cooling output. The results of this identified the coupled cycle and double boiler with evaporator tap off to be less effective at lowering evaporator temperatures, in the conditions investigated, than using a smaller difference in solution concentration. The most energy effective way to generate low evaporator temperatures was to use a small difference (2%) between the strong and weak solution concentrations. However the investigations did suggest that there may be an application for the coupled cycle at high ambient temperatures which result in high evaporator temperatures. An absorption refrigerator powered by a large waste heat source such as the CPV could cool the absorber and condenser of an absorption refrigerator powered by a smaller heat source such as the genset radiator to simulate cooler conditions, providing more versatile evaporator temperatures. Though further investigation is required.

It can be concluded that at a 25°C reference ambient temperature (used for energy and exergy analysis) acetone and zinc bromide absorption refrigeration with a 2% solution concentration difference powered by the waste heat from the CPV at 60°C and the genset radiator at 80°C has the potential to provide 33.4 kW·h of cooling per day at 6°C and 6.3 kW·h at 0°C respectively. The cooling can be quantified as the equivalent of 12.7 kW·h per day of electricity that would have been consumed by a typical vapour compression refrigerator. This is equivalent to 22% of the electricity that is being provided to the end user (the village). This is 75% of the exergetic value which quantifies the output based on a theoretical Carnot heat engine. This indicates that the absorption refrigeration systems proposed can utilise these low grade heat sources but in this configuration they do not surpass the theoretical maximum work output.

An area for further investigation to identify the effectiveness of absorption refrigeration in low grade waste heat utilisation would be comparing the avoided electrical energy to the amount of electrical energy that could be

generated from a physical heat engine, rather than the theoretical maximum provided by a Carnot heat engine. For example the results of Glover et al. (2015), Peris et al. (2015) and Desideri et al. (2016) on organic Rankine cycle generators, which is a common form of heat engine, suggest efficiencies of 1% to 5% from heat sources under 100°C. Using these efficiencies instead of the Carnot efficiencies of 10.5% for the CPV and 15.5% for the genset radiator, the avoided electricity consumption from utilising these low temperature waste heat sources for absorption refrigeration outperforms, by at least a factor of two, using the heat sources to generate electricity directly.

These waste heat sources used for absorption refrigeration produce cooling that can be used for either food and medicine storage or space cooling in a health centre. The evaporator temperatures are affected by ambient temperature and careful planning on how to use the cooling and the size of the reservoirs will be required to maximise its benefit. It was identified that for the average ambient temperatures expected in the case study area (Kaligung Pearson-Palli, Santiniketan, West Bengal, India) of 24°C to 35°C an absorption refrigerator powered by the CPV would be suitable for space cooling of a room in a medical centre for 6 to 9 hours per day. An absorption refrigerator powered by the genset radiator could provide the equivalent of 6 to 8 domestic refrigerator units.

This thesis identified a technology that could utilise low grade waste heat, an energy source which accounts for an estimated 7% of global energy consumption. Extrapolating the results of this thesis the 7% wasted energy (as low grade heat) if used through absorption refrigeration could mitigate electrical consumption equal to 0.6% of global energy consumption. 0.6% of global energy consumption is approximately equal to the energy consumption of Poland. It should be noted that this analysis compares avoided electricity consumption to global energy consumption and does not take into consideration the conversion efficiency of producing electricity due to the variances

of electricity generation methods globally. Therefore the mitigated 0.6% of global energy consumption is a conservative figure and provides a case for further investigation into utilising low temperature waste heat for absorption refrigeration to reduce rising global energy consumption.

During the research that lead to this thesis a number of areas of further work have been identified, these include:

- Analysis of the operating performance of integrating absorption refrigeration into a physical pilot plant similar to that proposed by the BioCPV group. This could include investigating the temperature operating limits of the plant and its effect on plant lifetime and combined system performance.
- Modelling and improving the physical aspects of heat and mass transfer in acetone and zinc bromide absorption refrigeration systems and its effects on cooling output and evaporator temperature through its effects on boiler and absorber performance. This could involve investigating the specifics of absorber and boiler design to maximise fluid surface area.
- Improving heat and mass transfer characteristics in acetone and zinc bromide solution through additives such as nano-fluids, these could facilitate the use of lower grade heat sources and provide lower temperature refrigeration.
- The suitability of ambient air cooling (and its alternatives such as underground cooling or evaporative cooling) and the effect of ambient humidity. The models presented here can be refined with the use of physical data and further configuration optimisation analysis can be conducted.
- Investigating absorption refrigerator system stability, for example: maintaining solution concentration differences, managing heat and mass

transfer within the refrigerator and the associated control mechanisms for this. Moreover both acetone and zinc bromide are hydrophilic and over time may degrade due to leakages, loading and general maintenance. The effects of this should be understood to gain insight into long term operating performance.

- The modelled absorption refrigerators have varying evaporator temperatures to maximise the heat source in a given environment. The physical process of managing this and the use of the cooling output requires investigation. This could include control mechanisms such as feedback loops automating valve positioning and pump speed based on temperature and flow detection. Optimisation of the storage in the reservoirs together with the utilisation of weather forecasting data should be investigated to mitigate the effects of unfavourable conditions.
- Engineering design challenges of integrating the boiler of an absorption refrigerator directly to a PV cell assembly in a CPV system. These include: material compatibility, physical flexibility to allow for solar tracking and the prevention of PV cell assembly overheating.
- Investigating theoretical and physical operating limits for the configurations of absorption refrigeration described in this thesis. This could be in terms of temperatures or cooling quantity ratio.

Bibliography

Agnew, B. et al. (2015). "Maximum output from a tri-generation cycle". In: *Applied Thermal Engineering* 90, pp. 1015–1020. ISSN: 13594311. DOI: 10.1016/j.applthermaleng.2015.04.063. URL: http://linkinghub.elsevier.com/retrieve/pii/S135943111500407X (visited on 02/27/2016).

Ajib, Salman and Karno, Ali (2008). "Thermo physical properties of acetone - zinc bromide for using in a low temperature driven absorption refrigeration machine". en. In: *Heat and Mass Transfer* 45.1, pp. 61–70. ISSN: 0947-7411, 1432-1181. DOI: 10.1007/s00231-008-0409-1. (Visited on 07/05/2013).

Ammar, Y., Chen, Y., et al. (2011). "Absorption process: An efficient way to economically transfer low grade heat from industrial sources to domestic sinks". In: *The 2nd PRO˙TEM Network Conference*. Ed. by Ling J Chin and S Spokes.

Ammar, Y., Joyce, S., et al. (2012). "Low grade thermal energy sources and uses from the process industry in the UK". In: *Applied Energy* 89.1, pp. 3–20. ISSN: 0306-2619. DOI: 10.1016/j.apenergy.2011.06.003.

Bajpai, Prabodh and Dash, Vaishalee (2012). "Hybrid renewable energy systems for power generation in stand-alone applications: A review". In: *Renewable and Sustainable Energy Reviews* 16.5, pp. 2926–2939. DOI: doi:10.1016/j.rser.2012.02.009.

Balghouthi, M., Chahbani, M. H., and Guizani, A. (2012). "Investigation of a solar cooling installation in Tunisia". In: *Applied Energy* 98, pp. 138–148. ISSN: 0306-2619. DOI: 10.1016/j.apenergy.2012.03.017.

Banerjee, Rangan (2006). "Comparison of options for distributed generation in India". In: *Energy Policy* 34.1, pp. 101–111. ISSN: 0301-4215. DOI: http://dx.doi.org/10.1016/j.enpol.2004.06.006.

Bejan, A (1997). *Advanced Engineering Thermodynamics second edition*. New York: John Wiley & Sons, Inc.

Cameo (2016). *Blomberg SSM9450 white freestanding fridge*. URL: http://www.cameokitchens.co.uk/ (visited on 02/24/2016).

Castro, J. et al. (2009). "Comparison of the performance of falling film and bubble absorbers for air-cooled absorption systems". In: *International Journal of Thermal Sciences* 48.7, pp. 1355–1366. ISSN: 1290-0729. DOI: 10.1016/j.ijthermalsci.2008.11.021.

Cengel and Boles (2006). *Thermodynamics: An engineering approach*. New York: Mc Graw-Hill.

CIA (2015). *The World Factbook*. URL: https://www.cia.gov/library/publications/the-world-factbook/ (visited on 12/27/2015).

Dannen, Gene (1995). *Leo Szilard Online*. URL: http://www.dannen.com/szilard.html/ (visited on 09/11/2014).

Delano, Andrew (1998). "Design Analysis of the Einstein Refrigeration Cycle". English. PhD. Georgia Institute of Technology.

Deng, J., Wang, R. Z., and Han, G. Y. (2011). "A review of thermally activated cooling technologies for combined cooling, heating and power systems". In: *Progress in Energy and Combustion Science* 37.2, pp. 172–203. ISSN: 0360-1285. DOI: 10.1016/j.pecs.2010.05.003.

Desideri, Adriano et al. (2016). "Experimental comparison of organic fluids for low temperature ORC (organic Rankine cycle) systems for waste heat recovery applications". In: *Energy* 97, pp. 460–469. ISSN: 03605442. DOI:

10.1016/j.energy.2015.12.012. URL: http://linkinghub.elsevier.com/retrieve/pii/S0360544215016540 (visited on 02/25/2016).

DOE (2008). *Waste Heat Recovery: Technology and Opportunities in U.S. Industry*. URL: http://www1.eere.energy.gov/manufacturing/intensiveprocesses/pdfs/waste_heat_recovery.pdf (visited on 12/29/2015).

— (2014). *Fuel Economy where energy goes*. URL: http://www.fueleconomy.gov/feg/atv.shtml (visited on 04/03/2014).

DuPont Suva (2016). *Thermodynamic Properties of HFC-134a*. URL: https://cdm.unfccc.int/filestorage/8/J/K/8JKOV024N9F16TYGISCUZAEM3P5XDW/ (visited on 02/24/2016).

Eames, I. W. and Wu, S. (2003). "A valve operated absorption refrigerator". In: *Applied Thermal Engineering* 23.4, pp. 417–429. ISSN: 1359-4311. DOI: 10.1016/s1359-4311(02)00210-7.

EEB (2015). *EU ban 'Beginning of the End' for climate changing F gases - EEB*. URL: http://www.eeb.org/EEB/index.cfm/news-events/news/eu-partial-ban-e28098beginning-of-the-ende28099-for-climate-changing-f-gases/ (visited on 12/20/2015).

EIA (2015). *EIA Projects world energy consumption will increase by 56% by 2040 - Today in Energy - US Energy Information Administration*. URL: https://www.eia.gov/todayinenergy/detail.cfm?id=12251 (visited on 12/20/2015).

Einstein, Albert and Szilard, Leo (1930). "Refrigeration". US1781541 A. U.S. Classification 62/110, 62/490, 62/112; International Classification F25B15/10, C09K5/04; Cooperative Classification Y02B30/62, C09K5/047, F25B15/10; European Classification C09K5/04D, F25B15/10. URL: http://www.google.co.uk/patents/US1781541 (visited on 12/17/2014).

ESRL (2015). *ESRL Monitoring Division Halocarbons and other Atmospheric Trace Species*. URL: http://www.esrl.noaa.gov/gmd/hats/publictn/elkins/cfcs.html (visited on 12/20/2015).

Freidberg, Susanne Elizabeth (2009). *Fresh : A Perishable History*. Cambridge, MA, USA: Harvard University Press. ISBN: 9780674053854. URL: http://site.ebrary.com/lib/uon/docDetail.action?docID=10402511.

FSA (2007). "Guidance on Temperature Control Legislation in the United Kingdom, EC Regulation 852/2004, The Food Hygiene Regulations 2006 (as amended)". In: URL: http://www.food.gov.uk/sites/default/files/multimedia/pdfs/tempcontrolguiduk.pdf (visited on 02/24/2016).

— (2015). *[Archived Content] Chilling Food Standards Agency*. URL: http://webarchive.nationalarchives.gov.uk/+/http://www.food.gov.uk/northern-ireland/nutritionni/niyoungpeople/survivorform/dontgetsick/chilling (visited on 02/24/2016).

Ge, Y.T., Tassou, S.A., and Chaer, I. (2009). "Modelling and performance evaluation of a low-temperature ammonia-water absorption refrigeration system". In: *International Journal of Low-Carbon Technologies* 4.2, pp. 68–77. ISSN: 1748-1317. DOI: 10.1093/ijlct/ctp015. URL: http://ijlct.oxfordjournals.org/cgi/doi/10.1093/ijlct/ctp015 (visited on 02/27/2016).

Ghosh, Sajal (2002). "Electricity consumption and economic growth in India". In: *Energy Policy* 30.2, pp. 125–129. ISSN: 0301-4215. DOI: http://dx.doi.org/10.1016/S0301-4215(01)00078-7.

Glover, Stephen et al. (2015). "Simulation of a multiple heat source supercritical ORC (Organic Rankine Cycle) for vehicle waste heat recovery". In: *Energy* 93, pp. 1568–1580. ISSN: 03605442. DOI: 10.1016/j.energy.2015.10.004. URL: http://linkinghub.elsevier.com/retrieve/pii/S0360544215013596 (visited on 02/25/2016).

González-Gil, A. et al. (2011). "Experimental evaluation of a direct air-cooled lithium bromide - water absorption prototype for solar air conditioning". In: *Applied Thermal Engineering* 31.16, pp. 3358–3368. ISSN: 1359-4311. DOI: 10.1016/j.applthermaleng.2011.06.019.

Gutiérrez-Urueta, G. et al. (2011). "Experimental performances of a LiBr-water absorption facility equipped with adiabatic absorber". In: *International Journal of Refrigeration* 34.8, pp. 1749–1759. ISSN: 0140-7007. DOI: 10.1016/j.ijrefrig.2011.07.014.

Haddad, Cynthia et al. (2014). "Some Efficient Solutions to Recover Low and Medium Waste Heat: Competitiveness of the Thermoacoustic Technology". In: *Energy Procedia* 50, pp. 1056–1069. ISSN: 18766102. DOI: 10.1016/j.egypro.2014.06.125. URL: http://linkinghub.elsevier.com/retrieve/pii/S1876610214008613 (visited on 12/29/2015).

Harrison, H C (1996). "Storing Vegetables at Home". In: URL: http://nchfp.uga.edu/how/store/wisc_vegetables.pdf (visited on 12/28/2015).

Hawkins, G (2011). "BSRIA Rules of Thumb Guidelines for Building Services, 5th Edition". In: URL: https://www.bsria.co.uk/download/product/?file=zxrulZgWBrY= (visited on 01/20/2016).

Herold, K. E. (1996). *Absorption chillers and heat pumps*. In collab. with Reinhard Radermacher and Sanford A. Klein. Boca Raton, FL: CRC Press. 329 pp. ISBN: 0849394279.

Howard, John P (1980). "A history of refrigeration throughout the world by Roger Thevenot". In: *New Scientist* 87. 1210, p. 219. URL: http://books.google.co.uk/books?id=a9hgb5uSVF8C&pg=PA219&dq=history+of+refrigeration+technology&hl=en&sa=X&ei=uH-JT-XBJs6z8QPr3s30CQ#v=onepage&q=history%20of%20refrigeration%20technology&f=true.

HP (2015). *HP Online Store*. URL: http://store.hp.com/UKStore (visited on 01/14/2015).

HSE (1997). *Lighting at Work Web-Friendly Version of HSG38*. URL: http://www.hse.gov.uk/pubns/priced/hsg38.pdf (visited on 01/04/2015).

Hua, Junye et al. (2014). "Thermodynamic analysis of ammonia-water power/chilling cogeneration cycle with low-grade waste heat". In: *Applied Thermal Engineering* 64.1, pp. 483–490. ISSN: 13594311. DOI: 10.1016/j.applthermaleng.2013.12.043. URL: http://linkinghub.elsevier.com/retrieve/pii/S135943111300940X (visited on 02/27/2016).

Jelinek, M. and Borde, I. (1998). "Single and double stage absorption cycles based on fluorocarbon refrigerants and organic absorbents". In: *Applied Thermal Engineering* 18.9-10, pp. 765–771. ISSN: 1359-4311. DOI: 10.1016/s1359-4311(97)00114-2.

Jelinek, M., Levy, A., and Borde, I. (2002). "Performance of a triple-pressure-level absorption cycle with R125-N, N'- dimethylethylurea". In: *Applied Energy* 71.3, pp. 171–189. ISSN: 0306-2619. DOI: 10.1016/s0306-2619(02)00003-x.

Jeong, Chulyoung et al. (2009). "Generating efficiency and emissions of a spark-ignition gas engine generator fuelled with biogas–hydrogen blends". In: *International Journal of Hydrogen Energy* 34.23, pp. 9620–9627. ISSN: 0360-3199. DOI: http://dx.doi.org/10.1016/j.ijhydene.2009.09.099.

Jeong, Jongsoo, Saito, Kiyoshi, and Kawai, Sunao (2011). "Static characteristics and efficient control of compression- and absorption-type hybrid air conditioning system". In: *International Journal of Refrigeration* 34.3, pp. 674–685. ISSN: 0140-7007. DOI: 10.1016/j.ijrefrig.2011.01.003.

Jordan, Richard C and Priester, Gayle B (1950). *Refrigeration and air conditioning*. 512th ed. New York: Prentice-Hall Inc.

Karno, Ali and Ajib, Salman (2008). "Thermodynamic analysis of an absorption refrigeration machine with new working fluid for solar applica-

tions". In: *Heat and Mass Transfer*, p. 40. ISSN: 0947-7411. DOI: 10.1007/s00231-008-0408-2. (Visited on 07/05/2013).

Kim, D S and Infante Ferreira, C A (2009). "Air-cooled LiBr-water absorption chillers for solar air conditioning in extremely hot weathers". In: *Energy Conversion and Management* 50.4, pp. 1018–1025. ISSN: 0196-8904. DOI: 10.1016/j.enconman.2008.12.021.

Kim, Jin Kyeong, Jung, Jun Young, and Kang, Yong Tae (2007). "Absorption performance enhancement by nano-particles and chemical surfactants in binary nanofluids". en. In: *International Journal of Refrigeration* 30.1, pp. 50–57. ISSN: 01407007. DOI: 10.1016/j.ijrefrig.2006.04.006.

Lide, David R (2004). *Handbook of Chemistry and Physics*. 85th ed. Boca Raton: CRC.

Mathkor, Ratha et al. (2015). "Exergetic Analysis of an Integrated Tri-Generation Organic Rankine Cycle". In: *Energies* 8.8, pp. 8835–8856. ISSN: 1996-1073. DOI: 10.3390/en8088835. URL: http://www.mdpi.com/1996-1073/8/8/8835/ (visited on 02/27/2016).

Mei, V. C. et al. (1992). *An assessment of desiccant cooling and dehumidification technology*. Tech. rep.

Miró, Laia, Brückner, Sarah, and Cabeza, Luisa F. (2015). "Mapping and discussing Industrial Waste Heat (IWH) potentials for different countries". In: *Renewable and Sustainable Energy Reviews* 51, pp. 847–855. ISSN: 13640321. DOI: 10.1016/j.rser.2015.06.035. URL: http://linkinghub.elsevier.com/retrieve/pii/S1364032115006073 (visited on 12/29/2015).

Mohammad, Abdulrahman Th. et al. (2013). "Historical review of liquid desiccant evaporation cooling technology". In: *Energy and Buildings* 67, pp. 22–33. ISSN: 0378-7788. DOI: 10.1016/j.enbuild.2013.08.018.

Moss, Stephen (1989). "Out of the Ice Box, into the Fire". In: *New Scientist, Google Books* 1696/1697, p. 85. URL: http://books.google.co.uk/

books?id=yINSqbNUNM0C&pg=PA85&dq=einstein+szilard+fridge&hl=en&sa=X&ei=TB3aU9_JDKnG7AbCo4DIAQ&ved=0CCoQ6AEwAA#v=onepage&q=einstein%20szilard%20fridge&f=false (visited on 07/31/2014).

Munters, Carl Georg and Platen, Baltzar Carl von (1928). "Refrigeration". US Patent 1,669,269. URL: https://www.google.co.uk/patents/US1669269 (visited on 09/11/2014).

NIST (2011). *NIST Acetone*. URL: http://webbook.nist.gov/cgi/cbook.cgi?ID=C67641&Mask=4&Type=ANTOINE&Plot=on#ANTOINE (visited on 12/20/2015).

NREL (2014). *National Residential Efficiency Measures Database*. URL: http://www.nrel.gov/ap/retrofits/ (visited on 12/14/2014).

— (2016). *India Solar Resource Data: Hourly*. URL: http://rredc.nrel.gov/solar/new_data/India/nearestcell.cgi (visited on 10/14/2016).

NUT (2015). *Space Requirements in Classrooms: NUT Health and Safety Guidance*. URL: https://www.teachers.org.uk/files/space-requirements-in-classrooms.doc (visited on 09/27/2015).

Oluleye, Gbemi et al. (2016). "Evaluating the potential of process sites for waste heat recovery". In: *Applied Energy* 161, pp. 627–646. ISSN: 0306-2619. DOI: http://dx.doi.org/10.1016/j.apenergy.2015.07.011.

Pátek, J. and Klomfar, J. (2006). "A computationally effective formulation of the thermodynamic properties of LiBr - H_2O solutions from 273 to 500 K over full composition range". In: *International Journal of Refrigeration* 29.4, pp. 566–578. ISSN: 0140-7007. DOI: 10.1016/j.ijrefrig.2005.10.007.

Pennington, N.A. (1955). "Humidity changer for air-conditioning". US Patent 2,700,537. URL: http://www.google.com/patents/US2700537 (visited on 09/11/2014).

Peris, Bernardo et al. (2015). "Experimental characterization of an ORC (organic Rankine cycle) for power and CHP (combined heat and power)

applications from low grade heat sources". In: *Energy* 82, pp. 269–276. ISSN: 03605442. DOI: 10.1016/j.energy.2015.01.037. URL: http://linkinghub.elsevier.com/retrieve/pii/S0360544215000614 (visited on 02/25/2016).

Petela, Richard (2010). *Engineering Thermodynamics of Thermal Radiation*. 1st ed. McGraw-Hill. ISBN: 9780071639620.

Pita, Edward (1984). *Refrigeration principles and systems: An energy approach*. New York: John Wiley & Sons.

Ramachandra, T.V., Jain, Rishabh, and Krishnadas, Gautham (2011). "Hotspots of solar potential in India". en. In: *Renewable and Sustainable Energy Reviews* 15.6, pp. 3178–3186. ISSN: 13640321. DOI: http://dx.doi.org/10.1016/j.rser.2011.04.007.

Reddy, K. S. and Veershetty, G. (2013). "Viability analysis of solar parabolic dish stand-alone power plant for Indian conditions". In: *Applied Energy*. Special Issue on Advances in sustainable biofuel production and use - XIX International Symposium on Alcohol Fuels - ISAF 102, pp. 908–922. ISSN: 0306-2619. DOI: http://dx.doi.org/10.1016/j.apenergy.2012.09.034.

Rogers, G.F.C. and Mayhew, Y.R. (1995). *Thermodyanmic and Transport Properties of Fluids (SI Units)*. Fifth. Blackwell Publishing. ISBN: 0631197036.

Said, Syed A. M., El-Shaarawi, Maged A.I., and Siddiqui, Muhammad U. (2012). "Alternative designs for a 24-h operating solar-powered absorption refrigeration technology". In: *International Journal of Refrigeration* 35.7. ISSN: 0140-7007. DOI: http://dx.doi.org/10.1016/j.ijrefrig.2012.06.008.

Saravanan, R. and Maiya, M. P. (1998). "Thermodynamic comparison of water-based working fluid combinations for a vapour absorption refrigeration system". In: *Applied Thermal Engineering* 18.7, pp. 553–568. ISSN: 1359-4311. DOI: 10.1016/s1359-4311(97)00072-0.

Shah, R. K., Subbarao, E. C., and Mashelkar, R. A. (1988). *Heat Transfer Equipment Design*. New York: Hemisphere Publishing Corperation.

Sharma, Naveen Kumar, Tiwari, Prashant Kumar, and Sood, Yog Raj (2012). "Solar energy in India: Strategies, policies, perspectives and future potential". en. In: *Renewable and Sustainable Energy Reviews* 16.1, pp. 933–941. ISSN: 13640321. DOI: http://dx.doi.org/10.1016/j.rser.2011.09.014.

Sieres, Jaime and Fernández-Seara, José (2007). "Experimental investigation of mass transfer performance with some random packings for ammonia rectification in ammonia - water absorption refrigeration systems". In: *International Journal of Thermal Sciences* 46.7, pp. 699–706. ISSN: 1290-0729. DOI: 10.1016/j.ijthermalsci.2006.09.003.

Srikhirin, Pongsid, Aphornratana, Satha, and Chungpaibulpatana, Supachart (2001). "A review of absorption refrigeration technologies". In: *Renewable and Sustainable Energy Reviews* 5.4, pp. 343–372. ISSN: 1364-0321. DOI: 10.1016/s1364-0321(01)00003-x.

Sun, Jian, Fu, Lin, and Zhang, Shigang (2012). "A review of working fluids of absorption cycles". In: *Renewable and Sustainable Energy Reviews* 16.4, pp. 1899–1906. ISSN: 1364-0321. DOI: 10.1016/j.rser.2012.01.011.

Tae Kang, Yong, Akisawa, Atsushi, and Kashiwagi, Takao (2000). "Analytical investigation of two different absorption modes: falling film and bubble types". In: *International Journal of Refrigeration* 23.6, pp. 430–443. ISSN: 0140-7007. DOI: 10.1016/s0140-7007(99)00075-4.

Tamura, Moriyoshi (2008). "An Investigation of a Natural Gas HCCI Engine for 5kW Class Co-genergation System". In: *IGRC Paris 2008*. International Gas Union Research Conference.

Tassou, S.A. et al. (2010). "A review of emerging technologies for food refrigeration applications". In: *Applied Thermal Engineering* 30.4, pp. 263–276. ISSN: 13594311. DOI: 10.1016/j.applthermaleng.2009.09.001. URL:

http://linkinghub.elsevier.com/retrieve/pii/S1359431109002737 (visited on 02/27/2016).

Todd, Daniel (1995). *Timetoast Timelines: Internal Combustion Engine Timeline*. URL: https://www.timetoast.com/timelines/119674 (visited on 10/01/2014).

Vent-Axia (2015). *Reversible Hi Line Vent Axia*. URL: http://www.vent-axia.com/range/reversible-hi-line.html (visited on 09/27/2015).

Wang, R and Oliveira, R (2006). "Adsorption refrigeration - An efficient way to make good use of waste heat and solar energy". en. In: *Progress in Energy and Combustion Science* 32.4, pp. 424–458. ISSN: 03601285. DOI: 10.1016/j.pecs.2006.01.002.

WHO (2016). *Guidelines for the Storage of Essential Medicines and Other Health Commodities*. URL: http://apps.who.int/medicinedocs/en/d/Js4885e/6.5.html (visited on 02/24/2016).

Xie, Guozhen et al. (2012). "A novel lithium bromide absorption chiller with enhanced absorption pressure". In: *Applied Thermal Engineering* 38, pp. 1–6. ISSN: 1359-4311. DOI: 10.1016/j.applthermaleng.2011.12.047.

Yanmar (2016). *Yanmar mCHP Catalogue*. URL: http://www.yanmar-es.com/uploads/files/349226-YAN-Catalog-Apr17_FINAL_DIGITAL_med.pdf (visited on 02/24/2016).

Zacarías, A. et al. (2011). "Experimental assessment of ammonia adiabatic absorption into ammonia-lithium nitrate solution using a flat fan nozzle". In: *Applied Thermal Engineering* 31.16, pp. 3569–3579. ISSN: 1359-4311. DOI: 10.1016/j.applthermaleng.2011.07.019.

Zohar, A. et al. (2009). "Performance of diffusion absorption refrigeration cycle with organic working fluids". In: *International Journal of Refrigeration* 32.6, pp. 1241–1246. ISSN: 0140-7007. DOI: 10.1016/j.ijrefrig.2009.01.010.

Appendix: Draft Paper

Design and initial assessments of a biomass/biogas and solar renewable power plant for rural electrification in India

Joel Hamilton[1], Nabin Sarmah[10], Donald Giddings[1], Gavin S Walker[1], Kunal Bandyopadhyay[3], Sambhu N Banerjee[3], Shibani Chaudhury[3], Prakash Ghosh[6], S. Lokeswaran[5], Leonardo Micheli[2] Mark Walker[4], Davide Poggio[9], Tapas Mallick[2], Kandavel Manickam [1], David Grant[1], Lin Ma[4], Tadhg O'Donovan[7], Xichun Luo[8], Marios Theristis[7], K. S. Reddy[5], Amit K Hazra[3], Mahesh Kumar[5], Srirama Srinivas[5], Anil K. Mathew[3], S. Balachandran[3], William Nimmo[4], Mohamed Pourkashanian[4]

[1]*University of Nottingham,* [2]*University of Exeter,* [3]*Visva Bharati University of West Bengal,* [4]*University of Sheffield,* [5]*Indian Institute of Technology Madras,* [6]*Indian Institute of Technology Bombay,* [7]*Heriot Watt University,* [8]*University of Strathclyde,* [9]*University of Leeds,* [10]*Tezpur University*

Abstract

This paper describes the method of predicting the demand requirement to promote sustainable development for a 45 household rural community in West Bengal, India and proposes an integrated renewable power plant to meet this demand. The daily demand profile of 55 kW·h includes lighting, fans, charging station, small machinery and computers. The plant consists of 10 kW (electrical) concentrated photovoltaic (CPV) and 5 kW (electrical) biogas-hydrogen internal combustion engine electrical generator. Providing 57 kW·h of electricity to the community at an electrical energy efficiency of 18% and an electrical rational (exergetic) efficiency of 20%. The biogas will be generated locally using food waste, crop waste and aquatic weeds in an anaerobic digester. The hydrogen will be generated from an electrolyser with excess solar power and stored in a metal-hydride system. Energy and exergy analysis of the proposed system finds that that the largest energy losses, 48%, of the total input energy into the system is low temperature waste heat. However the total exergy contained in these heat sources would only be equal to 6% of the total input exergy. Inferring that the waste heat in this system would not be well utilised if it were converted into work or electricity.

Keywords: Renewables, Rural renewable power, Concentrated photovoltaic (CPV), Anaerobic digestion, Biogas, Sustainable development, Energy and exergy analysis

1. Introduction

The economic growth of a country is directly related to the per capita energy consumption [Ghosh, 2002]. According to the data of Government of India 2011 census, 833 million (approximately 69% of total population) lives in 640,867 villages, out of which 56% and almost 400 million people are without grid connected electricity supply [Census of India, 2011]. In rural areas energy is required for both domestic and small-scale local industries, both of which contribute significantly to economic development. The geographical diversity and lack of proper infrastructure has become a barrier for the grid connection to the rural areas.

The Ministry of Rural Development, Government of India, has taken measures for poverty alleviation, skill development and employment generation through different schemes like Integrated Rural Development Programme (IRDP, 1980), Training of Rural Youth for Self Employment (TRYSEM), Development of Women and Children in Rural Areas (DWCRA), Supply of Improved Toolkits to Rural Artisans (SITRA), Ganga Kalyan Yojana (GKY), and the Million Wells Scheme (MWS). Among these, IRDP is the major programme meant for self-employment generation by providing subsidy and credit to below-poverty-line families with a view to bringing them above the poverty line. These are all separate programmes with little integration between them [MoRD, 2014]. Another important initiative launched by the Ministry of Rural Development

Email address: joelawhamilton@gmail.com (Joel Hamilton)

(MoRD), Government of India in June 2011 was National Rural Livelihoods Mission (NRLM). The Mission, partly aided by the World Bank, aims to create efficient livelihood development for the rural poor through sustainable enhancements and improved access to financial services [NRLM, 2014].

In spite of having such activities by the Government of India, basic infrastructural facilities in rural India like electricity, education, transport and healthcare are still far from satisfactory. In 2011, only 55.3% of rural household had access to electricity [Census of India, 2011] (Energy Statistics 2013). The Human Development Report 2011 quotes a percentage point gap between urban and rural areas of 17% in literacy, 19% in child immunisation and 38 in institutional delivery (giving birth within an institution rather than at home), [Gandhi, 2011].

Per capita annual grid connected electricity consumption in India during 2011 is 288 kW·h in urban areas and 96 kW·h in rural areas. Though this is higher than The World Energy Outlook (WEO) analysis of the International Energy Agency (IEA) (2012) which considers 250 kW·h and 500 kW·h as the minimum annual consumption levels for a household of five in rural and urban areas respectively.

This lack of facilities has crippled the socio-economic development of the rural masses; who are dependent to a large extent on natural resources for making their livelihood and wellbeing. The quality of life of these people living in rural India can be improved by widespread electrification, which can infuse visible changes in their livelihood. As the natural resources like plant biomass, agricultural by-products and solar radiation are in abundance in rural areas, efficient management of these resources in a sustainable manner can provide holistic development of rural communities. Electrification can help improve facilities in terms of education, healthcare, lifestyle and rural enterprises; thereby alleviating poverty and ushering in an era of self-sufficiency and better competitiveness to take on the challenges of the rest of the world.

Decentralised hybrid power plants with different renewable technologies can provide efficient, cheap and sustainable options for rural electrification [Bajpai and Dash, 2012] and [Ghosh, 2002]. The integration of a variety of renewable sources coupled with storage to complement each other can provide a sustainable development solution all year round.

India had 20,556 MW of renewable power generation capacity by 30th June 2011 which was approximately 11% of the total power generation capacity of the country. There is an average intensity of solar radiation of 200 MW·km^{-2}. Through the Jawaharlal Nehru National Solar Mission (JNNSM) it is envisaged that India will have an installed solar capacity of 20,000 MW by 2020, 100,000 MW by 2030 and 200,000 MW by 2050. [Sharma et al., 2012]

The following research is part of a collaborative group, called BioCPV, with the objective of providing a sustainable development solution to rural India through renewable power. This research outlines the need for rural development in India and then describes the demographics of a particular community in Santiniketan, West Bengal, India. With this information a demand profile is forecast and a technology selection process to meet these needs is described. The initial design calculations for the proposed technologies are presented and followed with an energy (first law) and exergy (second law) analysis of the proposed system to identify areas for optimisation.

2. Description of Need for Micro Electrical Generation Plant

Two rural tribal villages, Kaligung and Pearson-Palli, adjacent to Visva-Bharati, Santiniketan have been selected because the majority of the tribal people do not have access to electricity owing to their socio-economic conditions. Although there is a grid connection in the village, the supply is weak, only providing a few hours of electricity per day and not all the houses are connected through this grid. The villages are comprised of 179 households with a population of approximately 821. Most the families in the village live below the poverty line. Out of the total population, 52% are women and 10% are children. The average income of each household is approximately INR 2500/month.

Basic facilities such as drinking water and sanitation are not available which leads to an unhygienic lifestyle. The houses are typical for an Indian village made from bamboo or wood and mud. There is a basic health centre in the village which provides primary health care through an arrangement with university, doctors and local health workers. Most of this care currently takes place outdoors. However for more serious illness, villagers visit the Block Primary Health Centre (BPHC) or University Hospital (3 and 2 km away respectively).

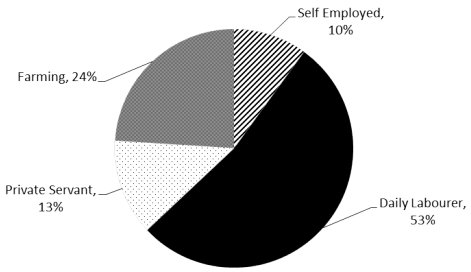

Figure 1: Breakdown of the villagers occupations

2.1. Lifestyle and Culture

Kaligung and Pearson-Palli are primarily tribal dominated, mostly belonging to Santal tribes (indigenous group found in East India and Nepal). The villages come within the Visva-Bharati University (a member of the BioCPV project) core area. Historically, these native tribes found work in agriculture, environment, gardening and forestation of the Santiniketan campus (Visva-Bharati, West Bengal). They are one of the oldest inhabitants in the area. But despite being the oldest inhabitants of the area, they are lagging behind from the rest of the local society in terms of development.

The people of Kaligung and Pearson-Palli are deprived of the basic privileges of a hygienic lifestyle and education mainly because of the lack of infrastructure in rural areas. A sample of the villagers showed that 70% households are not landowners and live on government land. 53% of these two villages' populations are daily labourers, 24% earn by farming and the remaining 23% are working as self-employed or private servants, see Figure 1. 31% of people in the villages are literate, but not well educated. Though most of the parents in the villages are illiterate, their children are in conventional school education. However acute poverty forces children to drop out from school in order to earn a living.

Women are involved in both household and income generating activities. Household activities include: collecting leaf litters and fuel woods from the nearest forest area 2–3 km from the village for cooking purposes and preparing meals for the rest of the members of the family. Income generating activities include: spice grinding and making small handicrafts using bamboo and other locally available materials. Some of them are involved in Self Help Groups (SHG) to generate opportunities for small scale businesses to improve their economic conditions.

Men are considered the "main worker" in families in the villages, this is typical for rural parts of this district. As seen in the Department of Statistics and Programme Implementation by the government of West Bengal in 2011, 43% out of the total population of the district are rural male "main workers". When they are not working men spend a lot of time in public areas, therefore developing these public areas so that they are suitable for education and training could also provide a positive impact for the villagers.

There is inadequate indoor and outdoor lighting in the villages. This results in the majority of the work and learning taking place during the day. Moreover a survey carried out within the village found that it was difficult for children to study at home due to lighting issues, the current solution of kerosene lamps has health implications as their emissions impair indoor air quality.

There is a need for reliable electricity to aid the sustainable development of this community. It can improve the quality of life through improving the educational environment and reduce the use of technologies that are damaging to health (such as kerosene lamps). This electricity needs to be provided in a sustainable manner which can promote the self sufficiency of these people.

2.2. Weather and conditions

Like most of the remote areas of eastern India, the region of Kalijung and Pearson-Pally is warm and humid with generous rainfall (1500 mm from June to September) and temperatures (24°C to 35°C). Data collected from local weather station on Visva-Bharati, West Bengal.

2.3. Resources available

India is blessed with an abundance of solar energy with annual daily average solar irradiance on a horizontal surface of 5 to 7 kWh·m^{-2}. Nearly 58% of the geographical area represents regions of exceptional solar power potential [Ramachandra et al., 2011]. The eastern part of India is rich in both solar irradiation and biomass resources [Reddy and Veershetty, 2013] and [Banerjee, 2006]. A survey also estimated that there is access to a minimum of 200 kg food waste generated on a daily basis from the university hostels in the nearby area of the village and plenty of aquatic weeds provided by the nearby ponds.

3. Community Power Demand Rationale

The following section describes the process for designing a small rural distributed renewable power plant. The process requires a demand estimation and a detailed overview of the technologies available allowing appropriate selection. The section is followed with the design considerations and sizing calculations for each technology within the plant.

3.1. Demand Estimation

The World Energy Outlook analysis for the minimum electricity consumption of a 5 person household is calculated using the assumption that following technologies could be used: floor fan, a mobile telephone, and two compact fluorescent lamp (CFL) bulbs in rural areas, and might include an efficient refrigerator, a second mobile telephone, and another appliance, such as a small television or a computer, in urban areas. Electric lighting is seen to be an influential technology to provide development, from 2001 to 2011 the shares of households in rural areas using electricity as their prime source of lighting changed from 43.5% to 55.3%, and in urban areas from 87.6% to 92.7% (Census of India, 2011).

In light of these findings and studies of the local needs together with the desire to provide sustainable development through improving the educational environment and overall quality of life, the following items in Table 1 have been selected for the demand profile.

Previous work with these communities carried out by Visva-Bharati, West Bengal found that successful adoption of change requires a holistic approach where the villagers are involved throughout the project, training and education are provided and that everything is compatible with their customs and traditions.

The following subsections describe the method for calculating the predicted demand.

Ventilation - Fans

Guidelines in the United Kingdom suggest 70 m^2 is required for primary or middle school class of 30 students [NUT, 2015]. A typical ceiling fan such as Vent-Axia Reversible Hi-Line + requires 60 W at full load and suggests in tropical climates that they should be placed 3 m apart (and 6 m in temperate climates) [Vent-Axia, 2015]. There are currently 104 students at the school which are accommodated by 2 large rooms (approximately 11 m x 5 m) and one small one (3 m x 4 m). For the purposes of repeatable demand profiling and as the number of students can vary, and the building may have additional rooms built on to it, the remaining analysis is based on the guidelines mentioned earlier. Therefore the school would require 3 classrooms allowing for a comfortable learning environment for 90 children. Each 70 m^2 classroom can be allocated 2 fans depending on dimensions. An assembly hall which can house activities and exercise classes as well is assumed to be the size of 3 classrooms and would require 6 fans. Another room the same size as a classroom used as an office for the teachers and staff would require a further 2 fans. This totals 14 fans, however it will be very unlikely that all the fans were on maximum load at the same time. For the purposes of load estimating an average of 10 fans at 60 W each has been assumed.

Lighting

The efficacy of compact florescent light bulb (CFL) = 55 $\mathrm{lm \cdot W^{-1}}$ [NREL, 2013]. The lighting requirements for a bright office space requiring perception of detail is 200 lx and for dull workspaces not requiring perception of detail 100 lx is needed [HSE, 1997]. By definition

$$efficacy = \frac{lumen}{electrical\ power} \tag{1}$$

And

$$lux = \frac{lumen}{area} \tag{2}$$

Therefore using Equations 1 and 2 the lit area depending on the lighting requirements can be found using Equation 3

$$area = \frac{efficacy \times electrical\ power}{lux} \tag{3}$$

Using this information a 15 W CFL should provide 4.125 m^2 of bright workspace and 8.25 m^2 of dull workspace. Therefore 40 × 15 W CFLs are considered for public lighting, providing a bright area of 165 m^2 and a dull area 330 m^2. Taking natural light into consideration as well, the estimate of 40 bulbs provides an average load of public lighting to meet the daytime and evening needs.

Table 1: Appliance itinerary to create demand profile, including typical energy consumption and quantity required

	Energy Per Item (W)	Quantity	Total Energy (kW)
School / Public light bulb	15	40	0.75
Fan	60	10	0.6
Domestic light bulb	10	90	0.9
Lantern / Phone charging	10	100	1
Desktop PC	100	10	1
Small Machinery	200	8	1.6

Likewise the same analysis can be used to determine that 10 W CFLs in a domestic setting can provide the equivalent of 2.75 m^2 of bright workspace and 5.5 m^2 of dull workspace. Assuming that 2 rooms per household require lighting, then 90 $\times$ 10 W CFL bulbs are required.

Lantern and Phone Charging

Lantern and phone charging was based on modern high powered USB chargers outputting approximately 10 W for mobile phone charging for example the Innergie ADP 21AW D. Since a large number of battery powered devices can be charged by these it was assumed to be suitable for lanterns as well. It was assumed that there would be 2 lanterns per household and 10 phones in the community resulting in a quantity of 100 $\times$ 10 W devices requiring charge.

Desktop PC

The power demand for a typical PC found on the market is 100 W based on a basic specification of an HP 110-352na Desktop PC at 65 W and a typical monitor such as the HP ENVY 24 60.5 cm at 26 W to 54 W [HP, 2015]. It was assumed the school could have an average PC load of 10 PCs.

Small Machinery

Small machinery such as spice grinders and sewing machines were estimated at 200 W based on a range available in the market. A quantity of 8 was estimated allowing a gentle introduction of the technology, so that those who want to work together with the machinery can and those who prefer the traditional methods can maintain their current approach.

3.2. Demand Profile

Figure 2 shows the expected demand profile of the village over 24 hours. The demand is divided in to a day

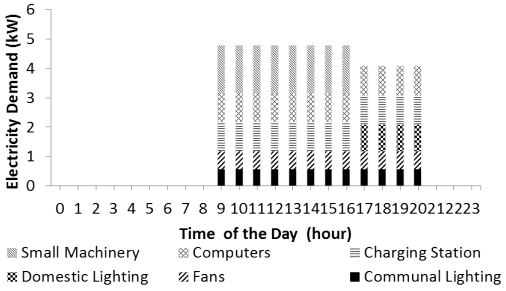

Figure 2: Maximum predicted demand profile elected for the community on a typical day irrespective of the season

load which is from 09:00 to 17:00 and an evening load from 17:00 to 21:00. public area lighting, fans, computers and the charging station are assumed to be used all day from 09:00 to 21:00. This is a result of the community buildings being used as a school during the day and then a community centre. The small machinery load is assumed to only take place during the day, this is mainly because they are noisy.

3.3. System Requirements

This demand profiling analysis shown in Figure 2 and Table 1 has found that there is a minimum system requirement of 4.8 kW of electricity during the day (09:00 to 17:00) and 4.1 kW in the evening (17:00 to 21:00). Totalling 55 kW·h per day of electrical supply to the village. An additional 26 kW·h has been allocated for system ancillaries (12 kW·h), 14 kW·h solar trackers and 7 kW·h for hydrogen production (1 kW for the 7 hours of CPV operation). Therefore there is an minimum electrical generation requirement of 88 kW·h per day.

4. Appropriate Generation Technologies

The main available renewable resources are solar and biomass.

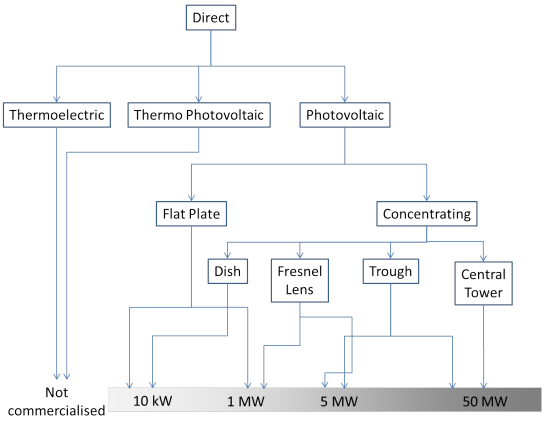

Figure 3: Current direct solar generation technologies

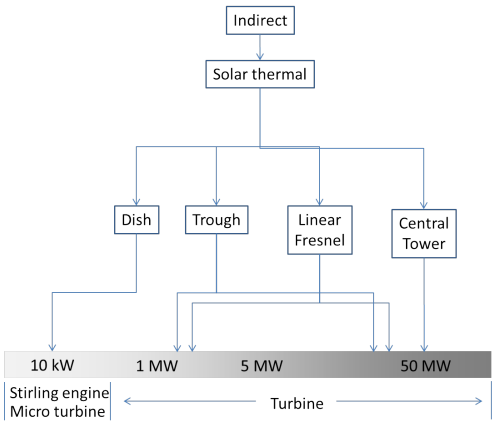

Figure 4: Current indirect solar generation technologies

4.1. Solar

Solar is a globally available, abundant, clean energy source. Solar energy technology has a fast growing global market for example solar photovoltaic has an increase in installation to 31 GW in 2012 compared to 0.3 GW in 2000 [Zheng and Kammen, 2014]. Solar Energy can be converted to electricity either by solar thermal or photovoltaic process. Whilst solar thermal is an indirect way of converting solar energy into electricity by using a working fluid and engines with electrical generators, photovoltaic (PV) is a direct process where the solar radiation is used to excite electrons which generate electricity. Figures 3 and 4 display the different solar power generation technologies and their scale.

4.1.1. Concentrated Solar (thermal) Power (CSP)

The heat energy (radiation) from the sun is captured in some form of solar collector. This heats a working fluid, which drives a heat engine, which powers an electrical generator. Electricity generation in a solar thermal plant occurs in two stages. The concentrator usually consists of a system of mirrors to concentrate the sunlight on to an absorber, where the heat is transferred to the working fluid. The type of concentrator, concentration ratio, flow rate of the working fluid and receiver design will determine the operating temperature of the power plant. For small scale decentralised systems Stirling engines can be effective. For small to medium sized applications scroll expanders and micro turbines are being developed and coming on to the market. For larger systems a turbine driven by steam or other vaporous working fluid is often used. Sometimes solar concentrators are used with existing fossil power plants in a hybrid mode to supply renewable heat energy, when available, reducing the fossil fuel requirement. [Viebahn et al., 2011], [Hoffschmidt et al., 2012]

Figure 4 shows that only solar thermal dish is appropriate in terms of size for this application. However, due to the number of moving parts there is usually a higher maintenance requirement which can be logistically difficult in rural locations, diminishing the viability of this option.

4.1.2. PV

The higher frequency radiation (visible, ultra violet) from the sun is captured in an array of semiconductors known as photovoltaic cells which convert the radiant energy directly into electricity. The current global photovoltaic market is dominated by silicon solar cells which have higher efficiency and production capacity compared to thin-film and dye-sensitise cells [Luque and Hegedus, 2003], [Kazmerski, 2012]. Typical efficiencies are 10% - 17%, though the maximum efficiency of a flat plate silicon module is reported to be 20.5% [Green et al., 2014]. The lowest price of the PV modules was 0.72 $^{USD}/_{W}$ in September 2013 [Zheng and Kammen, 2014], though this has started to increase. Whilst PV is the simplest method of solar electricity generation, its low conversion efficiency means that it requires a large amount of solar cells and space to accommodate them. Moreover most systems operate close to ambient conditions providing little to no scope for thermal energy harvesting.

4.1.3. CPV

The drawbacks of conventional photovoltaic are overcome by concentrating a large amount of sunlight onto a small area of solar photovoltaic materials to generate electricity using cost effective optics resulting a low cost-per-Watt. This technology is widely known as concentrated photovoltaic (CPV). Multi-junction solar cells are used here to capture more photons in wider wavelengths, allowing higher conversion efficiency (approaching 40%). The CPV receiver can be mounted on the focal plane with a passive or active cooling arrangement to extract surplus heat. Utilising this heat increases the combined or cogeneration efficiency. CPV using dishes [Verlinden et al., 2008] or micro dishes [Kribus et al., 2006], [Feuermann and Gordon, 2001] are well established compared to other concentrators because of its high concentration ratio (currently up to 500 suns), resulting in more electrical output. Application of the Tower approach to CPV is also under development. The maximum system efficiency of a CPV system is reported to be 35.9% [Green et al., 2014]

The technologies such as Concentrator Thermoelectric Generator (CTEG) and Solar thermo photovoltaic (STPV) are still in laboratory scale with maximum conversion efficiency reported 2.9% [Fan et al., 2011] and 23% [Wernsman et al., 2004] respectively.

CPV provides direct electricity generation, resulting in fewer mechanical parts than CSP, which may result in less maintenance requirements which can be logistically difficult in rural settings. The cost-per-Watt of CPV is lower than PV and has the potential to recover waste heat at higher temperatures than PV. Making CPV the most viable technology for this application, out of the technologies discussed here.

4.2. Biomass

Biomass can be used as a resource for rural electrification using a range of physico-chemical (e.g. transesterification), thermochemical (combustion, gasification, pyrolysis, liquefaction) and biochemical (fermentation, anaerobic digestion (AD)) processes [Appels et al., 2011]. In all of these four cases the resultant energy vector (heat, biodiesel, bioethanol, methanol, syngas, biogas and pyrolysis oils) requires another technology for eventual conversion to electricity. The choice of biomass conversion technology must take into account several factors including the cost and the appropriateness of the technology in rural India, but predominantly the best option will be clear given the properties of the biomass itself (In this case its moisture content and composition). For this location the identified available biomass was a mixture of aquatic weeds collected from surrounding ponds, and food/market waste from the nearby university campus and settlements. Both of these biomass types contain a large quantity of moisture as collected (75-95%) and contain a broad mixture of organic macromolecules (polysaccharides, lignocellulose, fats, proteins). In general the thermal conversion technologies (combustion and gasification) lend themselves to dry biomass sources since the vaporisation of large quantities of water can reduce the net energy output. Furthermore the development of these technologies has focused on large scale applications and in the case of gasification, despite being available for several decades and marketed by a number of companies, there are relatively few installations. Similarly despite the high levels of interest in pyrolysis due to the high oil yield and flexibility in terms of biomass composition and moisture content, as a technology it is still in its development stage and therefore was deemed inappropriate for current use in rural India. Biodiesel and bioethanol production from these mixed biomass sources is possible but the biofuel yields would be low due to the low oil and (poly and mono) saccharide content of the biomass respectively. Based on the available biomass conversion options anaerobic digestion is the best fit for electrification in rural India, since it has already been demonstrated from micro (i.e. single household) to industrial scale, it is appropriate in terms of the materials and skills available, and can be used to convert biomass with a high moisture content, with minimal pre-treatment, to biogas, which can subsequently be burned in a conventional internal or external combustion engine. It is estimated that there are over 2 million small biogas plants in the Indian subcontinent; these are generally very simple unheated systems with few moving parts, suitable for biogas production from animal slurries only with the biogas used for domestic cooking. Unheated anaerobic digestion systems are subject to daily and seasonal temperature variations caused by ambient conditions which can negatively affect both the process performance and stability [Nallathambi Gunaseelan, 1997].

Aside from the traditional Indian small-scale biogas plant, there are many other designs of anaerobic digestion systems with increased technical complexity that can be classified in a variety of ways and operated in either continuous or batch modes. These include; single and multi-stage continuously stirred tank reactor (CSTR) systems; phase separated system such as leach beds and sequenced batch reactors; liquid/effluent treat-

ment systems such as anaerobic filters, baffles reactors, anaerobic sludge blankets and membrane bioreactors, and a variety of systems that combine the above reactor types [Gerardi, 2003]. Although there is a huge amount of research into multistage/phase anaerobic digestion systems the most predominant are single stage (partially or completely) mixed systems due to their simpler, robust designs and lower capital and operating costs [Bouallagui et al., 2005]. Two-stage anaerobic digestion systems have yet to show their process benefits in the market [Hartmann and Ahring, 2006].

Anaerobic digestion is usually conducted in the mesophilic (≈37°C) or moderately thermophilic temperature ranges (50-60°C) and whilst there are some process advantages to operating at the higher temperatures it is recognised that the process becomes increasing sensitive to disturbances and more difficult to control [Hilkiah Igoni et al., 2008].

Due to the nature of the sustainable fuels available biogas generation via anaerobic digestion, is considered the most viable option for this situation out of the technologies discussed here. An internal combustion engine electrical generator will be use the biogas due the small size of this system and fast start up times.

5. Proposed System Design

Due to the abundance of solar irradiation and biomass in the vicinity, CPV and biogas (via an anaerobic digestion and used in an internal combustion engine generator) were selected as the main energy generation methods. These technologies complement each other as the biogas electrical generator can be operated when the CPV is unavailable. Moreover the production and use of biogas are decoupled; therefore, depending on storage capacity, it can support both seasonal and diurnal variation. Hydrogen storage will be used to optimise the solar electricity generation and increase the quality of the biogas. A schematic of the system can be seen in Figure 5.

For system sizing purposes a generation load of 90 kW·h per day will be used as it exceeds the estimated daily demand of 88 kW·h. This can be allocated to a daytime solar generation load 70 kW·h which can be simplified to 7 hours of generation at 10 kW (electric) and an evening biogas - hydrogen electrical generator load of 5 kW (electric) for 4 hours per day.

5.1. CPV

There are many CPV system designs have been reported so far, in order to increase the overall system efficiency. CPV are commercially available manufactured by companies such as Amonix, Zenith Solar, Soitec, Heliotrop etc. [Amonix, 2014], [Zenith Solar, 2013], [Soitec, 2014] and [Heliotrop, 2014]. The CPV system in this project aims to eliminate the fuzziness of concentrated light at the receiver and to achieve high optical efficiency (over 80%) by eliminating losses in the optical components. Additionally the CPV design needs to be simple to transport, assemble and install in remote locations. Therefore an optimum CPV design with a large area parabolic dish and densely packed receiver assembly with active cooling was adopted for BioCPV system.

The CPV system consists of four CPV units with two axis tracking. Each CPV unit consist of two primary concentrators and receivers. The primary concentrator is a parabolic dish with a square opening and made up of four sections to achieve an entry aperture area of 9 m^2. The receiver consists of a solar cell assembly of 144 solar cells, secondary concentrator (Crossed Compound Parabolic Concentrator (CCPC)) and cooling system. The specifications of the CPV unit are given in Table 2 and a CAD model of the system in Figure 6.

The solar cell used in the CPV system are commercially available triple junction solar cells 37.6% electrical conversion efficiency when used with a high (500X) concentrating system maintained at 60°C. This data is based on the data sheets provided by the solar cell manufacturer AZUR SPACE Solar Power and the efficiencies stated are inline with the NREL report titled “Opportunities and Challenges for Development of a Mature Concentrating Photovoltaic Power Industry” [Kurtz, 2012]. A novel cooling system was developed for efficient heat recovery from the CPV units, which will be used in the Anaerobic Digestion system and hydrogen storage system [Reddy et al., 2013].

It is assumed for design and modelling purposes that the CPV generates the equivalent of 10 kW for 7 hours per day.

To size the CPV system based on the specifications in Table 2 the following equations are required:

The solar energy entering the cell ($Q_{CPV_{cell}}$) can be calculated with the known electrical energy requirement

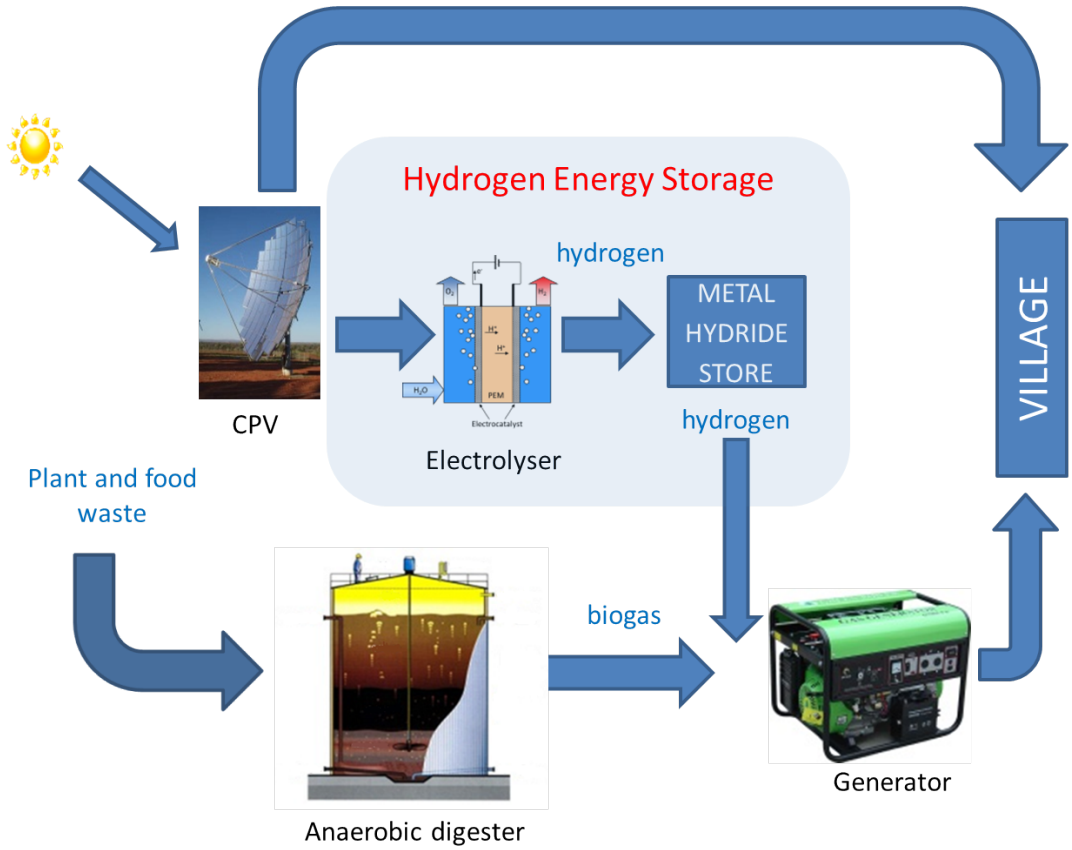

Figure 5: BioCPV renewable power plant schematic

($E_{CPV_{cell}}$) and the PV cell efficiency ($\eta_{CPV_{cell}}$)

$$Q_{CPV_{cell}} = \frac{E_{CPV_{cell}}}{\eta_{CPV_{cell}}} \tag{4}$$

The solar energy required to enter into the CPV collectors ($Q_{CPV_{concentrator}}$) can be found using the optical efficiency ($\eta_{CPV_{optical}}$) of the system

$$Q_{CPV_{concentrator}} = \frac{Q_{CPV_{cell}}}{\eta_{CPV_{optical}}} \tag{5}$$

The concentrator area ($A_{CPV_{concentrator}}$) can be found using the Direct Normal Irradiance (DNI) and the solar energy falling on the concentrator ($Q_{CPV_{concentrator}}$)

$$A_{CPV_{concentrator}} = DNI \times Q_{CPV_{concentrator}} \tag{6}$$

5.2. *Anaerobic Digester*

The proposed AD system represents a typical medium sized Indian biogas plant with some low cost upgrades with the aim of maintaining the appropriateness of the technology whilst improving the versatility and efficiency of the AD process. The upgrades include a biogas mixing system which should extend the life of the plant and allow feeding of the chosen biomass due to reduced sedimentation in the digester, and a heating system allowing stable and efficient biogas production independent to ambient temperature. The selected design for the AD system is a single stage Continuously Stirred Tank Reactor (CSTR) and the system will consist of an electrical chopper that will reduce the particle size of the biomass to around 20-30 mm, a pre-feeding tank with a volume of 1.5 m^3 where the processed biomass will be stored before feeding, a 14.6 m^3 buried fixed dome digester with internal heat exchanger and biogas mixing spargers, biogas and hot water pumps, a 12.1 m^3 water gasometer for biogas storage and a digestate storage la-

Table 2: CPV specifications rated at 25°C and 1 atmosphere

Total Installation power rating	E_{CPV}	10 kW
Number of CPV modules	n_{CPV}	8
Direct Normal Irradiance	DNI	550 W·m^2
Power output of each unit	$E_{CPV_{unit}}$	1.3 kW
Rated voltage of the each unit	V_{CPV}	216 V
Area of one cell	$A_{CPV_{cell}}$	1 cm^2 (1 × 1 cm)
Concentration ratio	CR_{CPV}	500X
Optical efficiency	$\eta_{CPV_{optical}}$	80%
PV Cell efficiency at 60°C	$\eta_{CPV_{cell}}$	37.6%
Power output of one cell	$E_{CPV_{cell}}$	8.3 W
Area of each cell assembly (receiver) for 1.3 kW system (With secondary concentrator)	$A_{CPV_{receiver}}$	580 cm^2
Effective concentrator entry aperture area	$A_{CPV_{concentrator}}$	7.565 m^2
Primary concentrator dish dimensions	$w \times l$	3 m × 3 m

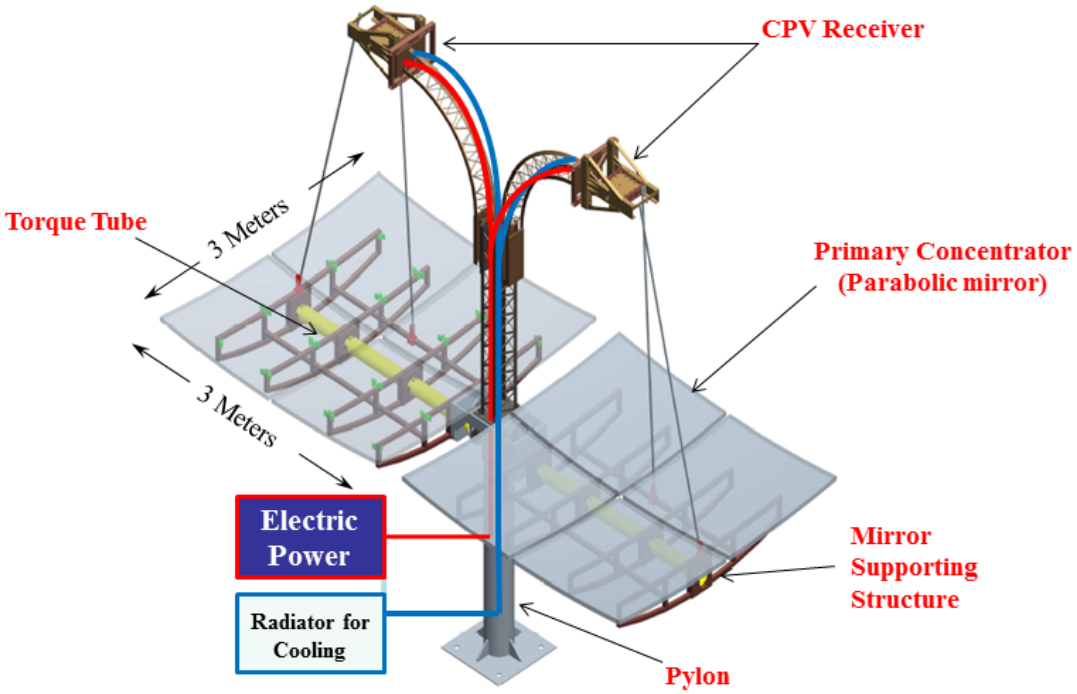

Figure 6: CAD model of one of the four CPV modules

Table 3: Anaerobic digester design specifications

Design		STR
Tank volume	V_{AD}	15.6 m^3
Tank height	H_{AD}	2.7 m
Tank diameter	D_{AD}	2.7 m
Hydraulic Retention Time	HRT	30 days
Organic Loading Rate	OLR	4 $kg{\cdot}VS{\cdot}\ m^{-3}{\cdot}day^{-1}$
Operational temperature	T_{AD}	37 °C
Thermal conductivity of tank walls	U_{AD}	1 $W{\cdot}m^{-2}{\cdot}{}^{\circ}C^{-1}$
Pre-mixing tank volume	$V_{Pre-mix}$	1.5 m^3
Pre-mixing tank operational temperature	$T_{Pre-mix}$	Ambient

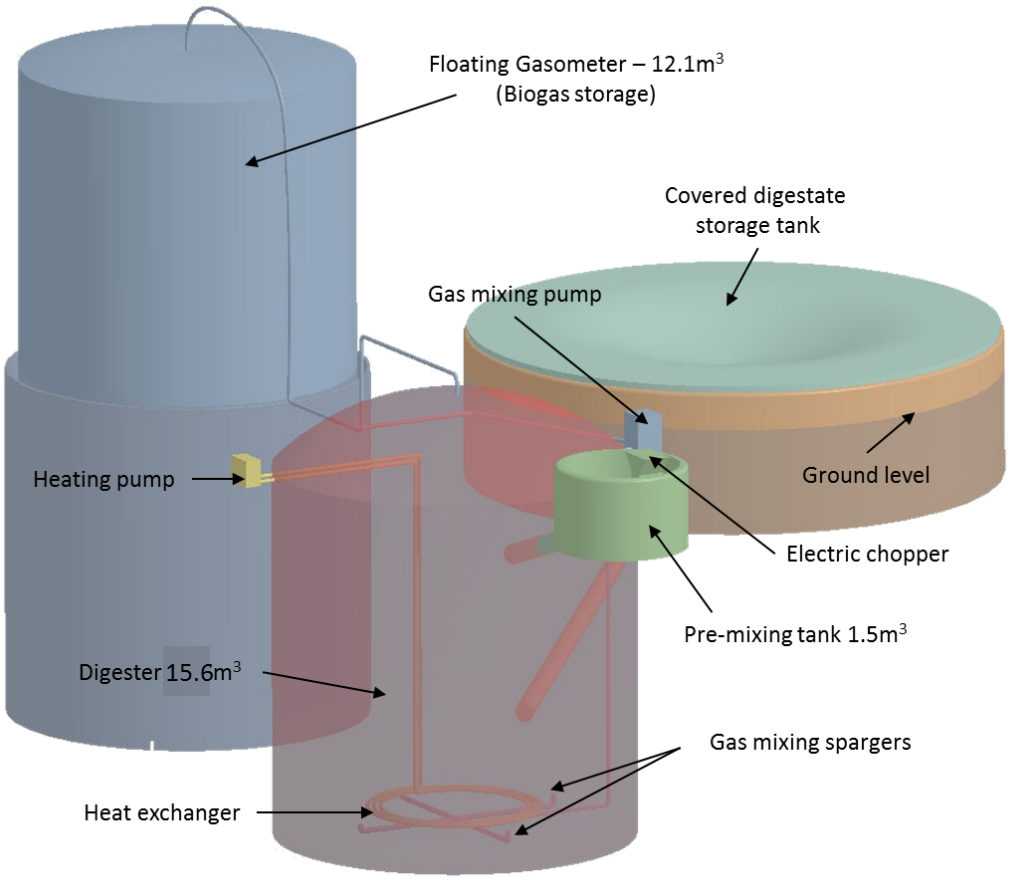

Figure 7: CAD model of the anaerobic digestion system

goon. See Figure 7 and Table 3 for the design layout and specifications.

Design Calculations for Anaerobic Digester

The following describes the preliminary design calculations required for an anaerobic digester.

Biomass Requirement

Total biogas calorific energy required from AD system, Q_{AD} is 76 kWh·day^{-1}

$$Q_{AD} = 76 \text{ kWh·day}^{-1} = 273.6 \text{ MJ·day}^{-1} \tag{7}$$

and

$$LHV_{CH_4} = 50 \text{ MJ·kg}^{-1} \tag{8}$$

therefore,

$$m_{CH_4} = \frac{Q_{AD}}{LHV_{CH_4}} \tag{9}$$

$$m_{CH_4} = 5.472 \text{ kg·day}^{-1} \tag{10}$$

or at Standard Temperature and Pressure (STP) the volume of methane required, V_{CH_4},

$$V_{CH_4} = 7.77 \text{ m}^3\text{·day}^{-1} \tag{11}$$

Since biogas is approximately 60% methane by volume the daily biogas requirement is 12.95 m^3·day^{-1} (STP).

Using Water Hyacinth (Eichhornia crassipes) as a model biomass for calculation purposes and using data from [Chanakya et al., 1992]

BMP (Biochemical methane potential) of biomass, P_{CH_4}

$$P_{CH_4} = 0.21 \text{ m}^3_{CH_4}\text{·kg}^{-1}_{VS_{added}} \tag{12}$$

Volatile solids (VS) concentration, C_{VS}

$$C_{VS} = 0.079 \text{ kg}_{VS}\text{·kg}^{-1}_{wet} \tag{13}$$

Assume the effectiveness of the process, α_{AD}

$$\alpha_{AD} = 0.9 \tag{14}$$

(i.e. we expect to get around 90% of the BMP in the continuous process).

To calculate the biomass requirement to provide the required amount of biogas

$$\dot{m}_{biomass} = \frac{Q_{CH_4}}{\alpha_{AD} P_{CH_4} C_{VS}} \tag{15}$$

$$\dot{m}_{biomass} = 520.5 \text{ kg·day}^{-1} \tag{16}$$

Digester Sizing

The size of an anaerobic digestion system can either be limited by hydraulic or organic conditions depending on the nature of the biomass.

Hydraulic conditions

The volumetric flow through the AD system must be such that the microorganisms are not washed out. This applies especially to the methanogenic organisms that are crucial to the anaerobic digestion process but have a relatively low growth rate. Therefore it is common to set a lower limit on the HRT (hydraulic retention time), t_R, defined by;

$$t_R = \frac{V_{HRT}\rho_{biomass}}{\dot{m}_{biomass}} \tag{17}$$

Common values of HRT are between 15 and 60 days and as a design constraint we have specified;

$$t_R \geq 30 \text{ days} \tag{18}$$

Organic Loading

The organic loading rate (OLR), $\dot{m}_{OLR}$, must be such that intermediate species are not accumulated in the anaerobic digester. This can occur when the OLR is too high such that the hydrolysis and fermentative organisms, which are fast growing and tolerant to changes in pH, produce volatile fatty acids (VFA) at a rate greater than that which can be consumed by the acetogenic

and methanogenic organisms. The mechanism of process failure is that the increased concentration of VFA, and the associated pH change, begins to inhibit the methanogenic organisms eventually resulting in almost complete cessation of methane production. For this reason a limit of OLR is imposed on an AD system. The OLR is defined by;

$$\dot{m}_{OLR} = \frac{C_{VS}}{V_{OLR}} \tag{19}$$

For mixed systems this can be in the range of 2–10 $\mathrm{kg{\cdot}m^{-3}{\cdot}day^{-1}}$ depending on the system design and biomass type. In our design we have specified;

$$\dot{m}_{OLR} \leq 4\ \mathrm{kg_{VS}{\cdot}m^{-3}_{digester}{\cdot}day^{-1}} \tag{20}$$

Digester Volume

To ensure that our system satisfies both the hydraulic and organic loading conditions imposed;

$$V_{AD} = max\,(V_{HRT}, V_{OLR}) \tag{21}$$

in the case of water hyacinth:

$$V_{HRT} = 15.6\ \mathrm{m^3} \tag{22}$$

and

$$V_{OLR} = 10.3\ \mathrm{m^3} \tag{23}$$

therefore,

$$V_{AD} = 15.6\ \mathrm{m^3} \tag{24}$$

to fulfil both conditions.
As a comparison, if food waste was the model biomass, using data from Banks et al. [2011] gives the following results;

$$\dot{m}_{biomass} = 78.1\ \mathrm{kg{\cdot}day^{-1}} \tag{25}$$

$$V_{HRT} = 2.4\ \mathrm{m^3} \tag{26}$$

$$V_{OLR} = 4.8\ \mathrm{m^3} \tag{27}$$

Thus not only is the food waste system organically, rather than hydraulically limited but also is much more compact than the system based on water hyacinth. Both of these are manifestations of the fact that food waste is much higher in organic material and much lower in water.

5.3. Hydrogen - Electrolyser and Metal Hydride Store

The input power for the electrolyser is assumed to be 1 kW of electricity from the CPV, if we assume 7 hours operation per day this is 7 kW·h . The total efficiency of PEM electrolyser is 60% and it produces about 3 standard litres of hydrogen per min. The total output power from the electrolyser in terms of 'hydrogen power' is 0.60 kW_{H_2} or 4.2 $\mathrm{kW{\cdot}h}_{H_2}$ per day, which is equal to 1260 standard litres of hydrogen per day.

The hydrogen storage system will be in charging mode during the day for 7 hours (when hydrogen is being produced). The system will absorb 180 litres of hydrogen per hour for these 7 hours during the day. The system will desorb hydrogen, when it is required, especially during the 4 hours when the biogas - hydrogen electrical generator is operational. Hence the system will release 1197 litres of hydrogen over 4 hours. [1].

5.4. Biogas-Hydrogen Electrical Generator

The genset will be a commercially available 5 kW biogas internal combustion engine modified to take a biogas–hydrogen mix. The electrical efficiency, was estimated at 25% based on common electrical efficiencies of 5 kW natural gas generators found in the market, for example Yanmar CP5WN [Yanmar, 2015]. For this analysis the ratio of hydrogen is 2% of the fuel mix by mass, based on the expected daily production of hydrogen and daily fuel energy required for the genset, though in reality it may vary depending on availability and need. Conveniently results from Jeong et al. [2009] show that there are diminishing returns from ratios greater than 2.3% hydrogen because the hydrogen displaces air and reduces volumetric efficiency. They also state the most significant increase in efficiency of 3.34% was achieved from 0% – 0.7% hydrogen, when compared to an increase of 1.24% with hydrogen ratios 1.5% – 2.3%.

[1] 11.2 litres of hydrogen gas is equal to one mole of H, weighs 1 gram.

There is also potential to increase the efficiency of the overall system by recovering waste heat from the exhaust and radiator.

6. Initial Energy Utilisation Analysis

The following section provides an energy (first law) and exergy (second law) analysis on the proposed renewable power plant. This quantifies amount of energy flowing through the plant and its quality. An energy utilisation analysis generates the necessary information to diagrammatically display the energy flows with a given system. This allows losses to be investigated and suggest improvements. In addition an exergy analysis can complement an energy analysis by quantifying the energy sources in terms of their quality, relative to a given environment. Together they provide insight into the use of energy within a system to optimise the useful outputs.

6.1. Energy

In order to conduct a theoretical energy analysis assumptions need to be made by either benchmarking to exciting systems and extrapolating the expected output or by using the design criteria.

6.1.1. CPV

The CPV specifications can be found in Table 2. The system is assumed to provide an electrical power (E_{CPV}) of 70 kW·h per day. Equations 4 and 5 provide energy falling entering the collector and CPV PV cell respectively.

For an energy flow analysis in the form of a Sankey diagram, the losses need to be determined. The optical losses ($L_{CPV_{optical}}$) are determined from the difference between the solar energy falling on the concentrator ($Q_{CPV_{concentrator}}$) and the energy reflected on to the PV cell ($Q_{CPV_{cell}}$).

$$L_{CPV_{optical}} = Q_{CPV_{concentrator}} - Q_{CPV_{cell}} \tag{28}$$

Reflective losses from the cell are assumed to be negligible, due to the dual reflector system. Therefore thermal losses ($L_{CPV_{thermal}}$) are assumed to be the difference between the solar energy falling on the PV cell ($Q_{CPV_{cell}}$) and the electrical output (E_{CPV}).

$$L_{CPV_{thermal}} = Q_{CPV_{cell}} - E_{CPV} \tag{29}$$

Table 4: Genset expected efficiency and electrical output

Electrical output	E_{genset}	5 kW
Genset efficiency	η_{genset}	25%
Energy input (fuel)	Q_{genset}	20 kW

6.1.2. Electrical Generator (Genset)

Using the efficiency (η_{genset}) stated in Table 4 (based on the information in Section 5.4) together with the required electrical output (E_{genset}), the energy input of the genset (i.e. the energy of the fuel) (Q_{genset}) can be calculated.

$$Q_{genset} = \frac{E_{genset}}{\eta_{genset}} \tag{30}$$

The US Department of Energy suggest that there are 10% ancillary losses ($L_{genset_{ancillary}}$) on average with automotive internal combustion engines. [DOE, 2014]

$$L_{genset_{ancillary}} = Q_{genset} \times 0.1 \tag{31}$$

The energy content within the exhaust ($L_{genset_{exhaust}}$) was calculated by assuming a biogas (60% methane, 40% carbon dioxide) - hydrogen fuel mix. Genset operation is assumed to be 4 hours, consuming 4 kW·h of hydrogen and 76 kW·h of biogas per day. The products of combustion leave the exhaust at 350°C this figure lies between the exhaust temperatures determined by Tamura [2008] on natural gas engines. The combustion was assumed to take place with 1.2 excess air based on Tamura [2008] findings. For simplicity the excess air in the exhaust remains as oxygen and nitrogen (i.e. no NOx formed). The enthalpy data was extracted from Cengel and Boles [2006] using linear extrapolation for 350°C (623K) and taking the environmental temperature to be 25°C (298K). Subscript i denotes a single component of the products of combustion in the exhaust.

$$L_{genset_{exhaust}} = \sum m_{genset_{exhaust_i}} \times h_{genset_{exhaust_i}} \tag{32}$$

For simplicity the radiator is assumed to contain the remaining losses ($L_{genset_{radiator}}$), though in reality there will be losses through the engine casing.

$$L_{genset_{radiator}} = Q_{genset} - L_{genset_{ancillary}} - L_{genset_{exhaust}} - E_{genset} \tag{33}$$

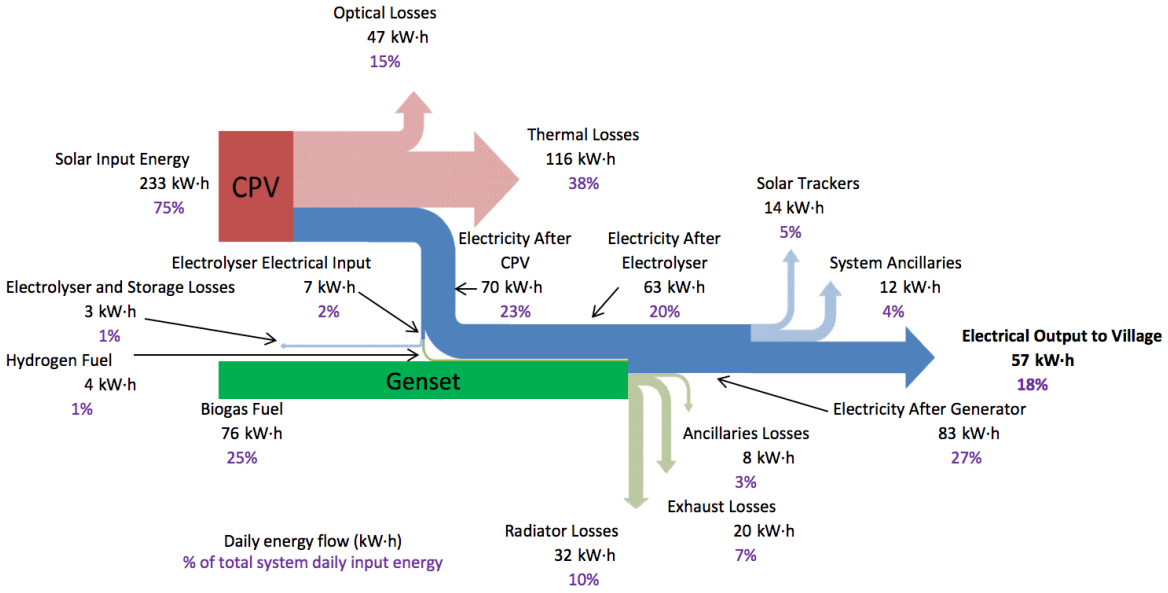

Figure 8: Sankey diagram of daily energy production from BioCPV power plant

6.2. *Exergy*

Exergy rationalises energy in terms of its quality. It does this by relating the energy to its maximum possible work output relative to its environment. As work is (generally) independent of environmental temperature it has the highest energy quality thus the exergy and energy values are equal. Likewise electricity can almost entirely be converted to work, therefore electrical energy and exergy are also equal. Other forms of energy have to be exergetically rationalised. An alternative way to view exergy is quantity of reversible work from a given energy source. Conversely exergy losses are irreversiblities.

6.2.1. *Thermal Exergy (Radiator and PV cell)*

Thermal exergy uses the Carnot efficiency to calculate the maximum work output of a given stationary heat source. The Carnot efficiency uses the temperature difference between a hot source (this is usually the waste heat) and a cold source (this is often the surroundings) to predict the efficiency of an ideal heat engine.

$$\eta_{Carnot} = \frac{T_{hot} - T_{cold}}{T_{hot}} \tag{34}$$

$$\varepsilon_{thermal} = Q \times \eta_{Carnot} \tag{35}$$

6.2.2. *Flow exergy (Exhaust)*

Exhaust gasses are a flow, (whereas the radiator is a stationary a heat source) so flow exergy will be used. Flow exergy uses the entropy generated in the surroundings to determine the maximum reversible work output of a flow. It can be simplified by neglecting the kinetic and potential terms.

$$\varepsilon_{flow} = \dot{m}[(h_1 - h_{surroundings}) - T_{surroundings}(s_1 - s_{surroundings})] \tag{36}$$

When there are several components of a flow the previous equation can be altered to sum the individual components, where subscript i denotes a component of the flow, in the case of the exhaust this will be the products of combustion.

$$\sum \varepsilon_{flow_i} = \sum \dot{m}_i[(h_i - h_{surroundings}) - T_{surroundings}(s_i - s_{surroundings})] \tag{37}$$

6.2.3. *Chemical Exergy (Fuels)*

Chemical exergy quantifies the maximum work output of a chemical reaction in a given environment. The

chemical exergy of fuels has been tabulated by Bejan [1997] at 25°C and 1 atmosphere. This conveniently lies within the conditions expected for the BioCPV power plant environment, and is compatible with the data for the CPV system which is rated to the same conditions. Only the methane content of the biogas has been considered for the exergetic value of the fuel.

- Hydrogen = 235.2 kJ· mol^{-1}
- Methane = 830.2 kJ· mol^{-1}

[Bejan, 1997]

To determine the input (fuel) exergy of the genset for the total period of operation

$$E(kJ) = \tilde{E}(kJ \cdot mol^{-1}) \times \frac{1000}{\tilde{m}(kg \cdot kmol^{-1})} \times m(kg) \tag{38}$$

or for instantaneous (flow) exergy

$$E(kW) = \tilde{E}(kJ \cdot mol^{-1}) \times \frac{1000}{\tilde{m}(kg \cdot kmol^{-1})} \times \dot{m}(kg \cdot s^{-1}) \tag{39}$$

6.2.4. Radiative exergy

This section extrapolates the technique described by Petela [2010] exergetic analysis of a PV cell to a CPV system.

Petela [2010] calculates the total thermal exergy from the sun falling on a PV cell as

$$\varepsilon_{CPV_{concentrator}} = F_{SunEarth} \frac{\sigma}{3} A_{PV} \times \left(3T_{Sun}^4 + T_{environment}^4 - 4T_{environement} T_{Sun}^3\right) \tag{40}$$

To extrapolate to the 8 CPV modules being used in this analysis an effective solar collector area needs to be calculated. This is equivalent to flat area to collect the same out of solar energy as the CPV concentrator.

$$A_{effective} = \frac{Q_{CPV_{concentrator}}}{F_{SunEarth} \times \sigma \times T_{Sun}^4} \tag{41}$$

Table 5: Data for radiative exergy calculations

σ	Stephan-Boltzmann coefficient	$5.67 \times 10^{-}8$ $J{\cdot}s^{-1}{\cdot}m^{-2}{\cdot}K^{-4}$
$F_{Sun-Earth}$	Sun-Earth factor (dimensionless)	2.16^{-5}
T_{Sun}	Sun surface Temperature	5800 K
$T_{environment}$	Environmental temperature	298 K
$A_{effective}$	Calculated effective area of collector	23 m^2

$$\varepsilon_{CPV_{concentrator}} = F_{SunEarth} \frac{\sigma}{3} A_{effective} \times n_{CPV} \times \left(3T_{Sun}^4 + T_{environment}^4 - 4T_{environement} T_{Sun}^3\right) \tag{42}$$

7. Results and Discussion

The surveys and anthropological investigations indicated that improving the environment for education and training would provide the foundation for sustainable development in the selected community. Due to a lack of electrical infrastructure there is inadequate lighting both in public areas such as the school and their homes. The current solutions include kerosene lamps which have adverse health implications when used indoors. There is no provision for thermal comfort such as fans which can significantly aid a learning environment.

To address the development needs of the village a daily electrical demand requirement of 55 kW·h, shown in Figure 2 based on: 7.2 kW·h of public lighting, 3.6 kW·h of domestic lighting, 7.2 kW·h of fans, 12 kW·h of charging appliances such as mobile phones, torches and lanterns, 12 kW·h of computers and 12.8 kW·h of small machinery. This selection of technologies should improve the learning environment in the public areas and alleviate some of the labour intensive income generating activities of the community.

The technologies selected are based on the main renewable energy sources being solar and biomass. Electricity generation will be provided by 10 kW (electric) concentrated photovoltaic (CPV) during the day and a 5 kW (electric) biogas-hydrogen internal combustion electrical generator during the evening. The biogas will be provided by an anaerobic digestion system and the hydrogen from the excess electricity from the CPV via an

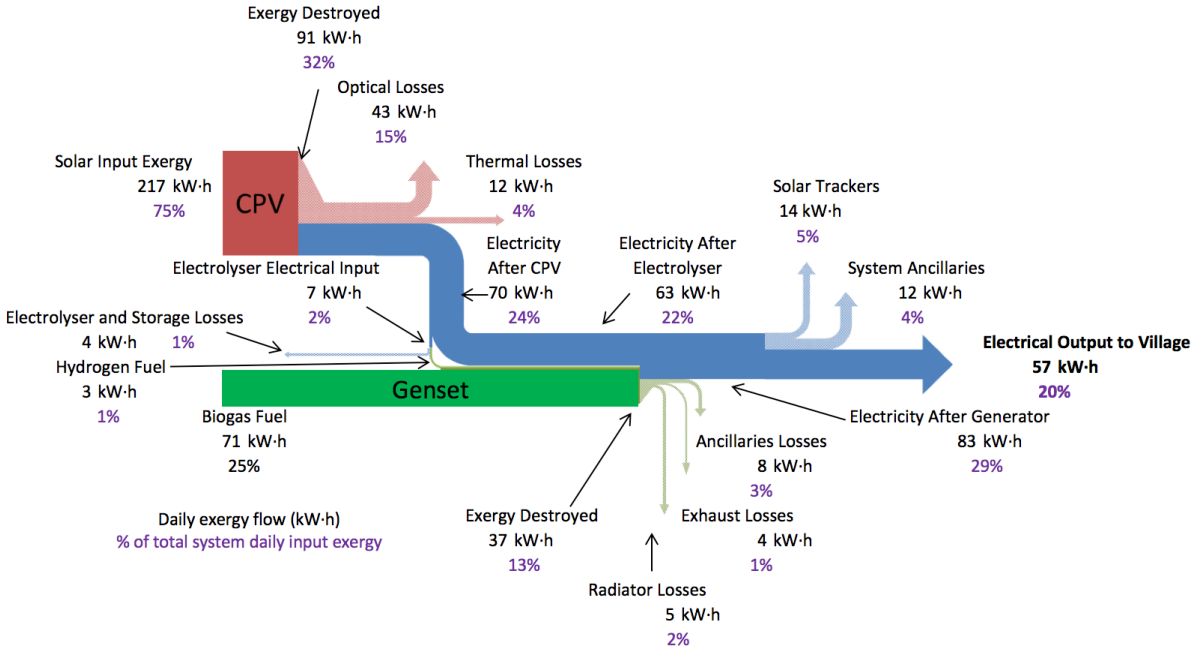

Figure 9: Grassman diagram of daily exergy flow from BioCPV power plant

electrolyser and metal hydride store. The biogas and hydrogen also act as a long term energy store which can be released and used with almost instantaneous start up times.

Using the Sankey diagram (energy flow) in Figure 8 the proposed system should provide 57 kW·h of electricity per day to match and slightly exceeds the estimated demand of 55 kW·h. The system has an electrical efficiency of 18% based on daily quantities from the expected total daily energy input of 309 kW·h, (233 kW·h of solar irradiance and 76 kW·h biogas fuel).

The greatest thermal losses are from the CPV and account for 38% of the total energy input and the radiator from the genset at 10%. Other recoverable thermal losses are from the exhaust of the genset which are 7% of the total energy input. The other losses in the system are: 15% CPV optical losses, 5% solar trackers, 4% system ancillaries and 3% genset ancillaries. Though there is potential to reduce these to increase the overall system performance, the total of these losses is 27%, which is less than the thermal losses of the CPV. Therefore, to improve the system efficiency from an energy perspective, efforts should be directed at utilising the waste heat sources.

However the energy analysis does not take into consideration the quality of the energy. The heat from the CPV and the radiator from the biogas-hydrogen electrical generator at 60°C and 80°C respectively is measured with the same metric as the electricity powering the solar trackers. Therefore an analysis that can compare these quantities in terms of energy quality is required.

The following paragraphs refer to Figure 8 when describing energy and Figure 9 when describing exergy.

The exergy analysis in the form of a Grassman diagram in Figure 9 rationalises the energy flow of the system in terms of its energy quality. For example the daily input exergies; solar radiation falling on the CPV is 217 kW·h and the biogas fuel is 71 kW·h compared to the respective daily energy quantities of 233 kW·h and 76 kW·h. As a result of this and electricity having the same exergetic and energetic quantity, the rational (exergetic) efficiency of the system is 20% whereas the system (energy) efficiency is 18%.

This analysis shows the irreversiblities within the system by the exergy destroyed, 32% of the total system exergy is destroyed in the CPV and 13% in the Genset. This is largely a result of the low Carnot efficiencies of the 60°C CPV thermal losses of 10.5% and the 80°C genset radiator at 15.6%. In reality this means that the maximum theoretical daily work that can be produced

from 116 kW·h of thermal energy in the CPV is 12 kW·h. Likewise the 32 kW·h of daily thermal energy in the radiator of the genset could only produce 5 kW·h of work. The exhaust of the genset is a flow so although its temperature is 350°C, its energy of 20 kW·h only contains 4 kW·h of exergy.

From an exergy perspective the greatest losses are the optical losses from the CPV which amounts to 15% of the total system exergy, as well the electrical loss of the system ancillaries 4% and the solar trackers 5%. In comparison the thermal losses from the CPV are 4% and the genset radiator is 2%. This may seem like it would be more valuable to try to reduce these larger losses but it will not recuperate the 45% of total system exergy input destroyed. The destroyed exergy is a result of the low temperatures of the CPV and genset radiator and indicates that the amount of work that is generated from these outputs is low. There are several options which could use them more appropriately and improve the system efficiency and rational efficiency. Such as direct utilisation e.g. hot water, heat powered refrigeration and water purification.

Though this research is focused on a specific location its approach can be applied to other rural community settings and the findings may be applicable to other CPV and biogas power generation systems.

8. Conclusion

This paper addresses a number of socio-economic aspects of the selected village. Supplying sustainable and renewable electricity to the households is expected to increase the quality of life through improving the educational environment for the children and reducing the manual labour load often burdened by the women. Small scale handwork industries such a craft making and spice grinding can be operated electrically, with the potential to work during the night as well. Lighting and fans in the school will improve comfort and concentration, together with lighting in the home, making it possible for children to study at night. The implementation of a charging station for torches can improve the overall safety of the village. The food waste and other biomass sources will be used as feedstock for an anaerobic digester, providing a sustainable fuel and acting as a source of education for sustainability in general.

A 10 kW (electric) CPV combined with a 5 kW (electric) biogas - hydrogen generator will supply the electricity needs of the community. The energy and exergy analysis has shown that the greatest potential to improve the system efficiency is through utilising the waste thermal energy in the CPV. This amounts for 38% of the total input energy into the system. There is also potential to recover a further 10% of the total input energy from the radiator of the genset. However the exergy analysis showed that there is little work potential in these waste heat sources as they are at low temperatures, 60°C and 80°C respectively. Investigations into alternative uses of low temperature heat are required to make use of this waste energy to improve the system efficiency.

9. Acknowledgements

This work has been carried out as a part of BioCPV project jointly funded by DST, India (Ref No: DST/SEED/INDO-UK/002/2011) and EPSRC, UK, (Ref No: EP/J000345/1). Authors acknowledge both the funding agencies for the support. The authors also acknowledge the support of their respective universities which include: University of Exeter, Indian Institute of Technology Bombay, Indian Institute of Technology Madras, University of Nottingham, Herriot Watt University, Visva-Bharati (West Bengal) and University of Leeds.

10. References

Amonix, 2014. Solar Power Concentrated Photovoltaic Systems. `http://amonix.com/`, Accessed: 2014-08-05.

Appels, L., Lauwers, J., Degrève, J., Helsen, L., Lievens, B., Willems, K., Van Impe, J., Dewil, R., 2011. Anaerobic digestion in global bio-energy production: Potential and research challenges. Renewable and Sustainable Energy Reviews 15 (9), 4295–4301.

Bajpai, P., Dash, V., 2012. Hybrid renewable energy systems for power generation in stand-alone applications: A review. Renewable and Sustainable Energy Reviews 16 (5), 2926–2939.

Banerjee, R., 2006. Comparison of options for distributed generation in India. Energy Policy 34 (1), 101–111.

Banks, C. J., Chesshire, M., Heaven, S., Arnold, R., 2011. Anaerobic digestion of source-segregated domestic food waste: Performance assessment by mass and energy balance. Bioresource Technology 102 (2), 612–620.

Bejan, A., 1997. Advanced Engineering Thermodynamics second edition. John Wiley & Sons, Inc., New York.

Bouallagui, H., Touhami, Y., Ben Cheikh, R., Hamdi, M., 2005. Bioreactor performance in anaerobic digestion of fruit and vegetable wastes. Process Biochemistry 40 (3-4), 989–995.

Cengel, Boles, 2006. Thermodynamics: An engineering approach. Mc Graw-Hill, New York.

Chanakya, H., Borgaonkar, S., Rajan, M., Wahi, M., 1992. Two-phase anaerobic digestion of water hyacinth or urban garbage. Bioresource Technology 42 (2), 123–131.

DOE, 2014. Fuel Economy where energy goes, http://www.fueleconomy.gov/feg/atv.shtml, Accessed 03-04-2014.

Fan, H., Singh, R., Akbarzadeh, A., 2011. Electric Power Generation from Thermoelectric Cells Using a Solar Dish Concentrator. Journal of Electronic Materials 40 (5), 1311–1320.

Feuermann, D., Gordon, J. M., 2001. High-concentration photovoltaic designs based on miniature parabolic dishes. Solar Energy 70 (5), 423–430.

Gandhi, A. (Ed.), 2011. India human development report, 2011: towards social inclusion, 1st Edition. Institute of Applied Manpower Research, Planning Commission, Govt. of India : Oxford University Press, New Delhi.

Gerardi, M. H., 2003. Types of Anaerobic Digesters, in The Microbiology of Anaerobic Digesters. Wastewater Microbiology Series. John Wiley & Sons, Inc., Hoboken, NJ, USA.

Ghosh, S., 2002. Electricity consumption and economic growth in India. Energy Policy 30 (2), 125–129.

Green, M. A., Emery, K., Hishikawa, Y., Warta, W., Dunlop, E. D., 2014. Solar cell efficiency tables (version 43): Solar cell efficiency tables. Progress in Photovoltaics: Research and Applications 22 (1), 1–9.

Hartmann, H., Ahring, B., 2006. Strategies for the anaerobic digestion of the organic fraction of municipal solid waste: an overview. Water Science & Technology 53 (8), 7.

Heliotrop, 2014. Heliotrop - Innovative and low cost CPV solar systems. `http://www.heliotrop.fr/en-index.php`, Accessed: 2014-08-05.

Hilkiah Igoni, A., Ayotamuno, M., Eze, C., Ogaji, S., Probert, S., 2008. Designs of anaerobic digesters for producing biogas from municipal solid-waste. Applied Energy 85 (6), 430–438.

Hoffschmidt, B., Alexopoulos, S., Rau, C., Sattler, J., Anthrakidis, A., Boura, C., O'Connor, B., Hilger, P., 2012. 3.18 - Concentrating Solar Power. In: Sayigh, A. (Ed.), Comprehensive Renewable Energy. Elsevier, Oxford, pp. 595 – 636.

HP, 2015. HP Online Store, http://store.hp.com/UKStore, Accessed 14-01-2015.

HSE, 1997. Lighting at Work Web-Friendly Version of HSG38, http://www.hse.gov.uk/pubns/priced/hsg38.pdf, Accessed 04-01-2015).

Jeong, C., Kim, T., Lee, K., Song, S., Chun, K. M., 2009. Generating efficiency and emissions of a spark-ignition gas engine generator fuelled with biogas–hydrogen blends. International Journal of Hydrogen Energy 34 (23), 9620–9627.

Kazmerski, L., 2012. 1.03 - Solar Photovoltaics Technology: No Longer an Outlier. In: Sayigh, A. (Ed.), Comprehensive Renewable Energy. Elsevier, Oxford, pp. 13 – 30.

Kribus, A., Kaftori, D., Mittelman, G., Hirshfeld, A., Flitsanov, Y., Dayan, A., 2006. A miniature concentrating photovoltaic and thermal system. Energy Conversion and Management 47 (20), 3582–3590.

Kurtz, S., 2012. Opportunities and Challenges for Development of a Mature Concentrating Photovoltaic Power Industry (Revision). Tech. Rep. NREL/TP-5200-43208, 935595.

Luque, A., Hegedus, S. (Eds.), 2003. Handbook of photovoltaic science and engineering. Wiley, Hoboken, NJ.

MoRD, 2014. Ministry of Rural Development (Government of India), http://rural.nic.in/, Accessed 05-09-2014.

Nallathambi Gunaseelan, V., 1997. Anaerobic digestion of biomass for methane production: A review. Biomass and Bioenergy 13 (1-2), 83–114.

NREL, 2013. NREL: National Residential Efficiency Measures Database - Retrofit Measures for Light Bulbs. `http://www.nrel.gov/ap/retrofits/measures.cfm?gId=5&ctId=30`, Accessed: 2014-10-07.

NRLM, 2014. Aajeevika - National Rural Livelihoods Mission (NRLM), http://aajeevika.gov.in/, Accessed 05 September 2014.

NUT, 2015. Space Requirements in Classrooms: NUT Health and Safety Guidance, https://www.teachers.org.uk/files/space-requirements-in-classrooms.doc, Accessed 27-09-2015.

Petela, R., 2010. Engineering Thermodynamics of Thermal Radiation, 1st Edition. McGraw-Hill.

Ramachandra, T., Jain, R., Krishnadas, G., 2011. Hotspots of solar potential in India. Renewable and Sustainable Energy Reviews 15 (6), 3178–3186.

Reddy, K. S., Lokeswaran, S., Agarwal, P., Mallick, T., 2013. Numerical Analysis of Micro Channel Heat Sink Cooling System for Solar Concentrating Photovoltaic Module. In: Ghosh, P. C. (Ed.), 4th International Conference on Advances in Energy Research. Mumbai, India.

Reddy, K. S., Veershetty, G., 2013. Viability analysis of solar parabolic dish stand-alone power plant for Indian conditions. Applied Energy 102, 908–922.

Sharma, N. K., Tiwari, P. K., Sood, Y. R., 2012. Solar energy in India: Strategies, policies, perspectives and future potential. Renewable and Sustainable Energy Reviews 16 (1), 933–941.

Soitec, 2014. Soitec - Revolutionary semiconductor materials for energy and electronics. `http://www.soitec.com/en/index.php`, Accessed: 2014-08-05.

Tamura, M., 2008. An Investigation of a Natural Gas HCCI Engine for 5kW Class Co-generation System. In: IGRC Paris 2008. International Gas Union Research Conference.

Vent-Axia, 2015. Reversible Hi Line Vent Axia, http://www.vent-axia.com/range/reversible-hi-line.html, Accessed 27-09-2015.

Verlinden, P., Lewandowski, A., Kendall, H., Carter, S., Cheah, K., Varfolomeev, I., Watts, D., Volk, M., Thomas, I., Wakeman, P., Neumann, A., Gizinski, P., Modra, D., Turner, D., Lasich, J., 2008. Update on two-year performance of 120 kWp concentrator PV systems using multi-junction III-V solar cells and parabolic dish reflective optics. IEEE, pp. 1–6.

Viebahn, P., Lechon, Y., Trieb, F., 2011. The potential role of concentrated solar power (CSP) in Africa and Europe—A dynamic assessment of technology development, cost development and life cycle inventories until 2050. Energy Policy 39 (8), 4420 – 4430.

Wernsman, B., Siergiej, R., Link, S., Mahorter, R., Palmisiano, M., Wehrer, R., Schultz, R., Schmuck, G., Messham, R., Murray, S., Murray, C., Newman, F., Taylor, D., DePoy, D., Rahmlow, T., 2004. Greater Than 20% Radiant Heat Conversion Efficiency of a Thermophotovoltaic Radiator/Module System Using Reflective Spectral Control. IEEE Transactions on Electron Devices 51 (3), 512–515.

Yanmar, 2015. Yanmar mCHP Catalogue, http://www.yanmar-es.com/uploads/files/349226-YAN-Catalog-Apr17˙FINAL˙DIGITAL˙med.pdf, Accessed 24-02-2016.

Zenith Solar, 2013. Zenith Solar. `http://www.zenithsolar.com/solar-engineering.aspx`, Accessed: 2014-08-05.

Zheng, C., Kammen, D. M., 2014. An innovation-focused roadmap for a sustainable global photovoltaic industry. Energy Policy 67, 159–169.